ANGLIA RUSKIN UNIVERSITY

FINITE ELEMENT ANALYSIS AND OPTIMISATION OF EGG–BOX ENERGY ABSORBING STRUCTURES

MARYAM SANAEI

A Thesis in partial fulfilment of the requirements of Anglia Ruskin University for the degree of Doctor of Philosophy

Submitted: December 2013

AKNOWLEDGMENT

On top of all, I thank God for giving me the opportunity to discover, study and grow.

I would like to present my gratitude to my supervisory team, Prof. Shirvani, Dr. Nwaubani and Dr. Shirvani at the Faculty of Science and Technology at Anglia Ruskin University, and Dr. Miraj at the Department of Civil and Environmental Engineering at UCI, for their invaluable advice and support along the journey of this research. My appreciation also goes to Cellbond Composites Ltd. for offering their time and information to assist the initiation of this project.

I am also grateful to Prof. Mosallam at UCI for his kind consideration and guidance and Mr. Cartillieri, Mr. Metzner, Mr. Rutz and Mr. Kim for offering their facilities and advice as well as Mr. Becerra for his novel ideas.

I also take this opportunity to thank my family (my parents, parents in law, husband, sister, brother and son), without whose continuous moral encouragement and financial support, starting and completing this research would not have been possible.

DEDICATIONS

To my Parents;
for their infinite love, unconditional support and invaluable advice.

To my Husband;
for understanding, caring and standing by me along the way.

And last but certainly not least,

To my Sister and Brother;
for always being there and completing my life.

ANGLIA RUSKIN UNIVERITY

ABSTRACT

FACULTY OF SCIENCE AND TECHNOLOGY

Doctor of Philosophy

MARYAM SANAEI
December 2013

This study investigates the mechanical and geometrical attributes of egg–box energy absorbing structures as crash safety barriers in the automotive industry. The research herein was originated from the earlier work of Prof. Shirvani, patented and further investigated by Cellbond Composites Ltd. who has invested in further research, for developing an analytical tool for geometric optimisation as an enhanced resolution to various shapes and materials. Energy absorption in egg-box occurs through plastic deformation of cell walls, examined through non–linear finite element simulations using ANSYS® and ANSYS/LS–DYNA® FE packages. Experimental dynamic crash tests have been designed to verify the validity of the FE simulations. Geometrical models are defined as 3D graphical representations, outlined in detail. Further, the impact behaviour of commercially pure aluminium egg-box energy absorbers is studied to identify the optimum design parameters describing the geometry of the structure. A simulation-based multi-objective optimisation strategy is employed to find a set of Pareto-optimal solutions where each solution represents a trade-off point with respect to the two conflicting objectives: the maximum impact force and the energy absorption capacity of the structure. The aim is to simultaneously minimise the former and maximise the latter, in the attempt to find purpose–specific optimal egg–box geometries. In light of the associated outcomes, it is shown that egg–box geometries with most favourable performance in the initial stage of an impact have large vertical apical angles ($70^{\circ} < \omega < 89^{\circ}$), thin walls ($t$ < 1mm), short inter–peak distances and small peak diameters. Maximum deformation lengths occur in egg–box geometries with smaller vertical apical angles ($0^{\circ} < \omega < 20^{\circ}$), thin walls ($t$ < 1mm), lengthy inter–peak distances and smaller peak diameters. It is concluded that, egg–box structures combined in the form of sandwich panels can be designed per application to act as optimised energy absorbers. Results of the proposed optimised sandwich structure are verified using analytical techniques.

CONTENTS

NOMENCLATURE

Abbreviation	Description	Units
Al	Aluminium	
CP	Commercially Pure (99% Al Alloy)	
EA	Energy Absorber	
FE	Finite Element	
KE	Kinetic Energy	
LCS	Local Coordinate System	
PE	Potential Energy	
ε	Nominal Axial Strain	
$\bar{\varepsilon}$	Strain Rate	s^{-1}
ε_D	Densification Strain	
Θ	Cone Angle with Horizontal	degree
ρ	Density of Crushed Structure	ton/mm^3
ρ_a	Density of Commercially Pure Aluminium Sheet	ton/mm^3
$\bar{\rho}$	Ratio of Egg–box Mass to Mass of Solid Block	
σ	Nominal Axial Stress	MPa
σ_i	Stress due to Impact	MPa
σ_Y	Material Yield Strength	MPa
ω	Epical Angle (Cell Wall Angle to the Vertical)	degree
A	Cross Sectional Area of Impacted Structure	mm^2

a	Acceleration	mm/s^2
a_{crush}	Crush Acceleration	mm/s^2
d	Diameter at Top of Cell	mm
D	Base Diameter of Frusta	mm
E_L	Energy Absorber per Unite Length	N.mm/mm
E_{total}	Total Crush Energy Absorbed	N.mm
F_{avg}	Average Value of Total Load Applied	N
Fi	Applied Impact Load	N
g	Gravitational Acceleration	mm/s^2
h	Egg–box Cell Cone Height	mm
H	Egg-box Total Cell Height = 2h	mm
k	Geometrical Constant	
m	Impacting Mass	kg
P	Applied Load	N
p	Inter–peak Distance in between Egg–box Cells	mm
r	Fillet Radius at Wall to Peak Transition Egg–box	mm
R	Radius of Peak/Base Curvature	mm
SEA	Specific Energy Absorption	N.mm/ton
t	Cell Wall Thickness	mm
t_{crush}	Total Time of Deformation	s
V	Velocity	mm/s

V_i	Velocity of Impact	mm/s
W	Cross–sectional Cell Width	mm
$W_{Bending}$	Work due to Structural Bending	J
$W_{Compression}$	Work due to Structural Compression	J
$W_{Flattening}$	Work due to Flattening of Structure Curves	J
$W_{Friction}$	Work due to Surface Friction	J
W_{Hinge}	Work due to Emergence of Plastic Hinges	J
W_m	Energy Absorbed per Unit Mass	N.mm/ton
$W_{Stretch}$	Work due to Material Stretching	J
W_{Total}	Total Work Done	J
W_{Twist}	Work due to Structure Twisting	J
W_v	Energy Absorption Capacity per Unit Volume	$N.mm/mm^3$
x	Deformation Distance	mm
x_i	Distance of Densification Point	mm
Y	Yield Strength	MPa

LIST OF FIGURES

LIST OF TABLES

1. INTRODUCTION AND THEORETICAL BACKGROUND

The ability to absorb and reduce the effect of kinetic energy has led to the production of specific structures called energy absorbers (EA). Use of such parts imbedded in the design of dynamically sensitive structures such as motor vehicles will increase their safety characteristics. A shock or crash enduring structure is one that handles the impact forces and the safe transfer of kinetic energy by collapsing through a predictable behaviour (Du Bois et al., 2004). As a result of this controlled collapse, the possibility of the vehicle occupants being injured can be reduced. Factors such as structural stiffness, maximum strength and the ability to absorb energy beyond the elastic limit, directly determine the level of the crashworthiness of a system*.

In addition to the front and rear bumpers, energy absorbing structures can be multi–functionally implanted in doors, bonnet, dashboard, heat exchanger, air filter, liquid storage components and other parts of a vehicle body (Ashmead et al., 2000). The presence of such systems could also play a key role in making roads safer for both pedestrians and passengers, by cushioning them against the impact of an accident.

---

* Readers are referred to Appendix A for further review and detailed information on subjects studied here forth.

In order for a structure to absorb the energy of an impact and reduce its effect, it would have to consist of builds such as lattice (periodic truss) structures (Evans, 2001, Fleck, 2001, Chiras et al., 2002, Wadely et al., 2003 and Kooistra et al., 2004), tubes (Abramowicz et al., 1984, Kim et al., 1998-1999, Markiewicz et al., 1998, Reid, 2003, Jensen et al., 2004, Morris et al., 2006-2007, Mahdi et al., 2006, Olabi et al., 2007-2008, Melo et al., 2007, Yuen et al., 2007, Zhang et al., 2009), repetitive cells (Wu et al., 1996, Kim et al., 2002, Yu et al., 2005, Avalle et al., 2006, Hou et al., 2007), or porous/perforated foam (Chen et al., 1999, Deshpande et al., 1999, Hanssen et al., 1999(1,2), Zhou et al., 2003, Fleck, 2001, Jeon et al., 2008-2010, Said et al., 2008, Yoo et al., 2010, Zarei et al., 2010), geometrical features. Such structures collapse through desirable patterns that can be studied and predicted to fit the needs of specific applications.

The absorption of energy by deformation in cellular absorbers can be through collapse processes such as plastic buckling (Figure 1.1), plastic yield or folding through stationary plastic hinges and travelling plastic hinges (Figure 1.2), depending on the type of the geometry (Alexander, 1960, Meng, 1983, Abramowicz et al. 1984). Alexander was the first researcher to provide a theoretical model for axial collapse of tubes. The mean crush force in Alexander's model is derived based on the balance of internal and external work. This simple theoretical model was later adopted and modified by Abramowicz and Jones into a more precise model. In some geometrical cases EA structures can fail due to material tearing (Qiao, 2008).

For applications such as cushioning of passengers in vehicles, low density energy absorbing structures are preferable, to reduce the total weight of the vehicle as associated with its performance. Lattice materials have greater density values in comparison to their cellular and foam counterparts (Jacobsen et al., 2010). Structures such as hexagonal honeycomb blocks of various depths, metal and plastic foams and egg–box panels are candidates falling in this desirable category.

The manufacturing methods of these structures include fabrication through powder metallurgical techniques, injection moulding and cold or hot pressing of metal sheets. This leads to the next signifying factor i.e. the production costs. Experience shows that egg–box structures can be manufactured through less

expensive methods compared to lattice material, honeycombs or foams since they can be produced through a single action by cold or hot pressing of metal sheets (Deshpande et al., 2003 and Nowpada and Chirwa et al., 2009).

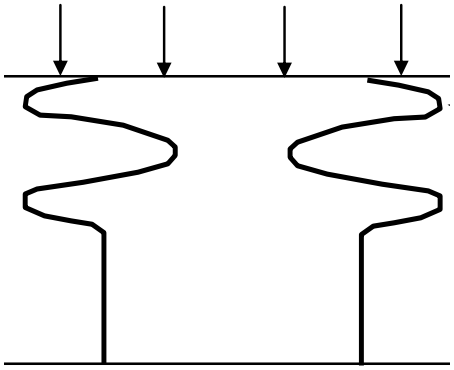

Figure 1.1 – Plastic Buckling Deformation

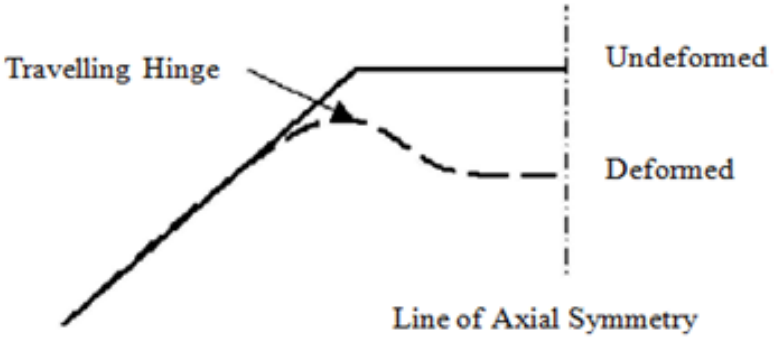

Figure 1.2 – Travelling Hinge Deformation

From the mechanics point of view, the purpose behind using an energy absorbing structure is the ability to absorb energy at a stress level which would be lower than a prescribed value for specific circumstances.

1.1. Characteristics of Cellular Egg–box Energy Absorbing Structures

Automotive designers are always looking for efficient and cost effective absorbers in vehicle interiors to cushion the occupants. One solution is to use cellular solids or structures made up of an interconnected network of cells, which characterise the advantages of deforming with a comparatively regular force during a compressive impact event. The Egg–box structure is one such energy absorber.

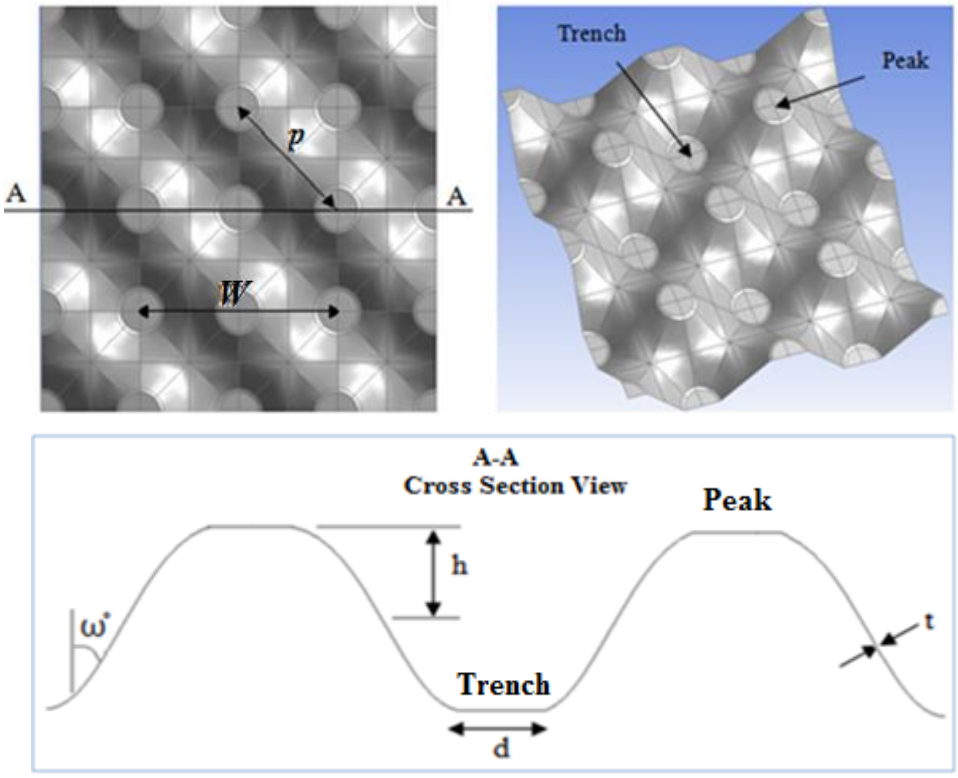

Figure 1.3 – Egg–box Absorber Structure (*W* is the distance between a consecutive peak and trench, *p* is the inter-peak distance, *h* is the cell height, *d* is the peak/base diameter, *ω* is the apical angle and *t* is the thickness)

The egg–box, as suggested by its name, is a structure consisting of a series of conical cells, forming the shape illustrated in Figure 1.3 with (*p*) showing the diagonal inter-peak distance and (*W*) being the distance between two consecutive peaks/trenches in lateral directions. This geometrical arrangement of regular flat–top cones is designed to provide axial strength against external forces. In addition, this

structure is renowned for its ability to deform in a predictable manner and produce consistent results under various impact angles (Ashmead et al., 2000). Based on the material involved in its production, the egg–box structure can come in relatively low weights and be manufactured to desired geometrical features for specific applications.

The quality and the relative length of the plateau for the absorber's force vs. displacement curve, provided in Chapters 3, 4 and 5, is a characterising criteria of a good energy absorber with the potential of being used as a design component for pedestrian and passenger protection. Figure 1.4 is a typical force-displacement curve as related to the performance of an egg-box structure.

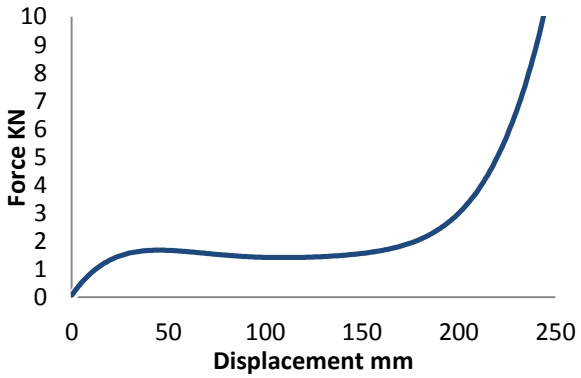

Figure 1.4 – Typical Force vs. Displacement Curve

1.1.1. Geometrical Configuration of Egg–box

The geometry of the egg–box structure contributes towards its suitability as an energy absorber.

Specific geometrical angles and distances in the structure of an egg–box cell can be adjusted to result in desired levels of energy absorption. Varying the peak to peak length (p), angle (ω), cell diameter (d) or wall thickness (t), in addition to the material type used and the level of constraints applied to the structure can result in

diverse energy absorption characteristics for this structure. For Example, research has shown that reducing the inter–peak distance, gives a higher density of cones throughout the structure which in turn results in an increased stiffness, hence, a higher stress level, i.e. greater amount of energy will be absorbed (Deshpande et al., 2003).

1.2. Why Egg–box as an Energy Absorbing Module?

In comparison to the classical energy absorbers, the egg–box structure has many advantages. Despite their satisfactory performance as energy absorbers, structures such as honeycomb blocks and metal foams are bulky and difficult to transfer from the manufacturer to the automotive companies. Egg–box absorbers, on the other hand, use minimum packaging space and are easy and safe to handle during installation. Moreover, similar to other energy absorbers, the egg–box structure has the benefit of being easily stackable and recyclable (Ashmead, 2000).

Due to its low manufacturing costs, and since it can be made from a range of metallic sheets by a single stage hot or cold pressing, or from plastic materials by injection moulding, the egg–box absorber is particularly suitable for high volume productions (Ashmead, 2000). As a result of this straightforward fabrication approach, it becomes possible to mould up the egg–box structure into complex shapes and tailor local crush strengths for specific applications. Its ability to be composed into sandwich structures can also offer many benefits to the designers with its exceptional flexural properties in sandwich systems (Ashmead, 2000). These features are all desirable to automotive and aviation companies.

An additional benefit that comes with the outline of the egg-box absorber is having an open structure along its length, which can be structurally useful in allowing for wirings to pass along the length of the panel, bending amongst the peaks and trenches.

A specific feature displayed in the deformation process of the egg–box structure, greatly contributes towards its aptness as an energy absorber; with the collapse of the egg–box geometry under impact loads, two main deformation

mechanisms can be observed, Travelling Hinge deformation and Plastic Buckling deformation (Figure 1.5, explained further in Appendix A). These two phases need to be investigated more thoroughly for the energy absorption of the egg–box structure to become more predictable and noticeably improved.

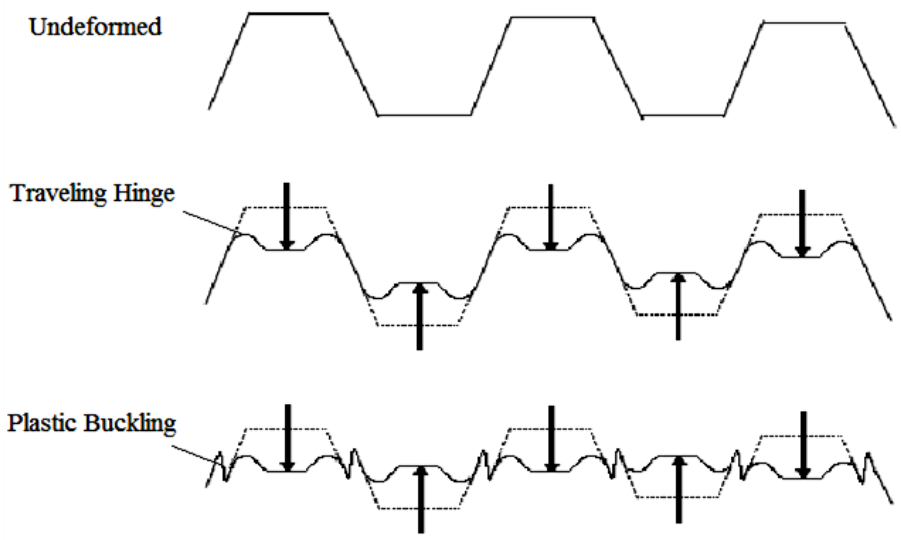

Figure 1.5 – Egg–box Deformation Procedure

It is common practice for the egg–box structures currently used in the industry to be fabricated from materials such as aluminium, steel, gun–metal and a variety of plastics by cold pressing and injection moulding, respectively.

An ideal absorber is one that, while performing adequately in reducing the effect of impact energy, would be light, mouldable and stackable. It is obvious that using tougher metals such as steel or gun–metal will result in stronger energy absorbers. Nevertheless, these metals are heavier in nature and much harder to mould into the desired shape. Aluminium alloys are comparatively light weighted, very mouldable, inexpensive and ultimately they can be recycled.

Currently aluminium parts are employed in the automotive industry, most importantly due to their significant weight saving features. Steel has a density value three times that of aluminium which leads to over 25% more weight when used in

vehicle body parts (Kim, 1998). Such amount of weight cutback can have a strongly positive effect on reducing the fuel consumption and emission of the vehicle. All these benefits as well as its high corrosion resistance, indicate that aluminium is the ideal material for the automotive industry.

To maintain the characteristics of an ideal absorber and as a most commonly used material in this industry, aluminium alloys are considered as optimum materials for the production of egg–box structures. Nevertheless, it should be noted that, an important determining factor remains to be the specific application for which the absorber is being manufactured.

1.3. Evaluation of the Performance of Egg–box Structure

The mechanism of deformation for a uniaxial compression is complex. Different variables are taken into account and controlled by the design engineer to evaluate the mode of deformation of the egg–box absorber for a specific application. Refinement of these factors can lead to improved performance, efficiency and design optimisation that would accommodate the specifications required by individual customers.

In addition, external factors such as the angle and magnitude of the loadings applied and the presence of other adjacent bodies will also determine the characteristics of the deformation pattern of an EA structure (Alexander, 1960). Examples are illustrated in Appendix A.

Traditionally, the main practical method to evaluate the effect of variations of geometric characteristics in the performance of a structure and its EA capacity was experimental testing (Alexander, 1960, Mamalis, 1986, Alghamdi, 1992). In more recent research this method is used to verify the results of numerical or theoretical techniques (Alghamdi, 2001, Deshpande, 2003, Zupan, 2003, Naik, 2004, Nowpada, 2009, 2010 a, b). Various methods of practical testing of energy absorber structures exist which can be divided into two main categories of static loading and dynamic impact testing. Past and current researches have been critically reviewed in the second chapter.

Another method of exploring the behaviour of energy absorbers is analysing the structures mathematically. However, despite its repeatability features, this analytical approach can become exceedingly time consuming with complicated situations such as the deformation of energy absorbing structures. To simplify, analysers tend to take advantage of geometrical symmetries to create less complicated two–dimensional illustrations of physical structures (Alexander, 1960, Mamalis, 1986, Alghamdi, 1992, 2001, Deshpande, 2003, Zupan, 2003, Naik, 2004). Although Alexander concludes that his theoretical model does not account for the effect of the superimposed axial stresses on the yield criterion or the detailed consideration of the deformation mode and equilibrium conditions, Calladine (1986) suggests that Alexander's relatively simple theoretical model gives a satisfactory approximation of the collapse behaviour of structures.

Numerical approaches, on the other hand, are beginning to take off as a key part of the design process of energy absorbers in general and specifically in egg–box structure as an innovative energy absorber. One of the best methods for designing, visualising, refining and calculating the performance of geometrically assorted structures produced from different materials is by using the finite element (FE) method.

As an advantage, commercially available advanced finite element computation packages, such as ANSYS®, ABAQUS®, LUSAS® and LS–DYNA®, allow for the creation of graphical representations of required components, in the form of numerical models, which can be tested through a number of different methods, both inexpensively and repeatedly under a variety of different conditions, via powerful processors. The accurate results of these simulations in comparison with experimental tests, has encouraged researchers all over the world to use this approach with firm validity and without using expensive experimental techniques. The works of such researchers, as related to the subject of this project, are critically reviewed in the next chapter.

For highly complex problems, highly professional finite element solver packages have been commercially designed, which substantially reduce the time and cost of experimental and mathematical analysis. The ANSYS® software is one of the

well established, widely distributed and popular commercial finite element analysis packages, which has continuously been in use and refined since 1970. Its historical background of development has resulted in a code with a vast range of capabilities.

In current researches on the analyses of mechanical behaviour of energy absorbing structures, the procedures mentioned above, including static and dynamic experimental methods, mathematical approaches and numerical techniques are being extensively used. Using numerical calculations and predictions, the FE method can in fact be used to determine the energy absorption characteristics of an EA structure prior to the geometrical design and manufacture. Additionally, FE analysis can be employed for structural optimisation.

1.4. ANSYS® and ANSYS/LS–DYNA® as Tools for Numerical Analysis

As a powerful numerical solver using finite element method, the ANSYS® package can be used to analyse a wide range of mechanical problems such as static and transient structural analysis. In fact, ANSYS® is most commonly used in this particular area of mechanical physics, since it can facilitate the analysis of structures as large as bridges or as small as vehicle parts.

In order to simulate dynamic loading conditions, the powerful processors of ANSYS® have been combined with the equally powerful solver of another finite element package known as LS–DYNA®. This software is designed to be used for analysing static and dynamic problems with large deformation. LS–DYNA® uses explicit time integration as its base solution approach (LSTC, 2007).

The combination of ANSYS® and LS–DYNA® gave existence to a powerful finite element package referred to as ANSYS/LS–DYNA®. Researchers and designers use this product, to model a structure or system in ANSYS®, then obtaining the explicit dynamic solution using the powerful LS–DYNA® solver, and eventually reviewing the results in the ANSYS® post–processing Graphical User Interface (GUI). The geometry and results information can also be transferred between ANSYS® and ANSYS/LS–DYNA® to help perform chronological

implicit–explicit and explicit–implicit analyses, such as those required for drop–test, spring–back and other applications (ANSYS/LS–DYNA® User's Manual, 2011).

1.5. Aims and Objectives of the Research

Recognising the energy absorption characteristics of structures is functional in analysing the damage caused by accidental or sudden controlled impacts. Identification of such properties is therefore necessary in order to improve the performance of an energy absorbing structures.

The main objective of this research is to develop a numerical simulation tool for geometric optimisation of egg–box energy absorbing structures as an enhanced resolution to various shapes and materials. The study focuses on the way in which egg–box structures can be best designed to absorb kinetic energy in a controllable and predictable manner. The aim of the project is to establish and define geometrical characteristics of egg–box structures which display optimum energy absorption performances.

To define limitations for the research hypothesis, commercially pure aluminium (commonly used in the industry for egg-box absorbers) has been employed as the base material for the egg–box structures. In these cellular structures energy absorption occurs through plastic deformation of the cell walls, which are to be modelled and examined using non–linear finite element simulation packages. The accuracy of the modelling approach has been evaluated and authenticated in comparison to the outcomes of experimental tests. Following the experimental work, the analytical technique has been used in deriving equations of total energy for the deformation procedure of the tested specimens. This method is used alongside the experimental results for the verification of the finite element simulations.

The geometrical modelling of the structures is defined as 3D graphical representations, outlined in detail. Further, deformation mechanisms of the geometrical variations are comparatively modelled and ultimate optimised structures within given boundary conditions are represented.

The effect of variations in the geometrical features of the egg-box is broadly examined based on the associated force–displacement curves, in the attempt to find purpose–specific optimal egg–box geometries.

By performing a comparative study of the force-displacement curves generated, optimised egg–box structures can be selected for specific functions. In addition, these curves can be used as a set of reference deformation pattern curves for various egg–box geometries.

Through modelling and optimisation, it will be the aim of this project to demonstrate the optimum cellular structural energy absorbing characteristics that will display a higher energy absorption capacity, while, simultaneously diminishing the destructive effect of a sudden impact at the initiation of its deformation process. The validity of these simulations will be verified against results of experimental tests as well as a developed mathematical model.

1.6. Scope of the Thesis

Road and automotive statistics around the world reveal that, despite taking an increasing number of safety measures on board to reduce the life threatening effect of road accidents, they still remain a main cause of human fatalities and severe injuries. Practical methods, such as making vehicle parts that would protect occupants through absorbing impact energy, should be developed to serve towards safer roads for both vehicle users and pedestrians.

Amongst available options, cellular EA structures perform efficiently by displaying predictable deformation patterns and desirable levels of energy absorption capacity in addition to having advantageous physical and geometrical attributes. Examples of cellular EA structures include conical frusta, circular and non–circular tubes and egg–box panels which consist of a directionally reversed arrangement of flat–top cones. This research concentrates on the behaviour of egg–box energy absorbers, due to their benefits over the other commercially available counterparts. The panel under investigation is of pure aluminium alloy, which is one of the main materials currently being used in the industry to fabricate egg–box structure.

Experimental impact tests have been conducted on both panel and cell specimens to provide principal bases for the assessment of the numerical method employed herein.

The ideal egg–box geometries that will display high levels of energy absorption capacities in specific applications and reduce the effect of an impact to a satisfactory level while maintaining a reasonably low structural weight and material consumption are identified and assessed. Finding such a supreme structure calls for a practical optimisation method. A follow through procedure is provided in this work that allows for modelling and testing egg–box structures of altered geometries, the comparison of which gives rise to optimal egg–box energy absorbing structures.

1.7. Research Methodology

Using tools such as ANSYS® and ANSYS/LS–DYNA®, the dynamic crash tests of egg–box structures of various geometrical characteristics and material conditions have been simulated. Such authentic simulation works can help observe the detailed behaviour of impact absorbers; studying their modes of deformation, benefits and drawbacks.

To create accurate FE simulation specifications for dynamic loading, comparison is made with the results of experimental dynamic crash tests of egg-box structures with known geometrical details. Two geometrically varied aluminium egg-box samples are selected based on size and commercial availability. The tests can be categorised into three groups based on the participating specimen; free-edged single cone, single cone within a panel and axial impact of the entire panel. In addition, the first two test groups are divided into two areas; flat impacts (at 90° to the horizontal) and oblique impacts (at 45°), to investigate the performance of the egg-box under different loading angels. The outcome of the experimental work validates the proposed numerical model.

Evaluation of the performance of these geometries is made through a comparative study of their load vs. deformation curves for dynamic buckling tests. A series of alterations have been made to the geometry of the egg–box, based on a

tabular arrangement of geometrical factors including base diameter (d), apical angle (ω), inter-peak distance (p) and wall thickness (t), which play significant roles in the deformation pattern of this structure. Modifying these factors has a direct effect on the performance and hence the optimisation of the egg–box while the structure can be improved in order to comply with the requirements of various end–users.

For the purpose of this project, sets of values are defined for each variable factor, in accordance to the geometrical measurements of the egg–box structures currently in commercial use.

The values given to each geometrical factor are chosen in a manner to allow a group of geometries to be covered within each range. An averaging technique can be used to estimate the energy absorption characteristics of the structures whose geometrical features fall between two or more parameter ranges. A comprehensive simulation procedure and an optimisation cycle are proposed in this thesis which can be used to model egg–box geometries with specifically defined measurements and fabricated of various materials to determine their precise behaviour as energy absorbers.

The final outcomes of the optimisation process conducted in the current research are validated using a developed analytical model.

1.8. Research Questions and Contribution to Knowledge

With the growing importance of the egg–box structure as functional energy absorbers in the automotive industry, it becomes necessary to have a validated system through which performance of the structure can be evaluated and improved. This calls for a repeatable and inexpensive technique such as finite element simulation.

In addition, whilst a great deal of recent research has taken place on the energy absorption behaviour of structures and materials and significant progress has been made in this area, the knowledge is widely scattered when it comes to geometrical modelling of the cellular structures. Methods of evaluating the performance of an

egg–box structure when subjected to dynamic loading, modelling its geometry and recognising its material properties are diffused amongst analysts, researchers and experts.

The modelling procedure presented and experimentally validated in the thesis can be used as a unified system which will facilitate information comparison for individuals who are associated with the structural design of the egg–box. Although the modelling procedure is based on the ANSYS® Graphical User Interface for the purpose of this study, it can be implemented in any similar 3D simulation software for different purposes.

It has been observed that in the multi–objective optimisation task of the deformation pattern of the egg-box energy absorber, one contributing factor cannot be changed without affecting others. A series of follow–through procedures have been developed in the course of this study, which allow for modelling and evaluation of the performance of aluminium egg–box structures with altered geometries. The effect of variations in the geometrical features of egg–box structures is broadly examined based on their associated force–displacement curves, in the attempt to find purpose–specific optimal egg–box geometries.

As the main contribution to knowledge, deformation patterns of egg–box structures of altered geometrical features have been comparatively examined to allow for the selection of appropriate geometries for certain applications. A series of optimum curves have been presented in Chapter 5 of the thesis. An analytical review of the curves, results in the introduction of an optimised combination of the egg–box absorbers, which satisfactorily displays the requirements of an improved structure.

1.9. Thesis Outline

A brief description of chapter contents of this thesis is presented below.

Chapter 1 provides introductory information on primary concepts and boundary conditions including materials used in this investigation. It further aims to define the hypothesis of the thesis and the rational for the investigation. These include details

on energy absorption and energy absorbing structures, egg–box energy absorber geometrical features, finite element analysis and its application towards the optimisation of egg–box energy absorbing structures. The objectives, research contributions and design methodology of the research are provided in this chapter.

The 2nd Chapter aims to explore and exhaust the subject area from other researchers prospective and to make sure this investigation has fulfilled the process of consolidating the various strands of past research into a single narrative structure, describing the evolution of the research domain. It follows by the work of previously performed researches on the subject of energy absorption and optimisation, by critically reviewing a series of past and recently published literature.

Chapter 3 covers the experimental work conducted as a part of this project. Information on the sample preparation, geometrical details of the sample, test equipment and scope, experiment procedure and result derivation are provided in this chapter. The results of the experimental works have been presented and comparatively discussed in the concluding section of Chapter 3.

The 4th chapter consists of two sections, exploring the deformation pattern of the egg-box both analytically and numerically. In the former part, the total energy equation has been developed per experimental test conducted as a part of satisfying the objectives of the project and preliminary calculations are made which comply with the experimental test results. The latter part of this chapter uses finite element technique and packages to model, simulate and analyse the energy absorbing characteristics of egg-box structures when subjected to an impact load. This section includes information on geometrical modelling details, material model definition, element selection, application of boundary conditions and loadings and result derivation using the pre and post processor and solver of ANSYS/LS-DYNA® FE package. The outcomes of the simulations are compared to that of the experimental work, achieving excellent correlation between results and hence, verifying the authenticity and accuracy of the finite element model and settings for the egg-box cell simulations.

In Chapter 5 the established finite element model of the previous chapter has been employed to model a series of geometrically altered egg–box structures, created

in accordance to the values provided in a tabular arrangement of various geometrical factors. These structures are then impacted in a simulated dynamic test, and their results, produced by finite element methods, are reviewed to find application–specific optimised geometries. Subsequently, an improved sandwich structure, formed by a combination of optimum egg–box geometries is introduced. The concluding outcome of this section is authenticated using an analytical method, developed to predict the performance of egg–box structures.

Chapter 6 includes a summary of the research, discussing the outcomes of each chapter and relating them and reviewing them with regards to the rest of the work.

The final chapter brings the current project to a close, providing concluding remarks on the achievements of this work presented herein. Possibilities of further works relevant to the subject area of this study have also been discussed in Chapter 7, introducing design recommendations of research for future investigation.

2. LITERATURE REVIEW

As related to the subject of this thesis, the published literature can be categorised into two main sections: energy absorption and optimisation. The former category reviews the researches and experiments focusing on the nature of structural energy absorption and techniques associated with this matter. In the second part of this chapter, studies exploring the optimisation methods of energy absorbing structures are studied. The objectives and outcome of these researches and their connection to the subject matter of this work are critically discussed following their citing. This review will elucidate the rationales of this research.

2.1. Energy Absorption and Crashworthiness

Energy absorption and structural crashworthiness are two main areas of concern in mechanical crash analysis. The Transportation Industry is the main sector where energy absorbing structures become applicable; not only in cars and small vehicles, but in fact in the fabrication of heavy vehicles, railway components, aerospace and ship manufacturing. Thus, this section looks at the works of researchers on the basics of these two concepts.

The term crashworthiness in definition was originally described by Johnson as “the quality of response of a vehicle when it is involved in or undergoes an impact. The less damaged the vehicle and/or its occupants and contents after the given event, the higher the crash quality of the vehicle or the better its crashworthy properties” (Johnson, 1978). Later, Wierzbicki (1983) defined structural crashworthiness as the

impact performance of a structure when it collides with another object. For many decades, crashworthiness has been a necessity in the structural design of vehicles.

In theory a crashworthy design transfers part of an impact load to the body of the vehicle. It is essential for the amount of this load to be less than the limit that would result in damage to the body that is being protected. The structure that can reduce the effect of this load to below its destructive limit can be called an energy absorbing structure. The peak of this load should also remain within a reasonable limit (Deb et al., 2004). Researchers have introduced various techniques for reducing this peak load (Hamada, 1997 and Yamazaki, 2000).

For a more practical application, energy absorbing crash boxes in the form of thin–walled tubular structures have been suggested (Hanssen et al., 2001). These crashworthy structures would be replaceable after damage or deformation, making it less costly for a vehicle to be repaired after an accident. It is preferable for the energy absorbing structures positioned in these crash boxes to deform in a manageable and predictable manner. This will ensure compliance between the applied load and the tolerable limit of the energy absorbing structure, and in return ensuring a reduction in the kinetic energy and thus the severity of possible injuries on the occupants (Zini, 2005). This is where the study of the deformational characteristics of energy absorbing structures becomes essential.

2.1.1. Energy Absorbing Structures

Many different energy absorbing structures, with individual properties and applications, are in existence for commercial use. These structures are currently employed in a number of applications as barriers, interior/exterior components of vehicles, wall/floor panels, etc. with many more potential applications still in development.

Most energy absorbing structures can be categorised in one of the following groups: Thin–walled Circular Tubes, Thin–walled Rectangular Tubes, Thin–walled Hat–Section Tubes (the cross section of this structure has the shape of a top hat), Thin–walled Tapered Rectangular Tubes, Thin–walled Conical Shells and frusta,

Metallic Foams, Polymeric (Non–Metallic) Foams (Ahmad, 2009) and Cellular Solids (Avalle, 2006). Images of energy absorbing structures are shown in Fig. 2.1. Investigations have been made on each group over the years, looking at the characteristics of the EA structures.

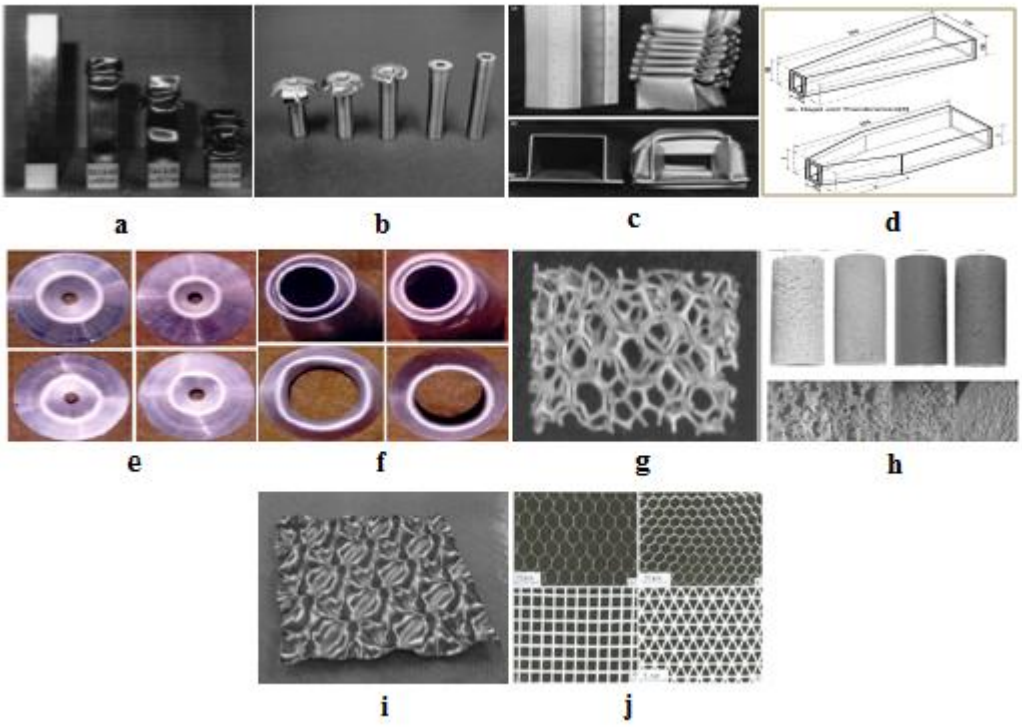

Figure 2.1 – Energy Absorbing Structures: (a) Thin–walled Rectangular Tubes (Langseth, 1998), (b) Thin–walled Circular Tubes (Olabi, 2007), (c) Thin–walled Hat–Section Tubes (Schneider, 2008), (d) Thin–walled Tapered Rectangular Tubes (Shariatpanahi, 2008), (e, f) Thin–walled Conical Shells and frusta (Gupta, 2006), (g) Metallic Foams (Deshpande, 1999), (h) Polymeric Foams (Subhash, 2006), (i, j) Cellular Solids (Deshpande, 2003, Gibson, 1997)

A wide range of collapsible energy absorbing structures can be categorised under the group of thin–walled tubes. Such structures, with various types of geometrical shapes and material properties, are being extensively used in different structural applications. The characteristics of these structures have been studied by many researchers. The works of Johnson et al. (1978), Reid (1993), Hanssen et al. (2000a–b), Alghamdi (2001), Jones (2003) and Abramowicz (2003) provide broad

descriptions of the attributes of these structures and their deformational behaviour. Each type of structure is reviewed below.

Zhang et al. (2009) found the energy absorption capacity of thin–walled tubes to be notably subjective to their material properties and geometrical features. A thin–walled tube could have various cross sectional shapes, including but not limited to circular, square, rectangular, tapered and hat–sections (Ahmad, 2009).

According to research done by Zarei et al. (2008), thin–walled circular tubes are light and, due to their geometry perform efficiently as energy absorbing structures. Another reason for their vast usage as EA structures is explained by Gameiro et al. (2007) to be due to their display of a reasonably constant operating load. A down point of this structure is its limited length, since as concluded by Zarei et al. (2006), the circular tube has a length limit above which it will buckle; hence a substantial reduction in its energy absorption capacity. As noted by Mamalis et al. (1983) and agreed by Yuen et al. (2008), a circular tube shows higher levels of energy absorption capacity compared to its square counterpart.

Square or rectangular based thin–walled tubes were originally looked into by Abramowicz et al. (1984). The response of these structures to static and dynamic loading was investigated more thoroughly over the years by researchers such as Reid et al. (1986), Otubushin (1998), Hanssen et al. (1999) and Meguid et al. (2007). Despite similarities in their load vs. deformation curves, rectangle based tubes deform in a different pattern, compared to circular tubes. Reid et al. (1986) found the collapse mode of these structures to be through global bending. This unstable deformation manner can cause major reduction in the energy absorption capacity of rectangular tubes. Such an unstable collapse can be avoided by the use of a tapering technique, as suggested by El–Hage et al. (2005). This method will help the structure to initiate into a folding pattern which leads to a more manageable crush mechanism. Published literature on the characteristics of hat–section tubes, as energy absorbing structures, include White et al. (1999), Tarigopula et al. (2006), Fyllingen et al. (2009), and Peroni et al. (2009). The studies state that when subjected to axial loading, a thin–walled hat–section tube displays behaviour similar to that of a square tube. It can be understood that the energy absorption characteristics of a tube with a quadrilateral cross section is not greatly affected by the ratio of length to width

dimensions. Hence, structures with appropriate geometrical dimensions can be used based on the limitations of the area of application.

An innovative form of rectangular tubes is the thin–walled tapered structures, which have been developed in recent studies as energy absorbing structures. In fact, the collapse mechanism of these structures was briefly looked into as early as 1986 by Reid et al. It was based on this study that Nagel (2005) began a thorough investigation on the deformation behaviour of tapered rectangular tubes under various loading conditions. Their work was followed by researchers such as Mirfendereski et al. (2008) and Shariatpanahi et al. (2008). The latter researchers came to a conclusion that tapered rectangular tubes not only increase the energy absorption capacity through their deformation pattern, they also decrease the initial peak load due to their geometrical tapered shape. This in return reduces the damage caused by the impact load on the protected bodies (Shariatpanahi et al. 2008). In fact, Reid et al. (1986) proposed that to react efficiently against diagonal loadings, it is preferable to use tapered structures as energy absorbing components. Hence, conical shells can also be categorised under this group, due to their tapered geometry with a circular cross section.

Thin–walled conical shells and frusta have been utilised in various types of energy absorption applications such as marine and aviation structures, due to their predictable crush pattern and high energy absorption attributes (Gupta et al. 2006). Researchers have studied the crush and energy absorption response of these structures, as subjected to axial compressive loading, axial inversion, axial splitting, lateral bending, lateral indentation, lateral flattening and dynamic loading (Jones, 1989; Singace et al., 2001; Lu et al., 2003; Prasad et al., 2005; Gupta et al., 2007; Sheriff et al., 2008 and Ahmad, 2009). The chance of buckling or global bending in a conical shell is much less than in a circular tube, which makes this structure a better substitute (Gupta et al., 1999). In comparison, it also shows a more stable deformation pattern and high levels of specific energy absorption (Mamalis et al. 2005). In 2003 Deshpande et al. studied the characteristics of closed top conical frusta in an effort to find a deformation pattern for egg–box cellular structures. They found that the behaviour of these structures displays a pattern that can be expanded into more complex structures consisting of arrangements of conical frusta. As an

enhancement factor, Reid et al. (1986) stated that all shell and tube–like structures can be reinforced using the method known as foam filling.

Foam filling can significantly enhance the energy absorption characteristics of a structure at very low additional weights. Foams can be open or closed–cell based on the connections between their pores (Lu et al., 2003). Gibson (1997) and his research team declared that foam material can deform extensively under low levels of stress prior to reaching the densification strain point. Advantage is being taken of these structures in the automotive industry where high energy absorbers of low weight are considered ideal (Cheon et al., 2004). Gibson et al. (1997) proposed a mathematical relationship between the stress–strain plateau of the foam material and its relative density. The equation directly relates the stress over strain ratio of the foam to the square of its relative density, multiplied by a constant which, from test data, is determined to be approximately equal to 1. From this equation it is deduced that foams with higher relative density display higher strength, while their deformation length shortens. It is therefore necessary to design foam material per application (Gibson et al., 1997).

Deshpande et al. (2000) and Reyes et al. (2003) have studied the behaviour of foam structures fabricated from different materials. These can be categorised into two main groups of metallic or non–metallic (polymeric) foam material.

Metallic foams are a relatively new class of energy absorbing structures, with the ability to absorb substantial amounts of impact energy as a positive result of their light weight (Banhart, 2001). Currently, metals such as magnesium, iron, copper, zinc, titanium and aluminium are used in the production of metal foams (Ahmad, 2009). However, according to a research performed by Lu et al. in 2003, aluminium has received the greatest attention in this area and aluminium metal foams count as superior foam structures. Zarei et al. (2006) reported a 25% weight reduction in vehicles containing energy absorbing aluminium foam parts in their design. Aluminium is also used in foam filling of hollow structures. An alternative is the use of low–density polymeric (non–metallic) foams. This energy absorbing structure offers a number of advantages such as the capability of undergoing large deformations and absorbing high amounts of energy, without displaying any large permanent distortions (Triantafillou et al., 1989).

In 2010, Jeon et al. performed a number of finite element analyses on the plastic collapse of closed–cell aluminium foams with X–ray computed tomography, claiming that an increase in the 0.2% offset yield stress of the foam material will increase the magnitude of the plateau stress, while a decrease in the power–law hardening exponent not only increases the magnitude of the plateau stress but also modifies the shape of the plateau stage. It has also been stated that an increase in the 0.2% offset yield stress with a decrease in the power–law hardening exponent, causes an extreme increase in the magnitude of the plateau stress (Jeon et al, 2010). Despite the favourable magnification of the plateau stress, the research group ignore its simultaneous effect on raising the initial load peak. Such a high load peak would mean a greater amount of the shock load transferred to the supported body in the initial stage of an impact.

The attributes of polymeric foams are widely recognised, as the new provisions in the Federal Motor Vehicle Safety Standards make the use of polymeric foam materials inside motor vehicles a compulsion in order to protect the occupants during accidents (FMVSS, Standard No. 302). Other characteristics of this structure include its rate–independent behaviour during loadings as well as its consistent performance in different loading directions (Sherwood et al., 1992).

As mentioned before, reinforcing the thin–walled structures with foams can increase their energy absorption to considerably higher levels. Many researchers have studied the performance of different foam–filled tube–like structures such as the studies made on foam–filled square tubes by Aktay et al. (2006), Hanssen et al. (2000b), Santosa et al. (2000); Seitzberger et al. (2000) and Zarei et al. (2008), Zhang et al. (2009) with the general conclusion that longitudinal compression load and energy absorption value of foam-filled square tubes is higher than the sum of that of aluminium foam and empty tube due to friction and interactions between the tube and foam. In transverse direction, the compression load and energy absorption ability of foam-filled square tubes are significantly lower than those in longitudinal direction.

In addition, investigations made on the characteristics of foam–filled circular tubes by researchers such as Borvik et al. (2003), Kavi et al. (2006), Toksoy et al. (2005) and Yan et al. (2007), also concluding that the combination of tube and foam

has stronger energy absorption characteristics compared to empty circular tubes or foams alone.

Foam–filled hat sections have also been looked into by researchers such as Chen (2001) and Song et al. (2005). The works of Mirfendereski et al. (2008) and Reid et al. (1986) provide information on the behaviour of foam–filled tapered rectangular tubes under various loadings while the effects of foam–filling conical shells have been investigated by Gupta et al. (1999). Contradictory comments have been made on the weight saving benefits of the foam filling technique. Lampinen et al. (1982) commented that below a certain wall thickness in the tubes and shells, the filling tends to become heavier than the original structure; hence the weight–saving benefits would no longer exist. On the other hand, researchers such as Santosa et al. (2000), Banhart (2001) and Reyes et al. (2004) claimed that aluminium foam filled metal tubes are weight effective with the increase in energy absorption capacity. Studies find foam–filling to be superior to thick tube walls, referring to the deformation pattern of the structure which can be influenced by the changes of the geometrical factors (Asavavisithchai et al. 2004).

Cellular solids are structures consisting of an arrangement of thin–walled tubes or shells, attached to each other at sides or corners. Cellbond Composites Ltd., a specialist in the production of energy absorber structures, currently utilises materials such as aluminium, polycarbonate, ABS (Acrylonitrile Butadiene Styrene) and combinations of them, to create purpose–specific impact absorbing structures. The Company expertises in the production of cellular solid EA structures including Honeycomb absorbers and egg–box structures. The latter is patented by the Company under the name of PressLoad (Ashmead, 2000). The structural details and geometrical properties of this structure were introduced in a conference paper released by the Company (Ashmead et al., 2000); this information will be provided later in the text. A great deal of emphasis has been put on improving the performance of Honeycomb energy absorbers within Cellbond as well as their simulation and numerical analysis (Asadi and Shirvani, 2006). A number of Honeycomb based energy absorbers have been introduced by the Company, varying in their structural design and material types, which are used as side and frontal impact barriers in the automotive industry. The characteristics of Honeycomb barriers have been

investigated by Cellbond engineers both experimentally and numerically. Studies include the evaluation of the accuracy of a finite element model representing the IIHS side impact barriers (Asadi et al., 2007a), generating an advanced FE model for the AE–MDB side impact barriers (Asadi et al., 2007b), development of a numerical model for NHTSA impact barriers (Asadi et al., 2008b), modelling and analysing the ODB impact barriers in LS–DYNA® using solid elements (Asadi et al., 2008a) and comparing the latter model with a shell–based simulation of the same barrier (Asadi et al., 2009). These Honeycomb barriers are designed to present the bumper of specific vehicles according to the regulations associated with their application.

A recent study was made on the crashworthiness of a new type of honeycomb sandwich, known as kagome honeycomb, under axial crushing loads (Zhang et al., 2010). The intention was to expand the plastic deformation zones of this structure and improve its energy absorption efficiency. It has been found that the kagome sandwich column has higher mean crash force and better energy absorption characteristics than a foam–filled column with the same foam density. Another group of researchers performed compressive tests on foam–filled composite egg–box panels, through collaboration between Chung–Ang University of Korea and UK's Cambridge University. It was found that the foam–filled composite egg–box sandwich panels offer a satisfactory energy absorption capacity with a stable collapse response resembling an ideal energy absorber (Yoo et al, 2010).

Research has also looked into the behaviour of cellular structures such as honeycombs and egg–box energy absorbers. Deshpande et al. (2003) look at the static loading of these structures, claiming that their mathematical and analytical model for predicting the behaviour of closed–top cones (frusta) can be expanded to study the characteristics of egg–box structures. The outcome has been validated against finite element simulations and experimental tests. The second group of researchers investigate the dynamic crushing of aluminium egg–box structures. The effect of variances of material properties and physical boundaries on the deformation response of these structures has been studied. With the aid of FE simulations and experimental testing they observe that velocity dependence present in the level of structural strength of the egg–box structure is mainly due to the strain–rate sensitivity of the aluminium material from which it has been manufactured Zupan et al. (2003).

It is concluded in both studies that the energy absorption capacity of aluminium egg–box structures is comparable to that of metallic foams (Deshpande, 2003 and Zupan, 2003).

More recently, Nowpada et al. (2009) have studied various stages of the collapse and crashworthiness of aluminium egg-box structure under quasi-static compressive loading. A comparison with the deformation behaviour of concertina tubes reveals that the drop in strength displayed with these structures is diminished in the egg-box structures. Thus they conclude that egg-box energy absorbers can play a significant role in improving the crashworthiness of vehicles. In 2010 Nowpada et al. looked at the use of egg-box panel for pedestrian safety and found it to be an adequate cushion to be utilized in HGV truck front as an additional energy absorbing layer (Nowpada et al., 2010a). Later the research group extended their work to investigate the deformation pattern of the egg-box geometry under quasi-static loading using numerical methods. They employed the FE packages HYPERMESH® and LS-DYNA® as their numerical simulation tools and successfully validated the FE models against experimental results. Comparing the energy absorption capacity of a number of different boundary condition situations, Nowpada et al. (2010b) concluded that the natural occurring restraint within the egg-box panel due to its repetitive geometry amplifies its energy absorption characteristics.

Among other studies, an investigation was made on the deformation and energy absorption capacity of composite silicon rubber egg–box panels by Chung et al. (2007). Their conclusion stated that the compressive behaviour of this composite structure is affected by the local stacking sequence of the layers of silicon as well as shear deformation during initial lay–up and draping (Chung, 2007).

Further investigations on the characteristics of the egg–box structures as an innovative and ideal group of energy absorbers can increase knowledge towards their optimisation and development. Previous scientists, such as Deshpande et al. (2003) and Nowpada and Chirva et al. (2010) have instigated the performance of the egg-box under static and quasi-static loading while this project intends to expand this investigation into reviewing the dynamic response of these structures.

2.1.2. Deformation Modes

The specific energy absorption and other mechanical and material characteristics of a structure must be investigated in order to meet detailed design requirements. All researchers working on the different types of energy absorption methods and components study the behaviour of their system prior to putting it to practice.

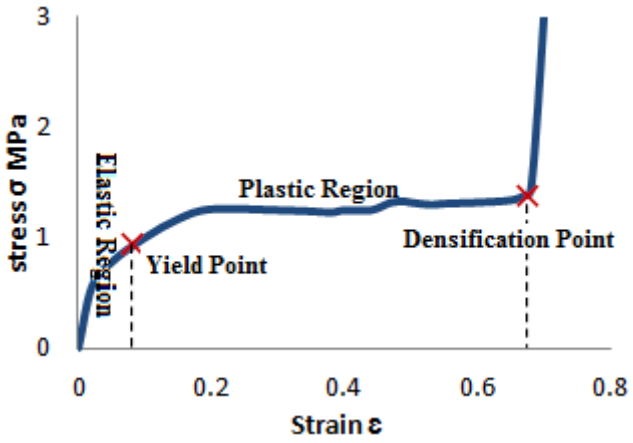

Figure 2.2 – Typical Stress vs. Strain Curve

The typical stress vs. strain curve of an energy absorbing structure, as shown in Fig. 2.2, consists of three sections; the deformation begins in the elastic region followed by a slightly increasing plateau beyond the yield point in the plastic region and a sudden increase in strength as the densification strain is reached (Deshpande et al., 2000 and Gibson et al., 1997). The collapse pattern of a structure plays a direct role in the amount of energy it absorbs. Reid (1993), Alghamdi (2001), and Ashby et al. (2000) define certain relationships between these two factors for different energy absorbers and loading types.

Many researchers have been studying the modes of deformation of energy absorbing structures such as thin–walled tubes, conical shells, metallic foams and cellular solids when subject to axial compressive loading (Mamalis et al., 1983 and 1986; Ashby et al., 2000; Bardi et al., 2003 and Deshpande et al., 2003). Through a

series of experimental, analytical and numerical analyses, these studies concluded that the energy absorption in thin–walled tubes and shells as well as both open–cell and closed–cell metal foams is mainly by the initiation of plastic hinges and the bending of cell edges. Other investigations agree that the collapse pattern of conical shells is the diamond mode with the exception of geometries that consist of apical angles of near 0° or 90° (Mamalis et al., 1984; Gupta et al., 1997; El–Sobky et al., 2001 and Prasad et al., 2005).

According to Deshpande (2003) cellular honeycomb structures deform through the formation of a series of folds occurring on each cell of a panel and hoop stretching of the cell walls among individual folds.

As one of the objectives of their study, this group of researchers demonstrates that, similar to that of conical frusta, the initiation of deformation in egg–box cellular structures is also due to the formation of travelling plastic hinges within every individual cell of this structure. The latter research group as well as Zupan et al. (2003) define three different collapse modes for the egg–box structure, based on its boundary conditions: 1) a simply constrained egg–box panel deforms through a travelling hinge mechanism, 2) an entirely unconstrained egg–box structure collapses through an inversion of the truncated cone followed by axisymmetric plastic buckling, and 3) an egg–box panel with bonded face sheets becomes deformed via an axisymmetric plastic buckling. Reference has been made to the works of these researchers in this thesis.

2.1.3. Experimental Testing

Repetitive compressive deformation tests and crash experiments are conventional methods of studying the behaviour of energy absorbing structures. Researchers such as Mamalis et al. (1986) based their investigations on experimental methods primarily, certifying their outcomes by comparison against approximate theoretical estimations. This method, as employed in this study, remains to be used as a tool for numerical and analytical data verification. Despite their accuracy benefits, such tests are not always desirable due to the expenses associated with their conductance and the complexities involved with repeating tests to exact measures.

Researchers have experimentally examined the collapse mechanism and energy absorption characteristics of tube–like structures. Abramowicz et al. (1989) successfully validated the theoretical results of their proposed analytical method for predicting the crush behaviour of multi–corner prismatic columns, against their experimental results. The energy absorption of aluminium rectangular and circular tubes under axial impacts have been experimentally investigated by Kim et al. (1999) to find that symmetric folds were formed in the circular tube specimens while asymmetric folds were formed mainly in the rectangular tube specimens. This results in a comparatively better energy absorption by the circular tubes.

During impact, the kinetic energy of the impactor is transferred into strain energy of the material; kinetic energy of the structure; and the energy created to form deformation (Finn et al., 1991). Studies show that a sharp impactor has a greater potential to induce impact damage than a blunter impactor does. A sharp impactor with smaller impact energy is able to generate the same damage as a blunt impactor of higher incident energy (Mosallam et al., 2008).

As relevant to the subject of this study, researchers such as Deshpande et al. (2003), Zupan et al. (2003), Akisanya et al. (2006), Chung et al. (2007) and, Nowpada et al. (2008, 2009, 2010) use quasi-static and dynamic experimental testing to investigate the deformation behaviour of the egg-box structure as an energy absorbing element. From these experimental works some researchers proceed to developing analytical and numerical models.

In practice, during an impact event, especially in road accidents, the load applied to the impacted body is not purely of axial or bending nature. In fact the collapse follows a complex manner under a combination of axial and off-axis or oblique loads. Such loadings cause energy absorbing structures installed in the vehicle body to deform through both axial and global bending collapse modes. The structure tends to deform through a global bending when subjected to an oblique load which reduces the energy absorption capacity of the structure. It is therefore important to study the behaviour of energy absorbing structures under oblique impacts in addition to axial loadings.

Some studies have investigated the oblique loading response of aluminium square and circular tubes both experimentally and numerically (Han and Park 1999; Reyes et al. 2002; Borvik et al. 2003; Reyes et al. 2003). These studies show that the initial peak load, the mean load and the energy absorption capacity drop drastically with increasing load angle away from the vertical. Reyes et al. (2004) and Borvik et al. (2003) examined the crush response of foam-filled square and circular tubes respectively, under axial and oblique quasi static loading with a load orientation range of 0-30° with the vertical. Numerical results showed that a global collapse mode tends to fully initiate when introducing a load angle of 15°, resulting in a reduction of the energy absorption capacity and the experimental results supported the outcome.

Karbhari et al. (2003) conducted experimental work to investigate the energy absorption characteristics of conical composite tubes under axial and off-axis loadings over a load angle range of 5°-35°. This study also showed that the angle of load orientation can significantly influence the energy absorption performance of conical tubes, in terms of the reduction in the energy absorption capacity. Ahmad (2009) also looked at the impact and energy absorption of empty and foam-filled conical tubes to facilitate their application in energy absorbing systems under axial and oblique loading conditions by designing quasi-static and dynamic experimental tests.

However, research information on the crush and energy absorption response of egg-box structures under axial or oblique impact loading is limited. As a validation method for the FE models simulated in this study, dynamic tests are conducted on egg-box structures. The experiments include impacting an entire panel axially as well as observing the behaviour of a single cone when impacted axially and at 45° angle both within an egg-box panel and as a free-edge part.

2.1.4. Analytical Modelling

For decades, the development of mathematical models has been a common means of exploring the energy absorption characteristics of a variety of energy absorbers under different loading conditions. Such theoretical methods are based on

simplified models of the problem alongside a number of assumptions. This can be a very approximate measure, since, due to its simplicity, it ignores many geometrical and physical factors that could potentially affect the outcome. However, along with an experimental or numerical model, analytical modelling can be a valuable source of result validation.

Prior to the introduction of commercial finite element codes, empirical modelling was widely used to study the energy absorption response. An analytical method was originally formulated by Alexander (1960) as a solution to analysing the axisymmetric crush of thin-walled cylindrical shells under static axial loads. Alexander uses simplified kinematic mechanisms by assuming a kinematically admissible deformation field on the basis of experimental observations or theoretical assumptions.

Many researchers work on developing more accurate theoretical models for solving the behaviour of complex deformation patterns and structures. Alexander (1960), Abramowicz et al. (1986), Grzebeita (1990), Gupta et al. (1997) and Deshpande et al. (2003) have made attempts on proposing and developing new and existing analytical models for measuring the collapse mechanism of energy absorbing structures. The derivation of such theoretical models involves comprehensive mathematical approaches. These models are generally based on the results of experimental tests. Theoretical approaches can be counted as suitable tools for initial measurements of the behaviour of a structure especially in less complex systems.

The less complicated theoretical model can be used in predicting the collapse response of structures. Sheh et al. (1992) developed a simple theoretical model, to provide approximations on a frontal vehicle crash. To increase the calculation speed and accuracy of the theoretical models of the complex system, methods such as finite element analysis were utilised.

2.1.5. Numerical Simulation and Analysis

The introduction of Finite Element (FE) packages to the world of structural and mechanical calculations has been an invaluable tool in studying the characteristics of energy absorbers. In general, these structures tend to display complex deformation behaviours which, in practice, cannot be accurately modelled using the traditional analytical methods. With the use of the correct FE software, designers can simulate accurate models representing the static or dynamic crushing of certain energy absorbers under different loads (Farley, 1986). This technique becomes extremely valuable in the initial design of energy absorbing structures such as vehicles body parts. Finite element analysis can be accurate, time–saving and inexpensively repeatable.

Many structures of various geometries and materials have been modelled by researchers as parts of their investigation on the energy absorption characteristic of the structures. The outcomes of the models can help validate the analytical or experimental results.

Researchers use different packages for the purpose of the structural analysis of the deformation of energy absorbers. Abramowicz (2003) used CRASH CAD® to study the bending and axial collapse of thin–walled energy absorbing tubes in vehicles. Through definition of the desired cross–section for the tube, their detailed analysis of the dynamic crash behaviour of the vehicle produced satisfactory outcomes which were in agreement with the experimental results. In their study of 1999, Langseth et al. modelled the axial impact of square aluminium tubes using the explicit finite element code LS–DYNA®. They studied the effect of impact mass and velocity on the deformation mechanism of the tube. In line with the time–saving benefits of using FE packages, Langseth et al. (1999) took advantage of the symmetrical geometry of a square tube and by applying the appropriate boundary conditions, modelled one quarter of the entire aluminium tube, thus reducing the time of analysis. The results obtained in their experimental programme were agreeably comparable to the predictions of their dynamic simulations. Their FE simulation gave good evaluation of the final profile shape in addition to a force-displacement curve with a ratio of 0.87–1.0 between FE and experiment.

The selection of the FE package is based on the material and geometrical attributes of the structure as well as the details required from the output data. Researchers such as Karagiozova et al., (2000 and 2004) used the explicit code of ABAQUS® for their simulation purposes. More simplified models can be solved using the implicit package such as ABAQUS/Standard V.5.8 used by Karagiozova et al. (2001).

Depending on the complexity of a structure and the conditions for which it is being tested, an FE replica can be produced by 2D axisymmetric modelling or 3D generation, representing the structure's geometrical and material attributes. Aljawi (2000) employed the 2D axisymmetric modelling technique to simulate the inversion of plastic tubes using ABAQUS® 5.7-3. Good agreement was obtained between the experimental results and their FE predictions. This 2D method can help save computation time by reducing the number of components.

Other studies on this subject area include the research of Santosa et al. (1998, 2000) on foam material and foam filling of EA structures. Chen et al. (2001) and Reyes et al. (2004) also studied the bending collapse and torsion deformation of these structures. Mamalis et al. (2001) carried out an FE simulation of the axial compression of metallic thin–walled square frusta. The FE code LS–DYNA® has largely been used by designers and engineers. Many researchers in the energy absorption area have used LS–DYNA® to simulate models and verify results against experimental and theoretical approaches. The investigation on the vehicular impact on a portable concrete barrier done by Ulker et al. in 2008 is one such example where LS–DYNA® pre and post–processor are used to model in details an available crash test in order to develop a set of charts for assessing the barrier displacement and related variables prior to entering the design phase (Ulker et al, 2008).

Researches performed on the characteristics of energy absorber structures using ANSYS® include Olabi et al.'s 2008 work on optimising the design of nested oblong tube energy absorbers. The implicit version of ANSYS® was used to simulate the quasi–static lateral compression of nested systems (Olabi et al., 2008). Morris et al. also used the implicit ANSYS® in 2006 in the analysis of nested tube type energy absorbers with different indenters and exterior constraints. In a more recent study at Dalian University of Technology in China, ANSYS® was used to investigate the

crashworthiness of kagome honeycomb sandwich cylindrical energy absorber columns under axial crushing loads (Zhang et al, 2010).

A group of researchers used the nonlinear ANSYS/LS–DYNA® code to analyse and simulate the inversion processes of a specific type of tube under axial compression (Zhang 2009). Another group used ANSYS/LS–DYNA® to investigate the relations between configuration parameters of double–walled hexagonal honeycomb cores and their out–of–plane dynamic plateau stresses at various impact velocities (Deqiang, 2010), all achieving satisfactory predictions of the experiments.

Within the Cellbond Composites Company, preliminary work has already been carried out looking at the finite element modelling of some egg–box geometries. Depending on the area of application, based on the maximum temperature, the level and angle of impact, and the boundary conditions that the structure will be subjected to, egg-boxes can be produced from metallic or non-metallic (polymeric) material (Ashmead et al, 2000).

Furthermore, Zupan et al. (2003) proposed a 3D finite element shell model of the egg-box since, despite the correct collapse modes, the calculations that had been made using their original axisymmetric finite element model gave less accurate predictions of the structure's deformation response. In this study, 3D FE models were developed and validated against the results of experiments in order to further analyse the geometrical features of egg-box structures and their effect on the deformation pattern of the absorber. Although their predictions were improved with the 3D simulation, the material model they defined to model the aluminium alloy, lacked adequacy in taking into account the rate sensitivity and failure of the material. This issue is addressed in the study in hand.

2.2. Optimised Energy Absorption

Modifications made to the vehicle safety standards and requirements call for constant improvements in the crashworthiness and performance of energy absorbing structures. In their research on the design optimisation of vehicle components, Avalle

et al. (2002) stated that vehicle parts should be redesigned regularly, in order to enhance the global performance of all means of transportation.

In order to find the optimal structures, many individuals and industries have endeavoured to improve the quality of their designs and processes. With the availability of advanced and powerful computing methods, a greater number of options can be examined and the objectives can be rapidly achieved (Choi, 2002).

Prior to designing an optimal energy absorber, it is necessary to study its deformational behaviour. As described by Harte et al. (2000) the force–displacement curve of an ideal energy absorber displays a long flat plateau at its plastic region. Tubes, shells and cellular solids satisfy this deformation pattern to different extents.

Mamalis et al. (2003) described three individual stages for the deformation pattern of an optimised energy absorbing structure:

- Stage 1: Initially the specimen behaves elastically and the load rises to a peak value followed by a sudden fall.

- Stage 2: The load increases with increasing deflection associated with the formation of lamina bundles bending inwards and outwards. The wedge formation is complete when the load starts oscillating.

- Stage 3: Stable crush with the formation of inward and outward fronds which spread radially in the form of a mushrooming failure. The external fronds develop axial splits due to the developed tension. Axial fibres bend inwards or outwards without fracturing, whilst fibres aligned in the hoop direction can only expand outwards by fracturing and inwards by fracturing or buckling.

These three stages can be individualised per structure type and function.

A research group from the University of Guilan explored the energy absorption of square aluminium tubes using multi–objective genetic algorithms for Pareto–approach optimisation of the energy absorption of square aluminium columns both with and without aluminium foam filler. Their findings suggested that non–filled columns were preferred over foam–filled ones for desired energy absorption levels of

no more than 4.8 kJ, however, where higher levels of energy absorption is of interest, foam-filled columns will perform more favourably (Nariman–zadeh et al. 2006).

Gupta et al. (2006) also looked at the deformation pattern and energy absorption attributes of circular tubes under quasi static and dynamic impact loading, both numerically and experimentally. They varied geometrical parameters such as the wall thickness and diameter to find that the energy absorption capacity of circular tubes in dynamic tests is around 1.56 – 12.3% higher than in quasi–static tests, while the initial peak load amplifies by about 14.33 – 40.25%. In addition, they came to the significant conclusion that both the crush load and energy absorption capacity increase with greater thickness and diameter values.

According to Nagel et al. (2006), a tapered rectangular tube can perform as an ideal EA structure in dynamic applications where combinations of both axial and oblique loads are present. The study concludes that, below a defined limit of critical load angle, the energy absorption capacity of a tapered rectangular tube decreases with the increase in the load angle. This claim was verified by Liu (2008) in a later research.

In 2007, Hou et al. investigated on the single and multi-objective optimisation of energy absorbers in general and thin-walled rectangular tubes specifically. The research group looked into optimising the cross-sectional dimensions of multi-cell tubes to enhance their energy absorption characteristics. Their study indicated that improvements implied to each objective will only enhance the overall behaviour of the system to a certain extent, while it simultaneously affects the other objectives negatively. In their research an optimisation algorithm was defined to seek optimal parameters for both criteria of maximising the energy absorption and reducing the peak crushing force. The group concluded that the former objective is achieved with more cross-sectional cells while the crush force does not follow a pattern in the cases of optimising either objective (Hou et al., 2007).

In the deformational performance of conical shells and frusta, geometrical features, such as wall thickness, diameter, angle, height, etc., and material properties, such as young’s modulus, yield point, densification strain, Poisson’s ratio, etc., can play a significant role. The relationship between geometrical and material features

and the critical buckling load of conical shells is expressed by Spagnoli et al. (1999) in the form of an equation, making evident the effect of these features on the behaviour of the structure. A set of experimental and numerical tests, performed by various researchers, helped describe the characteristics of an ideal conical shell (Gupta et al., 2006, 2007, 2008; Mamalis et al., 2005 and Sheriff et al., 2008). Gupta (2007) explained that the rate at which a load is applied also affects the energy absorption capacity of the structure. In dynamic loading, the increase is at approximately 8.93 – 49.6% while in quasi–static load cases, it is for angles varying between 6.84° and 65.35° and at mean diameter to thickness (D/t) ratios of between 22.32 and 79.29 that the load increases.

A comprehensive parametric study will reveal the effect of various geometrical and material parameters on the deformation mode, mean load and absorbed energy of the conical shell energy absorbing structures. The current study evaluates the effects of changing various geometrical parameters on the deformation pattern of egg–box energy absorbing structures under dynamic impact loads.

2.3. Optimisation of Egg–box Structures

Despite the significance of egg–box cellular solids as enhanced energy absorbing structures, not a great deal of research has been dedicated to investigating their performance and development.

In a 2010 study, Yoo et al. performed a series of compressive tests, at different loading and material conditions, on foam–filled composite egg–box panels. They came to the conclusion that foam–filled composite egg–box sandwich panels offer a good energy absorption capacity with a stable collapse pattern resembling the ideal energy absorber.

Works of researchers such as Nowpada et al. (2009, 2010a,b), Yoo et al. (2010), Chung et al. (2007), Akisania et al. (2006), Deshpande et al. (2003), Zupan et al. (2003) and Ashmead et al. (2000), focus on the effects of factors such as material alterations, loading conditions and some geometrical modifications, on the deformational pattern and energy absorption characteristic of the egg–box structure.

However, no comprehensive sets of data are available on the effects of geometrical alterations on the performance of egg–box energy absorbers.

According to Akisania et al. (2006), an egg–box is effectively a square array of conical frusta. Based on Gupta's (2007) comments, in conical frusta, modifications of geometrical factors directly affect the behaviour of the structure; hence, it can be concluded that an egg–box structure can be geometrically designed to perform in an optimum manner. Based on this conclusion, this project attempts to geometrically optimise the structure of the egg-box.

3. EXPERIMENTAL STUDIES

3.1. Introduction

For the purpose of validating the computer aided simulations proposed in this study as the optimisation tool for enhancing the energy absorption capacity of the egg-box structure, a series of experiments have been designed and conducted herein. The tests include axial and oblique impacts of free-edged single cells separated from egg-box panels, axial and oblique impacts of single cells situated within panels and axial impacts of entire egg-box panels. This chapter includes details on the specimens used, their material properties, preparation procedure, the test equipment as well as the techniques employed and the results of the experiments.

3.2. Material Details and Sample Preparation

In this study two geometrically different egg-box samples are impacted. The samples were fabricated from aluminium sheet metals. Commercially Pure (CP) annealed 1050 H111 aluminium sheets, consisting of 99% aluminium, with thicknesses of 0.8mm and 1.0mm were used in the production of specimens.

The 1XXX series aluminium alloys consist of 99.0% or higher levels of pure aluminium. The letter H applies to alloys which have their strength increased by strain-hardening, with or without supplementary thermal treatments, to produce partial softening. The H is always followed by two or more digits. The first digit indicates the specific combination of basic operations. H1 applies to aluminium alloys which are strain-hardened to obtain the desired mechanical properties without supplementary thermal treatment. The number following the designation indicates

the degree of strain-hardening with 0 being the softest and 9 designating an extra hard alloy. So the hardness of this alloy is of the first degree, i.e. it is a soft alloy. The third digit indicates that the degree of control of temper or the mechanical properties are different from, but within the range of, those for the two-digit H temper designation to which it is added. H111 applies to alloys which are strain-hardened less than the amount required for a controlled H11 temper (USA Dep of Defence, 1966).

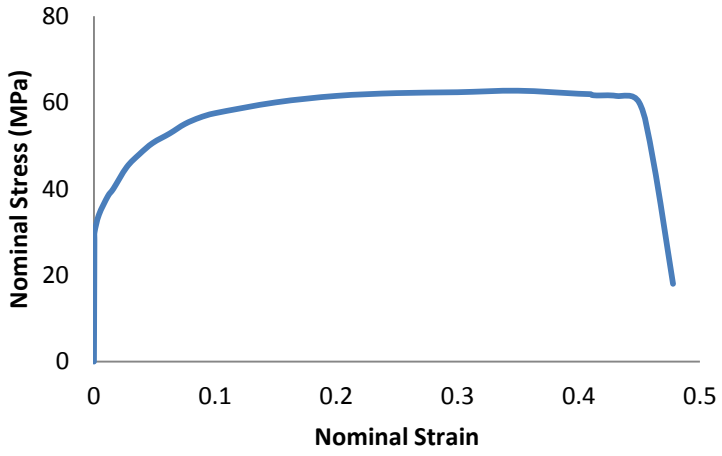

(a)

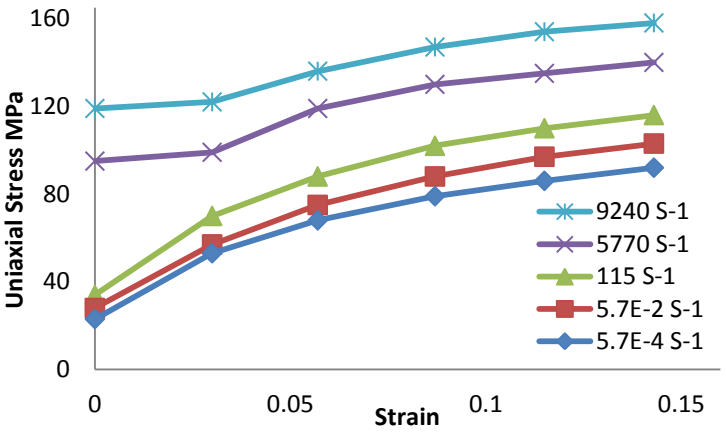

(b)

Figure 3.1 – Stress vs. Strain Curves of CP Aluminium Sheets (Zupan, 2003)

(a) Measured Tensile Behaviour of Al 1050 H111 Sheets

(b) Dynamic Stress vs. Strain of CP Al at Selected Strain Rates

Al1050 is a grade of aluminium used for general sheet metal work where moderate strength is required. The material properties of the alloy are provided in Figure 3.1(a). Figure 3.1(b) also shows the stress-strain curves of this material for a range of strain rates.

The sheets were cold–pressed between lubricated closed dies into egg–box shaped sheets, then cut to panels with overall cross dimensions of 300 × 300 mm^2, at Cellbond Composites Ltd. The dimensions and geometrical details of the two sample sets are presented in Table 3.1 in accordance to the factors shown in Fig. 3.2. Factors (*R*) and (*r*) are approximate measures. From a comparison between the dimensions of the samples it is evident that they were selected to vary in size in order to consider structures of different relative densities and strengths.

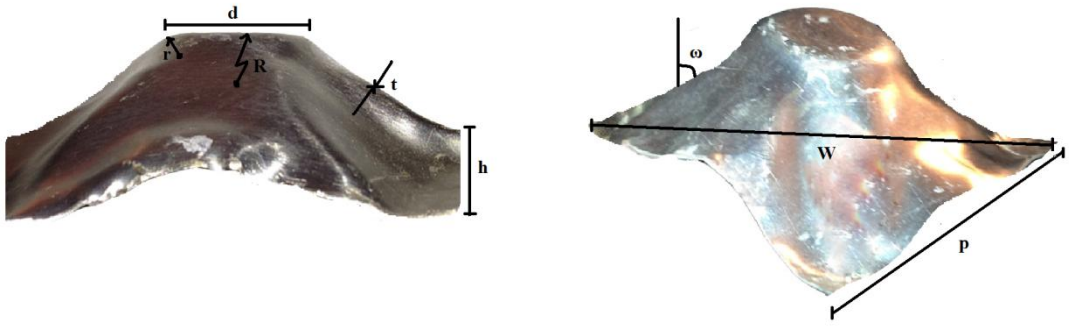

Figure 3.2 – Geometrical Dimensions of Egg-box Cells

Geometrical Factors	*W* (mm)	*d* (mm)	*p* (mm)	*h* (mm)	*t* (mm)	*R* (mm)	*r* (mm)	*ω* (deg)
Sample 1	75	24	103	12	0.8	50	2	48
Sample 2	36	10	52	6	1.0	50	2	53

Table 3.1 – Egg–box Cell Dimensions

3.3. Impacting System and Data Recording Devices

The egg-box panel specimens are impacted by drop masses of 5500g and 225g, for the entire panel and the single cells respectively, as shown in Fig. 3.3. The weights are directed to free fall at a contact speed of $6ms^{-1}$. The loading mass and velocity of the impactor can be increased or decreased as appropriate. Zupan et al. (2003) suggest impacting egg–box panels of below $1m^2$ cross sectional area with an impactor mass of 5.5kg moving at a velocity of 6m/s.

A cubic mass of 225g with cross-sectional dimensions of 72mm × 72mm which is approximately 70% of the plan view area of a cell is used for impacting free-edge single cells. Cylindrical weights are made per sample with dimensions relative to the peak diameter of the sample. These impactors are used for impacting single cones within a panel. A flat impactor is used for drop tests on the entire egg-box panels with a surface area of approximately 70% of that of the panel. The edges of the impactors are given a 1mm, 45° chamfer to reduce the damage from a sharp corner as described in Mosallam et al. (2008).

Figure 3.3 – Dimensions of Impactors Used in Dynamic Tests

A drop tower (Fig. 3.4), designed and built within the laboratory for experimental work of similar nature, is used to conduct the dynamic tests. To impact the cells obliquely, the base of the drop tower is tilted by 45° and placed on rigid metal wedges for stability as shown in Figure 3.5.

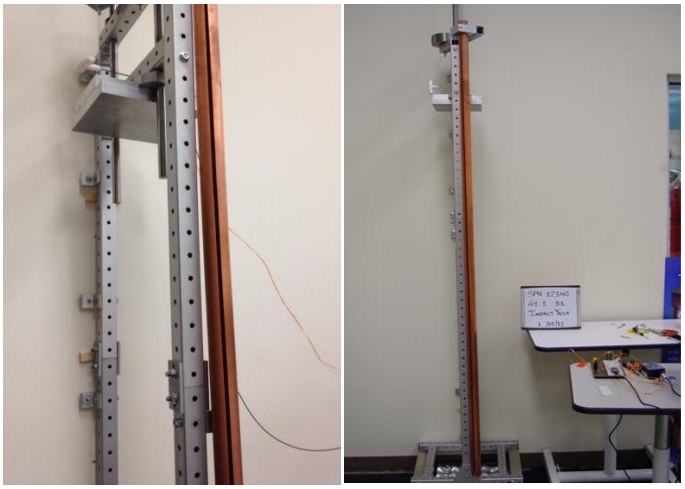

Figure 3.4 – Drop Tower and Boundary Fixtures

In the flat tests involving single free-edge cones cut from the panel the body will be resting freely on the solid and rigid surface below with no constraints. For the oblique tests of the same specimen, the structure is freely placed at the bottom of the tilted support where it is resting on the end bracket to prevent it from sliding.

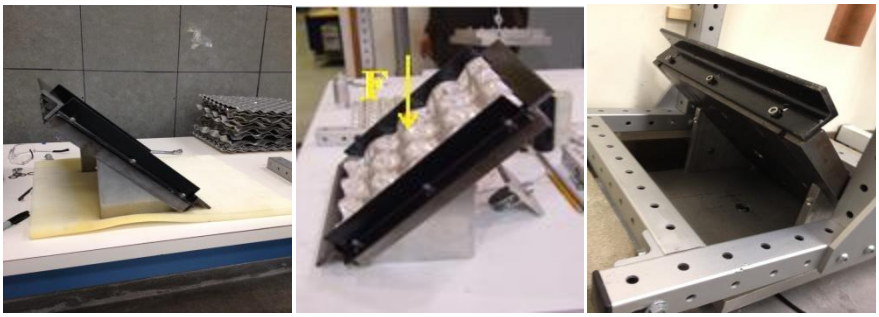

Figure 3.5 – 45° Wedges Placed Below Impact Surface for Oblique Loading

Where the entire panel is taking part in the test, the samples are required to be simply supported by the base of the tower and boxed in from four sides to prevent any lateral movements.

Initially a simple hollow box, as shown in Fig. 3.6, was proposed to stop the panels from being laterally displaced. However, since the egg-box samples obtained were not cut in an entirely square cross section, it would not have been possible to box all samples at all four edges.

As a resolution to the boundary condition issue, an alternative adjustable boxing technique was proposed and designed which covers all irregularities of panel edges and allows for full restraining of the samples against all lateral shifts. It can be seen in Fig. 3.7 that brackets with L-shaped cross sections are placed on four sides of the rigid support surface. Each bracket has three oval shaped bolt holes. The screws are loosened to allow for moving and tilting of the brackets. Once the sample panel is fully restrained with the brackets, the screws are tightened and all lateral movements are prevented.

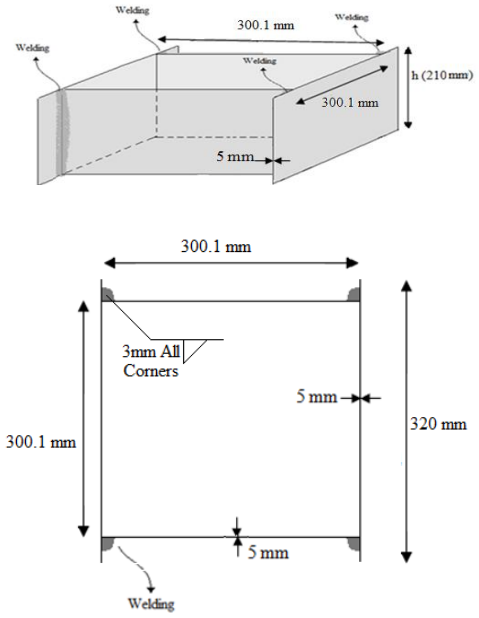

Figure 3.6 – Initial Design of Device for Boxing Egg-box Cell

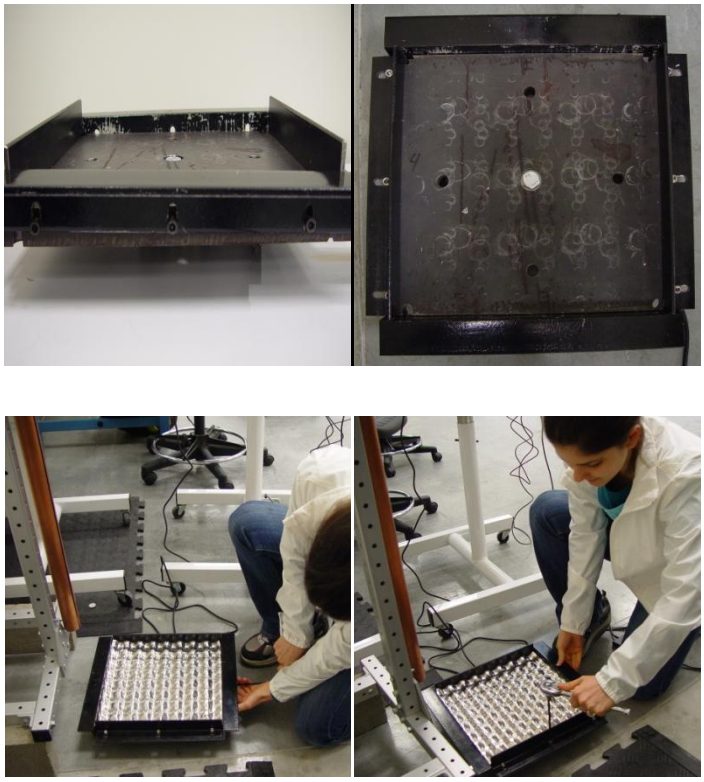

Figure 3.7 – Boxing Technique

The applied force is measured using a Loadstar® universal low profile pancake load cell with ±0.05% accuracy class and the data is recorded through a 1000kg capacity Loadstar® digital interface with 5000Hz data update rate.

To measure the acceleration over time from which the relative displacement is derived, an accelerometer is needed to be installed on the system. A simple calculation can be made in order to select the appropriate accelerometer. Assuming an approximate total time of t=0.003s for a typical impact at a contact speed of v=6m/s, acceleration (a) could be measured as:

$$a = \frac{v}{t} = \frac{6}{0.003} = 2000 \ {}^{m}/_{s^2}$$

then to find the required G-levels for an accelerometer:

$$\frac{a}{g} = \frac{2000}{9.81} = 204G > 200G.$$

Therefore, the accelerometer to be used must be sensitive for G-levels of more than 200G. A high frequency industrial accelerometer with ±500G is placed on the impactor for this purpose. The high frequency output rate will allow for enough data to be recorded in a small fraction of time. With the short duration associated with an impact, the high frequency sensor would be able to trace adequate data per microsecond.

The outputs of the sensors are transferred to a computer equipped with appropriate software which can save the data for future calculations and graphing.

3.4. Dynamic Impact Experiments on Egg-box Specimens

Three sets of tests are performed per sample type including flat impact of the entire panel, flat impact of a single cell within the panel and oblique impact of a single cell within a panel. For sample type 1 two extra set of tests are conducted including flat impact of a free edge single cell and oblique impact of a free edge single cell. Due to the small geometrical features of sample type 2 and the velocity of the impact, the latter test has been omitted for this sample type. The samples are simply supported in all cases, with no lateral movements in the first three test types.

To reduce experimental errors and ensure data accuracy, each experiment is repeated for 5 specimens from each sample, giving a total of 40 tests.

In the flat impact experiment, the 5500g drop mass is designed and directed to freely fall on the egg-box panels. The samples are aligned within the drop tower and the load is released. The measured data are accumulated and saved through the system. The results of 5 flat impact tests on sample type 1 and 5 flat tests on sample type 2 are provided in the upcoming section and discussed later in the text.

A tube-like structure is used to guide the cylindrical drop weights towards single cells within the egg-box panels. The drop masses although different in diameter, weigh the same 225grams. The guiding tube is designed to have a groove along its length to reduce the effect of air pressure below the falling weight as well as avoiding turbulence.

The drop masses are centred with the cell as well as the load cell prior to the impact taking place. Out of axis loads applied on the load cell can reduce its accuracy and functionality. For both flat and oblique tests of single cones data are recorded to be further analysed.

3.5. Results of Flat and Oblique Impact Experiments

Provided in this section are the results of the experimental work explained above. The outcomes are briefly discussed in this chapter. The main objective is to use this information towards the validation study of the finite element models presented in the following chapters. Upon achieving reasonable precision, it can be shown that the response of test specimens could be predicted using numerical models with sufficient accuracy.

Free-edged single cells of sample 1 are initially impacted with a 225g mass at a contact velocity of 6m/s both vertically and diagonally at 45° (load direction shown in Fig. 3.5). As explained previously, for the oblique loading, the rigid support surface is tilted and the cell is aligned with the bottom bracket to avoid sliding. The results of these tests are provided in Figure 3.8 and 3.9 for the 5 specimens.

In quasi-static deformation of free-edged single egg-box cones, as reported by Nowpada et al. (2010), the deformation procedure initiates with the flattening of the peak curvature. However, in the dynamic impact, due to the speed of the loading, following the initial contact, the material begins to stretch. The signs of low strength displayed by the structure at this stage are due to the friction present between the cell and the supporting surface. With no constraints present at the edges, the trench corners at the edge of the cell begin to curl upwards, slightly increasing the strength level in return. The force level is continuously elevated as the deformation

progresses. In a respective order the deformation continues by plastic hinges forming at the peak to trench transition lines, peak curvature flattens and then goes through inversion, the top cone of the cell is plastically deformed and eventually, the force level rises at a steep slope as full compaction occurs.

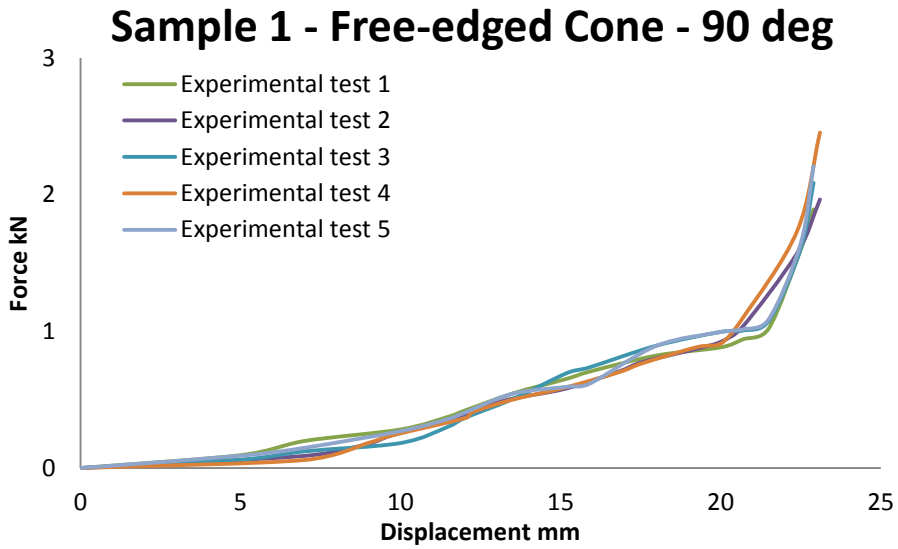

Figure 3.8 – Result Curves for Impacting Free-edge Single Cell at 90°

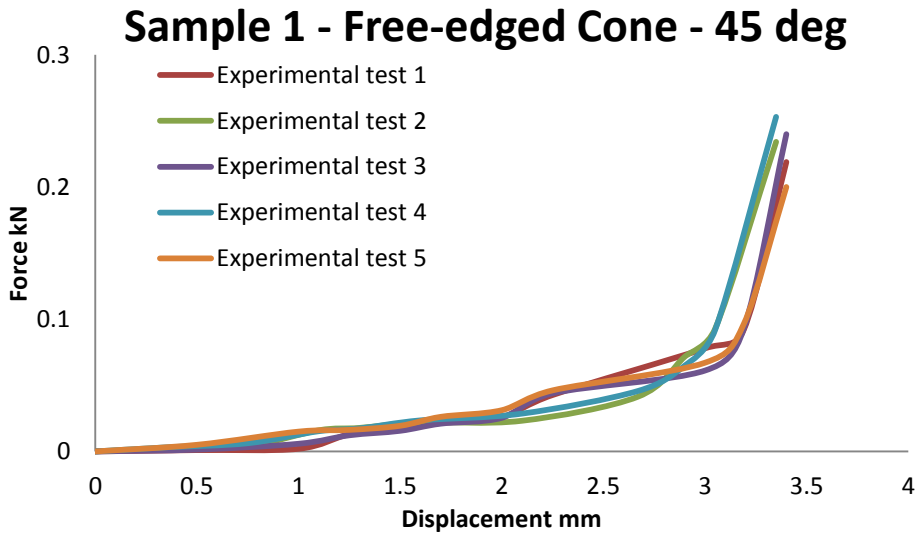

Figure 3.9 – Result Curves for Impacting Free-edge Single Cell at 45°

When a similar free-edged single cone specimen is subjected to an oblique load, the side of the cell which is initially touched by the edge of the impactor starts bending at the contact line. The thin shell structure shows very little resistance to this preliminary load. Due to the presence of the support surface extension acting as a stop at the bottom of the cell, as the deformation progresses, this end begins to curl upwards, causing a slight rise in the force-displacement curve. The impacting surface eventually reaches the peak cone and the entire structure begins to fold, hence the force level begins to increase further. Finally the impactor hits the tilted support surface resulting in a steep rise in the curve. This is shown in Fig. 3.9 for loading at an angle of 45°. As a consequence of the freedom present at the cell edges in the first two test types, the force-displacement curves enter the plastic region at very early stages of deformation.

Illustrated in figures 3.10 – 3.13 are the resultant curves of the impacts on single cones within the egg-box panel structure at 90° and 45°. A brief review of the force-displacement curves resulted from these tests reveals the effect of the continuity of the egg-box panel. With the adjacent cells partially restricting the lateral stretch of the impacted cell, the strength level of the cell rises to almost 1.6 times the free-edged specimen as shown in Table 3.2. Additionally, the entire deformation behaviour of the cone would be different.

Once the cell is impacted by the cylindrical weight, an inversion process of the peak cone begins with travelling hinges forming at the peak circle circumference. The translation of this occurrence in the curve is the initial steep rise. Simultaneously, the neighbouring trench cones show minor signs of deformation in the base curvature region. The procedure will continue until the travelling hinges are no longer present and the inversion of the cone will cease.

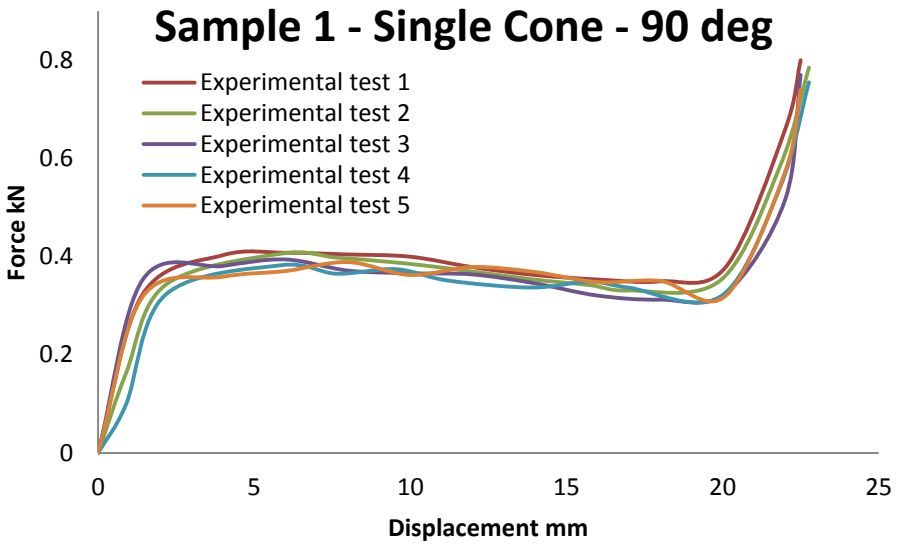

Figure 3.10 – Result Curves for Impacting Single Cone of Sample 1 at 90°

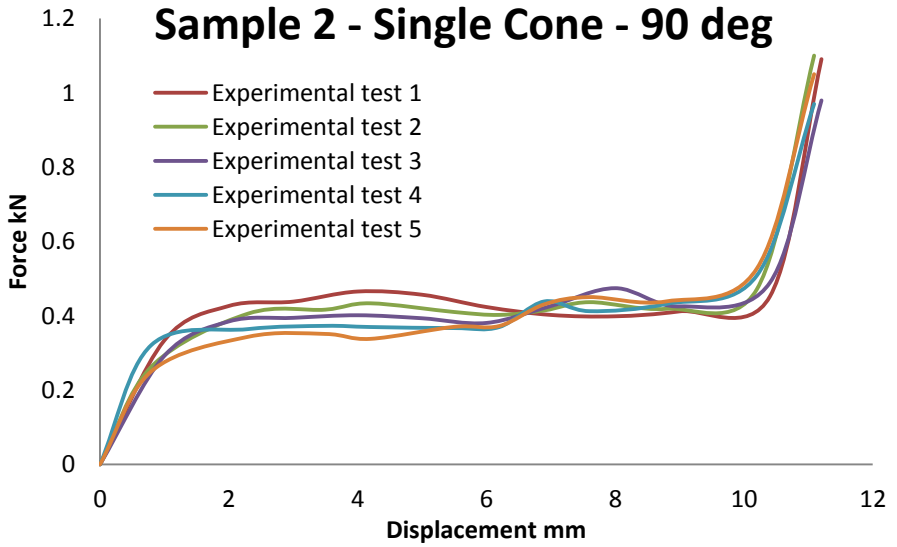

Figure 3.11 – Result Curves for Impacting Single Cone of Sample 2 at 90°

In the oblique impact of a single cone situated within an entire egg-box panel, the cylindrical mass, centred with the peak diameter, initially comes into contact with a corner of the peak curvature. Meanwhile, the cone is bent over a diameter of the peak circle inline with the impactor edge. The four neighbouring cones in this situation will be acting contradictorily; the two cells positioned above the impacted

cell, in terms of the impact location, will be stretched in tension while the lower two cells will be slightly compressed as part of the impacted cone tilts in their direction.

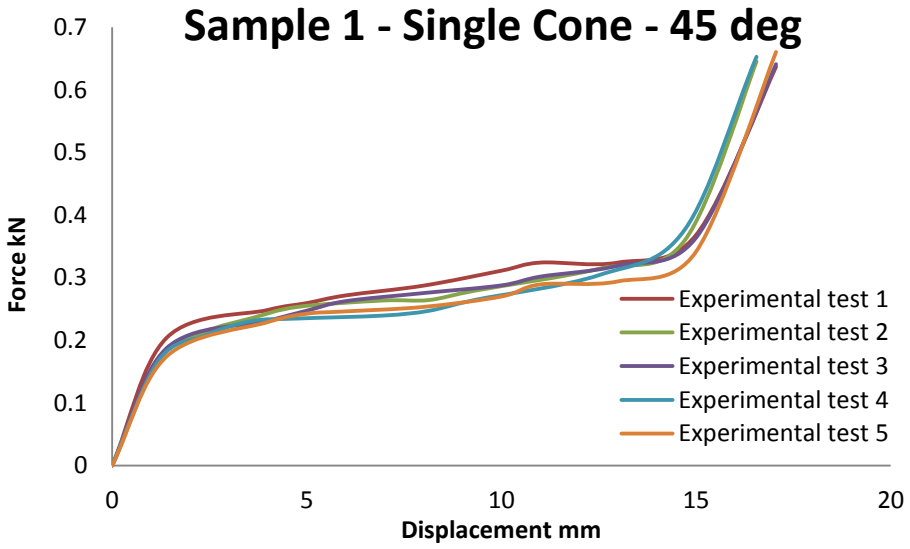

Figure 3.12 – Result Curves for Impacting Single Cone of Sample 1 at 45°

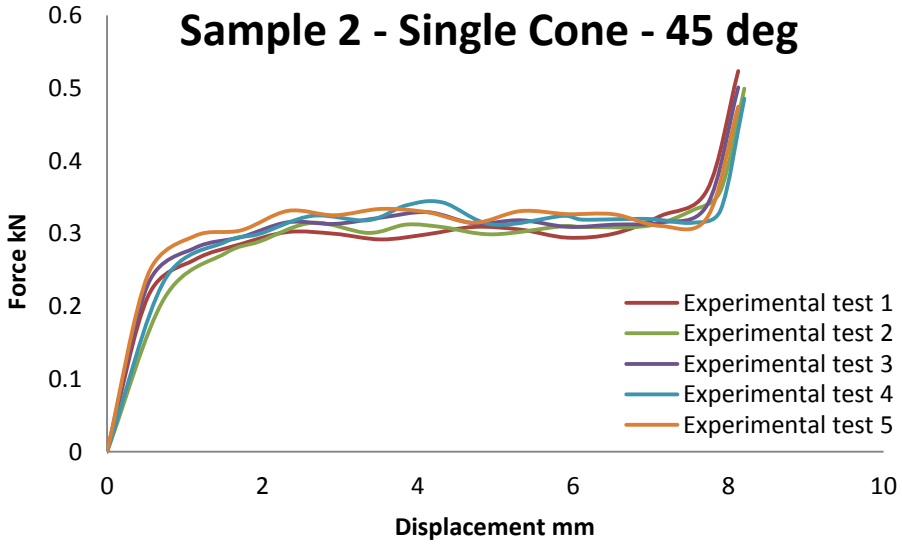

Figure 3.13 – Result Curves for Impacting Single Cone of Sample 2 at 45°

From a comparison between curves of Figures 3.10 and 3.11 with Figures 3.12 and 3.13, respectively, it can be seen in Table 3.2 that a single cone loaded obliquely has an average load which is approximately half of that of the same cone loaded vertically. This proves the fact that with more acute angles between the impact direction and the horizon, the strength of the egg-box energy absorbing structure decreases.

On another note, despite different geometrical measurements, both samples are showing similar average force levels. This is due to the larger concentration of cells in sample type 2 in comparison to sample type 1. As mentioned in the Introduction chapter, shorter inter-peak lengths mean higher cell density within constant panel cross-sectional dimensions.

Figures 3.14 and 3.15 show the results for the 90° impact test for sample type 1 and 2, respectively. It can be seen that both cases follow the same pattern. The crush response curve shows a primary rise in load in the elastic region with the initiation of deformation corresponding to the bending/flattening of the peak curvature about its circumference. This is followed by a kink and change in the slope of the curve as it enters the plastic region with the appearance of travelling plastic hinges at the top and bottom, and eventually at the mid-point of the cell walls.

The presence of neighbouring cells and the assumption of the panel being continuous, minimises the effect of material stretching in the deformation process due to flat impact. The crush load remains moderately constant with the progression of deformation up to the point where the peak and base of the cells reach the same point. The steep rise in the curve emerging past the point of densification illustrates the bottoming phase where no more plastic hinges will appear. It can be seen that the densification is occurring at around 75% of the entire height of the panel.

As expected, comparison between the graphs of single cone and entire panel for each sample shows that the average load level of a single cone is less than 10% (Table 3.2) of that of the entire panel in cases with restricted boundaries.

Fig. 3.16 shows the samples as impacted with regard to each test type. The disfiguration patterns can be linked to the deformation procedures described earlier in this section.

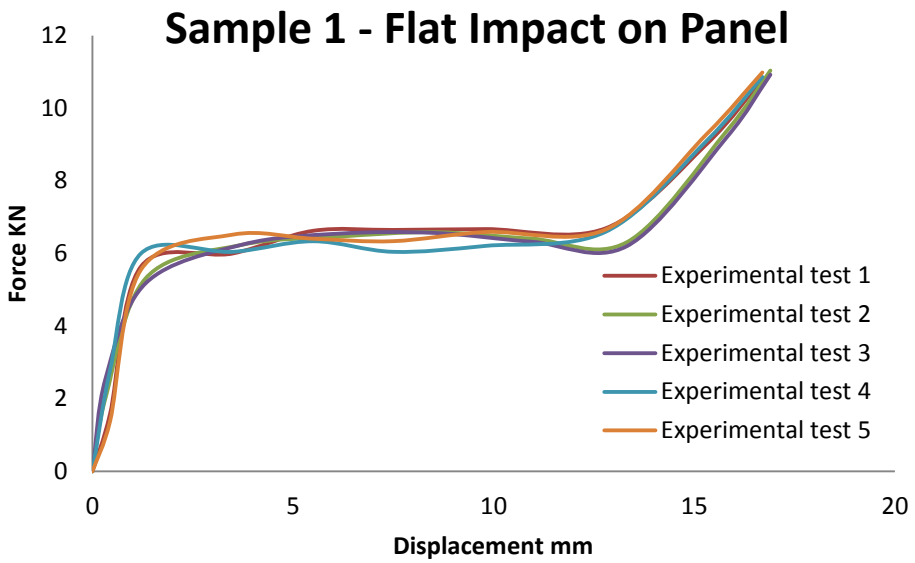

Figure 3.14 – Result Curves for Dynamic Impact of Sample 1 Panels at 90°

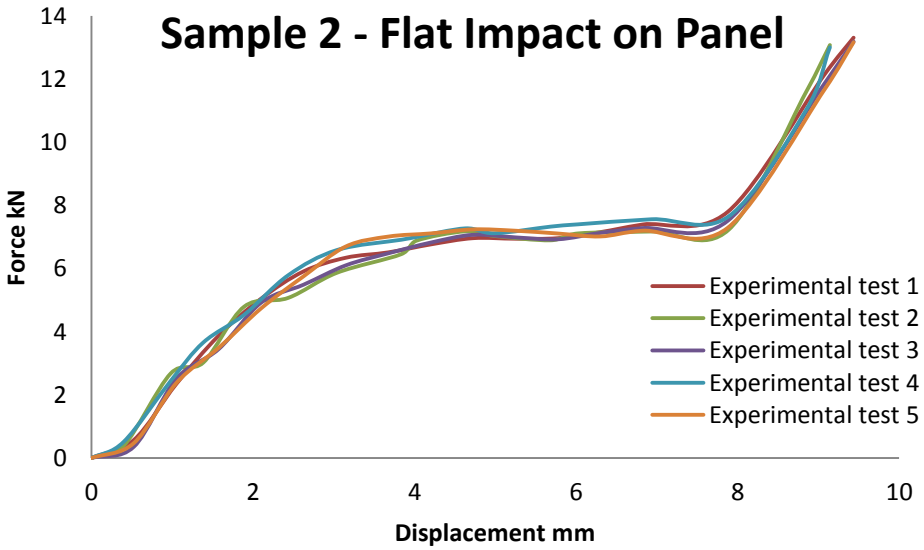

Figure 3.15 – Result Curves for Dynamic Impact of Sample 2 Panels at 90°

The experimental work reported in this chapter will be used in conjunction with analytical equations presented in the following chapter to validate finite element simulations associated with each test procedure. Upon agreement in results of the three methods, the numerical technique can be developed to be employed in the

study of the effect of geometrical alterations in the behaviour of egg-box structures, diminishing the need for performing destructive and expensive experimental tests.

Figure #	Sample #	Body Tested	DOF	Angle of Impact	E_{Total} (kN.mm)
3.8	1	Single Cone	No Constraint	Flat	4.55
3.9	1	Single Cone	No Constraint	Oblique	0.12
3.10	1	Single Cone	Within Panel	Flat	7.40
3.11	2	Single Cone	Within Panel	Flat	3.60
3.12	1	Single Cone	Within Panel	Oblique	3.45
3.13	2	Single Cone	Within Panel	Oblique	2.36
3.14	1	Full Panel	Laterally Fixed	Flat	77.89
3.15	2	Full Panel	Laterally Fixed	Flat	67.76

Table 3.2 – Total Energy Absorbed by Structures under Experimental Impact

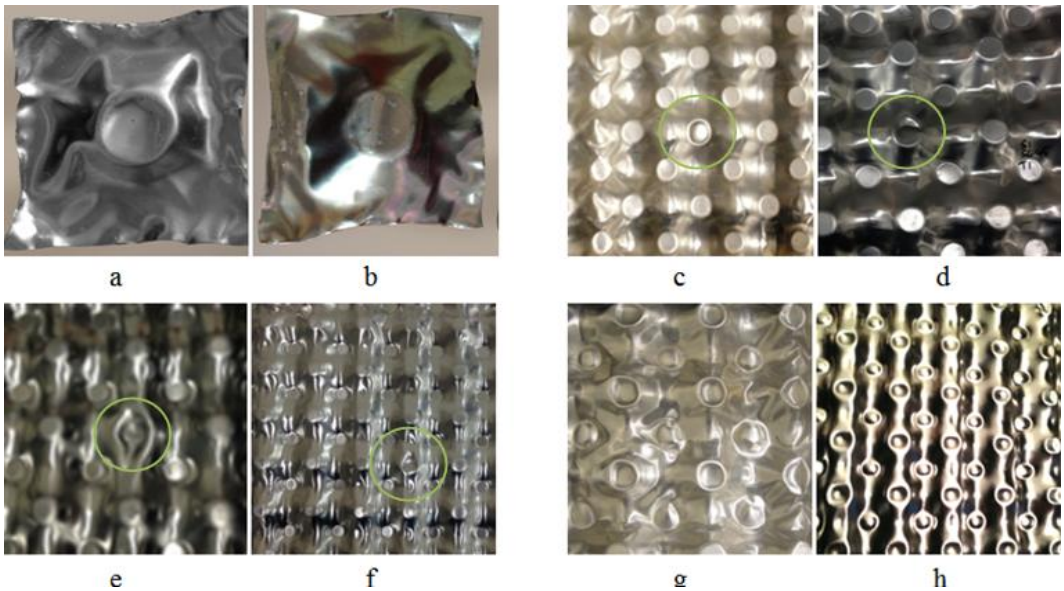

Figure 3.16 – Post-impact Deformed Samples (a) Free-edged Single Cone Impacted at 90°, (b) Free-edged Single Cone Impacted at 45°, (c) Sample 1 Single Cone within Panel Impacted at 90°, (d) Sample 1 Single Cone within Panel Impacted at 45°, (e) Sample 2 Single Cone within Panel Impacted at 90°, (f) Sample 2 Single Cone within Panel Impacted at 45°, (g) Sample 1 Full Panel Vertical Impact, (h) Sample 2 Full Panel Vertical Impact

4. THEORETICAL CONSIDERATION

4.1. Introduction

In order to enhance the performance of egg-box energy absorber structures under impacts, it is necessary to understand their behaviour in detail. It would, hence, be beneficial to have the means to study the progresses of the deformation procedure at various stages. However, with the very short duration of an experiment between the moment of impact and full compaction, it would not be possible to perform such in depth analysis. Such exploration becomes possible using methods such as analytical and numerical techniques to model an impact scenario. This allows for a thorough evaluation of the deformation process at any stage as it progresses. Such theoretical tools can also be used in predicting the behaviour of a structure prior to the application of physical loading.

Analytical models of the experimental impact tests conducted on various egg-box cell samples, as reported in the last chapter, are generated in the first section of this chapter. The developed equations are then used to review the outcomes of Chapter 3. Additionally, in the subsequent section of the current chapter, finite element technique has been used to simulate the aforementioned experiments. As well as presenting the modelling details, this section explores the requirements of a finite element simulation to ensure maximum result precision. The FE output curvatures have been successfully validated in conjunction to the experimental resultant curves. The high level of data precision verifies the competence of the FE models.

4.2. Analytical Modelling

The analytical approach can be used to approximately measure and evaluate the energy absorption characteristics of the egg–box structures. By developing an energy equation for the impact scenario of the egg-box, the total amount of energy absorbed through structural deformation can be approximately calculated. The result would be valuable in the preliminary assessments of the outcomes of experimental impact tests.

As described in the work of Nowpada and Chirwa et al. (2010), the total energy absorbed by structures such as egg-box is equal to the total work done during the deformation procedure. Equations 4.1 to 4.5 are adaptations of the formula generated in the aforementioned research for quasi-static loading of egg-box cells, modified in accordance to the dynamic response of the identified specimen.

Equation 4.1 shows the works done in the vertical impact of the free-edged cells. The work quantities have been derived based on the developing deformation stages of the cell following an impact. Complete description of the procedures can be applied as explained in Chapter 3.

The deformation procedure initiates by the outward stretching of the cell edges with a work value of $(W_{stretch})$. (W_{twist}) relates to the work done to gradually coil the unconstrained base corners as the deformation proceeds. The first (W_{hinge}) is the work due to the formation of plastic hinges at the peak to trench transition lines which is followed by the flattening of the peak curvature, causing $(W_{flattening})$ to take place. Due to the appearance of an additional travelling hinge at the peak circumference, causing the inversion of the cone, the second (W_{hinge}) is done bringing the deformation process to an end. As the walls of the cell slide over the impactor and support surfaces, friction occurs between each two faces. Hence it is also important to take $(W_{friction})$, the work due to friction into account. The above works add up to be equal to the energy absorbed through the deformation of the cell.

$$W_{Total} = W_{stretch} + W_{twist} + W_{flattening} + W_{friction} + \sum_0^2 W_{hinge} \qquad 4.1$$

For the oblique impact of the free-edged cell, the total works done is derived as given in equation 4.2, where the deformation begins with the impacted side of the peak cone bending at line of contact with a work value equal to ($W_{bending}$). The structure begins to slide along the horizontal component of the applied load, causing the end corners of the cell to roll upwards against the supporting surface and creating (W_{twist}). The peak cone then starts to fold on the side left intact. The work due to the folding phenomenon is shown in the equation as ($W_{folding}$). ($W_{friction}$) also is work done due to the friction present between contacting surfaces.

$$W_{Total} = W_{bending} + W_{twist} + W_{folding} + W_{friction} \quad 4.2$$

The next test type includes impacting a single cone in-situ within a panel both axially and obliquely at 45°. When vertically impacted, the peak curvature initially flattens, at a work value of ($W_{flattening}$). This is followed by the formation of two sets of travelling hinges. First group of hinges appear over the circumference of the peak cone, resulting in the inversion of the cone. This is followed by travelling hinges appearing at the trench circumference, causing their inversion. With the presence of the neighbouring cells, the effect of stretching and twisting of the ends disappears. The sum of the works done due to each of these deformation patterns is shown in equation 4.3 as:

$$W_{Total} = W_{flattening} + \sum_0^2 W_{hinge} + W_{friction}. \quad 4.3$$

The oblique impact of the single cell within the panel, for both sample sizes, causes the peak cone to bend in the load direction, stretching the material behind it and compressing them beneath, at works of ($W_{bending}$), ($W_{stretch}$) and ($W_{compression}$), respectively. The friction present between the impactor surface and the egg-box shell will result in the work value ($W_{friction}$), shown in equation 4.4.

$$W_{Total} = W_{bending} + W_{stretch} + W_{compression} + W_{friction} \quad 4.4$$

As for the most momentous experiment, equation 4.5 can be used to evaluate the total energy absorbed in the flat impact test by adding the works involved in the deformation process. Subsequent to the impact, the deformation initiates by flattening of the peak curvature, done by ($W_{flattening}$). This is followed by the development of plastic hinges at top, bottom and middle of the cell walls with a work shown as (W_{hinge}). ($W_{bending}$) is the load due to bending of the cell walls with the progression of the deformation. Friction present both above and below the sample is dealt with via ($W_{friction}$) at all stages of the deformation.

$$W_{Total} = W_{flattening} + \sum_0^3 W_{hinge} + W_{bending} + W_{friction} \quad 4.5$$

Considering the rule of the conservation of energy, it can be assumed that the kinetic energy (KE) of the free falling impactor mass would be equal to the potential energy (PE) of deformation (eq. 4.6).

$$W_{Total} = KE = PE \quad 4.6$$

Expanding this equation gives:

$$\frac{1}{2} m {v_i}^2 = mgH \; or \; F_i H, \quad 4.7$$

where (m) is the impacting mass, (v_i) is the speed of the impactor, *(g)* is the gravitational acceleration, *(H)* is the total height of a cell and (F_i) is the force of the impact. The impact force can be defined as;

$$F_i = \sigma_i A. \tag{4.8}$$

Hence, based on equations 4.7 and 4.8, the impact stress (σ_i) can be derived as:

$$\sigma_i = \frac{\frac{1}{2} m {v_i}^2}{AH}, \tag{4.9}$$

with *(A)* being the area of the impacted structure which is in contact with the drop mass. The total energy absorbed in the impact event (E_{Total}) can, ultimately, be calculated from equation 4.9 as:

$$E_{Total} = \int_0^{x_i} F_i \, dx = \sigma_i A x_i. \tag{4.10}$$

The densification point of the panel (x_i), for egg-box panel structures starts at strain values of around 0.6-0.8 (Deshpande, 2003, Akisanya, 2006, Cheng, 2007) and can be mathematically defined as:

$$x_i = 0.75\, H, \tag{4.11}$$

which indicates the depth where the sample approaches the point of densification.

The total energy for the egg-box panel samples tested as reported in Chapter 3 is calculated in Table 4.1, from equation 4.10 to be approximately equal to 74kN.mm, at densification depths of 18mm and 9mm based on equation 4.11, for sample types 1 and 2, respectively.

As associated with the force-displacement curve of an impact, the total energy absorbed by an egg–box cell during crush can be defined as the area roofed by this curve up to the point of densification.

Equation	$\sigma_i = \frac{\frac{1}{2} m {v_i}^2}{AH}$	$x_i = 0.75\ H$	$E_{Total} = \int_0^{x_i} F_i\ dx = \sigma_i A x_i.$
Sample1	$\sigma_i = \frac{\frac{1}{2} \times 5.5 \times 6^2}{A \times 24} = \frac{4.1}{A} \frac{kg}{mm} \frac{m^2}{s^2}$	$x_i = 0.75 \times 24 = 18\ mm$	$E_{Total} = \frac{4.1}{A} A \times 18 = 73.8\ kN.mm$
Sample 2	$\sigma_i = \frac{\frac{1}{2} \times 5.5 \times 6^2}{A \times 12} = \frac{8.3}{A} \frac{kg}{mm} \frac{m^2}{s^2}$	$x_i = 0.75 \times 12 = 9\ mm$	$E_{Total} = \frac{8.3}{A} A \times 9 = 74.7\ kN.mm$

Table 4.1 – Total Energy Calculations

A review of the force-displacement curves of the two aforementioned experiments approves the analytical estimation. For sample 1, the area under the curve (Fig. 3.14) is approximately equal to 78kN.mm and the same value for the second sample type (Fig. 3.15) is 68kN.mm. The conformity of calculations from the analytical method and the test data force-displacement curves is used as a supporting initiative in conducting further experimental work.

The mathematical method considered here is based on the mechanics of a two dimensional profile of the samples. It is obvious that the analytical results are approximate. In the next section, the samples are modelled as 3D replica to analyse the performance of the structures under impact.

4.3. Finite Element Modelling

To be able to observe and analyse the behaviour of a structure under the influence of various physical stresses, it is initially necessary to accurately model its geometry. Depending on the type of the structure, severity of the need for outcome precision, the level of symmetry of its geometry and the loads it is subject to, this finite element model can be made in a 2D or 3D environment.

Finite element software such as ANSYS® can be used to produce two and three dimensional geometries. As an advantage ANSYS® offers modelling tools in its pre–processor division, while it supports both solid modelling techniques, referring to them as modelling via interface software, and modelling through ANSYS® Graphical User Interface (GUI).

4.3.1. Geometrical Model

The term "solid modelling" is used in the ANSYS® documentations as opposed to a technique, introduced in the same script as "direct generation," where the model of a structure is generated directly through the definition of nodes and elements without the presence of any geometrical shapes pre–defining the perimeters and corners of that structure. This method is very time consuming and complicated unless when used for geometrically simple systems where design optimisation is not of any interest. Solid modelling technique has been used in this study as the means to simulate impact of the egg-box structure. ANSYS® 13.0 documentations provide a list of the cons and pros of this technique (ANSYS® 13.0, 2010).

An evaluation of the structure in hand reveals that the egg–box geometry, being a three–dimensional complex volume which consists of curvatures and arches, requires the use of Boolean operations and mesh refinement. Hence solid modelling technique is selected to generate the cell geometry. In fact, when it comes to the optimisation of this structure, it would be greatly advantageous to have a parametric model which allows for further modifications of the geometry. It would be beneficial and time saving, to generate a model directly through ANSYS® pre–processor, whether this is by command definition or using ANSYS® GUI.

The finite element model, made to represent the egg–box geometry, can be generated by translating simple cones. However, to reduce the size of the model and, as its direct effect, the time of the analysis, advantage can be taken of the geometrical symmetry of cones ergo the egg–box structure.

The three dimensional egg–box cell models for each of the two sample sizes are presented in Figure 4.1. The cells are modelled in ANSYS® pre–processor to the most accurate dimensional approximations. It should be noted that the thickness of the aluminium surface of the egg–box is introduced in the pre–processor as the virtual thickness of a thin shell element. In other words, the geometrical model generated herein does not have a physical thickness. Instead, this value is designated in the form of a real constant to the elements, by which every part of the cell would be covered.

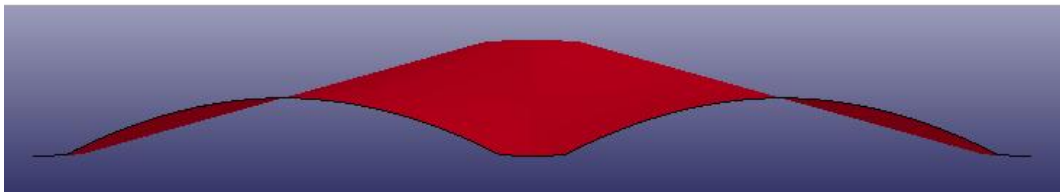

a) Sample 1

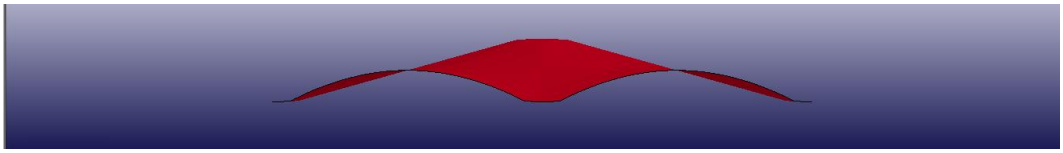

b) Sample 2

Figure 4.1 – FE Model of Egg-box Cells a) Sample Type 1 and b) Sample Type 2

Subsequent to the generation of the geometry of the specimen, the finite element model has to go through a preparation phase, where every physical aspect of the practical experiment, including boundary conditions and loadings, would be simulated and applied to the model.

The principal outcome of this section would be to generate and validate a finite element model with regards to the specifications of the dynamic impact experiments and explore the finite element results in comparison to the data obtained from the experimental works.

4.3.2. Material Properties

As stated in the previous chapter the egg–box samples were fabricated out of Commercially Pure (CP) Al1050 H111 aluminium alloy metal sheets which consist of 99% aluminium. The sheets were cold–pressed into egg–box shaped panels with overall dimensions of 300mm × 300mm lubricated closed dies.

The selection of a material model is extremely important in a simulation. To model materials in ANSYS® or ANSYS/LS–DYNA®, it is necessary to initially understand the characteristics of the material. In dynamic analysis, the strain rate dependency of a material plays a rather significant role in the behaviour of the structure. Therefore, to achieve result accuracy, a material model has to be defined which would account for this aspect of material physics.

ANSYS/LS–DYNA® offers a number of pre–defined rate dependent material models that are more or less similar in their physical behaviour, while their major differences is the solution methods and the input options of the model. Since its 1998 edition, LS–DYNA® offers a strain rate dependent multi–linear elastic–plastic material model called MAT_MODIFIED_PIECEWISE_LINEAR_PLASTICITY, which was specifically added for modelling the failure of aluminium material. This model takes multi–linear elastic–plastic material properties such as stress–strain curves in addition to taking the strain rate dependency of a material into consideration.

As opposed to that of its unmodified counterpart, this model offers enhanced failure criteria (ANSYS/LS–DYNA® User's Guide 12.0, 2009). The presence of such improved failure criteria in the formulation of the material model allows for the structural elements to collapse beyond their point of ultimate plastic strength. With

this option, the entire structure should demonstrate a more realistic behaviour. In this case, failure is based on effective plastic strain.

The Modified Piecewise Linear Plastic material was found to be most appropriate to represent the CP aluminium for the purpose of the test simulations. The material properties provided in Chapter 3 were implemented in the material model to represent the true characteristics of the aluminium alloys utilised.

4.3.3. Mesh Generation

The egg–box structure was modelled using the ANSYS/LS–DYNA® shell elements Shell163. This element is designed for dynamic simulations, therefore it has 12 degrees of freedom, translations, accelerations, and velocities in x, y and z directions and rotations about the nodal x, y and z axes, at each node. More thorough description of the properties of Shell163 can be accessed in ANSYS/LS–DYNA® User's Guide (2004).

The default Belytschko–Tsay method, which is recommended for most applications, was chosen as the element formulation. This method is known to be of high–speed in solving for elements since it uses reduced integration. However, in this study, three integration points were selected at all times for further accuracy of the results. The element was checked and approved for compatibility with the material model used.

Selective, yet continuous, mesh densities were used in different parts of the cell in order to take into consideration the miniature curves of the peak and base surfaces as well as the surface of transition from peak/base to walls, while maintaining a sensibly short solution time. The egg–box cell was divided into approximately 3900 shell elements and around 4000 nodes.

4.3.4. Boundary Conditions

In order to accurately model the symmetrical continuity of the cell in the egg–box panel, it is necessary to define appropriate boundary conditions. To prevent the

in–plane lateral expansion of the egg–box finite element model, as done in the experimental tests where the entire panel was involved, all the edge nodes of the single cell had to be restrained from translational movement in the horizontal directions as well as all rotational movements about the nodal axes. Also based on the practical test environment, it was assumed in all simulations that the egg–box panel was resting on a solid surface, with negligible horizontal movement. Hence, a solid surface was defined, positioned directly beneath the egg–box cell. The surface was limited to having no lateral or rotational movement, i.e. fully fixed in all directions.

The impactor surface was modelled in the form of another solid surface with the weight and physical properties of the drop mass. The only load set to be directly applied on the egg–box cell was its own gravitational weight.

To introduce the concept of structural solidity between objects represented, it was set for the entire model to have structural contact properties applied on all the outer surfaces both within one body and when in contact with other parts. The ANSYS/LS–DYNA® Surface to Surface and Automatic Single Surface contacts were used for this purpose. Properties such as static and dynamic friction coefficients and birth and death time of the contact were also introduced to the software based on the experimental test conditions, to ensure further accuracy.

The impact test simulations were categorised into three groups based on the level of lateral constraints applied to the system; a single cell with no lateral restrictions on its edges, a single cell situated amongst neighbouring cells and a cell representing any cell in-situ in the panel. The first model was simulated to characterise the flat and oblique impacts of the free-edged single cell. The second model corresponded to flat and oblique impact experiments conducted on one cone within the panel, while the flat impacts of the entire egg-box panel was simulated with the last cell model.

In the flat impact experiments of the entire egg–box panels, the samples were enclosed in a box, with a cross sectional area 1.4 times the surface of the drop mass to ensure enough number of cells are subjected to impact to replicate the continuous structure of an egg-box panel. This positioning restricted the egg–box panel from all

lateral movements. Hence, in order to reproduce the boundary conditions applied to the egg–box panel and to allow for the continuity of its cells, all the edge nodes of the simulated model were restrained from any lateral movement in the horizontal direction. Similar to the previous models, the cell was modelled to be resting on a solid and rigid surface, to be crushed from above by the impacting surface representing the drop weight.

The drop masses were modelled with identical cross-sectional dimensions and physical properties as those used in the experimental work. The weight of the flat panel impactor was adjusted to represent the share of a single cell from this mass. In all cases the surface was limited to travel in the vertical direction only. The effect of gravity was introduced to the impacting surfaces as an acceleration of 9810mm/s^2 applied on the nodes.

Once all the influential factors are taken into consideration, the egg–box cell model can undergo the dynamic analysis. Figure 4.2 shows a geometrical sketch of the egg–box cell resting on a solid surface with the impactor positioned above it.

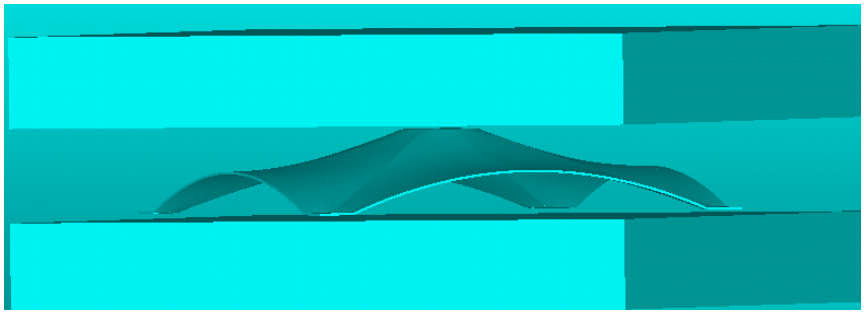

Figure 4.2 – Egg–box Cell Impact Simulation

4.4. Verification and Critical Analysis of the Results

Figure 4.3 to 4.10 show the force-displacement curves of the LS–DYNA® finite element analysis for the dynamic impact of egg–box cells. The resultant curves are compared to the outcomes of the experimental tests.

A reasonable correlation is evident between the results of the ANSYS/LS–DYNA® FE analyses and the experimental axial and oblique impact of the egg–box cells. Despite slightly different termination values, both curves commence the deformation process and reach the densification point at around the same displacement values.

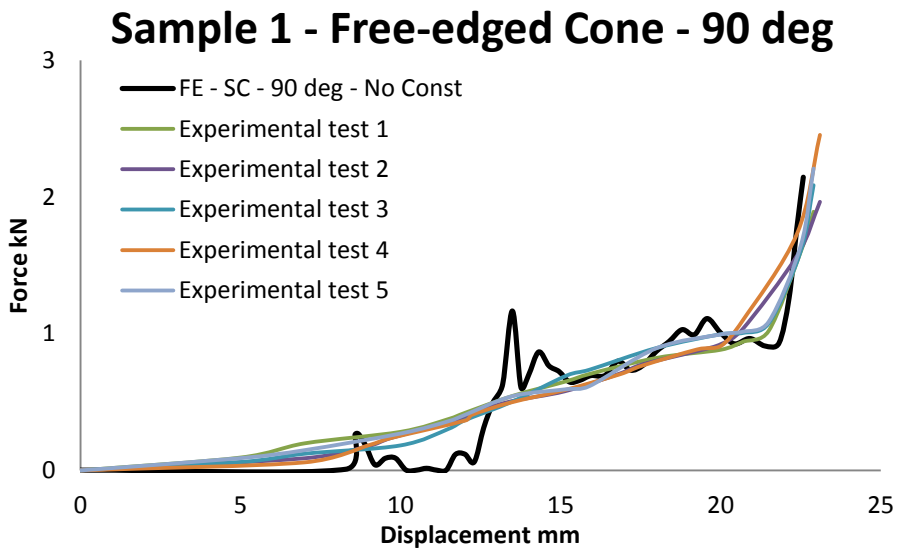

Figure 4.3 – Result Curves for Impacting Free-edge Single Cell at 90°

The equal areas beneath the curves up to the densification point validate the simulation accuracy by the total amount of energy absorbed. The smooth trend of the curves representing the outcome of the experimental tests is achieved by applying a low pass filter to the results received from the data recording devices.

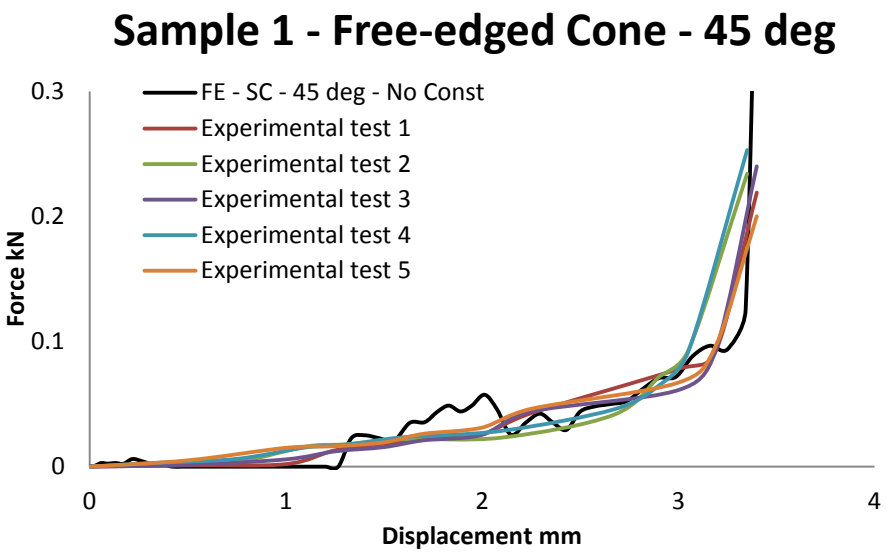

Figure 4.4 – Result Curves for Impacting Free-edge Single Cell at 45°

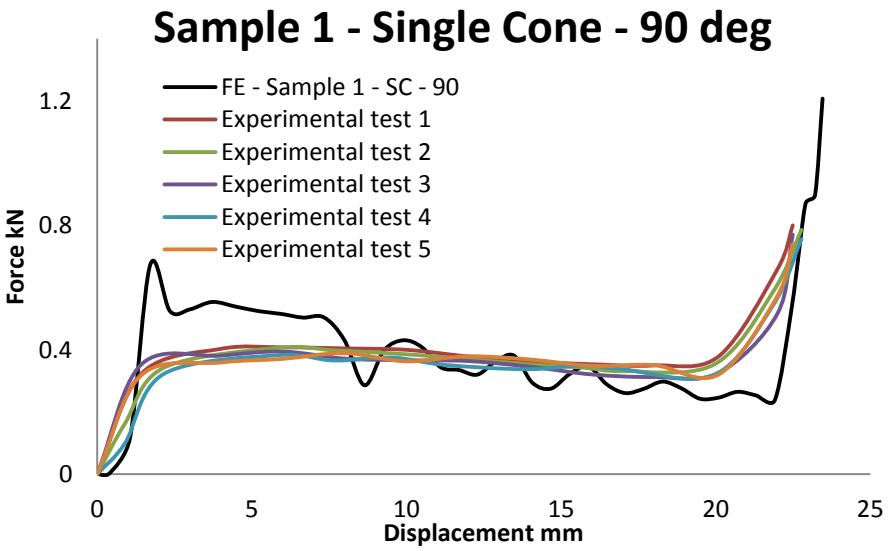

Figure 4.5 – Result Curves for Impacting Single Cone of Sample 1 at 90°

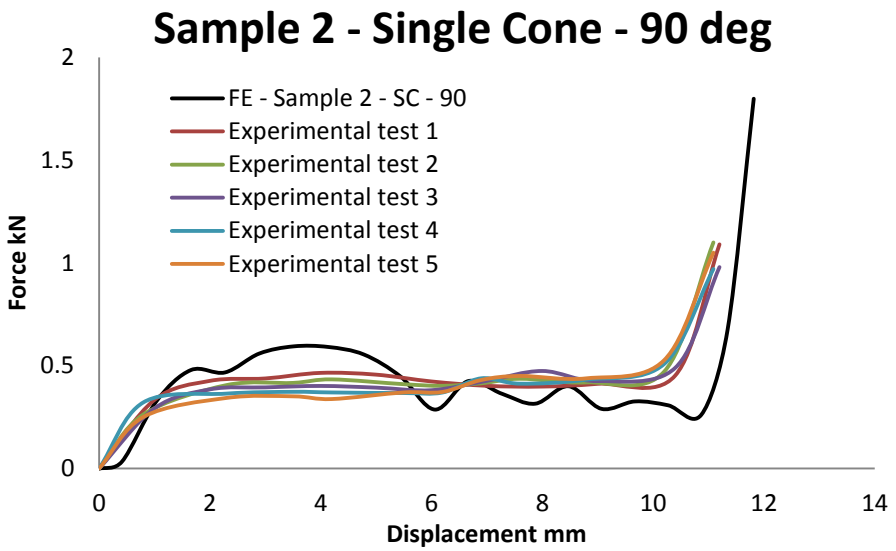

Figure 4.6 – Result Curves for Impacting Single Cone of Sample 2 at 90°

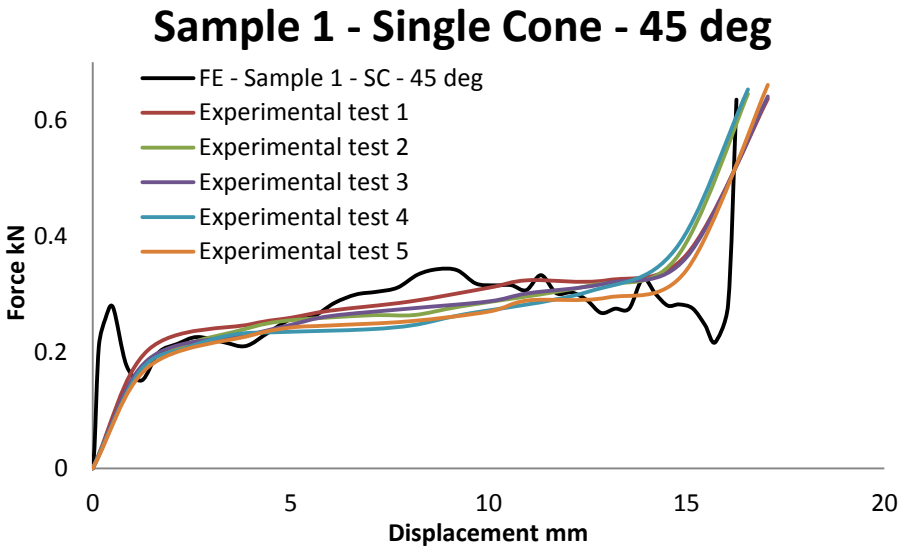

Figure 4.7 – Result Curves for Impacting Single Cone of Sample 1 at 45°

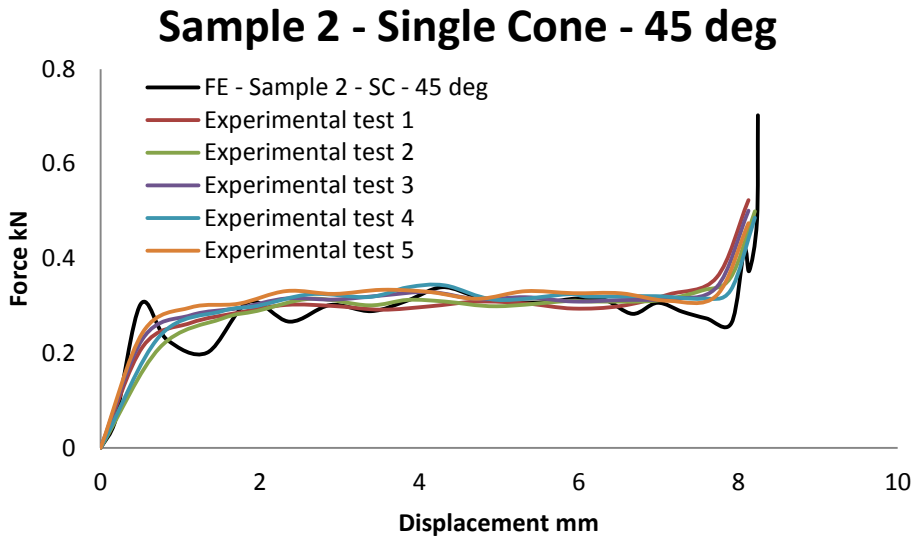

Figure 4.8 – Result Curves for Impacting Single Cone of Sample 2 at 45°

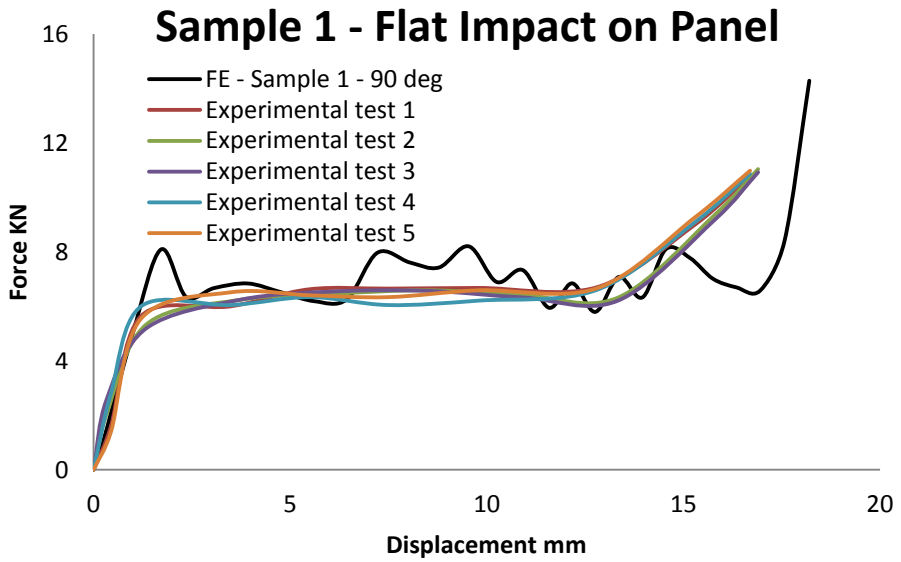

Figure 4.9 – Result Curves for Dynamic Impact of Sample 1 Panels at 90°

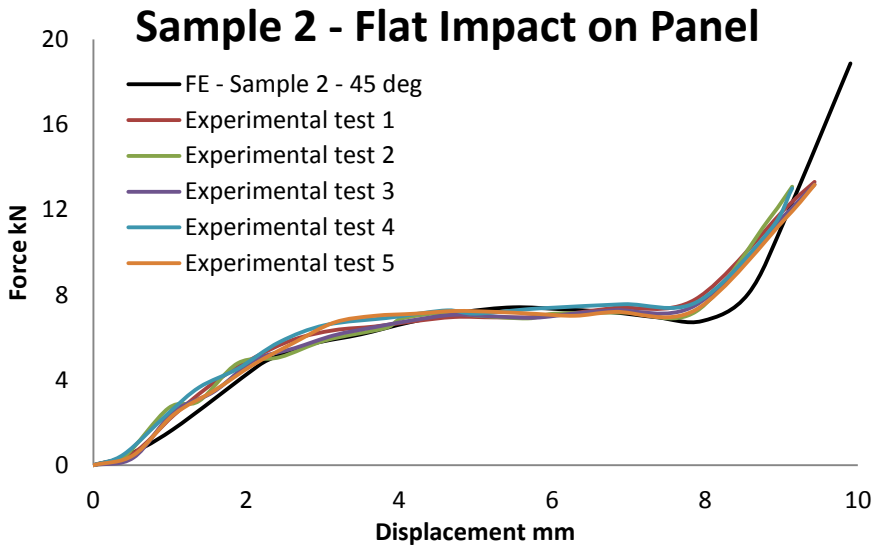

Figure 4.10 – Result Curves for Dynamic Impact of Sample 2 Panels at 90°

Fig. 4.11 shows the different stages of deformation for the axial impact of the entire panel, in association with the load-deformation curve. The structure has been circled in the image where a major transformation is in occurrence.

It can be deduced from the finite element curves of Figures 4.3 to 4.10 that the simulation specifications implemented in ANSYS/LS–DYNA® are rationally accurate. In the upcoming chapter the validated settings and constructed models will be used to perform dynamic impact analyses on egg–box structures of various geometries towards achieving the main research objective of developing purpose–specific optimised egg–box structures.

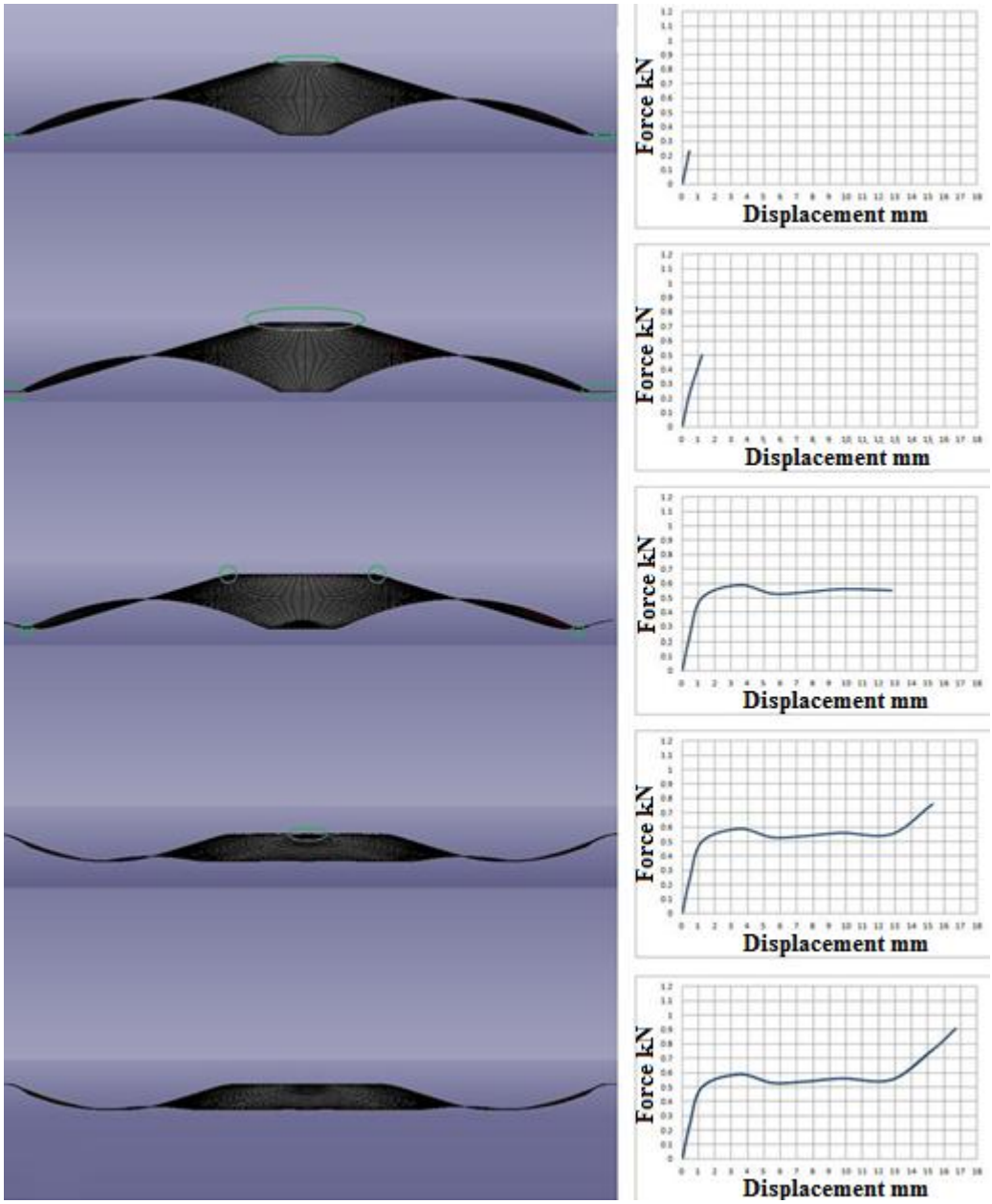

Figure 4.11 – Progression of the Deformation Procedure for Flat Impact

5. ANALYSIS AND OPTIMISATION OF MODIFIED EGG-BOX

5.1. Introduction

In this chapter, the constraints in the path towards the optimisation of egg–box structures have been discussed and the finite element model developed and validated in Chapter 4 has been employed en route for finding egg–box geometries that respond satisfactorily to the requirements of an optimal structure. The effects of geometrical variations on the performance of this energy absorber are explored based on the outcomes of the finite element analysis of the axial impact of the structure. Subsequently, a sandwich structure with optimum characteristics has been proposed in accordance to the analyses data which displays structurally desirable characteristics in comparison with its single panel counterparts. The enhanced performance of the proposed sandwich structure has been confirmed by the use of analytical approaches.

5.2. Geometrical Alterations

Various parameters, as detailed in the Introduction Chapter, can participate in the optimisation of structures such as egg–box energy absorbers. Systematic alteration of these factors will result in a set of design combinations which can consequently be compared in correspondence to one or more objectives, to establish an optimised model.

ω (deg)		15°									30°									45°									60°									75°								
t (mm)		0.8			1			1.2			0.8			1			1.2			0.8			1			1.2			0.8			1			1.2			0.8			1			1.2		
p (mm)		20	45	60	20	45	60	20	45	60	20	45	60	20	45	60	20	45	60	20	45	60	20	45	60	20	45	60	20	45	60	20	45	60	20	45	60	20	45	60	20	45	60	20	45	60
d (mm)	5	28	75	103	28	75	103	28	75	103	13	35	48	13	35	48	13	35	48	8	20	28	8	20	28	8	20	28	4	12	16	4	12	16	4	12	16	2	5	7	2	5	7	2	5	7
	10	19	65	93	19	65	93	19	65	93	9	30	43	9	30	43	9	30	43	5	18	25	5	18	25	5	18	25	3	10	14	3	10	14	3	10	14	1	5	7	1	5	7	1	5	7
	15	9	56	84	9	56	84	9	56	84	4	26	39	4	26	39	4	26	39	3	15	23	3	15	23	3	15	23	1	9	13	1	9	13	1	9	13		4	6		4	6		4	6
	20		47	75		47	75		47	75		22	35		22	35		22	35		13	20		13	20		13	20		7	12		7	12		7	12		3	5		3	5		3	5
	30		28	56		28	56		28	56		13	26		13	26		13	26		8	15		8	15		8	15		4	9		4	9		4	9		2	4		2	4		2	4
	40		9	37		9	37		9	37		4	17		4	17		4	17		3	10		3	10		3	10		1	6		1	6		1	6			3			3			3
	50			19			19			19			9			9			9			5			5			5			3			3			3									

Table 5.1 – Egg–box Cell Dimension Data for Geometrical Optimisation

- This table is in correspondence to the dimensional parameters of Figure 1.3.
- The main blocks of the table represent the value of cone height, (*h*) in mm for each combination. The actual height of each cell (*H*) would be twice this number.
- All combinations are designed to R = 50mm and r = 2mm.
- Cross hatched blocks indicate designs that are geometrically invalid or practically flat.
- The cell height decreases with an increase in the apical angle as well as an increase in the diameter.
- In each angle division, the height is greater with greater inter–peak distances.
- The cell height remains unchanged with the changes in the thickness.

The approach, used in this study, to achieve optimised outcomes is mainly based on Table 5.1. This table is categorised in terms of five geometrical variables, angle (ω) in degrees, thickness (t) in mm, inter–peak distance (p) and top diameter (d) both also in mm, and, as the result of their combination, cone height (h) in mm. It is assumed here, as a complexity reduction factor, that parameters (R in mm), base and peak curvature radius, and (r in mm), wall to top transition radius, remain constant for all combinations, since, in practice, their range of variance is relatively insignificant.

The series of values assigned to each parameter cover a reasonably wide range of possible inputs in consistence with the geometrical measurements currently in use in the industry. Various other inputs can be positioned among these arrays, which can go through a systemised procedure as required, for modelling and optimisation.

5.3. Simulation Configurations

All geometries of Table 5.1 have been modelled and simulated to be impacted by a loading mass of 5500g at a speed of 6m/s similar to the experimental tests conducted as a part of this project. As with the finite element model developed in Chapter 4, in the simulations presented in this section, cells are restrained to have no lateral movements to resemble a complete egg–box panel. A solid surface placed below the cells acts as the base of the test machine where the egg–box would be resting in a practical experiment.

The average value of the total force (F_{Avg}), applied by the impactor on the egg–box panels in the following impact tests can be calculated as,

$$F_{Avg} = m \times a_{crush} = m\frac{V_i}{t_{crush}} \qquad 5.1$$

where, (m) is he mass of the impactor and (a_{crush}) is the crush acceleration which can be expanded in definition by (V_i) which is the impact velocity, divided by the

time of the crush (t_{crush}). The latter value is taken as an average between all the models tested. Hence, implementing the relevant numbers in equation 5.1, the force value also becomes an average quantity and is equal to,

$$F_{Avg} = 5.5kg \times \frac{6^{m}/_{s}}{0.01s} = 3.3 \times 10^{3}N = 3.3\ kN.$$

As a measure of accuracy of a simulation, it can be checked that the average value of the impact load absorbed by the structure is reasonably less than and in agreement to the value of (F_{Avg}). Therefore, in the following impact simulations, the average value of the load–deformation curve on the load axis should be more or less around 3.3kN.

In order for the comparative analysis to be pragmatic, it was ensured for all FE tests to be based on identical factors in every area with the only discrepancy being the geometrical features of the egg–box cell model. After the solution phase, the Force vs. Displacement curve for each FE run is derived and used as the measure of behaviour assessment.

5.4. Systemised Assessment

To organise the large number of combinations of Table 5.1, an initial assessment is made amongst models sharing similar angles, thicknesses and inter–peak distances. This was achieved through evaluating models of different top/base diameters, which otherwise belong to the same category, against one another to generate the best diameter selection.

As explained previously, the evaluations presented herein seek two qualities in an improved model; maximised impact energy absorption and minimised impact peak load. The outcome curves of the combinations given in Table 5.1 are presented in the following sections along with the explanation of their characteristics.

5.4.1. Geometrical Variations at ω=15°

The force–displacement curves of egg–box geometries with vertical angles of 15° at peak to peak distances of 20, 45 and 60mm and 0.8, 1.0 and 1.2mm wall thicknesses are comparatively reviewed in the upcoming figures. Finite element models of the egg-box cells belonging to this group of geometries are shown in Figures 5.1, 5.5 and 5.9 for different diameter, (*d*) values. The shell elements can take the three thicknesses as per relevant case. Figures 5.1, 5.5 and 5.9 are individually associated with the curves following them. The cells illustrated in the same image vary in peak/base diameter. Each cell represents three models with different thicknesses while the apical angle and the inter-peak distance remain constant in all cells shown in the same figure. It is important to note that, with appropriate boundary conditions introduced to the models, each cell shown here represents an entire egg-box cell with a cross-sectional dimension of 300×300 mm^2.

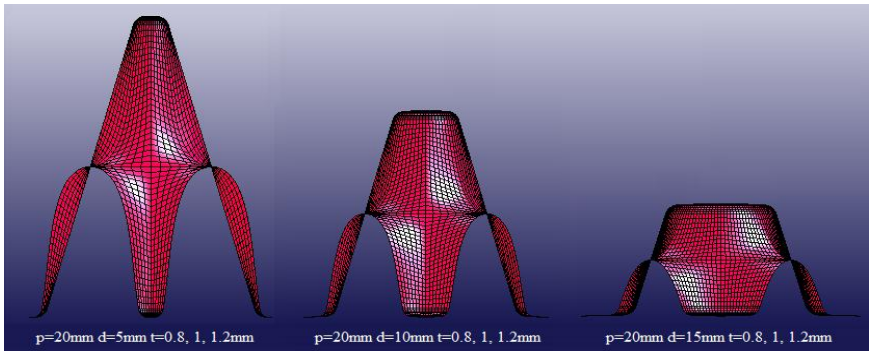

Figure 5.1 – FE Models of ω=15°, p=20mm, t=0.8, 1, 1.2mm for d=5, 10, 15mm

Evaluation is based on the increase or decrease in the peak/trench diameter in different geometries. The value of the diameter varies between 5mm to 50mm depending on the inter–peak distance of a particular model. It would not be geometrically practical for the (*d*) value to be larger than the (*p*) defined per model. Hence, as can be observed in the figures presented below, where curves are associated with a geometrical group of *p*=20mm, the value of (*d*) only rises up to 15mm, while with larger (*p*) values, such as 60mm, the top/base diameter can be increased to as large as 50mm.

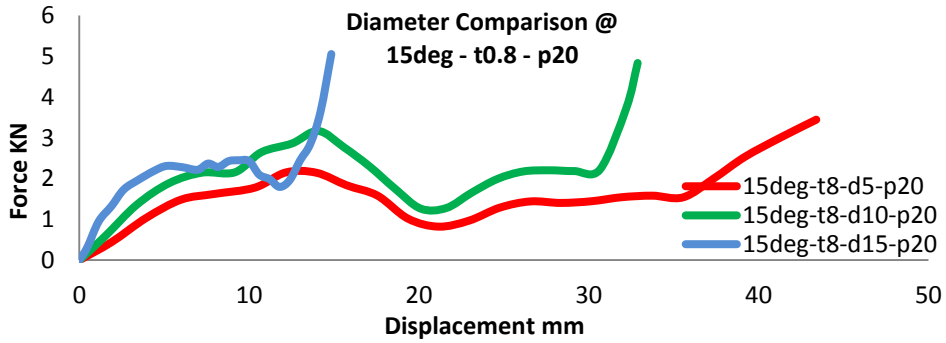

Figure 5.2 – Force vs. Displacement Curves of FE Simulations for ω=15°, t=0.8mm, p=20mm and d=5, 10, 15mm

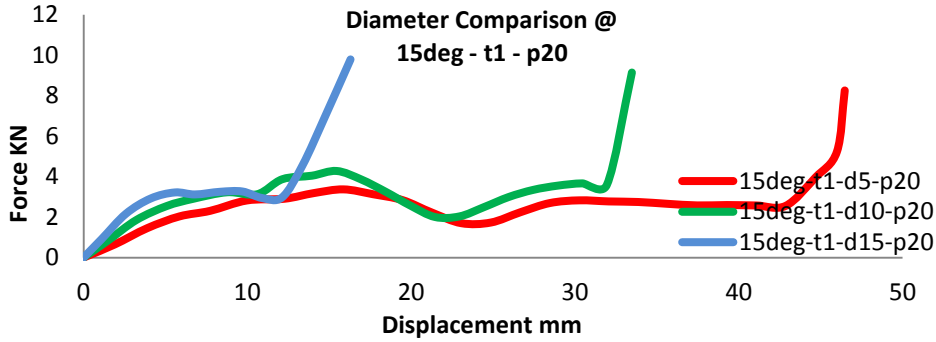

Figure 5.3 – Force vs. Displacement Curves of FE Simulation for ω=15°, t=1mm, p=20mm and d=5, 10, 15mm

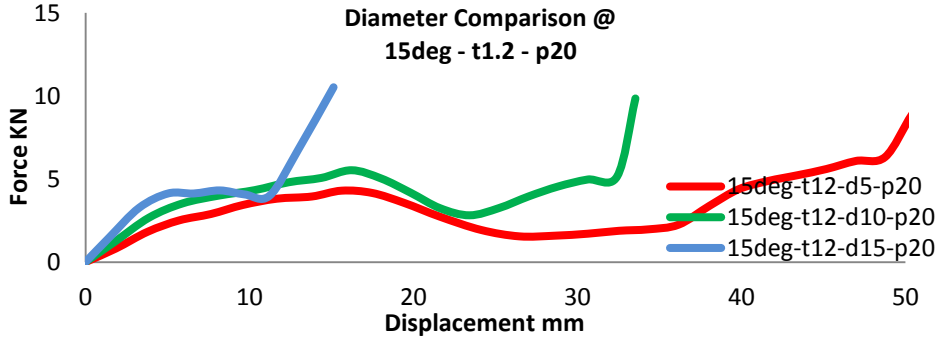

Figure 5.4 – Force vs. Displacement Curves of FE Simulation for ω=15°, t=1.2mm, p=20mm and d=5, 10, 15mm

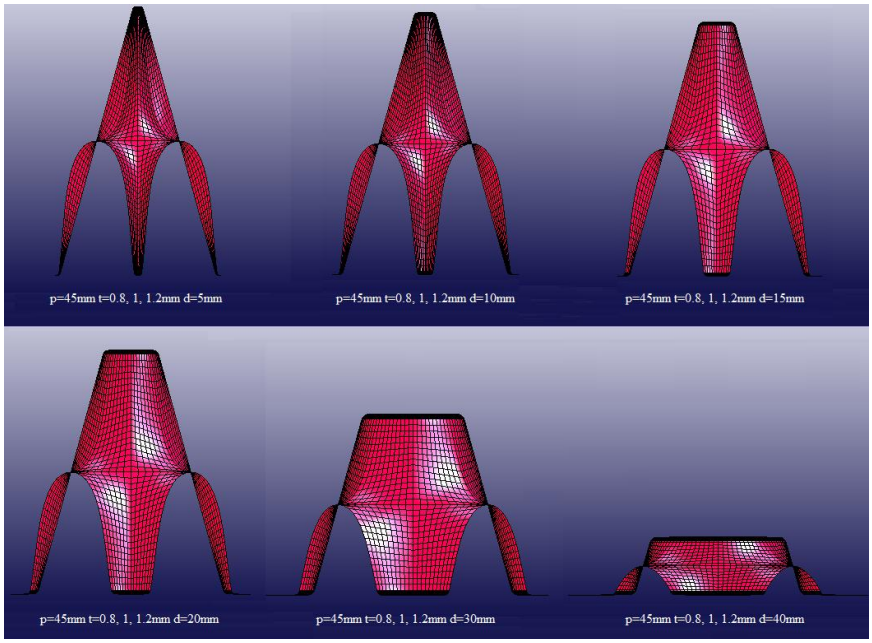

Figure 5.5 – FE Models of ω=15°, p=45mm, t=0.8, 1, 1.2mm for d=5, 10, 15, 20, 30, 40mm

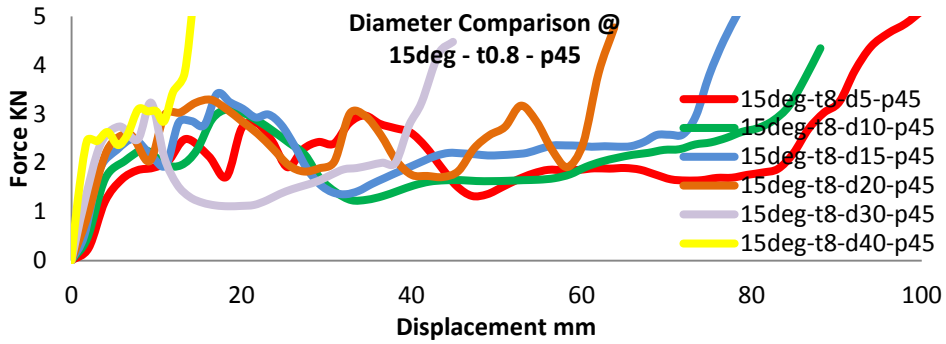

Figure 5.6 – Force vs. Displacement Curves of FE Simulations for ω=15°, t=0.8mm, p=45mm and d=5, 10, 15, 20, 30, 40mm

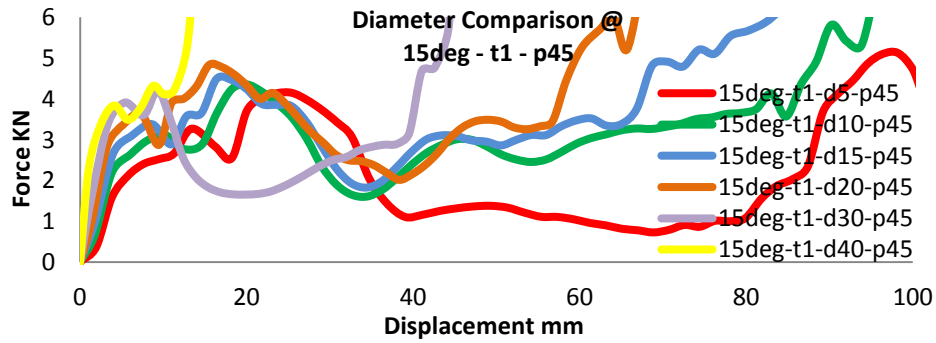

Figure 5.7 – Force vs. Displacement Curves of FE Simulations for ω=15°, t=1mm, p=45mm and d=5, 10, 15, 20, 30, 40mm

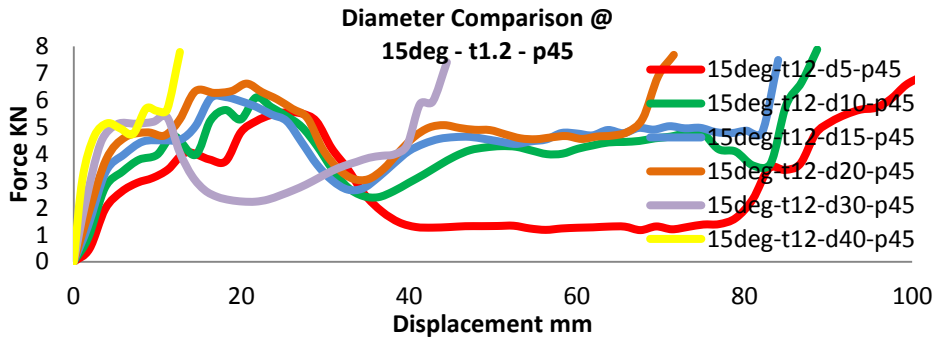

Figure 5.8 – Force vs. Displacement Curves of FE Simulations for ω=15°, t=1.2mm, p=45mm and d=5, 10, 15, 20, 30,40mm

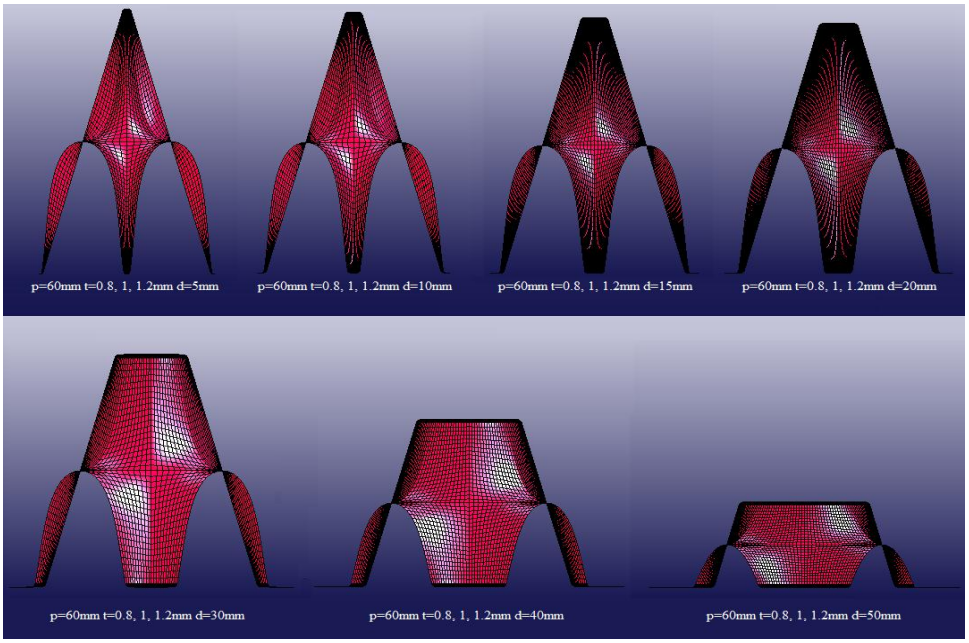

Figure 5.9 – FE Models of ω=15°, p=60mm, t=0.8, 1, 1.2mm for d=5, 10, 15, 20, 30, 40, 50mm

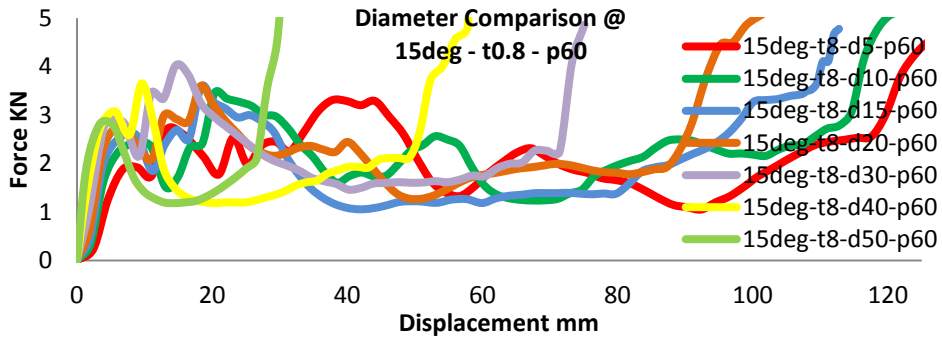

Figure 5.10 – Force vs. Displacement Curves of FE Simulations for ω=15°, t=0.8mm, p=60mm and d=5, 10, 15, 20, 30, 40, 50mm

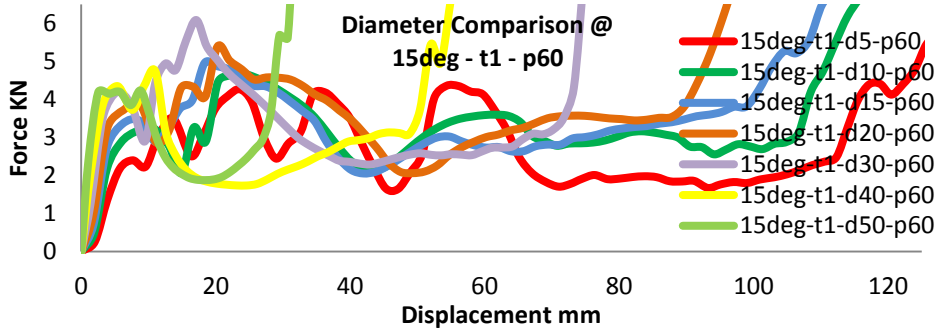

Figure 5.11 – Force vs. Displacement Curves of FE Simulations for ω=15°, t=1mm, p=60mm and d=5, 10, 15, 20, 30, 40, 50mm

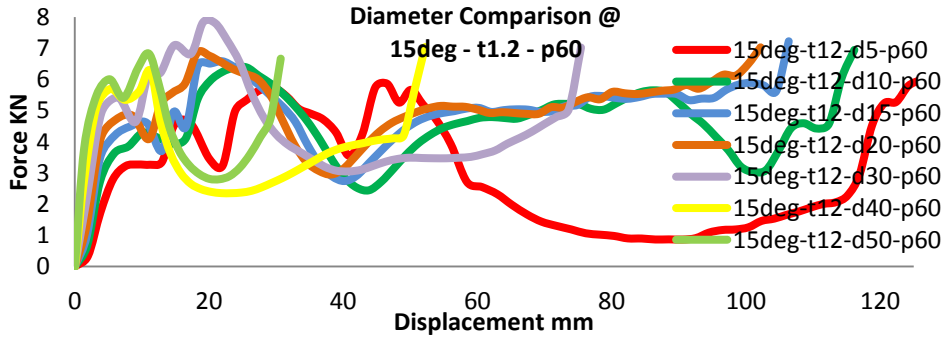

Figure 5.12 – Force vs. Displacement Curves of FE Simulations for ω=15°, t=1.2mm, p=60mm and d=5, 10, 15, 20, 30, 40, 50mm

Figures 5.2, 5.3, 5.4, 5.6, 5.7, 5.8, 5.10, 5.11 and 5.12 represent the force–displacement curves associated with the geometrical combinations of Table 5.1 that are categorised under (ω) of 15°. The increase in the peak to peak distance indicates wider cells hence egg–box panels with smaller cell densities. This means that in the same cross sectional area, a panel of p=20mm has more egg–box cells than a panel of p=60mm.

In accordance to the general characteristics mentioned in the previous section, it is evident from the curves of Figures 5.2 to 5.6 that with the increase of the inter–peak distance (p), the peak strength of the panel rises. This is a direct result of the greater cell density in the specimens with smaller (p) values. At the presence of more cells to initiate the deformation process, a larger amount of the impact shock is absorbed and vice versa.

From the effect of changes in the thickness factor and the inter–peak distance, it can be concluded that the egg–box panels of ω=15° with high cell densities and thin structure walls offer minimised initial load peak; hence, perform as efficient primary cushions against sudden impact to the bodies that are being protected.

It can also be deduced from the curves of Figures 5.2–5.4, 5.6–5.8 and 5.10–5.12 that the mean strength in geometries of similar diameter and thickness which disagree in (p), remains, reasonably, constant. Consequent to this consistency, it can be seen in the ω=15° curves that longer falls occur, following the sudden load peaks, in specimen of increased peak to peak distances.

The difference in load level becomes more evident in Figures 5.4, 5.8 and 5.12 as the walls of the egg–box cell become thicker, while, for all thicknesses, higher diameter models go through shorter falls. The exceptions to this pattern are specimens of d=5mm, which, due to their small top/base diameter, deform similar to cones. This effect is more evident in thicker models, since they show proximity to solid top conical structures, with their small diameter and large thickness.

By taking the aforementioned comparison into account for egg–box panels of ω=15°, it may be proposed that structures with relatively thinner walls and larger top/base diameters, show more satisfactory performance and are better energy absorbers in the primary stages of an impact.

5.4.2. Geometrical Variations at ω=30°

The FE simulation images and force–displacement curves associated with egg–box geometries of vertical angle ω=30° have been presented in Figures 5.13 to 5.24 and the curves have been compared among various diameters at 20, 45 and 60mm inter–peak distances and wall thicknesses of 0.8, 1.0 and 1.2mm.

In general, the characteristics observed with the previous category of egg–box structures also apply to this group. However, attributes specific to the models with (ω) of 30° will be discussed following the presentation of the force–displacement curves.

Similar rules regarding changes in top/base diameter, and their relationship with the inter–peak value, as explained in the previous section apply here and henceforth.

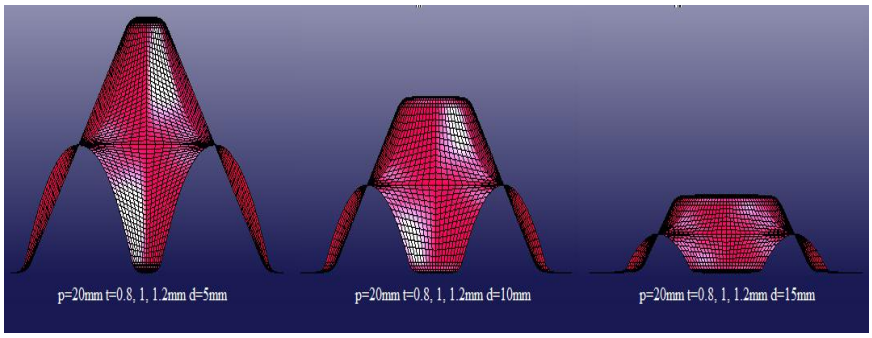

Figure 5.13 – FE Models of ω=30°, p=20mm, t=0.8, 1, 1.2mm for d=5, 10, 15mm

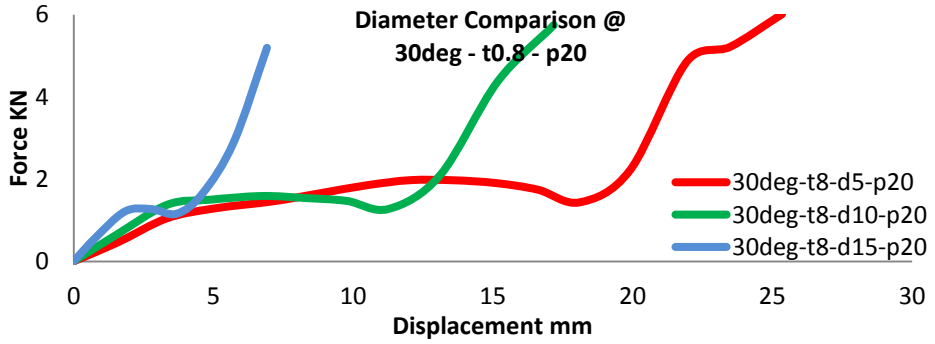

Figure 5.14 – Force vs. Displacement Curves of FE Simulations for ω=30°, t=0.8mm, p=20mm and d=5, 10, 15mm

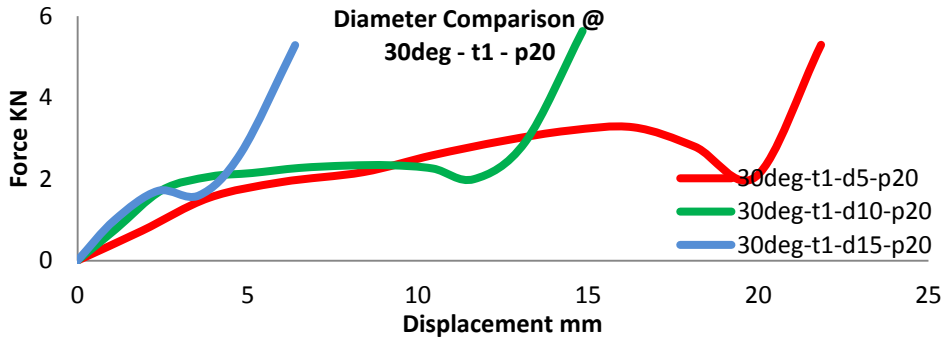

Figure 5.15 – Force vs. Displacement Curves of FE Simulation for ω=30°, t=1mm, p=20mm and d=5, 10, 15mm

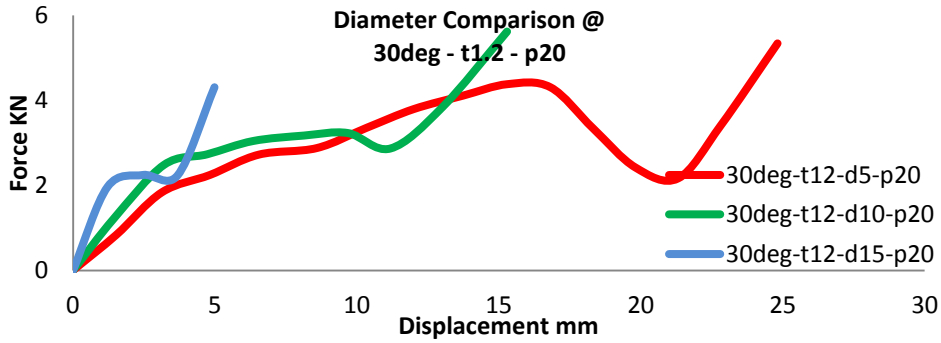

Figure 5.16 – Force vs. Displacement Curves of FE Simulation for ω=30°, t=1.2mm, p=20mm and d=5, 10, 15mm

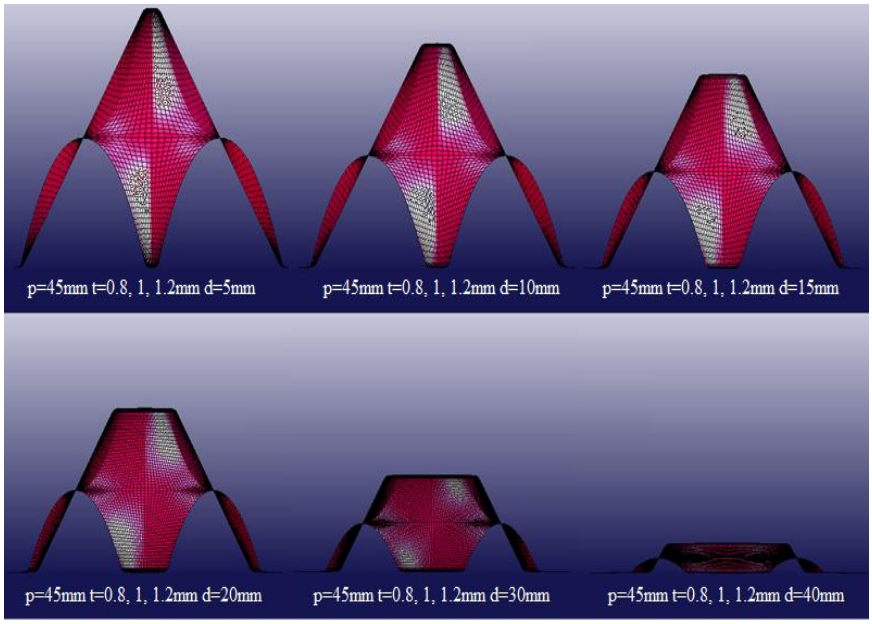

Figure 5.17 – FE Models of ω=30°, p=45mm, t=0.8, 1, 1.2mm for d=5, 10, 15, 20, 30, 40mm

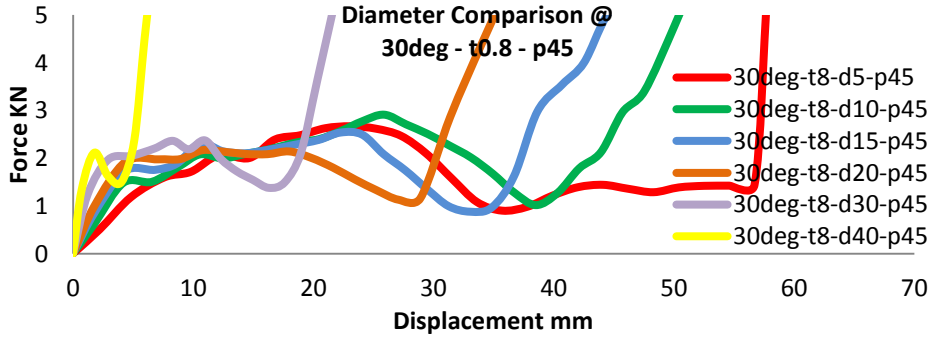

Figure 5.18 – Force vs. Displacement Curves of FE Simulations for ω=30°, t=0.8mm, p=45mm and d=5, 10, 15, 20, 30, 40mm

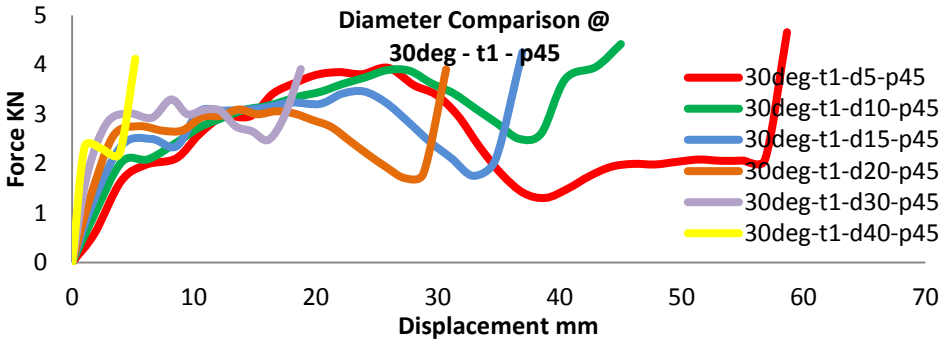

Figure 5.19 – Force vs. Displacement Curves of FE Simulations for ω=30°, t=1mm, p=45mm and d=5, 10, 15, 20, 30, 40mm

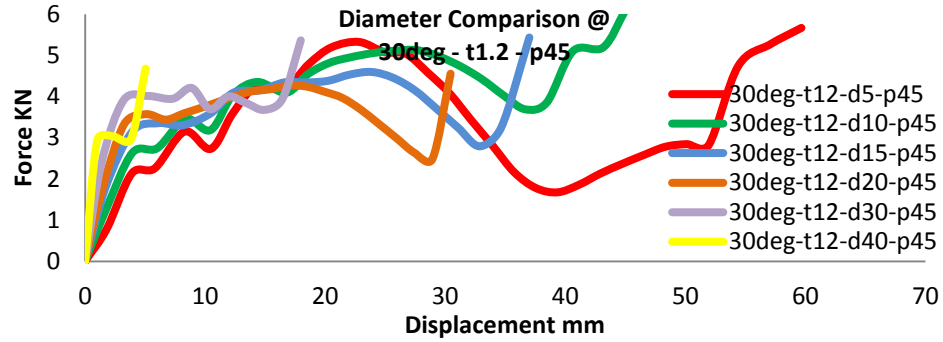

Figure 5.20 – Force vs. Displacement Curves of FE Simulations for ω=30°, t=1.2mm, p=45mm and d=5, 10, 15, 20, 30, 40mm

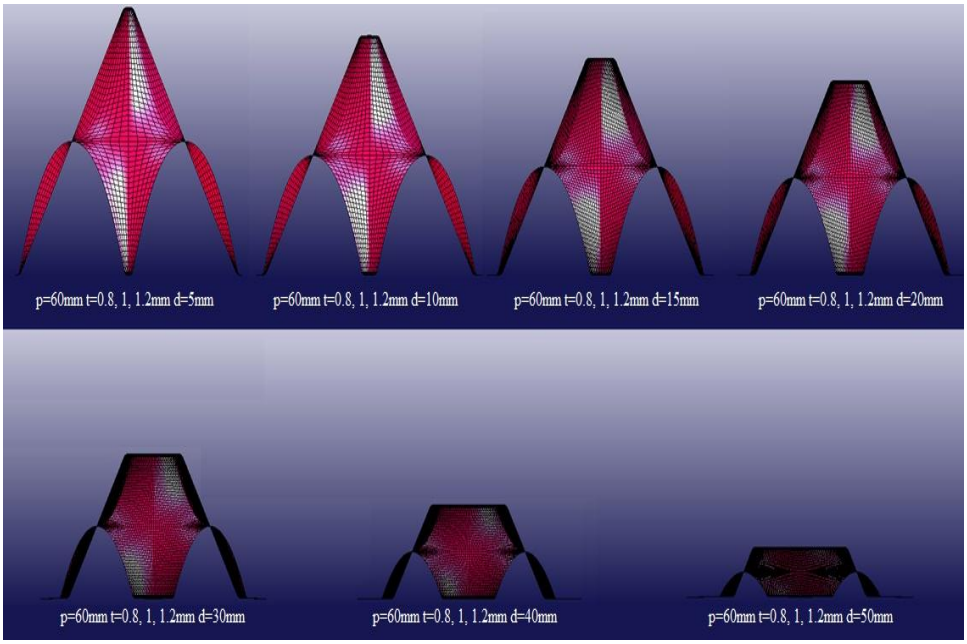

Figure 5.21 – FE Models of ω=30°, p=20mm, t=0.8, 1, 1.2mm for d=5, 10, 15, 20, 30, 40, 50mm

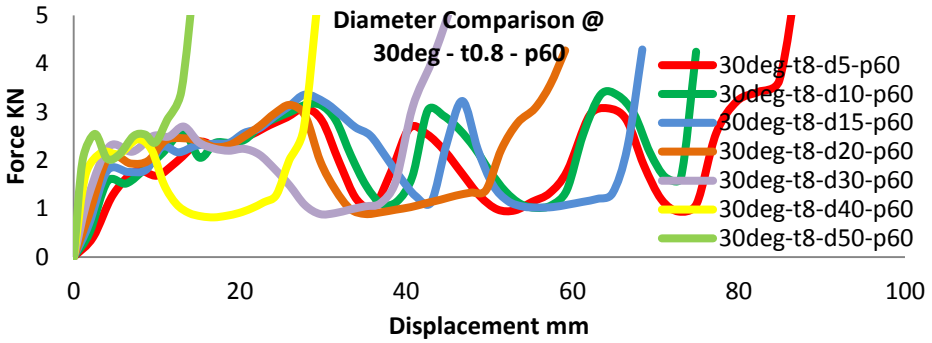

Figure 5.22 – Force vs. Displacement Curves of FE Simulations for ω=30°, t=0.8mm, p=60mm and d=5, 10, 15, 20, 30, 40, 50mm

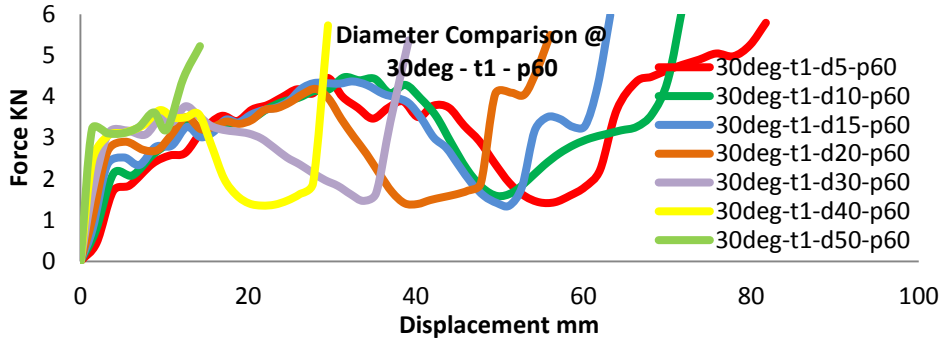

Figure 5.23 – Force vs. Displacement Curves of FE Simulations for ω=30°, t=1mm, p=60mm and d=5, 10, 15, 20, 30, 40, 50mm

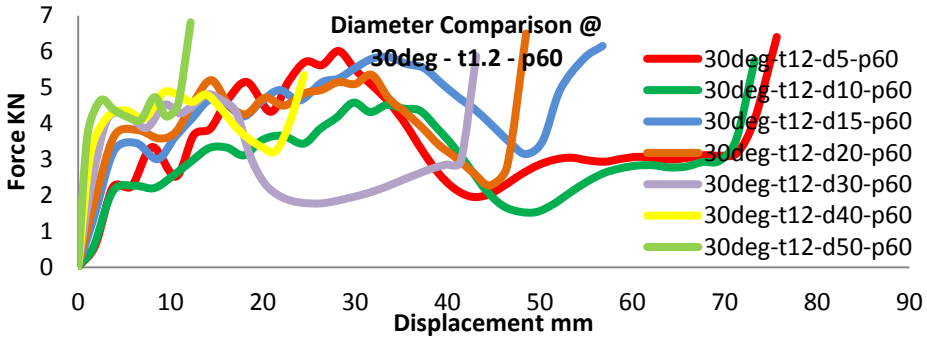

Figure 5.24 – Force vs. Displacement Curves of FE Simulations for ω=30°, t=1.2mm, p=60mm and d=5, 10, 15, 20, 30, 40, 50mm

As expected from the previous observations, progressing from Figures 5.14–5.16 to Figures 5.18–5.20 and finally to Figures 5.22–5.24, it can be seen that an increase in (p) results in a lengthier load–displacement plateau while it

simultaneously increases the level of the initial contact load. In addition, curve sets of each Figure, from 5.14 to 5.24, show that, smaller top/base diameters increase the length of the deformation, leaving the peak load level almost intact.

Upon comparing the characteristics of curves of Figures 5.2–5.12 with curves of Figures 5.14–5.24, it can be seen that the mentioned changes are constant between the two apical angles reviewed so far. Evaluating the models of similar diameter, thickness and inter–peak distance between ω=30° and ω=15°, reveals that with an increase in the apical angle the deformation length decreases. This is caused by a reduction in height which occurs in geometries with larger angles. In other words, there is a shorter structural depth to be deformed and hence less energy would be absorbed. On the other hand, models with the greater angle show smaller peak load values as opposed to their otherwise geometrically similar counterparts.

5.4.3. Geometrical Variations at ω=45°

Figures 5.25 to 5.36, presented in this section, illustrate images and curves linked with the egg–box models having a vertical apical angle measurement of 45°. Cells of various diameters have been compared for 9 combinations consisting of 20, 45 and 60mm inter–peak distances and of 0.8, 1.0 and 1.2mm wall thicknesses.

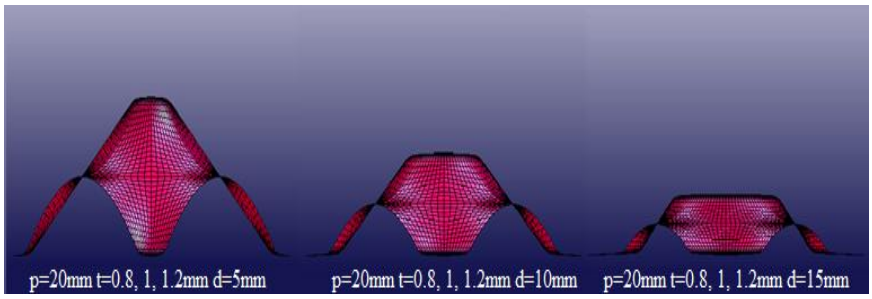

Figure 5.25 – FE Models of ω=45°, p=20mm, t=0.8, 1, 1.2mm for d=5, 10, 15mm

The curves belonging to this group are expected to display peak load and plateau variations similar to that of models with smaller angles presented in Figures

5.2 to 5.24. The performance of these models will be compared to the previous combinations following Figure 5.36.

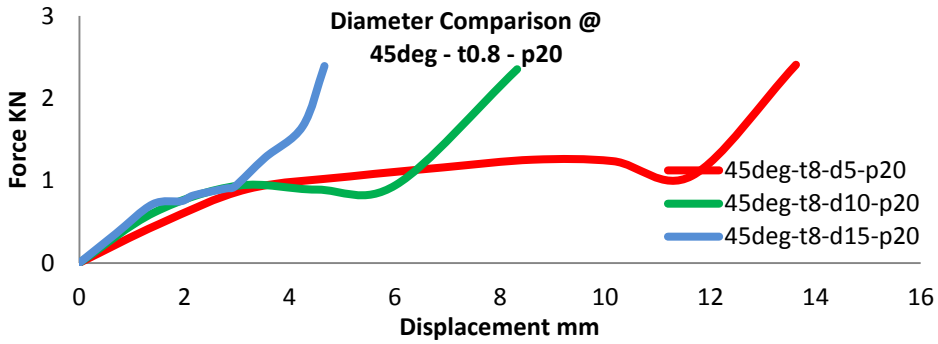

Figure 5.26 – Force vs. Displacement Curves of FE Simulations for ω=45°, t=0.8mm, p=20mm and d=5, 10, 15mm

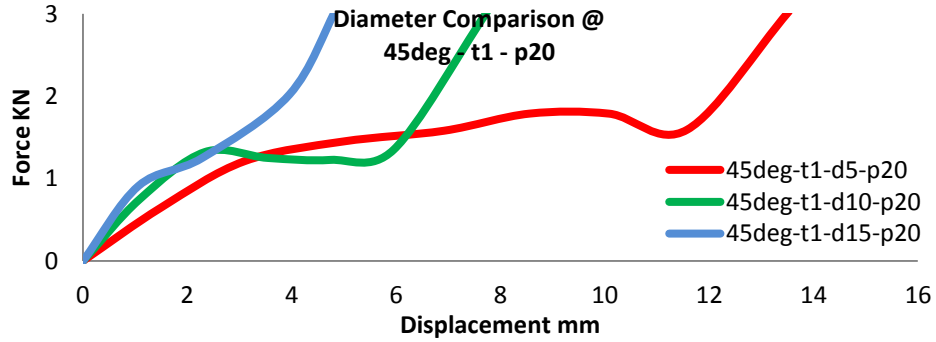

Figure 5.27 – Force vs. Displacement Curves of FE Simulation for ω=45°, t=1mm, p=20mm and d=5, 10, 15mm

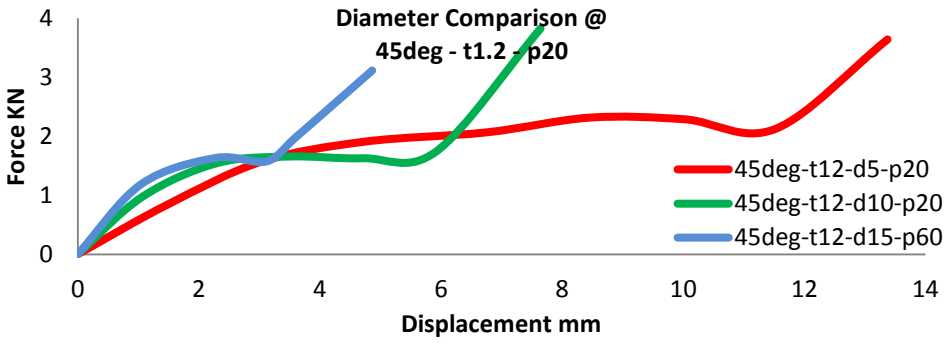

Figure 5.28 – Force vs. Displacement Curves of FE Simulation for ω=45°, t=1.2mm, p=20mm and d=5, 10, 15mm

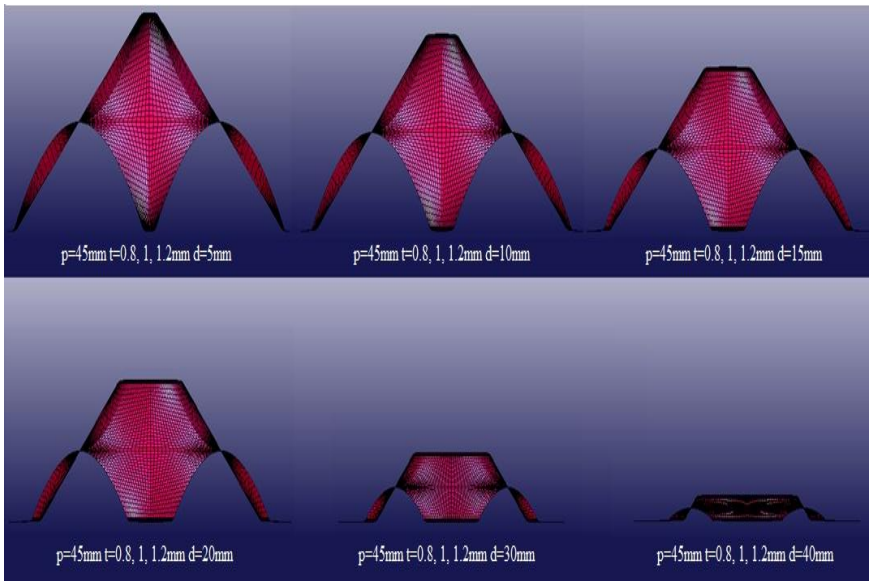

Figure 5.29 – FE Models of ω=45°, p=20mm, t=0.8, 1, 1.2mm for d=5, 10, 15, 20, 30, 40mm

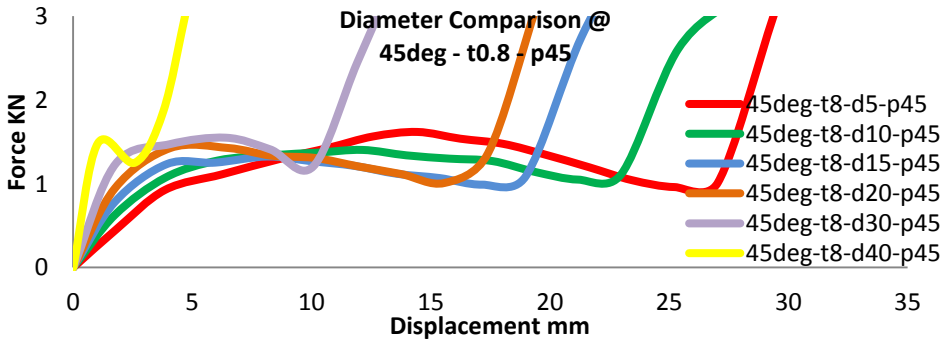

Figure 5.30 – Force vs. Displacement Curves of FE Simulations for ω=45°, t=0.8mm, p=45mm and d=5, 10, 15, 20, 30, 40mm

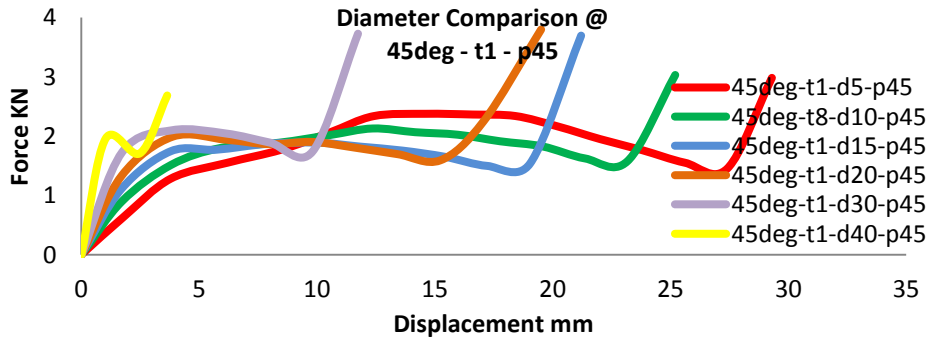

Figure 5.31 – Force vs. Displacement Curves of FE Simulations for ω=45°, t=1mm, p=45mm and d=5, 10, 15, 20, 30, 40mm

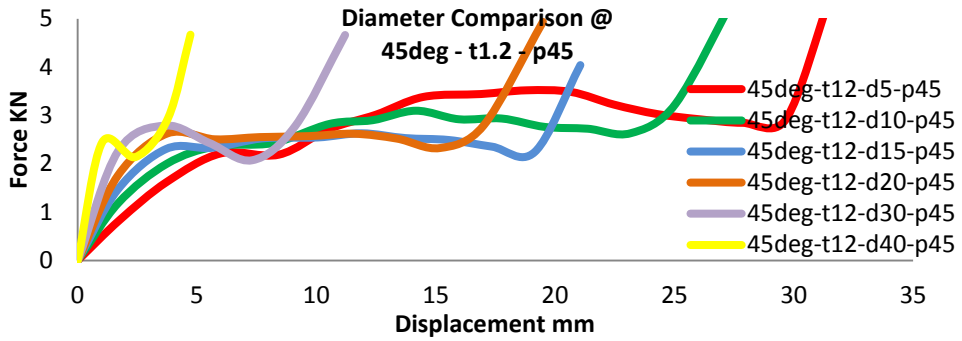

Figure 5.32 – Force vs. Displacement Curves of FE Simulations for ω=45°, t=1mm, p=45mm and d=5, 10, 15, 20, 30, 40mm

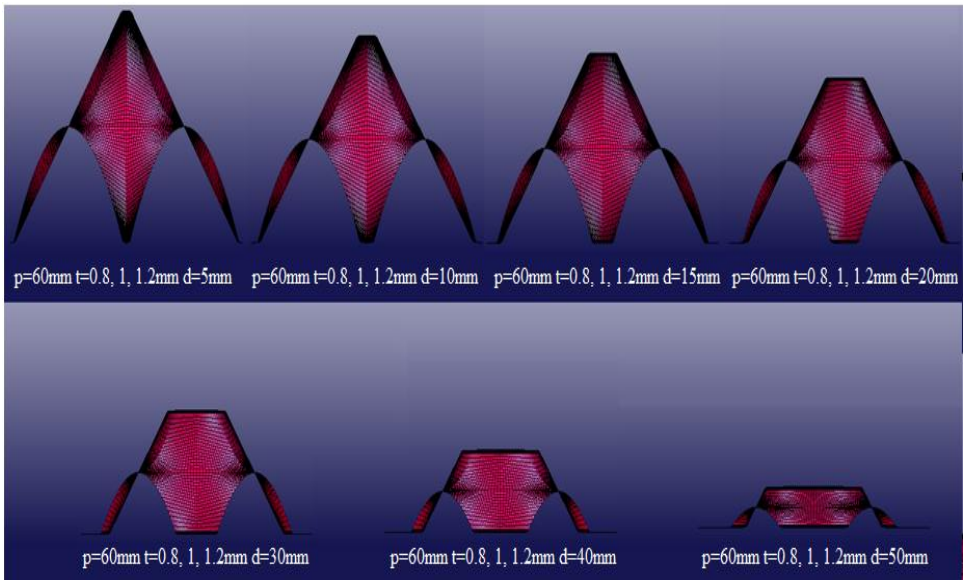

Figure 5.33 – FE Models of ω=45°, p=20mm, t=0.8, 1, 1.2mm for d=5, 10, 15, 20, 30, 40, 50mm

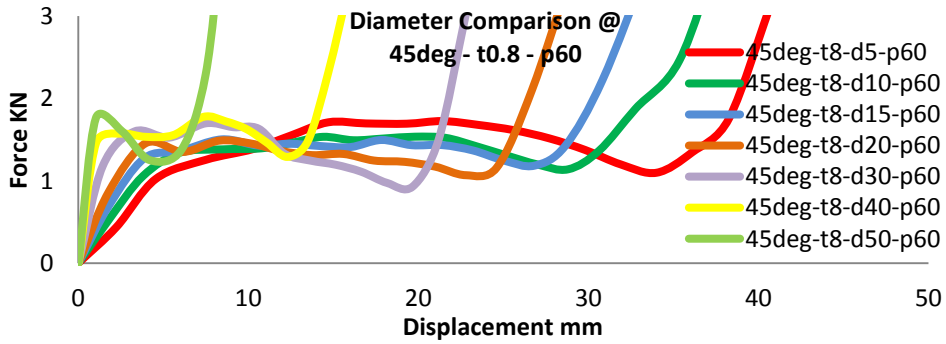

Figure 5.34 – Force vs. Displacement Curves of FE Simulations for ω=45°, t=0.8mm, p=60mm and d=5, 10, 15, 20, 30, 40, 50mm

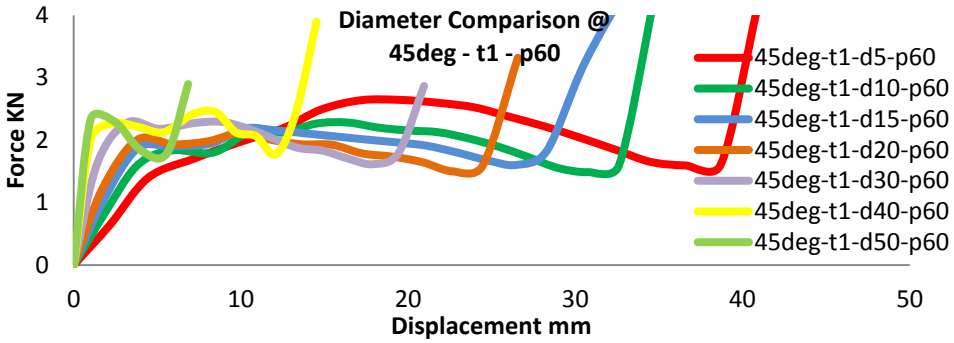

Figure 5.35 – Force vs. Displacement Curves of FE Simulations for ω=45°, t=1mm, p=60mm and d=5, 10, 15, 20, 30, 40, 50mm

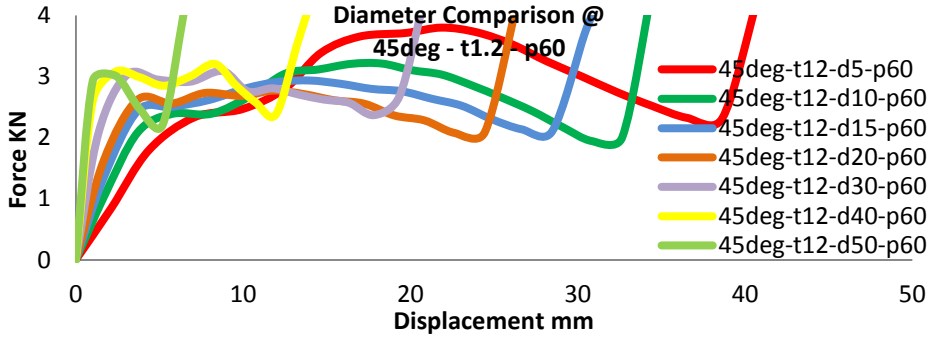

Figure 5.36 – Force vs. Displacement Curves of FE Simulations for ω=45°, t=1.2mm, p=60mm and d=5, 10, 15, 20, 30, 40, 50mm

It can be noted from the curves presented in Figures 5.26 to 5.36 that increasing the peak to peak distance enhances the energy absorption capacity of the egg–box, displayed by an increase in the length of the force–displacement plateau. As an adverse effect, however, the peak load becomes elevated with this change in the peak distance, practically increasing the initial damage to the protected body. Both effects can be sensed from a review of Figures 5.28, 5.32 and 5.36 as an example.

The changes in the measurement of the diameter are diversely related to the length of the plateau. An individual review of Figures 5.26 to 5.36 shows that with larger diameters, shorter deformation lengths occur at approximately the same load level. This is due to the reduction in the height of the cell.

A comparison between Figures 5.26–5.36 and models of ω=30° (Figures 5.14–5.24) and ω=15° (Figures 5.2–5.12) indicates that amongst models of similar

thickness, inter–peak distance and diameter, those with smaller angles, i.e. more elevated height, show greater strength. The load–displacement curves of the stronger models bend at higher load levels and reach their densification point at longer displacement measures.

5.4.4. Geometrical Variations at ω=60°

The next geometrical alteration according to Table 5.1 would be to increase the apical angle to a value of 60°. With the definition of the apical angle being the angle between the walls of the structure and the vertical axis, an (ω) of 60° indicates a flatter build as opposed to the previous models. It is, therefore, expected from this group to have shorter deformation lengths due to their decreased heights.

Based on the force–displacement curves presented in Figures 5.38 to 5.48, an assessment can be made of the effects of changing other geometrical components on the performance of the models with a 60° apical angle. The curves are associated with models having inter–peak measurements of 20, 45 and 60mm and ranging between 0.8, 1.0 and 1.2mm wall thicknesses. Figures 5.37, 5.53 and 5.57 show the finite element models for the geometries under investigation.

Evaluating the curves of Figures 5.38 to 5.48 against the curves previously introduced (Figures 5.2 to 5.36) gives an indication of the difference in behaviour of ω=60° models and models with smaller apical angles.

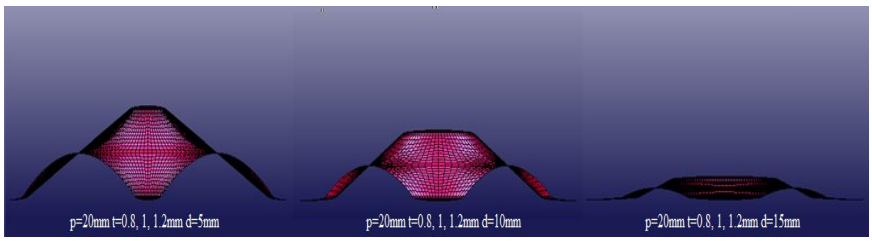

Figure 5.37 – FE Models of ω=60°, p=20mm, t=0.8, 1, 1.2mm for d=5, 10, 15mm

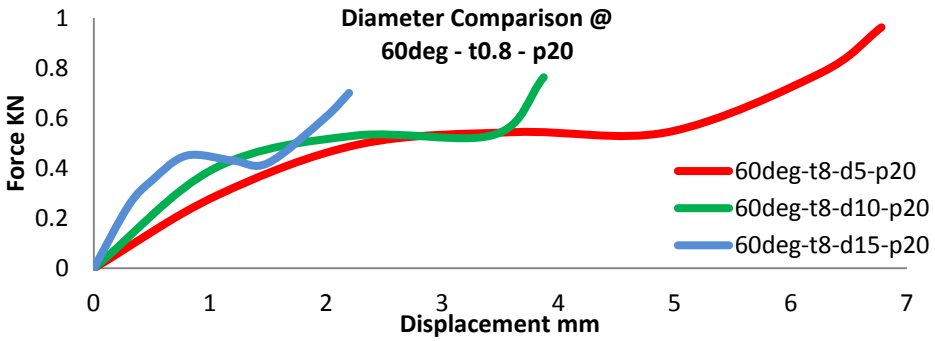

Figure 5.38 – Force vs. Displacement Curves of FE Simulations for ω= 60°, t=0.8mm, p=20mm and d=5, 10, 15mm

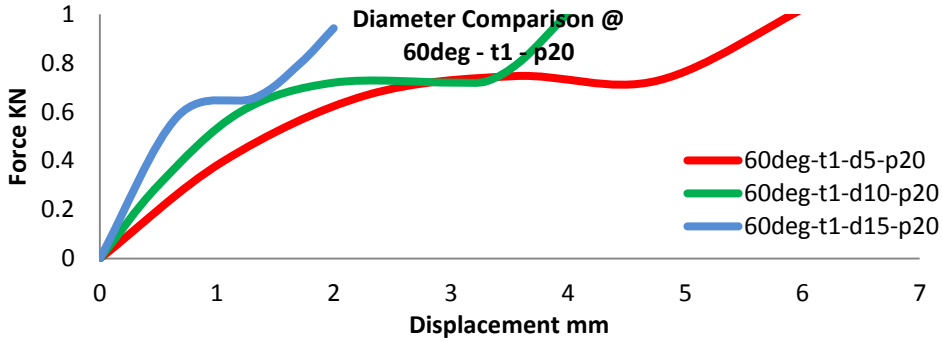

Figure 5.39 – Force vs. Displacement Curves of FE Simulation for ω=60° t=1mm, p=20mm and d=5, 10, 15mm

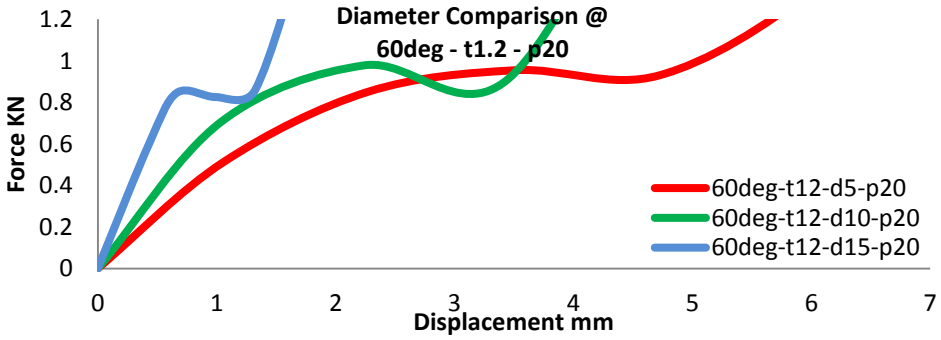

Figure 5.40 – Force vs. Displacement Curves of FE Simulation for ω=60°, t=1.2mm, p=20mm and d=5, 10, 15mm

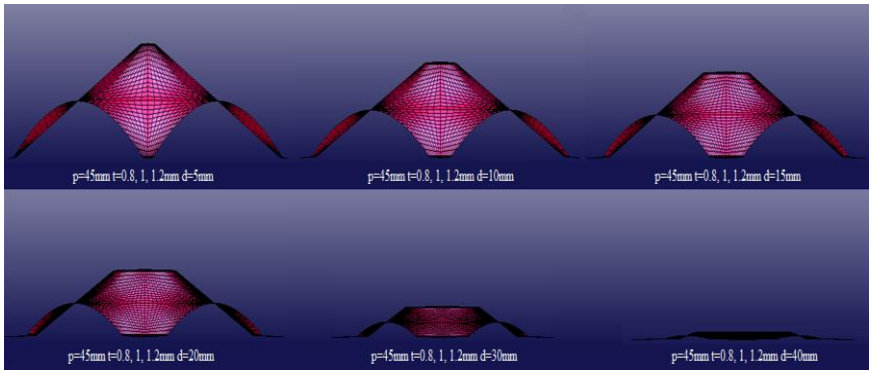

Figure 5.41 – FE Models of ω=60°, p=45mm, t=0.8, 1, 1.2mm for d=5, 10, 15, 20, 30, 40mm

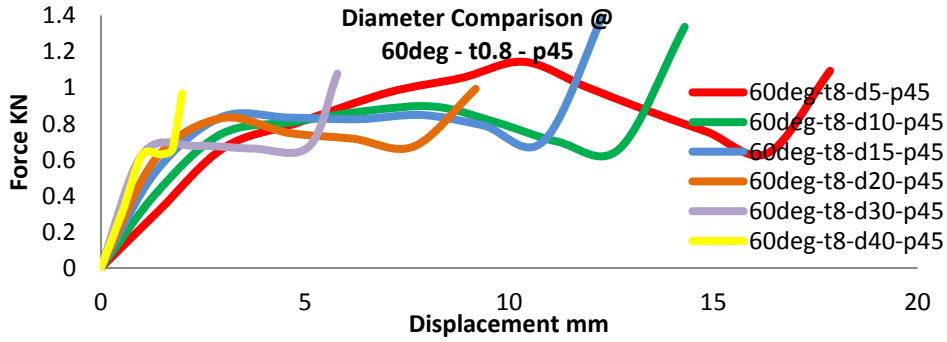

Figure 5.42 – Force vs. Displacement Curves of FE Simulations for ω=60°, t=0.8mm, p=45mm and d=5, 10, 15, 20, 30, 40mm

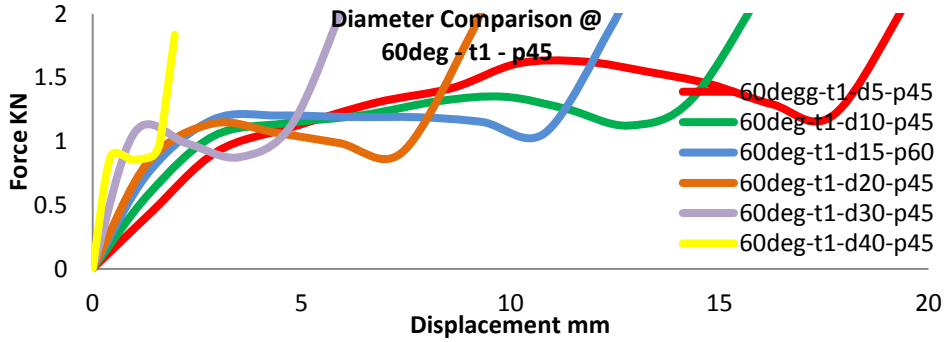

Figure 5.43 – Force vs. Displacement Curves of FE Simulations for ω=60°, t=1mm, p=45mm and d=5, 10, 15, 20, 30, 40mm

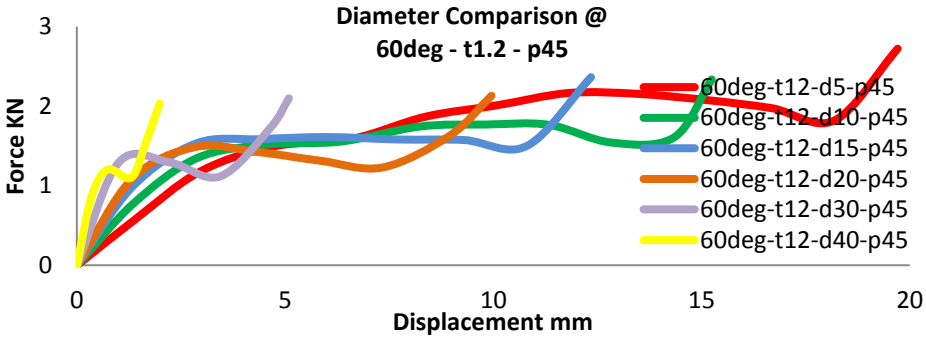

Figure 5.44 – Force vs. Displacement Curves of FE Simulations for ω=60°, t=1.2mm, p=45mm and d=5, 10, 15, 20, 30, 40mm

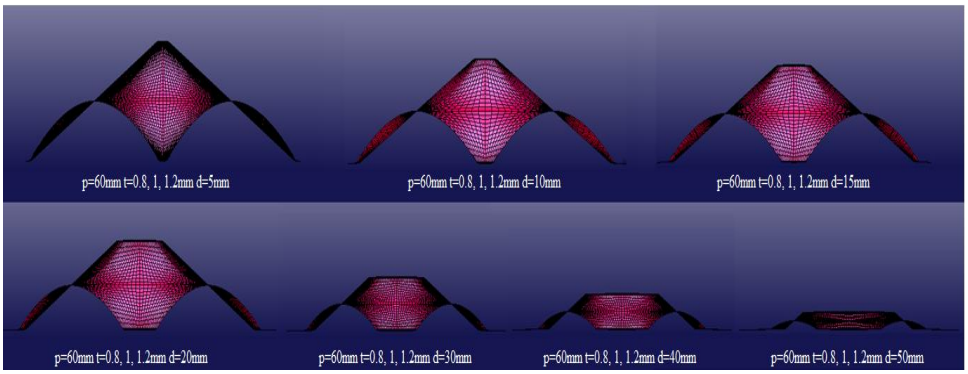

Figure 5.45 – FE Models of ω=60°, p=60mm, t=0.8, 1, 1.2mm for d=5, 10, 15, 20, 30, 40, 50mm

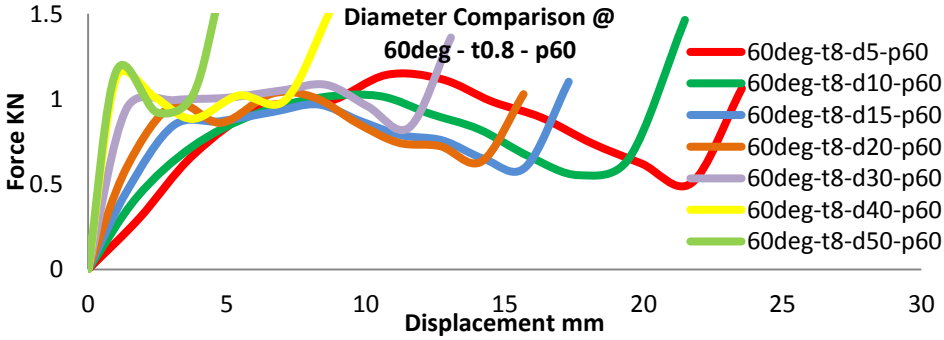

Figure 5.46 – Force vs. Displacement Curves of FE Simulations for ω=60°, t=0.8mm, p=60mm and d=5, 10, 15, 20, 30, 40, 50mm

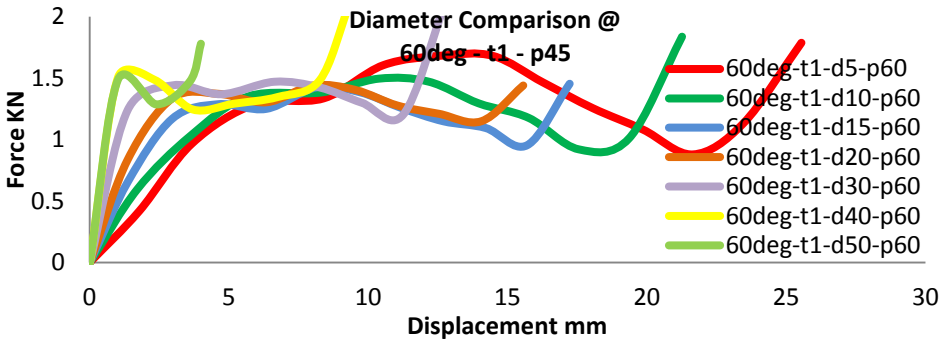

Figure 5.47 – Force vs. Displacement Curves of FE Simulations for ω=60°, t=1mm, p=45mm and d=5, 10, 15, 20, 30, 40, 50mm

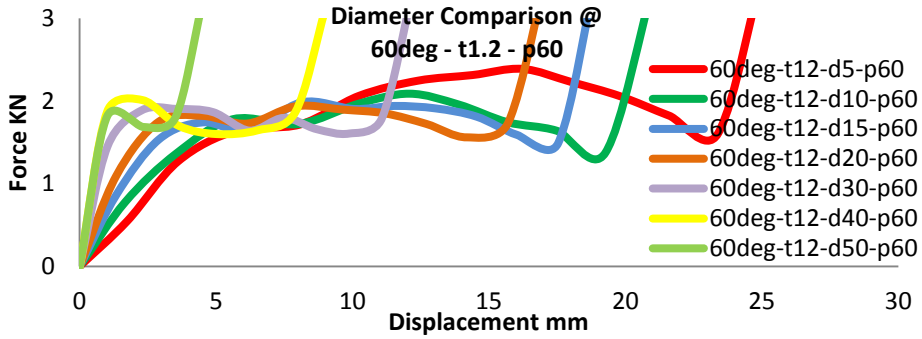

Figure 5.48 – Force vs. Displacement Curves of FE Simulations for ω=60°, t=1.2mm, p=60mm and d=5, 10, 15, 20, 30, 40, 50mm

It can be seen from the curves of Figures 5.38 to 5.48 that the energy absorption capacity of the cells becomes elevated in cells with more distant peaks according to the curves above. However, the same alteration increases the damaging effect of the initial impact. For example, in Figures 5.44 and 5.48 which give the force–displacement response of cells with identical apical angle and wall thicknesses, it can be viewed that the 5mm diameter geometry with 45mm inter–peak distance has a shorter deformation length, almost 18mm, while the cell with the same diameter at inter–peak distances of 60mm has a deformation length of around 23mm. The cell with shorter inter–peak distance, Figure 5.44, has an initial peak load value of 1.3kN in comparison to the geometry with longer peak to peak distance, Figure 5.48, which shows an initial load value of more than 1.5kN.

An assessment of the diametrical alterations amongst models presented in Figures 5.38 to 5.48 shows that as the top of a cell expands, its energy absorption

capacity decreases. In curve of Figure 5.39, for example, it can be seen that cells with greater (d) values have shorter force–displacement lengths. The reason behind this characteristic is the shorter cell height of the geometries with larger diameters in cells of equal (ω), (p) and (t). In additions, it can be observed from Figure 5.39, that changing the diameter has very minimal effect on the peak load value of the cells, since the apical angle and the inter–peak distance remain constant between these models.

A lower level of structural strength is exhibited in models of Figures 5.38 to 5.48 which have larger angles between the cell wall and the vertical line. Such behaviour is resulted from the decrease in the height of models with larger (ω) values. From the geometrical point of view, this can be justified by explaining that in egg–box cells of equal inter–peak distances and peak/trench diameters, larger apical angles mean shorter distances from centre to peak. Hence, models with ω=60° absorb less energy than cells of 15°, 30° and 45° apical angles presented in Figures 5.2–5.12, 5.14–5.24 and 5.26–5.36, respectively.

The peak load value also drops with larger angles which on the contrary to the decrease in energy absorption, is a positive effect in the performance of an egg–box structure. Therefore, geometries with larger apical angles are more desirable in the initial stage of an impact.

5.4.5. Geometrical Variations at ω=75°

In the process of evaluating the effect of the alterations of geometrical factors on the performance of egg–box energy absorbers, the value of apical angle (ω) is gradually increased to take a final value of 75°. Further increasing this component will result in cell models with practically flat geometrical shapes, considering the wall thickness of the egg–box cell. The (h) values of Table 5.1 support this theory.

The curves included in Figures 5.50 to 5.60 are linked with models categorised under ω=75°. Cells of 20, 45 and 60mm inter–peak distances and 0.8, 1.0 and 1.2mm wall thicknesses have been modelled for 5, 10, 15, 20, 30, 40 and 50mm top/base diameters. The curves produced here are results of finite element simulations solved

for the axial impacting of all the defined geometrical combinations. Images associated with the finite element models of this section are provided in Figures 5.49, 5.53 and 5.57 for p=20, 45 and 60mm, respectively.

The resultant curves of ω=75° group, Figures 5.50 to 5.60, are compared with the outcomes of the previous groups, Figures 5.2 to 5.48, to give an indication of the difference in behaviour of egg–box cells with altered geometrical features.

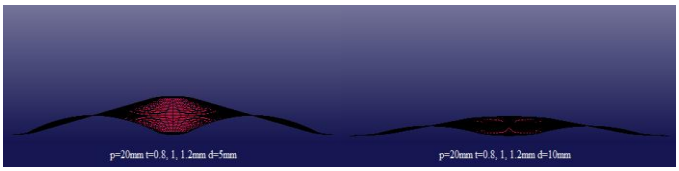

Figure 5.49 – FE Models of ω=55°, p=20mm, t=0.8, 1, 1.2mm for d=5, 10mm

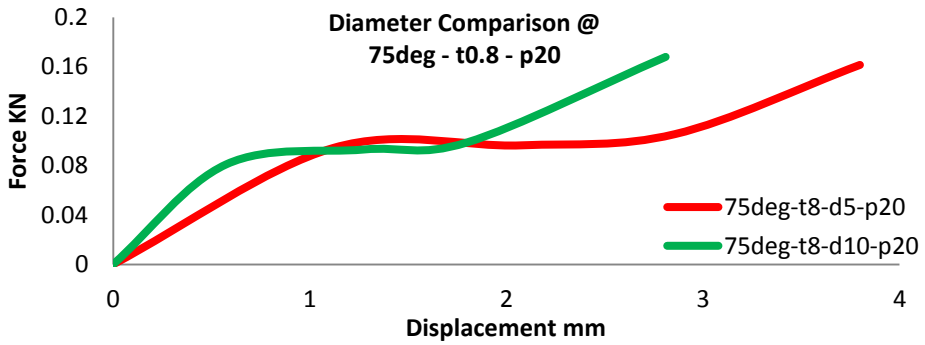

Figure 5.50 – Force vs. Displacement Curves of FE Simulations for ω=75°, t=0.8mm, p=20mm and d=5, 10mm

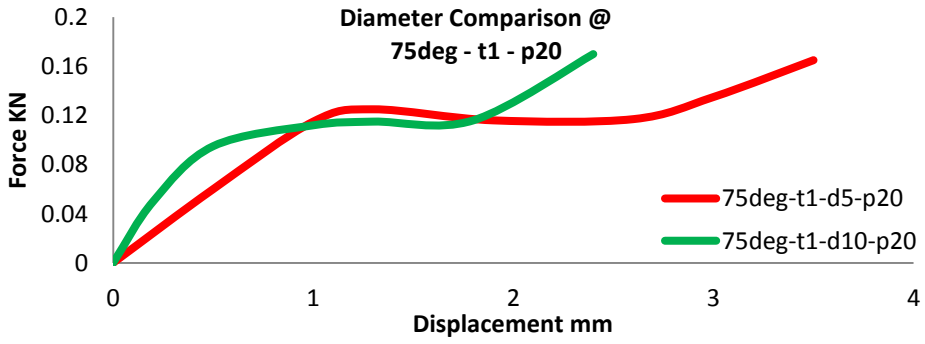

Figure 5.51 – Force vs. Displacement Curves of FE Simulation

for ω=75°, t=1mm, p=20mm and d=5, 10mm

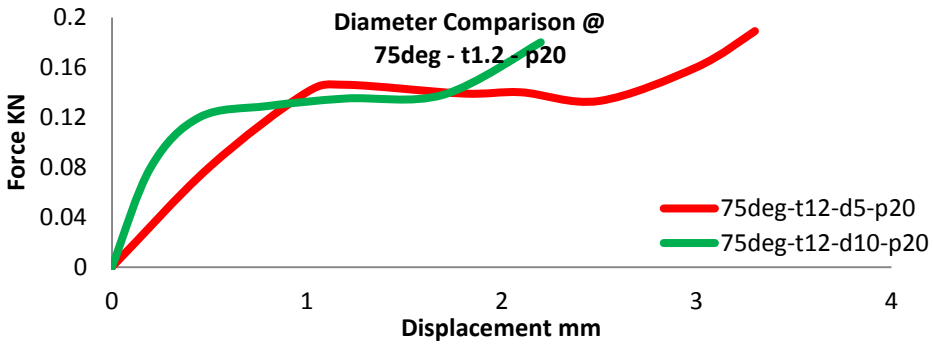

Figure 5.52 – Force vs. Displacement Curves of FE Simulation for ω=75°, t=1.2mm, p=20mm and d=5, 10mm

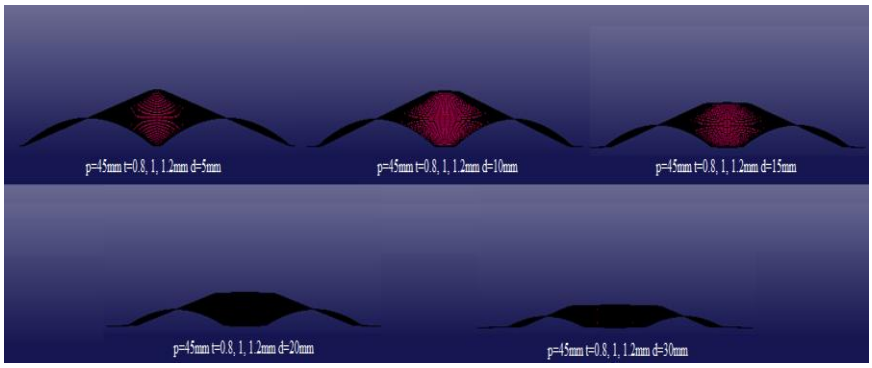

Figure 5.53 – FE Models of ω=75°, p=45mm, t=0.8, 1, 1.2mm for d=5, 10, 15, 20, 30mm

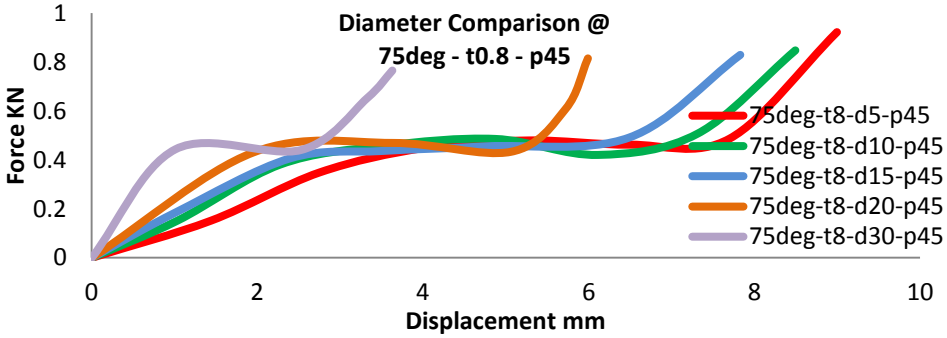

Figure 5.54 – Force vs. Displacement Curves of FE Simulations for ω=75°, t=0.8mm, p=45mm and d=5, 10, 15, 20, 30mm

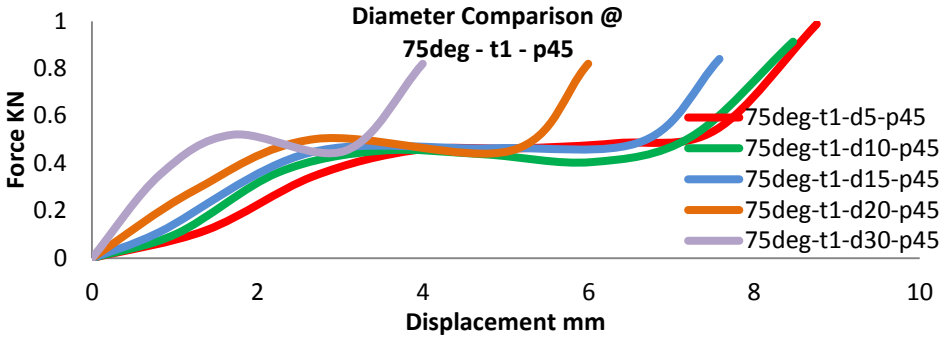

Figure 5.55 – Force vs. Displacement Curves of FE Simulations for ω=75°, t=1mm, p=45mm and d=5, 10, 15, 20, 30mm

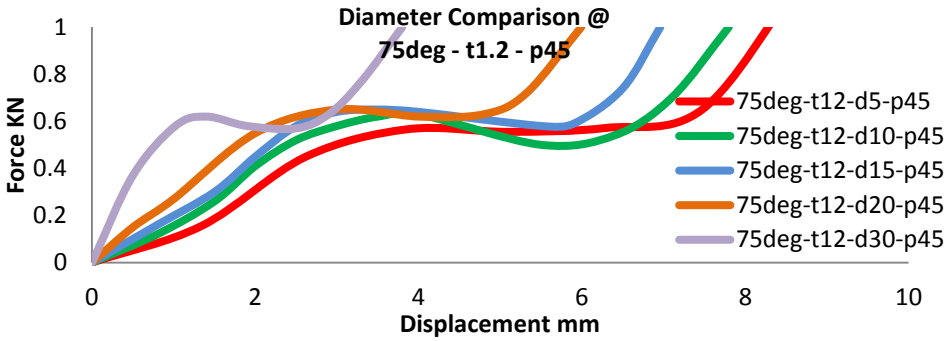

Figure 5.56 – Force vs. Displacement Curves of FE Simulations for ω=75°, t=1.2mm, p=45mm and d=5, 10, 15, 20, 30mm

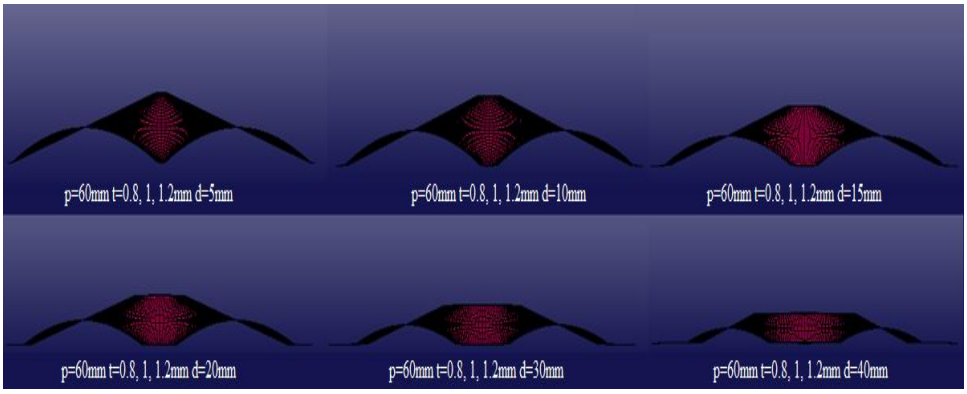

Figure 5.57 – FE Models of ω=75°, p=20mm, t=0.8, 1, 1.2mm for d=5, 10, 15,20, 30, 40mm

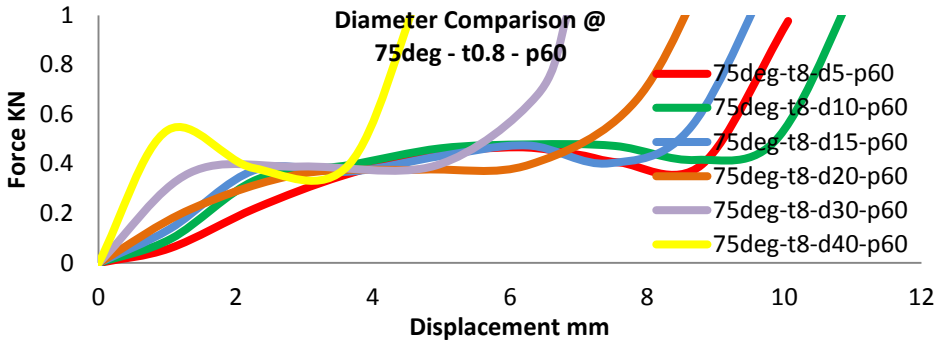

Figure 5.58 – Force vs. Displacement Curves of FE Simulations for ω=75°, t=0.8mm, p=60mm and d=5, 10, 15, 20, 30, 40mm

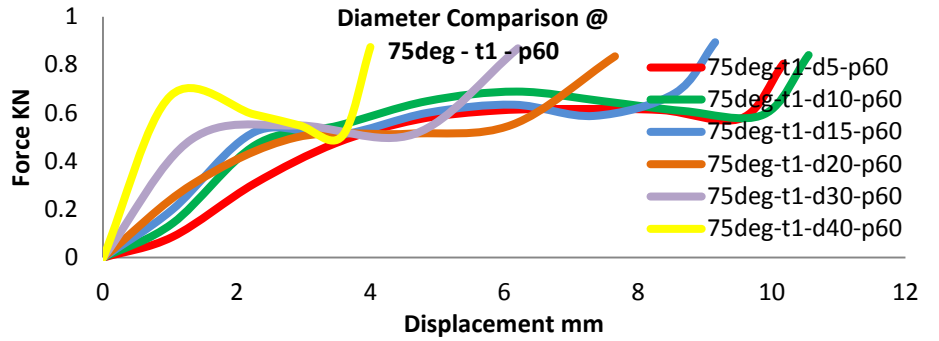

Figure 5.59 – Force vs. Displacement Curves of FE Simulations for ω=75°, t=1mm, p=60mm and d=5, 10, 15, 20, 30, 40mm

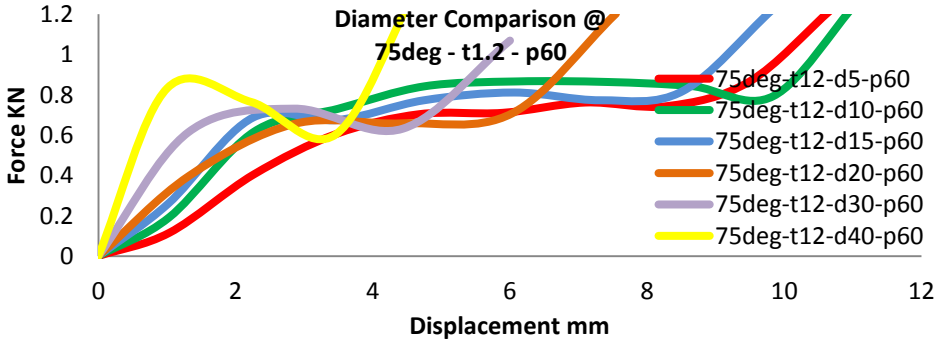

Figure 5.60 – Force vs. Displacement Curves of FE Simulations for ω=75°, t=1.2mm, p=60mm and d=5, 10, 15, 20, 30, 40mm

As previously explained, the large apical angle of this group of egg–box cells results in shorter cell heights, hence, for each set of geometries categorised under the

same (*p*) value, the top/base diameter factor is reduced to one less than the groups with smaller apical angles. Cell heights shorter than 1mm are invalid since with the largest thickness value of the egg–box walls being 1.2mm, a maximum of 0.6mm thickness will be below the central line of the cell wall. For smaller heights, the panel will act as a solid flat aluminium sheet with no significant energy absorption characteristics.

According to curves of Figures 5.50 to 5.60, the change in the peak load value for different thicknesses is very small in the current group due to their miniature structural dimensions. For example the comparison of Figures 5.54, 5.55 and 5.56 shows that the initial peak value is changing between 0.4 to 0.6kN while the deformation length remains the same.

A review of Figures 5.54 and 5.58 shows the direct effect of increasing the inter–peak value on the deformation length and the direct but negative effect of this increase on the initial peak load. It can also be seen in all figures that, as expected, larger peak/trench diameters result in shorter deformation lengths, hence lower energy absorption capacity.

An assessment of the final series of curves, presented in Figures 5.50 to 5.60, indicates that all the characteristics displayed by the previous geometrical models are being reflected in this group. It can, therefore, be proven that, regardless of the cell dimensions, a unique path of geometrical alterations results in energy absorption characteristics that can be predicted and evaluated.

5.5. Observation and Discussion of Results

Through a review of the curves presented in Figures 5.2 to 5.60, a series of general attributes can be deduced. The values given in Table 5.2 represent the area under the curves of the above figures which is equal to E_{Total}, the total amount of energy absorbed by each structure during the impact. Through a comparative study of the curves and their associated E_{Total} values, the effect of geometrical dimensions on the energy absorption of the egg-box structure can be evaluated.

Total Energy (kN.mm)

ω (deg)	15°									30°									45°									60°									75°								
t (mm)	0.8			1			1.2			0.8			1			1.2			0.8			1			1.2			0.8			1			1.2			0.8			1			1.2		
p (mm)	20	45	60	20	45	60	20	45	60	20	45	60	20	45	60	20	45	60	20	45	60	20	45	60	20	45	60	20	45	60	20	45	60	20	45	60	20	45	60	20	45	60	20	45	60
d (mm)=5	53	166	238	126	187	275	165	232	333	32	105	188	40	154	200	63	187	216	12	41	63	17	55	82	21	73	99	2.5	15	17	3.5	25	27	4.1	31	45	0.28	3.4	3.8	0.32	3.6	5.5	0.38	4.3	7.0
10	45	156	230	96	168	257	128	213	324	23	80	173	26	133	181	35	152	196	5.7	34	54	9.0	45	67	11	60	83	1.8	10	15	2.5	17	22	2.7	24	37	0.17	2.8	3.4	0.20	3.1	5.0	0.23	3.9	6.3
15	24	140	204	38	150	240	50	195	303	8.0	68	161	8.4	99	180	10	125	187	3.0	27	41	4.5	36	57	5.7	45	73	0.8	8.8	12	1.1	14	19	1.2	19	32		2.4	3.2		3.3	4.0		3.6	5.6
20		120	180		135	226		189	291		52	127		78	165		99	175		20	36		30	50		40	60		6.2	11		8.4	17		11	29		2.0	2.6		2.3	3.0		3.0	3.6
30		78	148		80	202		148	230		32	84		51	91		60	120		15	30		18	39		24	45		3.5	9.9		4.4	13		5.2	21		1.0	2.0		1.2	2.2		1.5	2.5
40		34	96		48	141		50	133		7	38		11	73		14	88		3.8	21		5.0	26		6.3	36		1.4	7.0		2.0	11		1.7	15			1.2			1.9			2.1
50			58			84			120			22			30			45			8.5			11			16		4.0			3.3			5.7									

Table 5.2 – Estimated Area under the Curve Representing E_{Total} for Geometrically Varied Egg–box Structures

By translating a curve pattern into practical deformation behaviour, it can be seen that a great peak load shows the presence of a high magnitude reaction force. The effect of this load can primarily cause severe damage to the protected body, followed by which the structure slides through a relatively smooth deformation procedure, lengthier with greater (p) values. As mentioned previously, the length of the deformation procedure of a structure has a direct relationship with its energy absorption capacity.

The opposite relationship between the minimised peak load and maximised deformation length can more clearly be seen through the curves of Figures 5.2 to 5.60. Hence, based on the specific requirements of a structure, a panel must be selected with an appropriate level of each of these characteristics, bearing in mind the level of required energy absorption capacity. This situation can be addressed through a simple mathematical explanation.

It has so far been established that the total energy absorbed by a structure is equal to the area below its force–displacement curve. If this area is approximated with a rectangle, it becomes clear that, the longer each length of the shape, the greater the area and hence the more energy absorbed. For example, in Figure 5.59, the area beneath the curve of ω=75°, t=1mm, d=10mm and p=60mm can be approximated by a rectangle of 10mm length by 0.5kN width.

The height of the rectangle represents the initial load peak, which is meant to be kept minimised for practical cushioning. Thus, based on their application, structures with longer deformation curves of lower load magnitudes can be preferable. Based on this theory, geometries with greater (p) values perform more ideally. The curve of ω=75°, t=1mm, d=10mm and p=45mm of Figure 5.55, absorbs an approximate total energy equal to 3.1kN.mm, as calculated in Table 3.2, compared to the 5kN.mm of the above example with a larger (p) value.

Per vertical angle (ω), the same characteristics apply amongst models of different geometrical features. A further step toward optimisation would be the comparison of desirable specimens amongst structures of different angles to clarify the effect of the increase in the vertical angle (ω) of an egg–box cell.

In the light of a comprehensive examination of the result curves comes proof that with more narrow apical angles, higher load peaks are displayed. The length of the deformation grows in an opposite manner to this rule; shorter deformations occurring with wider angles. This is in a sense expected, since as the heights of the egg–box cells decrease and the epical angles become wider, the cell density of the panels reduces.

From a review of the curves given in the figures above, a list of general attributes applicable to all of the modelled egg–box geometries can be deduced;

- In egg–boxes of small vertical angles, with the expansion of the top/base diameters and, as its result, the reduction of cell height, the deformation process of the egg–box becomes shorter.
- The mean level of strength, for diametrically variant models, remains constant.
- With reference to equation 4.10, it can be seen that the total energy absorbed by the structure increases with the increase in thickness.
- Egg–box structures with thicker walls show greater strength, hence, they initiate the deformation process at higher load peaks, which, as previously discussed, can lead to more disastrous bio mechanical injuries when used as human cushions.

5.6. Evaluation of the Effects of Geometrical Variations

From a critical observation of the curves of Figures 5.2 to 5.60, Table 5.3 presented below is derived, giving the effects of geometrical alterations on the performance of the egg–box structure.

Where the arrows are pointing up in the modification row, an increase in the value of the variable is indicated and vice versa. The next two rows show the effect of such increase or decrease, on both parts of the force–displacement response of the

egg–box structure. For instance, with an increase in thickness the level of the peak load rises while the length of the deformation curve remains unchanged.

Geometrical Factor	*t*		*ω*		*p*		*D*	
Modification	↑	↓	↑	↓	↑	↓	↑	↓
Deformation Length	–	–	↓	↑	↑	↓	↓	↑
Peak Load	↑	↓	↓	↑	↑	↓	–	–

Table 5.3 – Effects of Geometrical Changes on Egg–box Performance

The material properties and physical boundaries are assumed to remain constant in this comparison. Therefore, Table 5.3 can be used as a reference source for predicting the general change in behaviour caused by dimensional modifications of the egg–box structures subject to dynamic axial loading.

5.7. Optimised Egg–box Structure

An optimum egg–box structure is required to absorb maximum amount of energy while its initial impact load remains at a reasonably low value. It is evident from the result curves given in graphs of Figures 5.2 to 5.60 that these two requirements have an inverse relationship. Therefore, to find the best egg–box structure, some compromises have to be made on either phenomenon's part.

It has been established that geometries with smaller apical angles display higher plateau lengths and egg–box structures with flat builds, i.e. larger (ω) values, react less aggressively at the initiation of the impact.

Theoretically, it can be said that an egg–box cell which would satisfy both conditions of a crashworthy structure has to have an apical angle of average value. For example, the geometrical combination with ω=45°, t=1.0mm, p=45mm and d=5mm, displays a peak load of 2kN and a deformation length of 25mm. Compared

to the maximum peak load of 6kN in ω=15°, t=1.2mm and p=60mm, the value of 2kN is reasonably low, although it is still much higher than the 0.1kN initial impact load of ω=75°, t=0.8mm and p=20mm. The plateau length of 25mm, however, is rather short in the example model in contrast to the 120mm of ω=15°, t=0.8mm and p=60mm, although it is greater than the 2.5mm deformation length of ω=75°, t=1.2mm and p=20mm.

At a slightly higher peak value of 2.2kN, geometry of ω=30°, t=0.8mm and p=45mm shows a longer plateau length of 58mm. Hence, it could be a better choice towards compromising for optimisation. The geometry has approximately a medium sized apical angle, a thin structure and the expanded panel will have a reasonable cell density. Since the peak load does not practically change with the variations in the top/base diameter, and also because larger deformation lengths are displayed with smaller diameter, the model with d=5mm is assumed to be the most rational option among the available diameters.

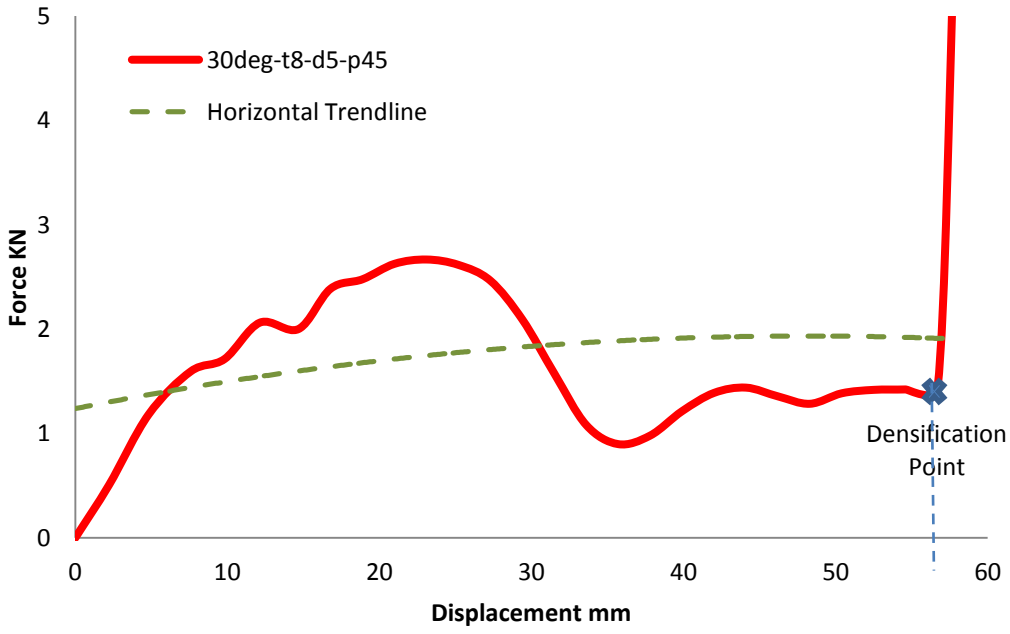

Figure 5.61 – Force–Displacement Curve of ω=30°, t=0.8mm, p=45mm and d=5mm

Despite the fact that the optimisation of energy absorbing structures is mainly linked to the function for which they are designed, for the purpose of this study, it is concluded that the egg–box cell of ω=30°, t=0.8mm, p=45mm and d=5mm performs in a comparatively enhanced manner as opposed to the other geometrical models examined here. The associated curve of this cell model is shown in Figure 5.61.

It can be seen in Fig. 5.61 that the average value of force in the force–displacement curve is approximately 1.5kN which complies with the outcome of equation 5.1, where (F_{Avg}) is required to be less than 3.3kN.

The maximum amount of energy absorbed by the optimised egg–box structure is equal to the area beneath its force–displacement curve up to the densification point, as explained mathematically in equation 4.10 of the thesis. To facilitate such measurements, it would be practical to approximate the enclosed area by a rectangle whose length would be equal to the deformation length in meters and its width would be equal to the average force in kN.

The total energy absorbed by the egg–box panel of ω=30°, t=0.8mm, p=45mm and d=5mm, as shown in Table 5.2, would approximately be equal to E_{total}=105kN.mm. This figure will be proportionately compared against the total energy absorption values of further geometries later in the current chapter following the path of finding optimum structures.

5.8. Optimum Sandwich Structures

An option towards finding the egg–box structure with the highest energy absorption capacity is the combination of two or more geometries in the form of sandwich structures. A sandwich panel can have many forms; from as simple as the addition of thin sheets on the top and base of an egg–box, to an arrangement of several egg–box structures of similar or different geometries, positioned on top of one another along the vertical axis. An egg–box sandwich panel sample is shown in Figure 5.62.

It is obvious that more than one egg–box in a structure would mean more energy absorption. However, as mentioned before, the strongest option is not always

the best and most practical. The rational requirements are for the force–displacement curve to have a low load peak and a lengthy plateau. Therefore, any sandwich combination should be studied to fit the needs of its specific application.

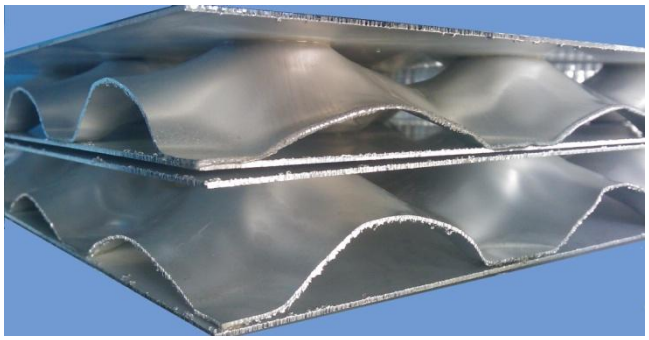

Figure 5.62 – Typical Aluminium Egg–box Sandwich Panel

As a result of a comparative review of Figures 5.2 to 5.60 provided in the previous section, a list of most and least appropriate geometries in terms of both peak load and plateau length is derived and presented in Table 5.4. This can be used to create optimised sandwich panels, by the combination of the aluminium egg–boxes simulated for the purpose of this study.

Aspect	Level	Force kN	Length mm	Geometry
Peak Load	Min	0.1	3	75deg – *t*0.8 – *p*20
	Avg–low	1.5	35	45deg – *t*0.8 – *p*60 @ *d*5
	Mean	2	25	45deg – *t*1.0 – *p*45
	Avg–high	2.2	58	30deg – *t*0.8 – *p*45
	Max	6	110	15deg – *t*1.2 – *p*60
Plateau Length	Min	0.14	2.5	75deg – *t*1.2 – *p*20
	Mean	2	25	45deg – *t*1.0 – *p*45
	Max	2.5	120	15deg – *t*0.8 – *p*60 @ *d*5

Table 5.4 – Egg–box Geometries with Distinctive Performance

The sandwich arrangement can consist of more than two geometries. However, bearing in mind the foremost use of egg–box structures as vehicle parts, combinations of more than two geometries can increase the height (depth) of the sandwich panel to impractically large values. It is important in the optimisation of the egg–box structure for its dimensions and shape to suit its function.

The egg–box sandwich panel can be made by combining the maximum plateau length and the minimum peak load. The setback is the opposite effect of these two factors. For a maximum plateau length, the peak load too rises to an undesired high value and vice versa. Hence, some compromise should be made to find geometries that attain both qualities. The geometries with the mean and average values provided in Table 5.4 satisfy the requirement to a reasonable extent.

In order for the sandwich panel produced to have maximum efficiency, the structures of ω=45°, t=0.8mm, p=60mm, d=5mm and ω=15°, t=0.8mm, p=60mm, d=5mm are selected to provide minimum peak load and maximum plateau length, respectively. The selected cell models have been highlighted in Table 5.4. It can be seen that both structures have the same thickness value; this counts as a facilitating factor in the fabrication of the geometries, serving towards the optimisation target.

When positioned at the top of the sandwich structure, the geometrical features of the model with the low peak load will act towards effectively reducing the damage by absorbing the sudden shock of the impactor. The sandwich structure then follows through an extended deformation procedure as the loads are transferred to the geometry, placed in the lower part of the sandwich.

A finite element model of the above combination is produced in ANSYS/LS–DYNA®. The model goes through the same impact exercise as the rest of the egg–box geometries in order to compare the outcome of this improved model with the result curves previously presented. Figure 5.63 (a) shows a cross section of the finite element model for the proposed sandwich panel. In Figure 5.63 (b) the model has been expanded to enable enhanced visualisation of the simulation. The aluminium sheet, the impactor and the supporting surface have also been scaled accordingly. The actual FE model consists of the single cells of part (a) of Figure 5.63.

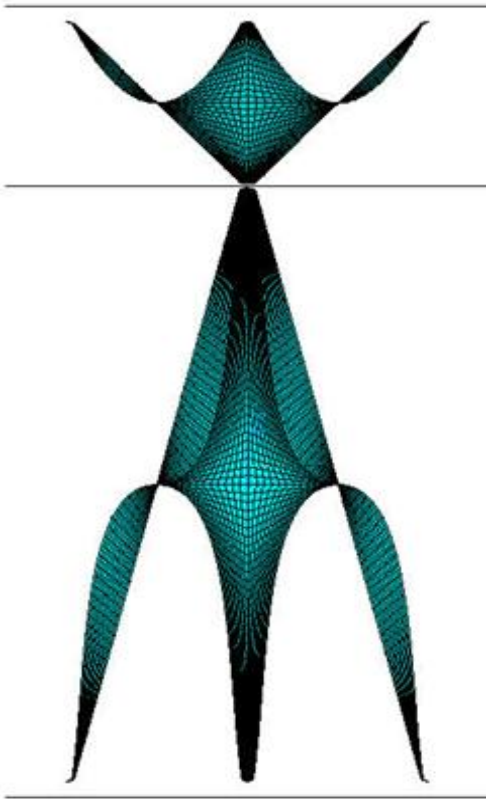

(a) Single Cell Cross Section

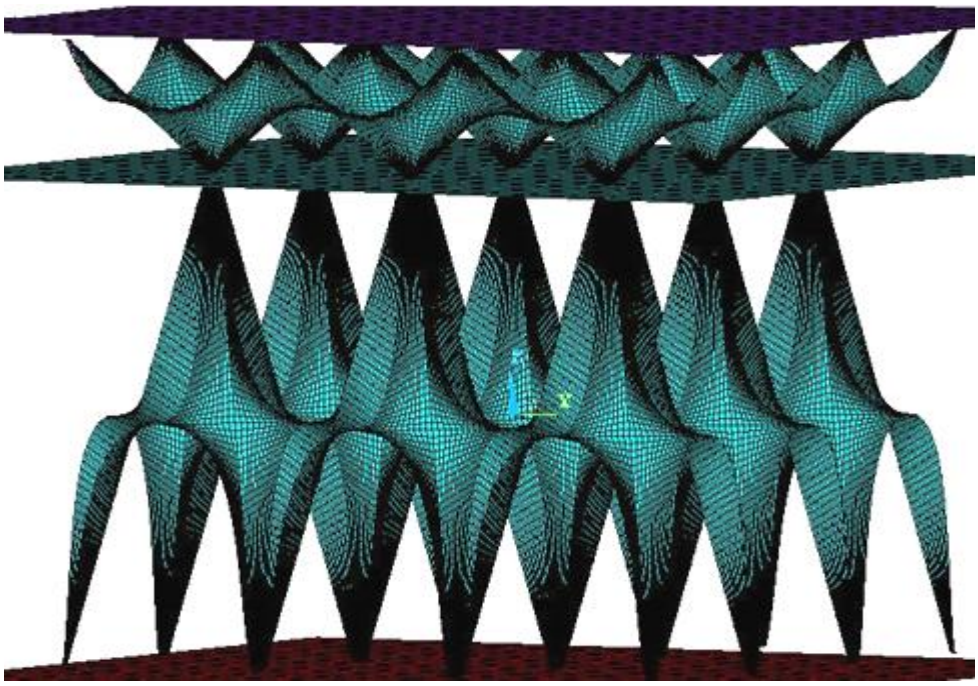

(b) 3D Expanded Sandwich Panel (Total Height of 265mm)

Figure 5.63 – FE Simulation Model of Proposed Sandwich Panel

To avoid unexpected deformations, a thin flat sheet of aluminium is placed between the two geometries as shown in Figure 5.63(a). The boundary conditions remain similar to those applied in the simulation of individual egg–box structures to allow for a true comparison of the outcomes.

Use of resins or welding in the production of the sandwich panel affects its performance and the accuracy of the comparative study of the results. It is therefore assumed that the two geometries and the middle sheet are restricted from movement in all lateral directions and contact conditions are applied to all outer surfaces as in the previous simulations. Hence, a condition in which the panels are boxed in by solid vertical surfaces is simulated.

The aluminium sheet placed between the two geometries has a thickness of 0.8mm, which will immediately deform when subject to forces, due to its flat, thin geometry. Thus, while keeping the geometries in their correct position, it does not significantly add to the strength of the sandwich structure, also allowing for a fair comparison of results.

Summing the height of the two geometries and the aluminium sheet, the entire structure has a total height of approximately 265mm, which in comparison, with the maximum height of the individual egg–boxes of this study being over 200mm, is a reasonably low height.

Figure 5.64 shows the force–displacement curves for the proposed sandwich structure (solid curve), the trend–line of this curve (dashed line) and the curves of each individual cell participating in the construction of the sandwich panel. It is evident that this structure displays a comparatively low peak load of less than 2kN, as expected and an exceptionally extended deformation length of 229mm which agrees with the entire height of the sandwich panel.

In addition, compared to the curves of each individual cell, it can be observed from Figure 5.64 that the ideal initial peak load of the 45deg–*t*0.8–*d*5–*p*60 model (obtained from Figure 5.34) is reflected in the sandwich panel while the length of the plateau in the proposed panel consists of the sum of the energy absorption length of 45deg–*t*0.8–*d*5–*p*60 and 15deg–*t*0.8–*d*5–*p*60 (from Figure 5.10) cells. The plateau

has in fact a desirable smooth consistency. This indicates that the proposed model is a comparatively optimised option.

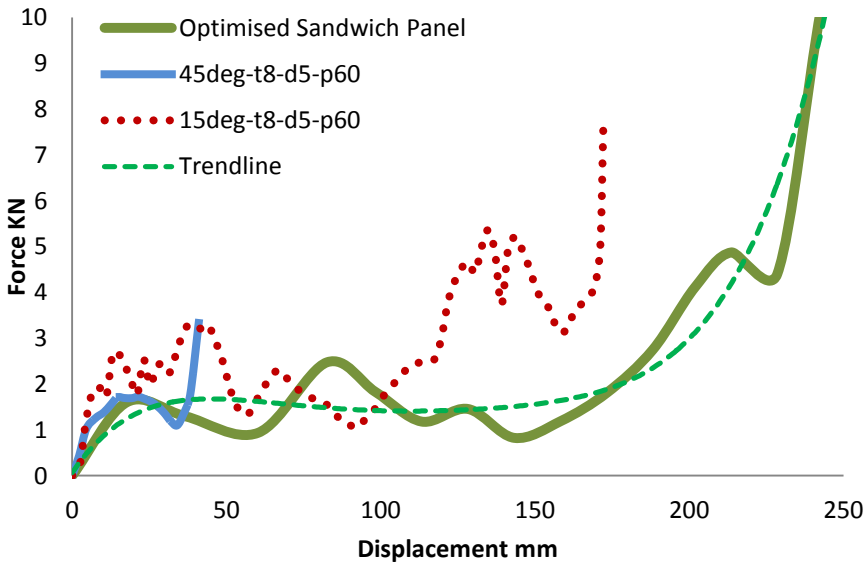

Figure 5.64 – Comparison of FE Analysis for Optimised Sandwich Panel and Individual Optimum Egg–box Components

It is expected from an optimised structure to have a reasonably low weight relevant to its energy absorption capacity. The entire sandwich structure, including the middle sheet, has a mass of 0.1kg per cell which results in a 2.5kg mass for a 5×5 cell unit panel.

From a review of the structural weight and the total energy absorbed by each of the individual egg–box cells used in the proposed sandwich panel against the same measures of the optimised sandwich structure, it is shown that: while the sandwich panel has an average weight gain of 3.5% in comparison to the two individual cells, its total amount of energy absorbed is increased by roughly 33%. Such level of increase in energy absorption capacity, in proportion to the amount of weight gain is commendable.

Additionally, the sandwich structure shows a 490% increase in the amount of energy absorbed, in comparison to the optimum egg–box structure with ω=30°, t=0.8mm, p=45mm, d=5mm, while there exists a 10% increase in structural weight between the two. Despite the large percentage of weight gain, the enhancement in the energy absorption, in addition to the comparatively similar initial peak load, makes the proposed sandwich structure an ideal candidate.

An experimental dynamic impact test of the sandwich structure can further confirm its suitability for use as an optimum aluminium energy absorber. However, the expensive and time consuming series of practical tests which lead to this structure have been prevented with the use of the less costly, repeatable finite element simulation method.

5.9. Critical Analysis of Optimised Sandwich Panel

In order to further evaluate the enhanced characteristics of the above sandwich panel, two counterexample case studies have been developed by the combination of different egg–box cells. To enable more efficient choices amongst the large number of possible cells, selection is made from the geometries of Table 5.4 which are already derived to be cases of worst or best performance. In all models, varieties are limited to a top/base diameter of 5mm, since it is evident in every curve of Section 5.4 that this dimension displays the most desirable force–displacement plateau.

5.9.1. Case Study 1

Initially a sandwich panel is made from the average high candidate of the peak load category and the mean level candidate of the plateau length category of Table 5.4. The geometrical measurements of the two models are ω=30°, t=0.8mm, p=45mm, d=5mm and ω=45°, t=1mm, p=45mm, d=5mm, respectively, as shown in figure 5.65.

The former geometry displays a high level of load peak and a rather lengthy plateau while the latter model has a comparatively average energy absorption capacity. The combination of the two allows for the evaluation of the role of a

geometry with a low peak load, as selected in the original sandwich panel, as well as the effect of its lengthier plateau on the total energy absorption of the system.

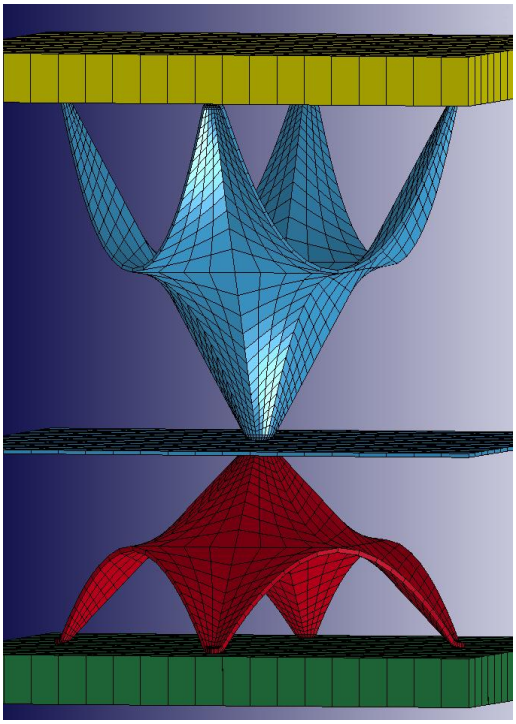

Figure 5.65 – 3D FE Simulation Model of Sandwich Panel Case Study 1

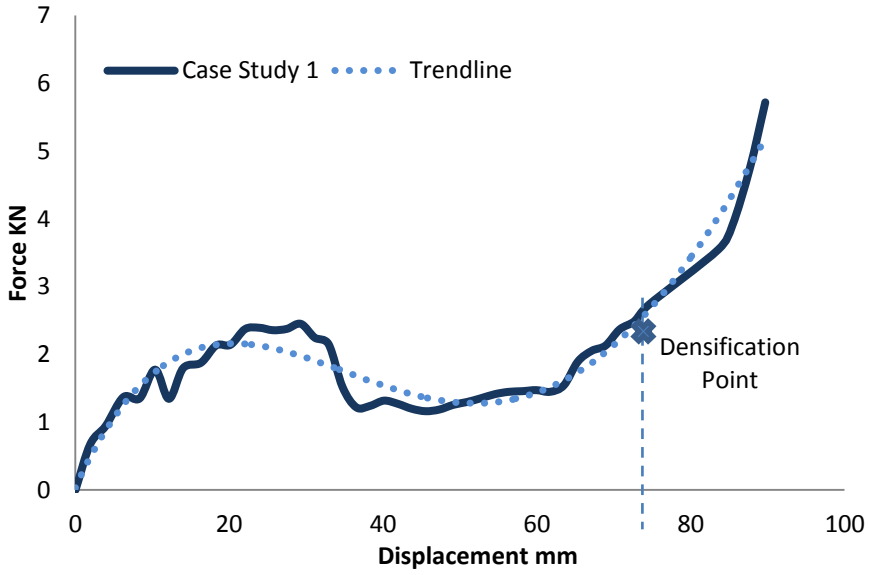

Figure 5.66 – FE Analysis for First Sandwich Panel Case Study

Similar to the previous sandwich model, a thin aluminium sheet of 0.8mm is placed between the two models and all parts of the simulation have been laterally fixed. All other loading conditions are similar to that of the originally proposed sandwich panel.

Figure 5.66 shows the force–displacement curve of the impact loading of the first case study. A dotted line follows the trend of the force–displacement curve to give a smoother pattern.

5.9.2. Case Study 2

The next sandwich panel, presented in Figure 5.67, is composed of two similar models; the mean value option of peak load category and the same from the plateau length category. The geometry has an apical angle of 45°, a thickness of 1mm, inter–peak distance of 45mm and a diameter of 5mm.

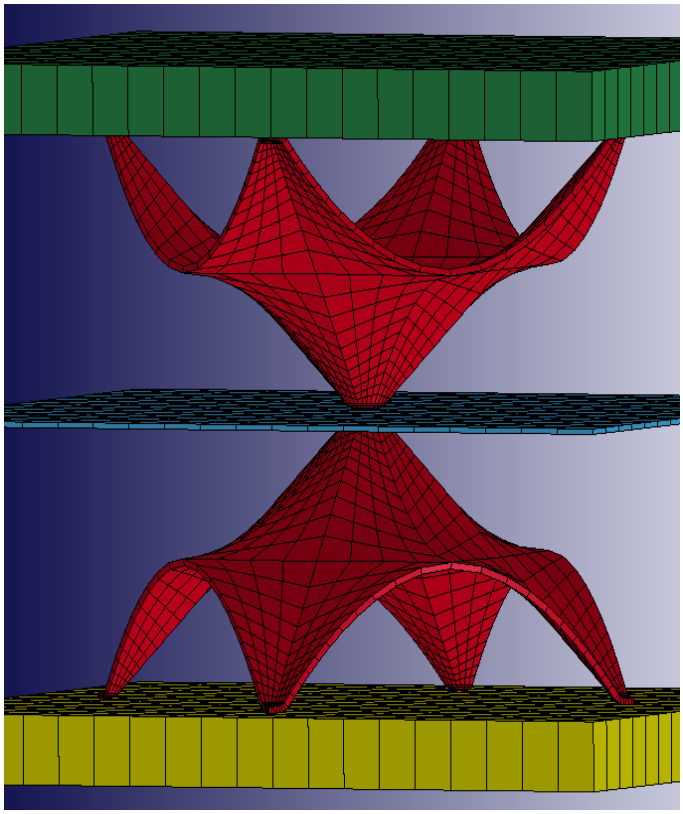

Figure 5.67 – 3D FE Simulation Model of Sandwich Panel Case Study 2

The upper model is rotated 180̊ to allow for the peak to be located on top of the peak of the lower egg–box. A 0.8mm thick aluminium sheet is placed between the two cells while the bottom cell rests on a supporting surface. All lateral movements have been restricted and an impactor surface is located above the entire sandwich model, similar to that of the originally proposed case.

A sandwich panel with such selection of egg–box cells can give information on the importance of using low peak load and high energy absorption models in the construction of a sandwich structure. The twice employed geometry has a comparatively high peak load value and a rather short plateau length.

Exploring the performance of the second sandwich panel example can help justify the improved characteristics of the proposed optimised sandwich panel. The force–displacement curve of case study number two alongside a trend line showing a smoothed out version of its path are illustrated in Figure 5.68.

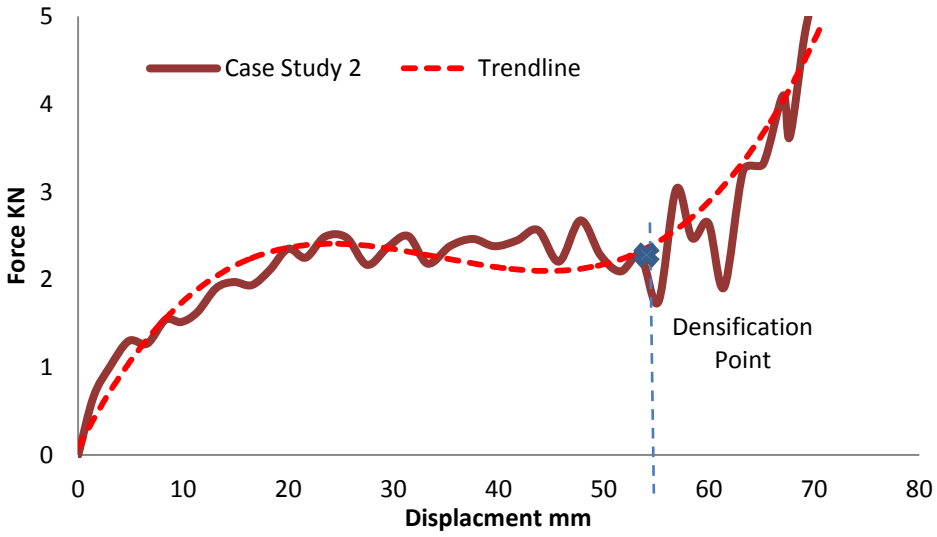

Figure 5.68 – FE Analysis for Second Sandwich Panel Case Study

5.9.3. Evaluation against Optimised Sandwich Structure

The curves of Figures 5.66 and 5.68 are compared to that of the proposed enhanced sandwich structure, in Figure 5.69. It can be seen that both case studies

have dramatically shorter plateau lengths compared to the optimised model. The peak loads are also relatively higher, at a force value of approximately 2.5kN, in contrast to the peak load value of the proposed panel which is below 1.9kN.

The percentage change in the weight of the three sandwich panels shows a 50% fall from the optimised structure to both case study 1 and case study 2, meaning that the optimised sandwich structure is 50% heavier than either of the other two. On the other hand there exists an approximately 200% rise in the total energy absorbed by the optimised structure.

Further combinations can be constructed from other geometrical combinations. However, it is expected for the performance of the proposed sandwich structure to extensively over rule the other candidates.

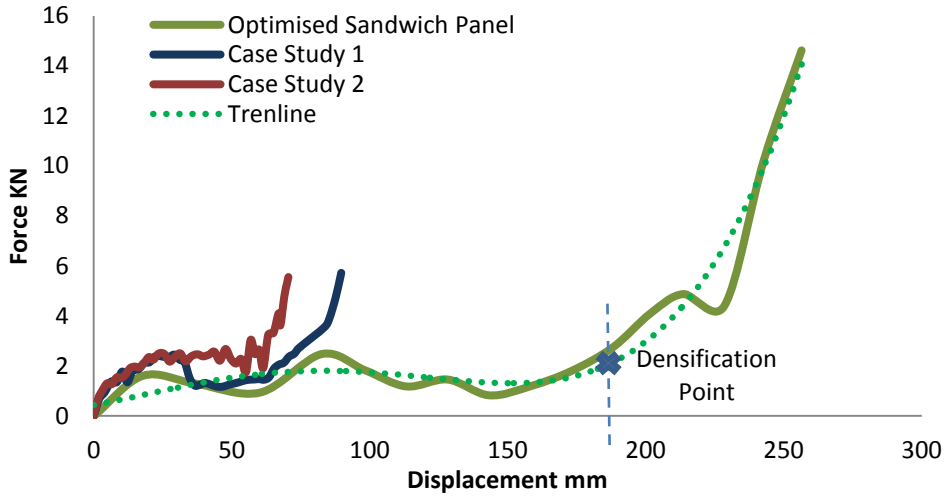

Figure 5.69 – Comparison between FE Outcomes of Proposed Sandwich Panels

It should be borne in mind that each individual egg–box structure or egg–box sandwich panel has to be designed for the specifications of the function for which it is responsible. Therefore, although the two case study structures have lower energy absorption capacities than the optimised sandwich panel, they might be ideal for other purposes.

5.10. Analytical Validation of Sandwich Panel

The analytical approach of investigating the deformation behaviour of egg–box structures can be used to evaluate and validate the enhanced performance of the proposed optimised sandwich panel.

It has been observed so far that following an impact, the egg–box structure deforms through a travelling plastic hinge. Hence, the analytical model developed for calculating the force value of the travelling plastic hinge in a rigid, ideally plastic solid, with the progression of deformation, presented in Deshpande et al. (2003), can be modified as;

$$F = 2\pi t\theta\sigma_Y . \tan\theta \sqrt{\frac{\frac{d}{2t}+\frac{x}{t}\cot\theta}{2\theta-\sin 2\theta}} \qquad 5.2$$

where, (F) is the impact load in kN, (σ_Y) is the material yield strength in MPa and (d) and (t) are geometrical factors of top/base diameter and thickness, respectively, both measured in mm and (x) is the deformation distance in mm. Angle (Θ) is complementary to the apical angle (ω) and therefore it would be calculated as $\frac{\pi}{2} - \omega$ in radians. In other words, (Θ) is the angle of the egg–box cell with the horizontal.

Equation 5.2 can be used to produce an approximate force–displacement curve for the deformation of individual egg–box structures subjected to impact. The analytical model can also be applied to a sandwich egg–box where the total force would be a function of the sum of the forces of the (n) number of egg–box cells enclosed in the structure of the sandwich panel.

$$F = \sum_{i=1}^{n} f(x_i, \theta_i, t_i, d_i) \qquad 5.3$$

Impact experiments show that in an energy absorbing structure, densification occurs roughly at 75% deformation of the height of the structure. In mathematical terms:

$$x = 0.75\,H \tag{5.4}$$

Equation 5.4 is used to estimate the termination point of the force–displacement plateau, where the curve transfers into a sudden steep rise. The behaviour of the structure past the point of densification is not of concern in the study of energy absorbers. Therefore, it will be assumed that the force value rises infinitively at the same point, while in practice the increase in force value happens gradually yet at a high rate.

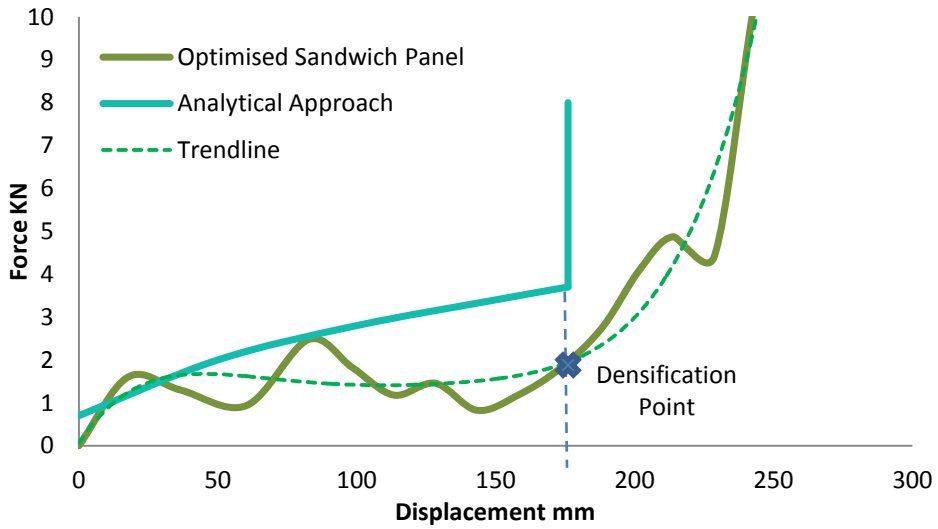

Figure 5.70 – Analytical Assessment (eq. 5.2 and 5.3) vs. FE Analysis of Proposed Optimised Sandwich Structure

Figures 5.70, 5.71 and 5.72 show the curves resulted from the application of equation 5.3 in conjunction with equation 5.2, to the proposed sandwich structure

and the subsequent case studies, respectively. The curves terminate at densification points estimated from the expression of equation 5.4. Evaluation is made against the finite element curve of each structure.

The resultant curve of the analytical approach in Figure 5.70 estimates force values in the vicinity of the outcome data of FE analysis of the proposed egg–box structure. The densification point is also in exact agreement among the two curves at a deformation value of x =175mm.

Due to the geometrical approximations made in the formation of the analytical model, the force value at termination is overestimated by the mathematical equation. In addition, the only material property detail implemented in the equation is the yield strength of the material, while the aluminium alloy used in the fabrication of egg–box structures under investigation has stress values sensitive to the strain rate. Bearing in mind the assumptions, it is argued that the current predictions of the analytical model are satisfactory and confirm the results of the finite element simulation performed.

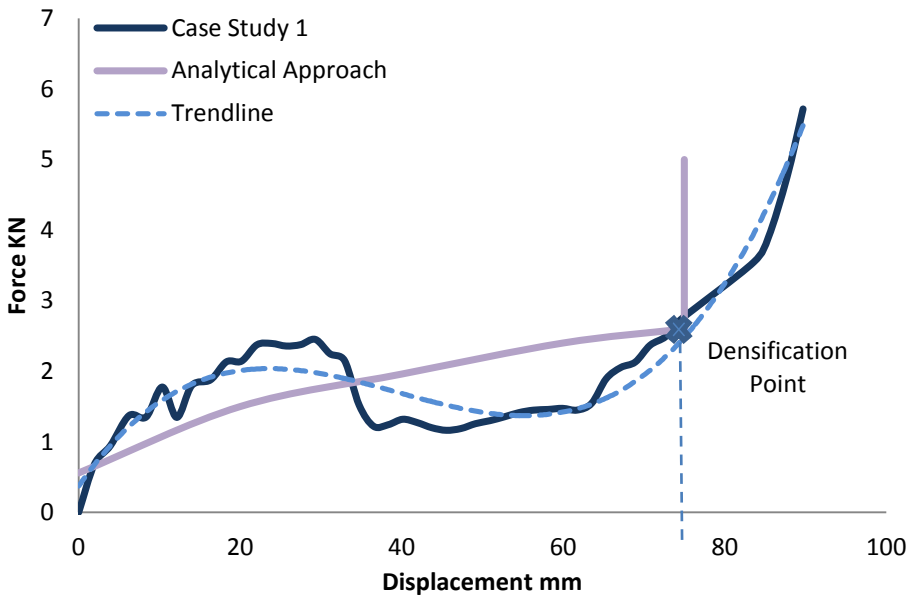

Figure 5.71 – Analytical Calculations vs. FE Analysis of Sandwich Case Study 1

To further examine the validity of the FE simulation results, the behaviour of the case study sandwich structures, which were formed to evaluate the performance of the proposed optimised structure, were also modelled with the analytical equation. Curves of these calculations are provided in Figures 5.71 and 5.72 for case study 1 and case study 2, respectively.

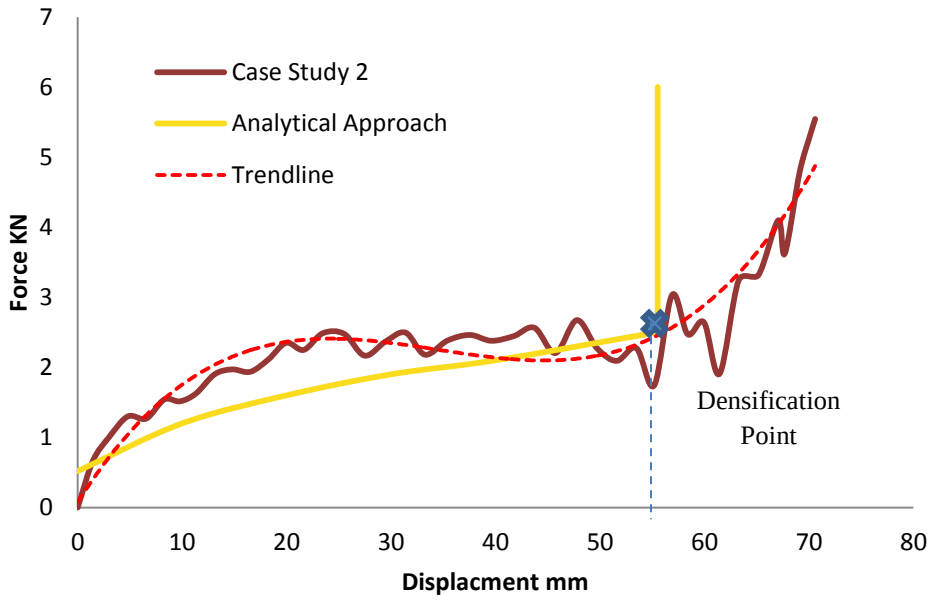

Figure 5.72 – Analytical Calculations vs. FE Analysis of Sandwich Case Study 2

Correlations are evident in both figures between the analytical curves and the FE outcomes. In each case the predicted densification point matches that of the simulated deformation curve. Sandwich panel of case study 1 reaches the densification point at almost 75mm and the second case study at x=55mm.

By estimating the area of the rectangle underneath the curves of Figures 5.70, 5.71 and 5.72, it can be seen that the total amount of energy absorbed as predicted by the analytical method agrees to the same calculations for FE analysis.

Implementation of equations 5.2, 5.3 and 5.4 in the above figures shows that the predictions of the finite element simulation are accurate and reliable.

6. DISCUSSION

In the present research an advanced finite element technique is developed for the modelling and simulation of aluminium egg–box structures in complex mechanical systems with specific boundary conditions. Following the establishment of accurate modelling and simulation specifications through a series of experimental tests and analytical models, a set of geometrically altered egg–box cells have been numerically modelled, tested and their results evaluated to propose optimised geometrical values which enhance the performance of an egg–box structure.

Following the presentation of introductory information on energy absorbing structures and the energy absorption concept, methods of improving occupant safety in vehicles were discussed in Chapter 1. Aluminium egg–box structures were presented to act as crush test barriers to assess car crashworthiness in impact test arrangements. It was established that varying the geometrical factors of the structure has a direct effect on its performance quality; hence, the energy absorption capacity of an egg–box structure can be improved by refining its geometrical features. The use of finite element numerical packages in evaluating the performance of complex structures such as the impact test of energy absorbers was introduced, providing a list of most common commercial FE packages used in static and dynamic structural analysis. In this chapter is was shown that the optimisation of egg–box energy absorbing structures is a multi–objective task where both the level of the peak impact load and the length of the deformation process are of importance.

In the second Chapter the works and studies previously performed in the subject area of the research in hand were reviewed. The evaluation of energy absorption characteristics and crashworthiness of various systems under diverse loading conditions were explored through investigating the past and recent literature. This was followed by a thorough investigation into the properties of currently available energy absorbing structures and their distinctive characteristics and performances. Reference was made to researchers who have employed experimental, analytical and numerical techniques in their projects. A review was also made of the work of researchers who have aimed to optimise the performance of energy absorbing structures and the techniques they utilised for this purpose. It became evident that, due to its recent development, the egg–box structure has not been studied as extensively as other energy absorbers. It was noticed in the literature review section that, inadequate knowledge exists on using innovative techniques to analyse highly complex energy absorbing structures and systems with pre–defined boundary conditions within an reasonable solution time and costs.

As a preliminary step in finding suitable tools to analyse the complex scenario of the dynamic impact of egg-box structure, experimental impact tests were conducted on various egg-box specimens as reported in Chapter 3. The samples included free-edged single cells cut from an egg-box panel, single cells in-situ within a panel and entire egg-box panels. The direction of the loading was altered in some test cases, to investigate the behaviour of the structures under oblique loadings in addition to flat impacts. The tests were conducted with drop masses free falling at a contact speed of $6ms^{-1}$. The applied load and the relative vertical movement of the egg-box specimens were recorded and presented in Chapter 3 as force-displacement curves. It became evident that with the oblique loading of egg-box cells, the strength displayed by the structure will greatly decrease. From conducting impact tests on samples with diverse boundary conditions, the important role of the continuous structure of egg-box was realised, since the amount of impact energy absorbed, was

noticeably higher in the impact of the panel in comparison to the single free-edged cell.

In Chapter 4 the deformation behaviour of the egg-box samples tested in Chapter 3 was examined and analytical total energy equations were derived per specimen. The total energy absorbed by the structures were also mathematically deduced and compared to the force-displacement curves presented in the previous chapter. In the subsequent section of Chapter 4, a finite element model was generated for the aluminium egg–box structure and the impact experiments performed in the previous chapter were simulated. The models were meshed using SHELL163 which is a thin shell element of ANSYS/LS-DYNA®. Using LS-DYNA®'s MAT_ MODIFIED_PIECEWISE_LINEAR_PLASTIC material model, the aluminium material was simulated with precise mechanical properties, taking into account the strain rate sensitivity of CP aluminium alloy. In addition appropriate boundary and loading conditions were introduced to the model. The outcome data of the FE simulations were then validated against numerical and experimental outputs. The precision of the results authenticated the simulation specifications, in terms of the accuracy of material models and boundary conditions, for further modelling of egg–box structures towards optimisation.

The validated FE modelling set up of Chapter 4 was used to simulate the dynamic impact tests of the egg-boxes with various dimensions to evaluate the effect of altering geometrical factors on their energy absorption characteristics. A table containing series of varying egg–box cell geometrical dimensions was presented in this chapter. The resultant force–displacement curves were analysed in cross comparison, to establish relationships between geometrical changes and the ultimate performance of a cell. The outcome of the analytical review was subsequently used to define best and worst geometries in terms of peak impact load level and length of deformation. It was determined that the two characteristics work in opposite manners and improvement in one results in the decline of another. Therefore, an optimum

egg–box structure was proposed which partially compromised to satisfy both specifications of an ideal energy absorber to a reasonable extent. Based on the findings, an improved sandwich structure, formed by a combination of two egg–box geometries with best performance in each area, was created which performed ideally as opposed to the individual egg–box structures. The exceptional energy absorption characteristics of the sandwich model were verified against the results of other sandwich panel combinations. In addition, an analytical method was developed to authenticate the outcomes of all sandwich panels. It was stated in Chapter 5 that the optimisation of egg–box structures is purpose–specific; meaning that for certain functions the structure may be required to perform in certain manners, hence it would be irrational for a single geometry to be called optimum for all purposes. This chapter was indeed a benchmark within the contributions of the present research, providing detailed load–deformation curves for a vast range of egg–box geometries, variations of which are currently in industrial applications. The vast number of simulations and their resultant graphs may be used as reference curves in the study of the performance of egg–box energy absorbers.

7. CONCLUSIONS

The present research has successfully achieved its aims and objectives as proposed in the introductory section of the thesis. The main objective of this project was to employ an advanced nonlinear finite element simulation tool to develop the best geometric design of commercially pure aluminium egg–box structure to absorb kinetic energy in a controllable and predictable manner.

In addition to meeting its initially proposed objectives, this research also presented broad techniques and arrangements to design and simulate tests, use material property data to produce practical material models and define realistic boundary condition and interface assumptions for finite element simulations. The main achievements in this investigation were to deliver FE simulations for the impact test of egg–box structures, validated against experimental impact tests, and to find cell geometries which would prove optimum in terms of their energy absorption characteristics under impact.

The study has successfully led into a time and cost efficient technique to simulate aluminium egg–box cells irrespective of their physical specifications such as cell measurements and wall thickness. Use of shell elements in the modelling of these structures has decreased the analysis time and associated costs due to the reduction in the number of nodes. Validated finite element models of such, greatly reduce the need for expensive, time consuming and irreversible practical tests.

The extensive variations of geometrical factors of the egg–box lead to different deformation responses and thus distinctive levels of energy absorption. Ideal egg–box geometries are expected to display high levels of energy absorption capacities in specific applications and reduce the initial effect of the impact to a satisfactorily low level while maintaining a reasonably low structural weight and material consumption. Experimental test outcomes showed that the strengths of the egg-box panels decrease substantially in oblique loading of the cells.

Modelling and testing egg–box structures of altered geometries and comparison of the output data gave rise to the development of optimal egg–box energy absorbing structures. From the combination of the most efficient geometries, an optimised sandwich structure was developed which showed ideal energy absorption characteristics in all anticipated areas.

The development of the FE modelling and simulations was on the basis of the assertion that accurate outcomes are results of accurately simulated models in terms of material models, boundary and loading conditions, geometrical symmetries and time values. It was shown in the modelling of the experimental dynamic tests that in finite element simulation, accounting for the strain rate sensitivity of materials leads to correct display of strength by the structure. Evaluation of the simulation results against the experimental tests data revealed that the simulations acquired from ANSYS/LS–DYNA® were valid and reliable for further repetitive modelling. In the process of the modelling thin shell elements were shown to be suitable for meshing the walls of thin–walled structures such as an egg–box.

In the path of optimising the structural performance of egg–box energy absorbers, it was concluded that as opposed to other materials used in the production of energy absorbers, the structural weight, recyclability, suppleness, price and industrial availability of aluminium alloys makes them ideal materials for use in the fabrication of egg–box absorbers.

Finite element simulations of one system, when based on different assumptions, produce results that are not in full agreement. The parametric modelling procedure enables outcome comparison between different users. The same procedure was used in the current project to produce an assortment of egg–box geometries which could be evaluated against one another for optimisation purposes.

The optimisation of energy absorbing structures is a multi–objective task where the variables create a Pareto set. An optimised egg–box has a force–displacement curve which displays a low initial peak (fatal injuries become less likely) and a lengthy plateau (greater energy absorption).

From the comparative analysis of the various egg–box geometries, it was concluded that structures with thicker walls have higher peak loads, while the change in thickness does not significantly affect the length of the plateau. The increment of the vertical angle of an egg–box, on the other hand, appeared to lessen the depth of the panel. Deeper egg–box panels produced longer deformation processes (plateau), but higher peak loads.

Comparison with regards to the inter–peak distance (p) revealed that with shorter (p) values, the initial response of the egg–box structure to an impact becomes more satisfactory; however, the length of the force–displacement curve plateau becomes shorter and hence less energy would be absorbed. The effect of changes in top/base diameter on the initial reaction of the egg–box was found to be negligible while it displayed a reverse relationship with the length of the deformation.

Amongst the simulated models, the egg–box geometry that would perform most satisfactorily in the initial stage of an impact consisted of a large angle ω=75° (70° < ω < 89°), thin walls t=0.8mm (t < 1mm), a short inter–peak length p=20mm, while the measurement of the top/base diameter (d) was not of major importance. It was, hence, concluded that egg–box panels with large apical angles (a flat build), thin walls and greater cell densities perform better in reducing the sudden initial

effect of an impact and protect the enclosed bodies against harmful injuries more effectively.

The length of the deformation process was maximised in an egg–box geometry with a small angle ω=15° (0° < ω < 20°), a lengthy inter–peak distance p=60mm and a small top/base diameter d=5mm while the thickness of the cell walls did not particularly influence this behaviour. The conclusions obtained from this geometry indicated that egg–box panels with smaller apical angles, less cell densities and smaller peak/trench diameters offer longer deformation lengths, thus, absorb more energy during a crush situation. In other words, a more efficiently reduced amount of the impact energy is transferred to the protected bodies.

It was noted that the optimised egg–box structure would be one that performs ideally in both of the above areas. From an analytical review of the geometries simulated, it was concluded that, at a fair level of compromise in either of the energy absorption characteristics, the geometry with ω=30°, t=0.8mm, p=45mm and d=5mm is the most optimum egg–box cell with a peak load of 2.2kN and a plateau length of approximately 58mm. The total amount of energy absorbed by this structure is equal to 105kN.mm.

Egg–box structures can be combined in the form of sandwich panels designed per application to act as optimised energy absorbers. In the current project, an innovative sandwich structure was proposed which displayed exceptional energy absorption characteristics in comparison to the individual egg–box geometries.

The sandwich panel consisted of two egg–box panels connected via a thin aluminium sheet. The participating egg–box cells were ω=75°, t=0.8mm, p=20mm and d=5mm on the top, to reduce the effect of the initial peak load, and ω=45°, t=0.8mm, p=60mm and d=5mm on the bottom, to provide maximum deformation length. The actual length of the deformation in this model was increased to 229mm by taking into account the sum of the heights of two geometries, while the initial

peak load remained at minimal level of less than 2kN, as expected from the top egg–box cell.

The total amount of energy absorbed by the sandwich panel is increased by roughly 33% in comparison to the two individual egg–box cells of which it is made. At such level of increase in energy absorption capacity, the average weight gain of 3.5% is acceptable. The optimised structure also shows a 200% rise in the total energy absorbed compared to either of the two counterexample case studies proposed in Chapter 5 of the thesis. A 50% weight gain comes with this enhancement in performance. It is concluded that the enhanced energy absorption capacity in the proposed structure over-performs the increase in its weight.

Authentication of the results of finite element analysis with analytical approaches verifies that the enhanced performance of the proposed sandwich model is valid and reliable.

7.1. Recommendations for further Investigation

The optimised structure proposed using the economical and repetitive finite element simulations and analyses, is required to be fabricated and experimentally investigated prior to being put into use in the industry. The experimental and FE tests studied and performed in this research assume loads or drop towers that impact the egg–box structure either at a right angle to the top of the panel or at a 45° angle. In practice, many impacts are made obliquely to the surface of a vehicle body where energy absorbing structures may be implemented. Further loading angles can be investigated per structure.

The analytical model which was proposed in this research to predict a pattern for the force–displacement curve of the impact of egg–box structure may be further developed to produce more accurate results in estimation.

Using the modelling and simulation procedures, the behaviour of the egg–box geometry can be investigated and analysed when subjected to any loading type or condition. The effect of using innovative metal alloys and other materials in the deformation mechanism of egg–box absorbers can be looked into to uncover more efficient materials for the production of ideal egg–box panels. Various geometrical modifications such as the addition of ribs amongst egg–box cells and corrugated or wavy structural shapes can be developed in the future which may perform more satisfactorily as energy absorbers. The follow–through procedures proposed in this study can be used for modelling other types of energy absorbing structures in the commercially available finite element analysis packages. Optimisation is purpose–specific; therefore, geometries not considered as ideal in this research may satisfy the requirements of certain applications.

REFERENCES

Abramowicz, W. (2003), *Thin–walled structures as impact energy absorbers*, Thin–Walled Structures, vol. 41(2–3), p. 91–107

Abramowicz, W. and Jones, N. (1984), *Dynamic axial crushing of square tubes,* Int. J. of Impact Engineering, vol. 2(2), p. 179–208.

Abramowicz, W. and Jones, N. (1986), *Dynamic progressive buckling of circular and square tubes,* Int. J. of Impact Engineering, vol. 4(4), p. 243–270

Abramowicz, W. and Wierzbicki, T. (1989), *Axial Crushing of Multicorner Sheet Metal Columns*, J. of Applied Mechanics, Transactions ASME, vol. 56, p. 113–120

Ahmad, Z. (2009), *Impact and energy absorption of empty and foam–filled conical tubes*, PhD thesis, Queensland University of Technology

Akisanya, A. R. and Fleck, N. A. (2006), *Plastic collapse of thin–walled frusta and egg–box material under shear and normal loading*, Int. J. of Mechanical Sciences, vol. 48(7), p. 799–808

Aktay, L., Toksoy, A. K. and Guden, M. (2006), *Quasi–static axial crushing of extruded polystyrene foam–filled thin–walled aluminium tubes: Experimental and numerical analysis*, Materials & Design, vol. 27(7), p. 556–565

Alexander, J. M. (1960), *An approximate analysis of the collapse of thin cylindrical shells under axial loading*, Quart. J. Mechanics. and Applied Mathematics, vol. 13, p. 10–15

Alghamdi, A. A. A. (2001), *Collapsible impact energy absorbers: an overview*, Thin–Walled Structures, vol. 29, p. 189–213

Aljawi, A. A. N. (2000), *Finite element and experimental analysis of axially compressed plastic tubes*, European J. of Mechanical and Environmental Engineering, vol. 45 (1), p. 3–10

ANSYS® 13.0 Help System (2010), *Mechanical Analysis User Guide*, ANSYS Inc

ANSYS/LS–DYNA® (2011), *ANSYS/LS–DYNA User's Guide*, ANSYS Inc

ANSYS/LS–DYNA® Introduction, ANSYS Website, accessed March 2011: http://www.ansys.com/products/%20lsdyna.asp

Asadi, M., Walker, B. and Shirvani, H. (2009), *An Investigation to Compare the Application of Shell and Solid Element Honeycomb Model in ODB*, 7th European LS–DYNA Conf.

Asadi, M., Walker, B. and Shirvani, H. (2008a), *Development of the Advanced Finite Element Model for ODB Impact Barrier*, LS–DYNA User Conf.: Japan

Asadi, M., Walker, B. and Shirvani, H. (2008b), *New Finite Element Model for NHTSA Impact Barrier*, 10th Int. LS–DYNA Users Conf.

Asadi, M., Walker, B. and Shirvani, H. (2007a), *Evaluation of New Finite Element Model for IIHS Side Impact Barrier*, LS–DYNA User Conf.: Japan

Asadi, M., Tattersall, P., Walker, B. and Shirvani, H. (2007b), *Advanced Finite Element Model for AE–MDB Side Impact Barrier*, 6th European LS–DYNA User Conf.

Asadi, M., Shirvani, H., Sanaei, E. and Ashmead, M. (2006), *A Simplified Model to Simulate Crash Behaviour of Honeycomb*, Proceedings of the Int. conf. on Advanced Design and Manufacture: China

Asavavisithchai, S., Slater, D. and Kennedy, A. R. (2004), *Effect of tube length on the bucking mode and energy absorption of Al foam–filled tubes*, J. of Materials Science, vol. 39(24), p. 7395–7396

Ashby, M. F., Evans, A. G., Fleck, N. A., Gibson, L. J., Hutchinson, J. W. and Wadley, H. G. (2000), *Metal foams: a design guide*, Butterworth–Heinemann: Boston, MA, USA

Ashmead, M. (2000), *Energy–absorbing structures Int. Patent*, Serial No. WO 00/31434

Ashmead, M., Bedus, S. and Bradley, S. (2000), *Advanced Materials for Enhanced Automotive Safety*, Automotive Composites and Plastics Conf.

Avalle, M., Belingardi, G., Ibba, A. (2007), *Mechanical models of cellular solids: Parametres identification from experimental tests*, Int. J. of Impact Engineering, vol. 34(1), p. 3–27

Avalle, M., Chiandussi, G., and Belingardi, G. (2002), *Design optimisation by response surface methodology: Application to crashworthiness design of vehicle structures*, Structural and Multidisciplinary Optimisation, vol. 24, p. 325–332

Banhart, J. (2001), *Manufacture, characterisation and application of cellular metals and metal foams*, Progress in Materials Science, vol. 46(6), p. 559–632

Bardi, F. C., Yun, H. D. and Kyriakides, S. (2003), *On the axisymmetric progressive crushing of circular tubes under axial compression*, Int. J. of Solids and Structures, vol. 40, p. 3137–3155

Birch, R. S. and Jones, N. (1990), *Dynamic and static axial crushing of axially stiffened cylindrical shells*, Thin–Walled Structures, vol. 9, p. 29–60

Belytschko, T. B. and Tsay, T. S. (1983), *A stabilization procedure for the quadrilateral plate element with one–point quadrature,* Int. J. of Numerical Methods in Engineering, vol. 19, p. 405–419

Belytschko, T. B., Lin, J. I. and Tsay, C. S. (1984), *Explicit algorithms for the nonlinear dynamics of shells*, Computer Methods in Applied Mechanics and Engineering, vol. 42, p. 225–251

Borvik, T., Hopperstad, O. S., Reyes, A., Langseth, M., Solomos, G. and Dyngeland, T. (2003), *Empty and foam–filled circular aluminium tubes subjected to axial and oblique quasi–static loading*, Int. J. of Crashworthiness, vol. 8 (5), p. 481– 494

Box, G. E. P. and Wilson, K.B. (1951), *On the Experimental Attainment of Optimum Conditions (with discussion)*, J. of the Royal Statistical Society, Series B, vol. 13(1), p. 1–45

Brown, J., C. (2002), *Introduction to the Basic Principles of Crashworthiness*, Cranfield University: Bedfordshire

Calladine, C. R. (1986), *Analysis of large plastic deformations in shell structures*, In: Inelastic Behaviour of Plates and Shells (IUTAM Symposium, Rio de Janeiro, 1985), ed. L. Bevilacqua et al., Springer, Berlin, p. 69–101

Calladine, C., R. and English, R., W. (1984), *Strain–rate and Inertia Effects in the Collapse of Two Types of Energy–absorbing Structure*, Int. J. of Mechanical Science, vol. 26(11–12), p. 689–701

CARE (EU road accidents database) or national publications (2011), *Road safety evolution in EU*, European Commission Road Safety, Directorate General Energy and Transport

Chen, C., Harte, A. M. and Fleck, N. A. (2001), *The plastic collapse of sandwich beams with a metallic foam core*, Int. J. of Mechanical Sciences, vol. 43, p. 1483–1506

Cheon, S. S. and Meguid, S. A. (2004), *Crush behaviour of metallic foams for passenger car design*, Int. J. of Automotive Technology, vol. 5(1), p. 47–53

Chiras, S., Mumm, D. R., Evans, A. G., Wicks, N., Hutchinson, J. W., Dharmasena, K., Wadley, H. N. G. and Fichter, S. (2002), *The Structural Performance of Near-Optimised Truss-Core Panels*, Int. J. Solids Struct., vol. 39, p. 4093–4115

Choi, K. K. and Youn, B. D. (2002), *An investigation of nonlinearity of reliability–based design optimisation approaches*, In: 28th Design Automation Conf., Sep 29–Oct 2 2002, Montreal, Que., Canada

Chung, J. G., Chang, S. H., Sutcliffe, M. P. F. (2007), *Deformation and energy absorption of composite egg–box panels*, J. of Composites Science and Technology, vol. 67, p. 2342–2349

Commission of the European Communities (2001), *European transport policy for 2010: time to decide*, White Paper: Brussels

Deb, A., Mahendrakumar, M. S., Chavan, C., Karve, J., Blankenburg, D. and Storen, S. (2004), *Design of an aluminium–based vehicle platform for front impact safety*, Int. J. of Impact Engineering, vol. 30(8–9), p. 1055–1079

Department for Transport (DfT) (2011), *Heavy Goods Vehicle Inspection Manual*, Consolidated Edition

Deqiang, S., Weihong, Zh., Yanbin, W. (2010), *Mean out–of–plane dynamic plateau stresses of hexagonal honeycomb cores under impact loadings*, Composite Structures, vol. 92(11), p. 2609–2621

Deshpande, V. S. and Fleck, N. A. (2000), *Isotropic constitutive models for metallic foams*, J. of the Mechanics and Physics of Solids, vol. 48(6–7), p. 1253–1283

Deshpande, V. S., Fleck, N. A., (2001), *Collapse of truss core sandwich beams in 3–point bending*, Int. J. Solids Structures, vol. 38(36–37), p. 6275–6305

Deshpande, V. S. and Fleck, N. A. (2003), *Energy absorption of an egg–box material*, J. of the Mechanics and Physics of Solids, vol. 51(1), p. 187–208

Du Bois, P., Chou, C. C., Fileta, B. B., Khalil, T. B., King, A. I., Mahmood, H. F., Mertz, H. J. and Wismans, J. (2004), *Vehicle Crashworthiness and Occupant Protection*, Sponsored by Automotive Applications Committee, American Iron and Steel Institute: Southfield, Michigan

El–Hage, H., Mallick, P. K. and Zamani, N. (2005), *A numerical study on the quasi–static axial crush characteristics of square aluminium tubes with chamfering and other triggering mechanisms*, Int. J. of Crashworthiness, vol. 10(2), p. 183– 195

El–Sobky, H., Singace, A. A. and Petsios, M. (2001*), Mode of collapse and energy absorption characteristics of constrained frusta under axial impact loading*, Int. J. of Mechanical Sciences, vol. 43(3), p. 743–757

Ellert, G. (1998–2008), *The Physics Hypertextbook*, Physics.info 2010: New York

European Commissions (EC) (2003), *Saving 20000 Lives on Our Roads*, Office for Official Publications of the European Communities: Luxembourg

Evans, A. G. (2001), *Lightweight Materials and Structures*, MRS Bull vol. 790

Farley, G. L. (1986), *Effect of Specimen Geometry on the Energy Absorption Capability of Composite Materials*, J. of Composite Materials, vol. 20, p. 390–400

Finn, S. R., Springer, G. S. (1991), *Composite Plates Impact Damage: An Atlas*, Research supported by NASA, Technomic Publishing Co: Lancaster: PA

Fleck, N. A. (2001), *Multi-Axial Strength of Metallic Foams and Lattice Materials*, J. of JSMS: Materials Science for the 21st Century, vol. A, p. 336-340

Fyllingen, O., Hopperstad, O. S. and Langseth, M. (2009), *Robustness study on the behaviour of top–hat thin–walled high–strength steel sections subjected to axial crushing*, Int. J. of Impact Engineering, vol. 36(1), p. 12–24

Gameiro, C. P. and Cirne, J. (2007), *Dynamic axial crushing of short to long circular aluminium tubes with agglomerate cork filler*, Int. J. of Mechanical Sciences, vol. 49(9), p. 1029–1037

Gibson, L. J. and Ashby, M. F. (1997), *Cellular Solids, Structure and Properties*, 2nd ed., Cambridge University Press: Cambridge, UK

Grzebeita, R. H. (1990), *An alternate method for determining the behaviour of round stocky tubes subjected to an axial crush load*, Thin–Walled Structures, vol. 9, p. 61–69

Gupta, N. K., Easwara Prasad, G. L. and Gupta, S. K. (1997), *Plastic collapse of metallic conical frusta of large semi–apical angles*, Int. J. of Crashworthiness, vol. 2, p. 349–366

Gupta, N. K., Mohamed Sheriff, N. and Velmurugan, R. (2008), *Experimental and theoretical studies on buckling of thin spherical shells under axial loads*, Int. J. of Mechanical Sciences, vol. 50(3), p.: 422–432

Gupta, N. K. and Velmurugan, R. (1999), *Axial compression of empty and foam filled composite conical shells*, J. of Composite Materials, vol. 33(6), p. 567–591

Gupta, N. K. and Venkatesh (2006), *A study of the influence of diameter and wall thickness of cylindrical tubes on their axial collapse*, Thin–Walled Structures, vol. 44(3), p. 290–300

Gupta, N. K. and Venkatesh (2007), *Experimental and numerical studies of impact axial compression of thin–walled conical shells*, Int. J. of Impact Engineering, vol. 34(4), p. 708–720

Hamada, H. and Ramakrishna, S. (1997) Fem *method for prediction of energy absorption capability of crashworthy polymer composite materials*, J. of Reinforced Plastics and Composites, vol. 16, p. 226–242

Hanssen, A. G.; Langseth, M. and Hopperstad, O. S. (1999), *Static crushing of square aluminium extrusions with aluminium foam filler*, Int. J. Mechanical Engineering, vol. 41(8), p. 967–993

Hanssen, A. G., Langseth, M. and Hopperstad, O. S. (2000a), *Static and dynamic crushing of circular aluminium extrusions with aluminium foam filler*, Int. J. of Impact Engineering, vol. 24(5), p. 475–507

Hanssen, A. G., Langseth, M. and Hopperstad, O. S. (2000b), *Static and dynamic crushing of square aluminium extrusions with aluminium foam filler*, Int. J. of Impact Engineering, vol. 24(4), p. 347–383

Hanssen, A. G., Langseth, M. and Hopperstad, O. S. (2001), *Optimum design for energy absorption of square aluminium columns with aluminium foam filler*, Int. J. of Mechanical Sciences, vol. 43(1), p. 153–176

Harte, A. M., Fleck, N. A. and Ashby, M. F. (2000), *Energy absorption of foam–filled circular tubes with braided composite walls*, Eur. J. Mechanics – A/Solids, vol.19, p. 31–50

Hartmann, F. and Katz, C. (2007), *Structural analysis with finite elements*, Springer: Berlin

Hibbeler, R. C. (2002), *Structural Analysis*, Fifth Edition, Prentice Hall, Upper Saddle River: New Jersey

Hibbitt, Karlsson and Sorensen Inc. (HKS) (2002), *Getting Started with ABAQUS/Standard Version 6.3*, Pawtucket, USA: HKS

Jacobsen, A. J., Kolodziejska, J. A., Doty, R., Fink, K. D., Zhou, C., Roper, C. S. and Carter, W. B. (2010), *Interconnected Self-Propagating Photopolymer Waveguides: An Alternative to Stereolithography for Rapid Formation of Lattice-Based Open-Cellular Materials*, Twenty First Annual International Solid Freeform Fabrication Symposium - An Additive Manufacturing Conference: University of Texas, Austin

Jeon, I., Asahina, T., Kang, K. J., Im, S. and Lu, T. J. (2010), Finite element *simulation of the plastic collapse of closed–cell aluminium foams with X–ray computed tomography*, J. of Mechanics of Materials, vol. 42, p. 227–236

Johnson, W. and Mamalis, A. G. (1978), *Crashworthiness of vehicles*, Mechanical Engineering Publications Ltd: London

Jones, N. (1989), *Structural Impact*, Cambridge University Press: Cambridge, UK

Jones, N. (2003), *Several phenomena in structural impact and structural crashworthiness,* Euro. J. of Mechanics – A/Solids General and plenary lectures from the 5th EUROMECH Solid Mechanics Conference, vol. 22(5), p. 693–707

Karagiozova, D., Alves, M. and Jones, N. (2000), *Inertia effects in axisymmetrically deformed cylindrical shells under axial impact*, Int. J. of Impact Engineering, vol. 24(10), p. 1083–1115

Karagiozova, D. and Jones, N. (2004), *Dynamic buckling of elastic–plastic square tubes under axial impact–II: structural response*, Int. J. of Impact Engineering, vol. 30(2), p. 167–192

Kavi, H., Tasoy, A. K. and Guden, M. (2006), *Predicting energy absorption in a foam–filled thin–walled aluminium tube based on experimentally determined strengthening coefficient,* Materials & Design, vol. 27(4), p. 263–269

Kim, D. K., Lee, S. (1999), *Impact energy absorption of 6061 aluminium extruded tubes with different cross–sectional shapes*, Materials & Design, vol. 20(1–5), p. 41–49

Kooistra, G. W., Deshpande, V. S. and Wadley, H. N. G. (2004), *Compressive Behavior of Age Hardenable Tetrahedral Lattice Truss Structures Made from Aluminium,* Acta Mater, vol. 52, p. 4229–4237

Lampinen, B. E. and Jeryan, R. A. (1982), *Effectiveness of polyurethane foam in energy absorbing structures,* SAE Technical Paper Series 820494

Langseth, M., Hopperstad, O. S. and Berstad, T. (1999), *Crashworthiness of aluminium extrusions: Validation of numerical simulation, effect of mass ratio and impact velocity,* Int. J. of Impact Engineering, vol. 22, p. 829–854

Lanzi, L., Castelletti, M. L. and Anghileri, M. (2004), *Multi–objective optimisation of composite absorber shape under crashworthiness requirements*, Composite Structures, vol. 65(3–4), p. 433–441

Liu, Y. (2008), *Design optimisation of tapered thin–walled square tubes,* Int. J. of Crashworthiness, vol. 13(5), p. 543–550

LSTC (2007), *LS–DYNA® Keyword Users' Manual V970*, Livermore Software Technology Corporation

Lu, G. and Yu, T. (2003), *Energy absorption of structures and materials*, Woodhead Publishing Limited: Cambridge, UK

Mamalis, A.G. and Johnson, W. (1983), *The quasi–static crumpling of thin–walled circular cylinders and frusta under axial compression*, Int. J. of Mechanical Sciences, vol. 25(9–10), p. 713–732

Mamalis, A. G., Johnson, W. and Viegelahn, G. L. (1984), *The crumpling of steel thin–walled tubes and frusta under axial compression at elevated strain rates: some experimental results*, Int. J. of Mechanical Sciences, vol. 26, p. 537–548

Mamalis, A. G., Manolakos, D. E., Ioannidis, N. B. and Kostazos, P. K. (2005), *Numerical simulation of thin–walled metallic circular frusta subjected to axial loading*, Int. J. of Crashworthiness, vol. 10(5), p. 505–513

Mamalis, A. G., Manolakos, D. E., Ioannidis, M. B., Kostazos, P. K. and Dimitriou, C. (2003), *Finite element simulation of the axial collapse of metallic thin–walled tubes with octagonal cross–section*, Thin–Walled Structures, vol. 41(10), p. 891–900

Mamalis, A. G., Manolakos, D. E., Ioannidis, M. B., Kostazos, P. K. and Hassiotis, G. (2001), *Finite element simulation of the axial collapse of thin–wall square frusta*. Int. J. of Crashworthiness, vol. 6(2), p.155–164

Mamalis, A. G., Manolakos, D. E., Saigal, S., Viegelahn, G. and Johnson, W. (1986), *Extensible plastic collapse of thin–wall frusta as energy absorbers*, Int. J. of Mechanical Sciences, vol. 28(4), p. 219–229

Meguid, S. A., Attia, M. S., Stranart, J. C. and Wang, W. (2007), *Solution stability in the dynamic collapse of square aluminium columns*, Int. J. of Impact Engineering, vol. 34(2), p. 348–359

Meng, Q., Al–Hassani, S.T.S. and Soden, P.D. (1983), *Axial crushing of square tubes*, Int. J. of Mechanical Sciences, vol. 25(9–10), p. 747–773

Mirfendereski, L., Salimi, M. and Ziaei–Rad, S. (2008), *Parametric study and numerical analysis of empty and foam–filled thin–walled tubes under static and dynamic loadings*, Int. J. of Mechanical Sciences, vol. 50(6), p. 1042–1057

Morris, E., Olabi, A. G. and Hashmi, M. S. J. (2006), *Analysis of nested tube type energy absorbers with different indenters and exterior constraints*, J. of Thin–Walled Structures, vol. 44, p. 872–885

Mosallam, A., Slenk, J., Kreiner, J. (2008), Assessment of Residual Tensile Strength of Carbon/Epoxy Composites Subjected to Low-Energy Impact, J. of Aerospace Eng., vol. 21, p. 249-258

Nagel, G. M. and Thambiratnam, D. P. (2005), *Computer simulation and energy absorption of tapered thin–walled rectangular tubes*, Thin–Walled Structures, vol. 43(8), p. 1225–1242

Nagel, G. M. and Thambiratnam, D. P. (2006), *Dynamic simulation and energy absorption of tapered thin–walled tubes under oblique impact loading*, Int. J. of Impact Engineering, vol. 32(10), p. 1595–1620

Nariman–zadeh, N., Darvizeh, A. and Jamali, A. (2006), *Pareto Optimisation of Energy Absorption of Square Aluminium Columns Using Multi–Objective Genetic Algorithms*, Proceedings of the Institution of Mechanical Engineers, Part B: J. of Engineering Manufacture, vol. 220(2), p. 213–224

Nettles, A. T., Douglas, M. J. (2000), *A Comparison of Quasi-Static Indentation to Low-Velocity Impact*, NASA, Marshall Space Flight Center: Hanover, MD

Nowpada, S., Chirwa, E. C., Myler, P. and Matsika, E. (2010), *Aluminium Egg-box panel as an energy absorber for pedestrian protection*, Advanced Engineering Materials, vol. 12(7), p. 591–595

Nowpada, S., Yang, Y., Chirwa, E. C., Myler, P., Matsika, E. and Qian, P. (2010), *Aluminium egg-box energy absorber in a commercial vehicle front for pedestrian protection: Energy absorption capability*, Proc. of The Int. Crashworthiness Conference, ICRASH2010 Washington, Edited by E C Chirwa, C-D (Steve) Kan, The National Conference Center: Leesburg, VA, USA

Nowpada, S., Chirwa, E. C., Myler, P., Chinnaswamy, G. K. and Matsika, E. (2009), *Egg-box panel for commercial vehicle front – compressive loading tests*, Int. J. Crashworthiness, vol. 15(1), p. 59–70

Nowpada, S., Chirwa, E. C., Myler, P., Chinnaswamy, G. K. and Matsika, E. (2008), *Egg-box panel for commercial vehicle front*, Proc. of The Int. Crashworthiness Conference, ICRASH2008 Edited by E C Chirwa, H Hamada and K Mizuno, Kyoto Institute of Technology: Kyoto, Japan

Olabi, A. G., Morris, E., Hashmi, M. S. J. and Gilchrist M. D. (2008), *Optimised design of nested oblong tube energy absorbers under lateral impact loading*, Int. J. of Impact Engineering, vol. 35, p. 10–26

Otubushin, A. (1998), *Detailed validation of a non–linear finite element code using dynamic axial crushing of a square tube*, Int. J. of Impact Engineering, vol. 21(5), p. 349–368

Peroni, L., Avalle, M. and Belingardi, G. (2009), *Comparison of the energy absorption capability of crash boxes assembled by spot–weld and continuous joining techniques*, Int. J. of Impact Engineering, vol. 36(3), p. 498–511

Prasad, G. L. E. and Gupta, N. K. (2005), *An experimental study of deformation modes of domes and large–angled frusta at different rates of compression*, Int. J. of Impact Engineering, vol. 32(1–4), p. 400–415

Preece, B. W. (1911), *Sand for Brass Molding*, The Foundry; University of Michigan, Cleveland, Ohio, vol. 38(2), p. 83–87

Qiao, P., Yang, M. and Bobaru, F. (2008), *Impact Mechanics and High–Energy Absorbing Materials: Review*, J. of Aerospace Engineering, vol. 21(4), p. 235–24

Reid, S. R. (1993), *Plastic deformation mechanisms in axially compressed metal tubes used as impact energy absorbers*, Int. J. of Mechanical Sciences, vol. 35(12), p. 1035–1052

Reid, S. R. and Reddy, T. Y. (1986), *Static and dynamic crushing of tapered sheet metal tubes of rectangular cross–section*, Int. J. of Mechanical Sciences, vol. 28(9), p. 623–637

Reyes, A., Hopperstad, O. S., Berstad, T., Hanssen, A. G. and Langseth, M. (2003), *Constitutive modelling of aluminium foam including fracture and statistical variation of density*, European J. of Mechanics – A/Solids, vol. 22(6), p. 815–835

Reyes, A., Hopperstad, O. S. and Langseth, M. (2004), *Aluminium foam–filled extrusions subjected to oblique loading: experimental and numerical study*, Int. J. of Solids and Structures, vol. 41(5–6), p. 1645–1675

Santosa, S. P. and Wierzbicki, T. (1998), *Crash behaviour of box columns filled with aluminium honeycomb or foam*, Computers & Structures, vol. 68(4), p. 343–367

Santosa, S. P., Wierzbicki, T., Hanssen, A. G. and Langseth, M. (2000), *Experimental and numerical studies of foam–filled sections*, Int. J. of Impact Engineering, vol. 24(5), p. 509–534

Schneider, F. and Jones, N. (2008), *Observations on the design and modelling of some joined thin-walled structural sections*, Thin-Walled Structures, vol. 46(7–9), p. 887–897

Seitzberger, M., Rammerstorfer, F. G., Gradinger, R., Degischer, H. P., Blaimschein, M. and Walch, C. (2000), *Experimental studies on the quasi–static axial crushing of steel columns filled with aluminium foam*. Int. J. of Solids and Structures, vol. 37(30), p. 4125–4147

Shariatpanahi, M., Masoumi, A. and Ataei, A. (2008), *Optimum design of partially tapered rectangular thin–walled tubes in axial crushing*, Proceeding of the Institution of Mechanical Engineers Part B–J. of Engineering Manufacture, vol. 222(2), p. 285– 291

Sheh, M. Y., Reid, J. D., Lesh, S. M. and Cheva, M. (1992), *Vehicle crashworthiness analysis using numerical and experimental method*, Int. Conference on Vehicle Structural Mechanics and CAE, Warrendale, Society of Automotive Engineering Inc

Sheriff, N. M., Gupta, N. K., Velmurugan, R. and Shanmugapriyan, N. (2008), *Optimisation of thin conical frusta for impact energy absorption*, Thin–Walled Structures, vol. 46(6), p. 653–666

Sherwood, J. A. and Frost, C. C. (1992), *Constitutive Modelling and Simulation of Energy Absorbing Polyurethane Foam under Impact Loading*, Polymer Engineering and Science, vol. 32(16), p. 1138–1146

Shetty, S. K. (2001), *Finite Element Modelling of Energy Absorption Characteristics of Hybrid Structures – Composite Wrapped on a Square Metal Tube*, B.Eng Thesis, Mysore University: India

Singace, A. A., El–Sobky, H. and Petsios, M. (2001), *Influence of end constraints on the collapse of axially impacted frusta*, Thin–Walled Structures, vol. 39(5), p. 415–428

Song, H. W., Fan, Z. H., Yu, G., Wang, Q. C. and Tobota, A. (2005), *Partition energy absorption of axially crushed aluminium foam–filled hat sections*, Int. J. of Solids and Structures, vol. 42(9–10), p. 2575–260

Spagnoli, A. and Chryssanthopoulos, M. K. (1999), *Elastic buckling and postbuckling behaviour of widely–stiffened conical shells under axial compression*, Engineering Structures, vol. 21(9), p. 845–855

Subhash, G., Liu, Q., Gao, X. (2006), *Quasistatic and high strain rate uniaxial compressive response of polymeric structural foams*, Int. J. of Impact Eng., vol. 32(7), p. 1113–1126

Tan, H. and Qu, S. (2009), *Impact of Cellular Materials*, Lecture note, International Centre for Mechanical Sciences, Udine, Italy, 28 Sept – 2 Oct

Tarigopula, V., Langseth, M., Hopperstad, O. S. and Clausen, A. H. (2006), *Axial crushing of thin–walled high–strength steel sections*, Int. J. of Impact Engineering, Int. Symposium on the Crashworthiness of Light–weight Automotive Structures, vol. 32(5), p. 847–882

Toksoy, A. K. and Guden, M. (2005), *The strengthening effect of polystyrene foam filling in aluminium thin–walled cylindrical tubes*, Thin–Walled Structures, vol. 43(2), p. 333–350

Triantafillou, T. C. and Gibson, L. J. (1989), *Debonding in Foam Core Sandwich Panels*, Material Structures, vol. 22, p. 64–89

Ulker, M. B. C. and Rahman, M. S. (2008), *Traffic Barriers under Vehicular Impact: From Computer Simulation to Design Guidelines*, J. of Computer–Aided Civil and Infrastructure Engineering, vol. 23, p. 465–480

USA Department of Defence (1966), *Aluminum and Aluminum Alloys*, Military Standardization Handbook: Washington, DC

Vanderplaats, G. N. (2007), *Multidiscipline Design Optimisation*, Vanderplaatz R&D, Inc.

Wadley, H. N. G., Fleck, N. A. and Evans, A. G. (2003), *Fabrication and Structural Performance of Periodic Cellular Metal Sandwich Structures*, Compos Sci Tech, vol. 63, p. 2331–2343

Walter, P. L. (2007), *Selecting Accelerometers for Mechanical Shock Measurements*, Sound and Vibration, vol. 41(12), p. 14–18

White, M. and Jones, N. (1999), *Experimental quasi–static axial crushing of top–hat and double–hat thin–walled sections*, Int. J. of Mechanical Sciences, vol. 41, p. 179–208

WHO (2004), *World Report on Road Traffic Injury Protection*, World Health Organisation Library Cataloguing–in–Publication Data

Wierzbicki, T. and Abramowicz, W. (1983), *On the crushing mechanics of thin–walled structures*, J. of Applied Mechanics, vol. 50, p. 727–734

Witteman, W. J., Kriens, R. F. C. (1998), *Modelling of an Innovative Frontal Car Structure: Similar Deceleration Curves at Full Overlap, 40 per cent Offset and 30 Degrees Collisions*, Proceedings of the Sixteenth Int. Technical Conference on the Enhanced Safety of Vehicles (ESV), Paper 98–S1–O–04, p. 194–212: Windsor, Canada

Wu, E. and Jiang, W. (1996), *Axial crush of Metallic Honeycombs*, Pergamon, Int. J. of Impact Engineering, vol. 19(5–6), p. 439–456

Yamazaki, K. and Han, J. (2000) *Maximization of the crushing energy absorption of cylindrical shells*, Advances in Engineering Software, vol. 31, p. 425–434

Yan, W. Y., Durif, E., Yamada, Y. and Wen, C. (2007), *Crushing simulation of foam– filled aluminium tubes*, Materials Transactions, vol. 48(7), p. 1901–1906

Yoo, S. H., Chang, S. H. and Sutcliffe, M. P. F. (2010), *Compressive characteristics of foam–filled composite egg–box sandwich panels as energy absorbing structures*, J. of Composites, Part A, vol. 41, p. 427–434

Yuen, S. C. K., Nurick, G. N. and Starke, R. A. (2008), *The energy absorption characteristics of double–cell tubular profiles*, Latin American J. of Solids and Structures, vol. 5(4), p. 289–317

Zarei, H. R. and Kroger, M. (2006), *Multiobjective crashworthiness optimisation of circular aluminium tubes*, Thin–Walled Structures, vol. 44(3), p. 301–308

Zarei, H. R. and Kroger, M. (2008), *Optimisation of the foam–filled aluminium tubes for crush box application*, Thin–Walled Structures, vol. 46(2), p. 214–221

Zhang, X., Cheng, G. and Zhang, H. (2009), *Numerical investigations on a new type of energy–absorbing structure based on free inversion of tubes*, Int. J. of Mechanical Sciences, vol. 51, p. 64–76

Zhang, Z., Liu, Sh. and Tang, Z. (2010), *Crashworthiness investigation of kagome honeycomb sandwich cylindrical column under axial crushing loads*, J. of Thin–Walled Structures, vol. 48, p. 9–18

Zini, G. (2005), *Reduction of crash severity through in–vehicle systems (IVS) speed Control*, In: 19th Int. Technical Conference on The Enhanced Safety of Vehicles, June 2005, Washington DC

Zupan, M., Chen, C. and Fleck, N. A. (2003), *The plastic collapse and energy absorption capacity of egg–box panels*, Int. J. of Mechanical Sciences, vol. 45(5), p. 851–871

BIBLIOGRAPHY

Abramowicz, W. (2003), *Thin–walled structures as impact energy absorbers*, Thin–Walled Structures, vol. 41(2–3), p. 91–107

Abramowicz, W. and Jones, N. (1984), *Dynamic axial crushing of square tubes*, Int. J. of Impact Engineering, vol. 2(2), p. 179–208.

Abramowicz, W. and Jones, N. (1986), *Dynamic progressive buckling of circular and square tubes*, Int. J. of Impact Engineering, vol. 4(4), p. 243–270

Abramowicz, W. and Wierzbicki, T. (1989), *Axial Crushing of Multicorner Sheet Metal Columns*, J. of Applied Mechanics, Transactions ASME, vol. 56, p. 113–120

Ahmad, Z. (2009), *Impact and energy absorption of empty and foam–filled conical tubes*, PhD thesis, Queensland University of Technology

Akisanya, A. R. and Fleck, N. A. (2006), *Plastic collapse of thin–walled frusta and egg–box material under shear and normal loading*, Int. J. of Mechanical Sciences, vol. 48(7), p. 799–808

Aktay, L., Toksoy, A. K. and Guden, M. (2006), *Quasi–static axial crushing of extruded polystyrene foam–filled thin–walled aluminium tubes: Experimental and numerical analysis*, Materials & Design, vol. 27(7), p. 556–565

Al–asady, N. A., Abdullah, S., Ariffin, A. K., Bedan, S. M. and Rahman, M. M. (2009), *Comparison between experimental road data and finite element analysis data for automotive lower suspension arm*, European J. of Scientific Research, vol. 29(4), p. 557–571

Alexander, J. M. (1960), *An approximate analysis of the collapse of thin cylindrical shells under axial loading*, Quart. J. Mechanics. and Applied Mathematics, vol. 13, p. 1–9

Alghamdi, A. A. A. (2001), *Collapsible impact energy absorbers: an overview*, Thin–Walled Structures, vol. 29, p. 189–213

Alghamdi, A. A., EL–Kalay, A. K., Mansour T. M. and Akyurt, M. (1992), *Absorption of energy by frusta*, J. Islamic Acad Sci, pp. 14–20

Aljawi, A. A. N. (2000), *Finite element and experimental analysis of axially compressed plastic tubes*, European J. of Mechanical and Environmental Engineering, vol. 45 (1), p. 3–10

ANSYS® 13.0 Help System (2010), *Mechanical Analysis User Guide*, ANSYS Inc

ANSYS/LS–DYNA® (2011), *ANSYS/LS–DYNA User's Guide*, ANSYS Inc

ANSYS/LS–DYNA® Introduction, ANSYS Website, accessed March 2011: http://www.ansys.com/products/%20lsdyna.asp

Arriaga, A., Pagaldai, R., Zaldua, A. M., Chrysostomou, A. and O'Brien, M. (2010), *Impact testing and simulation of a polypropylene component. Correlation with strain rate sensitive constitutive models in ANSYS and LS–DYNA*, Polymer Testing, vol. 29(2), p. 170–180

Asadi, M., Walker, B. and Shirvani, H. (2009), *An Investigation to Compare the Application of Shell and Solid Element Honeycomb Model in ODB*, 7th European LS–DYNA Conf.

Asadi, M., Walker, B. and Shirvani, H. (2008a), *Development of the Advanced Finite Element Model for ODB Impact Barrier*, LS–DYNA User Conf.: Japan

Asadi, M., Walker, B. and Shirvani, H. (2008b), *New Finite Element Model for NHTSA Impact Barrier*, 10th Int. LS–DYNA Users Conf.

Asadi, M., Walker, B. and Shirvani, H. (2007a), *Evaluation of New Finite Element Model for IIHS Side Impact Barrier*, LS–DYNA User Conf.: Japan

Asadi, M., Tattersall, P., Walker, B. and Shirvani, H. (2007b), *Advanced Finite Element Model for AE–MDB Side Impact Barrier*, 6th European LS–DYNA User Conf.

Asadi, M., Shirvani, H., Sanaei, E. and Ashmead, M. (2006), *A Simplified Model to Simulate Crash Behaviour of Honeycomb*, Proceedings of the Int. conf. on Advanced Design and Manufacture: China

Asavavisithchai, S., Slater, D. and Kennedy, A. R. (2004), *Effect of tube length on the bucking mode and energy absorption of Al foam–filled tubes*, J. of Materials Science, vol. 39(24), p. 7395–7396

Ashby, M. F., Evans, A. G., Fleck, N. A., Gibson, L. J., Hutchinson, J. W. and Wadley, H. G. (2000), *Metal foams: a design guide*, Butterworth–Heinemann: Boston, MA, USA

Ashmead, M. (2000), *Energy–absorbing structures Int. Patent*, Serial No. WO 00/31434

Ashmead, M., Bedus, S. and Bradley, S. (2000), Advanced Materials for Enhanced Automotive Safety, Automotive Composites and Plastics Conf.

Avalle, M., Belingardi, G., Ibba, A. (2007), *Mechanical models of cellular solids: Parametres identification from experimental tests*, Int. J. of Impact Engineering, vol. 34(1), p. 3–27

Avalle, M., Chiandussi, G., and Belingardi, G. (2002), *Design optimisation by response surface methodology: Application to crashworthiness design of vehicle structures*, Structural and Multidisciplinary Optimisation, vol. 24, p. 325–332

Banhart, J. (2001), *Manufacture, characterisation and application of cellular metals and metal foams*, Progress in Materials Science, vol. 46(6), p. 559–632

Bardi, F. C., Yun, H. D. and Kyriakides, S. (2003), *On the axisymmetric progressive crushing of circular tubes under axial compression*, Int. J. of Solids and Structures, vol. 40, p. 3137–3155

Birch, R. S. and Jones, N. (1990), *Dynamic and static axial crushing of axially stiffened cylindrical shells*, Thin–Walled Structures, vol. 9, p. 29–60

Belytschko, T. B. and Tsay, T. S. (1983), *A stabilization procedure for the quadrilateral plate element with one–point quadrature*, Int. J. of Numerical Methods in Engineering, vol. 19, p. 405–419

Belytschko, T. B., Lin, J. I. and Tsay, C. S. (1984), *Explicit algorithms for the nonlinear dynamics of shells*, Computer Methods in Applied Mechanics and Engineering, vol. 42, p. 225–251

Borvik, T., Hopperstad, O. S., Reyes, A., Langseth, M., Solomos, G. and Dyngeland, T. (2003), *Empty and foam–filled circular aluminium tubes subjected to axial and oblique quasi–static loading*, Int. J. of Crashworthiness, vol. 8 (5), p. 481– 494

Box, G. E. P. and Wilson, K.B. (1951), *On the Experimental Attainment of Optimum Conditions (with discussion)*, J. of the Royal Statistical Society, Series B, vol. 13(1), p. 1–45

Brown, J., C. (2002), *Introduction to the Basic Principles of Crashworthiness*, Cranfield University: Bedfordshire

Calladine, C. R. (1986), *Analysis of large plastic deformations in shell structures*, Inelastic Behaviour of Plates and Shells (IUTAM Symposium, Rio de Janeiro, 1985), ed. L. Bevilacqua et al., Springer, Berlin, p. 69–101

Calladine, C. R. and English, R. W. (1984), *Strain–rate and Inertia Effects in the Collapse of Two Types of Energy–absorbing Structure*, Int. J. of Mechanical Science, vol. 26(11–12), p. 689–701

CARE (EU road accidents database) or national publications (2011), *Road safety evolution in EU*, European Commission Road Safety, Directorate General Energy and Transport

Chen, C., Harte, A. M. and Fleck, N. A. (2001), *The plastic collapse of sandwich beams with a metallic foam core*, Int. J. of Mechanical Sciences, vol. 43, p. 1483–1506

Chen, C., Lu, T. J. and Fleck, N. A. (1999), *Effect of imperfections on the yielding of two–dimensional foams*, J. of the Mechanics and Physics of Solids, vol. 47(11), p. 2235–2272

Cheon, S. S. and Meguid, S. A. (2004), *Crush behaviour of metallic foams for passenger car design*, Int. J. of Automotive Technology, vol. 5(1), p. 47–53

Choi, K. K. and Youn, B. D. (2002), *An investigation of nonlinearity of reliability–based design optimisation approaches*, In: 28th Design Automation Conf., Sep 29–Oct 2 2002, Montreal, Que., Canada

Chung, J. G., Chang, S. H., Sutcliffe, M. P. F. (2007), *Deformation and energy absorption of composite egg–box panels*, J. of Composites Science and Technology, vol. 67, p. 2342–2349

Commission of the European Communities (2001), *European transport policy for 2010: time to decide*, White Paper: Brussels

Deb, A., Mahendrakumar, M.S., Chavan, C., Karve, J., Blankenburg, D. and Storen, S. (2004), *Design of an aluminium–based vehicle platform for front impact safety*, Int. J. of Impact Engineering, vol. 30(8–9), p. 1055–1079

Department for Transport (DfT) (2011), *Heavy Goods Vehicle Inspection Manual*, Consolidated Edition

Deqiang, S., Weihong, Zh., Yanbin, W. (2010), *Mean out–of–plane dynamic plateau stresses of hexagonal honeycomb cores under impact loadings*, Composite Structures, vol. 92(11), p. 2609–2621

Deshpande, V. S. and Fleck, N. A. (2000), *High strain rate compressive behaviour of aluminium alloy foams*, Int. J. Impact Eng, vol. 24, p. 277–298

Deshpande, V. S. and Fleck, N. A. (2000), *Isotropic constitutive models for metallic foams*, J. of the Mechanics and Physics of Solids, vol. 48(6–7), p. 1253–1283

Deshpande, V. S., Fleck, N. A., (2001), *Collapse of truss core sandwich beams in 3–point bending*, Int. J. Solids Structures, vol. 38(36–37), p. 6275–6305

Deshpande, V. S. and Fleck, N. A. (2003), *Energy absorption of an egg–box material*, J. of the Mechanics and Physics of Solids, vol. 51(1), p. 187–208

Du Bois, P., Chou, C. C., Fileta, B. B., Khalil, T. B., King, A. I., Mahmood, H. F., Mertz, H. J. and Wismans, J. (2004), *Vehicle Crashworthiness and Occupant*

Protection, Sponsored by Automotive Applications Committee, American Iron and Steel Institute: Southfield, Michigan

El–Hage, H., Mallick, P. K. and Zamani, N. (2005), *A numerical study on the quasi–static axial crush characteristics of square aluminium tubes with chamfering and other triggering mechanisms*, Int. J. of Crashworthiness, vol. 10(2), p. 183– 195

El–Sobky, H., Singace, A. A. and Petsios, M. (2001*), Mode of collapse and energy absorption characteristics of constrained frusta under axial impact loading*, Int. J. of Mechanical Sciences, vol. 43(3), p. 743–757

Ellert, G. (1998–2008), *The Physics Hypertextbook*, Physics.info 2010: New York

European Commissions (EC) (2003), *Saving 20000 Lives on Our Roads*, Office for Official Publications of the European Communities: Luxembourg

Evans, A. G. (2001), *Lightweight Materials and Structures*, MRS Bull vol. 790

Farley, G. L. (1986), *Effect of Specimen Geometry on the Energy Absorption Capability of Composite Materials*, J. of Composite Materials, vol. 20, p. 390–400

Finn, S. R., Springer, G. S. (1991), *Composite Plates Impact Damage: An Atlas*, Research supported by NASA, Technomic Publishing Co: Lancaster: PA

Fleck, N. A. (2001), *Multi-Axial Strength of Metallic Foams and Lattice Materials*, J. of JSMS: Materials Science for the 21st Century, vol. A, p. 336-340

Fyllingen, Ø., Hopperstad, O. S. and Langseth, M. (2009), *Robustness study on the behaviour of top–hat thin–walled high–strength steel sections subjected to axial crushing*, Int. J. of Impact Engineering, vol. 36(1), p. 12–24

Gameiro, C. P. and Cirne, J. (2007), *Dynamic axial crushing of short to long circular aluminium tubes with agglomerate cork filler*, Int. J. of Mechanical Sciences, vol. 49(9), p. 1029–1037

Garg, M., Abdi, F., Zammit, A., Bayandor, J., Suh, Y., Song, S. (2011), *Impact Damage Resistance and Compression–After–Impact Strength of Sandwich Composites with Graphite–Epoxy Facesheets and Nomex Honeycomb Core*, Technical Paper (ONLINE): http://www.sampe.org/store/paper.aspx?pid=5681 (Accessed 06 September 2010)

Gibson, L. J. and Ashby, M. F. (1997), *Cellular Solids, Structure and Properties*, 2nd ed., Cambridge University Press: Cambridge, UK

Grzebeita, R. H. (1990), *An alternate method for determining the behaviour of round stocky tubes subjected to an axial crush load,* Thin–Walled Structures, vol. 9, p. 61–69

Gupta, N. K., Easwara Prasad, G. L. and Gupta, S. K. (1997), *Plastic collapse of metallic conical frusta of large semi–apical angles*, Int. J. of Crashworthiness, vol. 2, p. 349–366

Gupta, N. K., Mohamed Sheriff, N. and Velmurugan, R. (2008), *Experimental and theoretical studies on buckling of thin spherical shells under axial loads*, Int. J. of Mechanical Sciences, vol. 50(3, p.: 422–432

Gupta, N. K. and Velmurugan, R. (1999), *Axial compression of empty and foam filled composite conical shells*, J. of Composite Materials, vol.33(6), p. 567–591

Gupta, N. K. and Venkatesh (2006), *A study of the influence of diametre and wall thickness of cylindrical tubes on their axial collapse*, Thin–Walled Structures, vol. 44(3), p. 290–300

Gupta, N. K. and Venkatesh (2007), *Experimental and numerical studies of impact axial compression of thin–walled conical shells*, Int. J. of Impact Engineering, vol. 34(4), p. 708–720

Hallquist, J. O. (2006), *LS–DYNA® Theory Manual*, Livermore Software Technology Corporation

Hamada, H. and Ramakrishna, S. (1997) Fem *method for prediction of energy absorption capability of crashworthy polymer composite materials*, J. of Reinforced Plastics and Composites, vol. 16, p. 226–242

Hanssen, A. G.; Langseth, M. and Hopperstad, O. S. (1999), *Static crushing of square aluminium extrusions with aluminium foam filler*, Int. J. Mechanical Engineering, vol. 41(8), p. 967–993

Hanssen, A. G., Langseth, M. and Hopperstad, O. S. (2000a), *Static and dynamic crushing of circular aluminium extrusions with aluminium foam filler*, Int. J. of Impact Engineering, vol. 24(5), p. 475–507

Hanssen, A. G., Langseth, M. and Hopperstad, O. S. (2000b), *Static and dynamic crushing of square aluminium extrusions with aluminium foam filler*, Int. J. of Impact Engineering, vol. 24(4), p. 347–383

Hanssen, A. G., Langseth, M. and Hopperstad, O. S. (2001), *Optimum design for energy absorption of square aluminium columns with aluminium foam filler*, Int. J. of Mechanical Sciences, vol. 43(1), p. 153–176

Harte, A. M., Fleck, N. A. and Ashby, M. F. (2000), *Energy absorption of foam–filled circular tubes with braided composite walls*, Eur. J. Mechanics – A/Solids, vol.19, p. 31–50

Hartmann, F. and Katz, C. (2007), *Structural analysis with finite elements*, Springer: Berlin

Hibbeler, R. C. (2002), *Structural Analysis*, Fifth Edition, Prentice Hall, Upper Saddle River: New Jersey

Hibbitt, Karlsson and Sorensen Inc. (HKS) (2002), *Getting Started with ABAQUS/Standard Version 6.3*, Pawtucket, USA: HKS

Higashi, K., Mukai, T., Kaizu, K., Tsuchida S. and Tanimura, S. (1991), *Strain rate dependence on mechanical properties is some commercial aluminium alloys*, J Phys III, vol. 1

Housner, G. W. and Vreeland, T. Jr. (1965), *The Analysis of Stress and Deformation*, California Institute of Technology: Pasadena, CA

Iyengar, N.G.R. and Gupta, S. K. (1980), *Structural Design Optimisation*, East West Press: New Delhi

Jacobsen, A. J., Kolodziejska, J. A., Doty, R., Fink, K. D., Zhou, C., Roper, C. S. and Carter, W. B. (2010), *Interconnected Self-Propagating Photopolymer Waveguides: An Alternative to Stereolithography for Rapid Formation of Lattice-Based Open-Cellular Materials*, Twenty First Annual International Solid Freeform Fabrication Symposium - An Additive Manufacturing Conference: University of Texas, Austin

Jeon, I., Asahina, T., Kang, K. J., Im, S. and Lu, T. J. (2010), Finite element *simulation of the plastic collapse of closed–cell aluminium foams with X–ray computed tomography*, J. of Mechanics of Materials, vol. 42, p. 227–236

Johnson, W. and Mamalis, A. G. (1978), *Crashworthiness of vehicles*, Mechanical Engineering Publications Ltd: London

Jones, N. (1989), *Structural Impact*, Cambridge University Press: Cambridge, UK

Jones, N. (2003), *Several phenomena in structural impact and structural crashworthiness*, Euro. J. of Mechanics – A/Solids General and plenary lectures from the 5th EUROMECH Solid Mechanics Conference, vol. 22(5), p. 693–707

Jones, D. L. and Miraj, R. (1995), *Analytical and Numerical Evaluations of the Biaxial Strength of Composite Laminated Circular Sandwich Panels*, Second International Conference on Composites Engineering, ICCE/2: New Orleans

Karagiozova, D., Alves, M. and Jones, N. (2000), *Inertia effects in axisymmetrically deformed cylindrical shells under axial impact*, Int. J. of Impact Engineering, vol. 24(10), p. 1083–1115

Karagiozova, D. and Jones, N. (2004), *Dynamic buckling of elastic–plastic square tubes under axial impact–II: structural response*, Int. J. of Impact Engineering, vol. 30(2), p. 167–192

Kavi, H., Tasoy, A. K. and Guden, M. (2006), *Predicting energy absorption in a foam–filled thin–walled aluminium tube based on experimentally determined strengthening coefficient*, Materials & Design, vol. 27(4), p. 263–269

Kim, D. K., Lee, S. (1999), *Impact energy absorption of 6061 aluminium extruded tubes with different cross–sectional shapes*, Materials & Design, vol. 20(1–5), p. 41–49

Kooistra, G. W., Deshpande, V. S. and Wadley, H. N. G. (2004), *Compressive Behavior of Age Hardenable Tetrahedral Lattice Truss Structures Made from Aluminium*, Acta Mater, vol. 52, p. 4229–4237

Lampinen, B. E. and Jeryan, R. A. (1982), *Effectiveness of polyurethane foam in energy absorbing structures*, SAE Technical Paper Series 820494

Langseth, M., Hopperstad, O. S. and Berstad, T. (1999), *Crashworthiness of aluminium extrusions: Validation of numerical simulation, effect of mass ratio and impact velocity*, Int. J. of Impact Engineering, vol. 22, p. 829–854

Lanzi, L., Castelletti, M. L. and Anghileri, M. (2004), *Multi–objective optimisation of composite absorber shape under crashworthiness requirements*, Composite Structures, vol. 65(3–4), p. 433–441

Liu, Y. (2008), *Design optimisation of tapered thin–walled square tubes*, Int. J. of Crashworthiness, vol. 13(5), p. 543–550

LSTC (2007), *LS–DYNA® Keyword Users' Manual V970*, Livermore Software Technology Corporation

Lu, G. and Yu, T. (2003), *Energy absorption of structures and materials*, Woodhead Publishing Limited: Cambridge,UK

Mahdi, E., Hamouda, A. S. A. and Sen, A. C. (2004), *Quasi–Static Crushing Behaviour of Hybrid and Non–Hybrid Natural Fiber Composite Solid Cones*, Composite Structures, vol. 66(1–4), p. 647–663

Mamalis, A. G. and Johnson, W. (1983), *The quasi–static crumpling of thin–walled circular cylinders and frusta under axial compression*, Int. J. of Mechanical Sciences, vol. 25(9–10), p. 713–732

Mamalis, A. G., Johnson, W. and Viegelahn, G. L. (1984), *The crumpling of steel thin–walled tubes and frusta under axial compression at elevated strain rates: some experimental results*, Int. J. of Mechanical Sciences, vol. 26, p. 537–548

Mamalis, A. G., Manolakos, D. E., Ioannidis, N. B. and Kostazos, P. K. (2005), *Numerical simulation of thin–walled metallic circular frusta subjected to axial loading*, Int. J. of Crashworthiness, vol. 10(5), p. 505–513

Mamalis, A. G., Manolakos, D. E., Ioannidis, M. B., Kostazos, P. K. and Dimitriou, C. (2003), *Finite element simulation of the axial collapse of metallic thin–walled tubes with octagonal cross–section*, Thin–Walled Structures, vol. 41(10), p. 891–900

Mamalis, A. G., Manolakos, D. E., Ioannidis, M. B., Kostazos, P. K. and Hassiotis, G. (2001), *Finite element simulation of the axial collapse of thin–wall square frusta*. Int. J. of Crashworthiness, vol. 6(2), p.155–164

Mamalis, A. G., Manolakos, D. E., Saigal, S., Viegelahn, G. and Johnson, W. (1986), *Extensible plastic collapse of thin–wall frusta as energy absorbers*, Int. J. of Mechanical Sciences, vol. 28(4), p. 219–229

Meguid, S. A., Attia, M. S., Stranart, J. C. and Wang, W. (2007), *Solution stability in the dynamic collapse of square aluminium columns*, Int. J. of Impact Engineering, vol. 34(2), p. 348–359

Meng, Q., Al–Hassani, S.T.S. and Soden, P.D. (1983), *Axial crushing of square tubes*, Int. J. of Mechanical Sciences, vol. 25(9–10), p. 747–773

Miraj, R. (2005), *An Investigation of The Nonlinear Bending Of Unsymmetrical, Dissimilar Orthotropic Circular & Rectangular Sandwich Plates*, Composites Part B

Mirfendereski, L., Salimi, M. and Ziaei–Rad, S. (2008), *Parametric study and numerical analysis of empty and foam–filled thin–walled tubes under static and dynamic loadings*, Int. J. of Mechanical Sciences, vol. 50(6), p. 1042–1057

Moaveni, S. (1999), *Finite Element Analysis: Theory and Application with ANSYS*, 1st Edition, Prentice Hall, Upper Saddle River: New Jersey

Morris, E., Olabi, A. G. and Hashmi, M. S. J. (2006), *Analysis of nested tube type energy absorbers with different indenters and exterior constraints*, J. of Thin–Walled Structures, vol. 44, p. 872–885

Mosallam, A., Slenk, J., Kreiner, J. (2008), Assessment of Residual Tensile Strength of Carbon/Epoxy Composites Subjected to Low-Energy Impact, J. of Aerospace Eng., vol. 21, p. 249-258

Nagel, G. M. and Thambiratnam, D. P. (2005), *Computer simulation and energy absorption of tapered thin–walled rectangular tubes*, Thin–Walled Structures, vol. 43(8), p. 1225–1242

Nagel, G. M. and Thambiratnam, D. P. (2006), *Dynamic simulation and energy absorption of tapered thin–walled tubes under oblique impact loading*, Int. J. of Impact Engineering, vol. 32(10), p. 1595–1620

Nariman–zadeh, N., Darvizeh, A. and Jamali, A. (2006), *Pareto Optimisation of Energy Absorption of Square Aluminium Columns Using Multi–Objective Genetic Algorithms*, Proceedings of the Institution of Mechanical Engineers, Part B: J. of Engineering Manufacture, vol. 220(2), p. 213–224

Nettles, A. T., Douglas, M. J. (2000), *A Comparison of Quasi-Static Indentation to Low-Velocity Impact*, NASA, Marshall Space Flight Center: Hanover, MD

Nowpada, S., Chirwa, E. C., Myler, P. and Matsika, E. (2010), *Aluminium Egg-box panel as an energy absorber for pedestrian protection*, Advanced Engineering Materials, vol. 12(7), p. 591–595

Nowpada, S., Yang, Y., Chirwa, E. C., Myler, P., Matsika, E. and Qian, P. (2010), *Aluminium egg-box energy absorber in a commercial vehicle front for pedestrian protection: Energy absorption capability*, Proc. of The Int. Crashworthiness Conference, ICRASH2010 Washington, Edited by E C Chirwa, C-D (Steve) Kan, The National Conference Center: Leesburg, VA, USA

Nowpada, S., Chirwa, E. C., Myler, P., Chinnaswamy, G. K. and Matsika, E. (2009), *Egg-box panel for commercial vehicle front – compressive loading tests*, Int. J. Crashworthiness, vol. 15(1), p. 59–70

Nowpada, S., Chirwa, E. C., Myler, P., Chinnaswamy, G. K. and Matsika, E. (2008), *Egg-box panel for commercial vehicle front*, Proc. of The Int. Crashworthiness Conference, ICRASH2008 Edited by E C Chirwa, H Hamada and K Mizuno, Kyoto Institute of Technology: Kyoto, Japan

Olabi, A. G., Morris, E., Hashmi, M. S. J. and Gilchrist M.D. (2008), *Optimised design of nested oblong tube energy absorbers under lateral impact loading*, Int. J. of Impact Engineering, vol. 35, p. 10–26

Otubushin, A. (1998), *Detailed validation of a non–linear finite element code using dynamic axial crushing of a square tube*, Int. J. of Impact Engineering, vol. 21(5), p. 349–368

Peroni, L., Avalle, M. and Belingardi, G. (2009), *Comparison of the energy absorption capability of crash boxes assembled by spot–weld and continuous joining techniques*, Int. J. of Impact Engineering, vol. 36(3), p. 498–511

Prasad, G. L. E. and Gupta, N. K. (2005), *An experimental study of deformation modes of domes and large–angled frusta at different rates of compression*, Int. J. of Impact Engineering, vol. 32(1–4), p. 400–415

Preece, B. W. (1911), *Sand for Brass Molding*, The Foundry; University of Michigan, Cleveland, Ohio, vol. 38(2), p. 83–87

Qiao, P., Yang, M. and Bobaru, F. (2008), *Impact Mechanics and High–Energy Absorbing Materials: Review*, J. of Aerospace Engineering, vol. 21(4), p. 235–24

Qiao, P., Yang, M. and Mosallam, A. (2004), *Impact analysis of I-Lam sandwich system for over-height collision protection of highway bridges*, J. of Engineering Structures, vol.26(7), p.1003–1012

Reid, S. R. (1993), *Plastic deformation mechanisms in axially compressed metal tubes used as impact energy absorbers*, Int. J. of Mechanical Sciences, vol. 35(12), p. 1035–1052

Reid, S. R. and Reddy, T. Y. (1986), *Static and dynamic crushing of tapered sheet metal tubes of rectangular cross–section*, Int. J. of Mechanical Sciences, vol. 28(9), p. 623–637

Reyes, A., Hopperstad, O. S., Berstad, T., Hanssen, A. G. and Langseth, M. (2003), *Constitutive modelling of aluminium foam including fracture and statistical variation of density*, European J. of Mechanics – A/Solids, vol. 22(6), p. 815–835

Reyes, A., Hopperstad, O. S. and Langseth, M. (2004), *Aluminium foam–filled extrusions subjected to oblique loading: experimental and numerical study*, Int. J. of Solids and Structures, vol. 41(5–6), p. 1645–1675

Santosa, S. P. and Wierzbicki, T. (1998), *Crash behaviour of box columns filled with aluminium honeycomb or foam*, Computers & Structures, vol. 68(4), p. 343–367

Santosa, S. P., Wierzbicki, T., Hanssen, A. G. and Langseth, M. (2000), *Experimental and numerical studies of foam–filled sections*, Int. J. of Impact Engineering, vol. 24(5), p. 509–534

Schneider, F. and Jones, N. (2008), *Observations on the design and modelling of some joined thin-walled structural sections*, Thin-Walled Structures, vol. 46(7–9), p. 887–897

Seide, P. (1956), *Axisymmetrical buckling of circular cones under axial compression*, J. of Applied Mechanics, Transaction ASME, vol. 23, p. 625–628

Seitzberger, M., Rammerstorfer, F. G., Gradinger, R., Degischer, H. P., Blaimschein, M. and Walch, C. (2000), *Experimental studies on the quasi–static axial crushing of steel columns filled with aluminium foam*. Int. J. of Solids and Structures, vol. 37(30), p. 4125–4147

Shariatpanahi, M., Masoumi, A. and Ataei, A. (2008), *Optimum design of partially tapered rectangular thin–walled tubes in axial crushing*, Proceeding of the

Institution of Mechanical Engineers Part B–J. of Engineering Manufacture, vol. 222(2), p. 285– 291

Sheh, M. Y., Reid, J. D., Lesh, S. M. and Cheva, M. (1992), *Vehicle crashworthiness analysis using numerical and experimental method*, Int. Conference on Vehicle Structural Mechanics and CAE, Warrendale, Society of Automotive Engineering Inc

Sheldon Imaoka, http://ansys.net/, Accessed frequently since 2006

Sheriff, N. M., Gupta, N. K., Velmurugan, R. and Shanmugapriyan, N. (2008), *Optimisation of thin conical frusta for impact energy absorption*, Thin–Walled Structures, vol. 46(6), p. 653–666

Sherwood, J. A. and Frost, C. C. (1992), *Constitutive Modelling and Simulation of Energy Absorbing Polyurethane Foam under Impact Loading*, Polymer Engineering and Science, vol. 32(16), p. 1138–1146

Shetty, S. K. (2001), *Finite Element Modelling of Energy Absorption Characteristics of Hybrid Structures – Composite Wrapped on a Square Metal Tube*, B.Eng Thesis, Mysore University: India

Singace, A. A., El–Sobky, H. and Petsios, M. (2001), *Influence of end constraints on the collapse of axially impacted frusta*, Thin–Walled Structures, vol. 39(5), p. 415–428

Song, H. W., Fan, Z. H., Yu, G., Wang, Q. C. and Tobota, A. (2005), *Partition energy absorption of axially crushed aluminium foam–filled hat sections*, Int. J. of Solids and Structures, vol. 42(9–10), p. 2575–260

Spagnoli, A. and Chryssanthopoulos, M. K. (1999), *Elastic buckling and postbuckling behaviour of widely–stiffened conical shells under axial compression*, Engineering Structures, vol. 21(9), p. 845–855

Subhash, G., Liu, Q., Gao, X. (2006), *Quasistatic and high strain rate uniaxial compressive response of polymeric structural foams*, Int. J. of Impact Eng., vol. 32(7), p. 1113–1126

Tan, H. and Qu, S. (2009), *Impact of Cellular Materials*, Lecture note, International Centre for Mechanical Sciences, Udine, Italy, 28 Sept – 2 Oct

Tarigopula, V., Langseth, M., Hopperstad, O. S. and Clausen, A. H. (2006), *Axial crushing of thin–walled high–strength steel sections*, Int. J. of Impact Engineering, Int. Symposium on the Crashworthiness of Light–weight Automotive Structures, vol. 32(5), p. 847–882

Toksoy, A. K. and Guden, M. (2005), *The strengthening effect of polystyrene foam filling in aluminium thin–walled cylindrical tubes*, Thin–Walled Structures, vol. 43(2), p. 333–350

Triantafillou, T. C. and Gibson, L. J. (1989), *Debonding in Foam Core Sandwich Panels*, Material Structures, vol. 22, p. 64–89

Ulker, M. B. C. and Rahman, M. S. (2008), *Traffic Barriers under Vehicular Impact: From Computer Simulation to Design Guidelines*, J. of Computer–Aided Civil and Infrastructure Engineering, vol. 23, p. 465–480

USA Department of Defence (1966), *Aluminum and Aluminum Alloys*, Military Standardization Handbook: Washington, DC

Vanderplaats, G. N. (2007), *Multidiscipline Design Optimisation*, Vanderplaatz R&D, Inc.

Wadley, H. N. G., Fleck, N. A. and Evans, A. G. (2003), *Fabrication and Structural Performance of Periodic Cellular Metal Sandwich Structures*, Compos Sci Tech, vol. 63, p. 2331–2343

Walter, P. L. (2007), *Selecting Accelerometers for Mechanical Shock Measurements*, Sound and Vibration, vol. 41(12), p. 14–18

White, M. and Jones, N. (1999), *Experimental quasi–static axial crushing of top–hat and double–hat thin–walled sections*, Int. J. of Mechanical Sciences, vol. 41, p. 179–208

WHO (2004), *World Report on Road Traffic Injury Protection*, World Health Organisation Library Cataloguing–in–Publication Data

Wierzbicki, T. and Abramowicz, W. (1983), *On the crushing mechanics of thin–walled structures*, J. of Applied Mechanics, vol. 50, p. 727–734

Witteman, W. J., Kriens, R. F. C. (1998), *Modelling of an Innovative Frontal Car Structure: Similar Deceleration Curves at Full Overlap, 40 per cent Offset and 30 Degrees Collisions*, Proceedings of the Sixteenth Int. Technical Conference on the Enhanced Safety of Vehicles (ESV), Paper 98–S1–O–04, p. 194–212: Windsor, Canada

Wu, E. and Jiang, W. (1996), *Axial crush of Metallic Honeycombs*, Pergamon, Int. J. of Impact Engineering, vol. 19(5–6), p. 439–456

Yamazaki, K. and Han, J. (2000) *Maximization of the crushing energy absorption of cylindrical shells*, Advances in Engineering Software, vol. 31, p. 425–434

Yan, W. Y., Durif, E., Yamada, Y. and Wen, C. (2007), *Crushing simulation of foam– filled aluminium tubes*, Materials Transactions, vol. 48(7), p. 1901–1906

Yoo, S. H., Chang, S. H. and Sutcliffe, M. P. F. (2010), *Compressive characteristics of foam–filled composite egg–box sandwich panels as energy absorbing structures*, J. of Composites, Part A, vol. 41, p. 427–434

Yuen, S. C. K., Nurick, G. N. and Starke, R. A. (2008), *The energy absorption characteristics of double–cell tubular profiles*, Latin American J. of Solids and Structures, vol. 5(4), p. 289–317

Yuen, S. W. and Van Erp., G. M. (1999) *Transient analysis of thin–walled structures using macro spline finite elements*, Engineering Structures, vol. 21(3), p. 255–266

Zarei, H. R. and Kroger, M. (2006), *Multiobjective crashworthiness optimisation of circular aluminium tubes*, Thin–Walled Structures, vol. 44(3), p. 301–308

Zarei, H. R. and Kroger, M. (2008), *Optimisation of the foam–filled aluminium tubes for crush box application*, Thin–Walled Structures, vol. 46(2), p. 214–221

Zhang, X., Cheng, G. and Zhang, H. (2009), *Numerical investigations on a new type of energy–absorbing structure based on free inversion of tubes*, Int. J. of Mechanical Sciences, vol. 51, p. 64–76

Zhang, Z., Liu, Sh. and Tang, Z. (2010), *Crashworthiness investigation of kagome honeycomb sandwich cylindrical column under axial crushing loads*, J. of Thin–Walled Structures, vol. 48, p. 9–18

Zini, G. (2005), *Reduction of crash severity through in–vehicle systems (IVS) speed Control*, In: 19th Int. Technical Conference on The Enhanced Safety of Vehicles, June 2005, Washington DC

Zupan, M., Chen, C. and Fleck, N. A. (2003), *The plastic collapse and energy absorption capacity of egg–box panels*, Int. J. of Mechanical Sciences, vol. 45(5), p. 851–871

APPENDECIES

APPENDIX A

A.1. Introduction

In order to recognise the importance of optimum crashworthiness in a structure, it is initially necessary to study the theoretical background of the subjects related to this criteria. The aim here is to give a basic foundation on the work presented in the thesis and, where applicable, reference has been made to the works reviewed in the Literature Review Chapter. The information provided herein includes subjects such as structural crashworthiness, energy absorption, EA structures and methods of analysis of energy absorbers.

A.2. Safety Evaluation in the Automotive Industry

Severe or fatal traffic accidents are considered to be one of the most threatening dangers in daily life. In a 2001 White Paper on European Transport Policy, the European Commission proposed that the European Union should set itself the target of halving the number of road deaths by 2010 (EC, 2003). In 2003, the European Union published a brochure reflecting this proposal, indicating that:

> "Road safety directly affects all of the territory of the European Union and all its inhabitants: in the 15 member European Union, 375 million road users, 200 million of them driving license holders, use 200 million vehicles on 4 million km of roads. Ever greater mobility comes at a high price: 1'300'000 accidents a year cause 40'000 deaths and 1'700'000 injuries on the roads. The direct and indirect cost of this carnage has been estimated at EUR 160 billion" (EC, 2003).

In May 2011 the European Commission released a series of statistical data, suggesting that the total number of deaths in road accidents over Europe fell by 28% to 34,800 in 2009 from 54,302 in 2001. According to the European Road Safety Observatory, in Great Britain 2,645 people were killed in road accidents in 2008, 1,312 (almost 50%) of which were passenger car occupants alone (CARE, 2011). In light of these statistical data, it can be said that despite a decrease in the number of fatalities over the past 10 years, the current situation is still socially unacceptable.

In order for a vehicle to be released to consumers, it has to undergo a set of crash tests to determine its crashworthiness and safety levels. There are a number of vehicle rating systems under the New Car Assessment Program (NCAP) such as Australasian NCAP (ANCAP), European NCAP (EURO NCAP), Safer Car (US), Japan JNCAP and Korean KNCAP. These programs test vehicles and rate their safety with one to five stars; the safer the vehicle, the more the number of stars.

To make the evaluation, NCAP investigates the effects of a number of crash tests on the vehicle occupant dummies. The tests are conducted at various speeds and include a front–on crash, side impact crash and hitting a pole with the side of the car. The tests also investigate how a crash can influence the pedestrians and how they can be protected against injurious accidents. The test procedures consist of velocity, ground clearance height and percentage overlap tests (WHO, 2004). According to the report published by WHO, the test specifications vary between the NCAP rating systems mentioned above.

A.3. Structural Crashworthiness and Impact Mechanics

The most important areas in crash analysis are a structure's crashworthiness and its mechanical properties when impacted. Therefore, in order to design an energy absorbing system, it is necessary to explore the basic concepts of structural crashworthiness and impact mechanics. Energy absorbing systems are commonly in use in the vehicle industry by car manufacturers as well as the producers of heavy vehicle, railway, aerospace and ship.

As a result of the complex behaviour of an impacted structure, the detailed mechanical response of the structure can be investigated by studying an individual structural component such as an energy absorber.

In general, crashworthiness can be defined as the capability of a structure to resist the load of an impact from another body, in a manner that it will protect a survival space. In the automotive industry, an increased emphasis has been placed on this criterion as a vehicle design requirement for the safety of its occupants.

The essential concepts of the crashworthiness requirement for the survival space of a vehicle are illustrated in Figure A.1 (Brown, 2002). It can be seen that the kinetic impact energy during a crash event is initially absorbed by the frontal energy absorbing system of the vehicle, thus the survival space, where the vehicle occupants are located has remained intact.

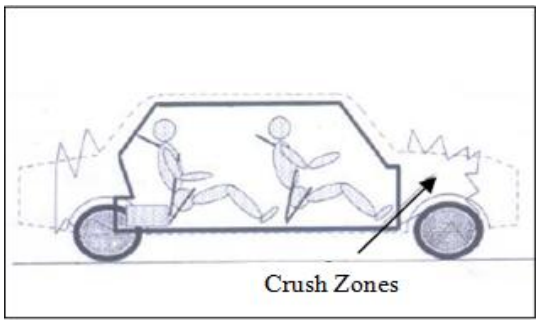

Figure A.1 – Crash Energy Management in Vehicles (Brown, 2002)

Theoretically, a crashworthy vehicle should be designed so the load that would be transferred to the vehicle body following an impact, (P_1) will be lower than the load which will damage the survival space (P_2). Brown (2002) provides the illustration of Figure A.2 to further explain this basic crashworthiness requirement. In other words, the deformation of the survival space must be kept to a minimum level. In addition, the peak deceleration should also be within a reasonable limit (Deb et al. 2004).

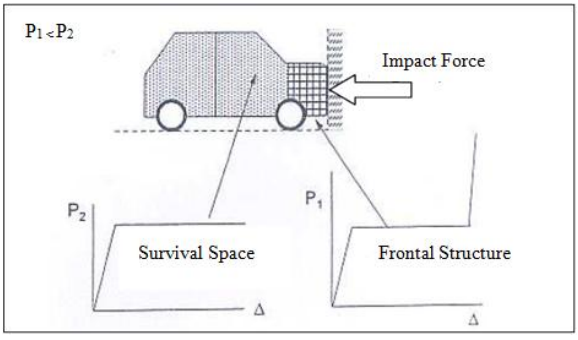

Figure A.2 – Crush Characteristics of Crashworthy Structures (Brown, 2002)

Alongside the collapse behaviour of a vehicle, its crashworthiness is also determined by aspects such as the ability of a vehicle to avoid accidents, the dynamics of the vehicle during and after an impact and the occupant motions. However, the focus of this study is on the components that improve the impact behaviour of a vehicle.

The performance of an energy absorbing structure depends on its collapse mode, the strain rate sensitivity of its material and the inertia effects. When a system is subjected to quasi–static loads, the loading rate is considered to remain constant and the inertia effects are relatively small. In a dynamic loading, however, due to the presence of inertia and strain rate effects, the collapse response varies.

A.3.1 Quasi–static and Dynamic Loads

Mechanics is concerned with the state of rest or motion of bodies subjected to the action of forces. The mechanics of physical rigid bodies is divided into two areas: statics and dynamics. To give a basic definition, static state is when a body is either at rest or moves with a constant velocity. When the velocity loses its consistency, the body becomes dynamic meaning that it has an accelerated motion. Hibbeler (2002) divides the dynamics into two branches itself; kinematics, which he explains as the branch dealing with the geometric aspects of the motion only, and kinetics, which is the analysis of the forces causing the motion.

Another classification of the branches of mechanics, done by Elert (1998, 2008) in his online textbook (The Physics Hypertextbook) is to categorise mechanics into three subdivisions. Here, the study of motion without regard to the forces or energies that may be involved is called kinematics. He believes that this is known as the simplest branch of mechanics. In contrast, the study of forces in the absence of changes in motion or energy is called statics. And finally, the branch of mechanics that deals with both motion and forces together is called dynamics.

In the current work, since the concentration is on finite element method and FE software, the below classification, used by many of such software, is preferred;

- Static (Linear)

- Quasi–static (Nonlinear Statics)
- Dynamics (Nonlinear)

In static analysis the effects of steady loading conditions on a system are calculated, ignoring effects such as those caused by time–varying loads. This type of analysis can, however, include loads with a steady inertia such as gravity and rotational velocity, and also time–varying loads that can be an equivalent of static loads such as the static equivalent wind and seismic loads commonly defined in many building codes. Static analyses determine the displacements, stresses, strains, and forces in systems and bodies caused by time varying loads. The loads and disturbances and the response of the system are assumed to vary slowly with respect to time. The types of loading that can be applied in a static analysis include (ANSYS 13.0 Help System, 2010):

- Externally applied forces and pressures
- Steady–state inertial forces (such as gravity or rotational velocity)
- Imposed (nonzero) displacements
- Temperatures (for thermal strain)
- Fluences (for nuclear swelling)

The dynamic response of a structure when subjected to time–dependent loads can be determined using a technique known as transient analysis. This method, also known as time–history analysis, can establish the displacements, strains, stresses, and forces in a structure as they vary with time. The inertial effects, mentioned in the previous sections becomes of importance in this area of analysis.

In comparison with static and transient analysis, dynamics is considered to be a technique more often used, since it accounts for both the forces applied to a body and its motion.

Energy Absorbing structures tend to collapse in an even mode when subjected to quasi–static loads. Sequential development of lobes on one end of the structure is known as progressive buckling. Progressive buckling can be divided into quasi–static progressive buckling and, when strain rate effects are taken into account for quasi static loading conditions, dynamic progressive buckling.

According to Karagiozova et al. (2000), in low velocity impacts the progressive buckling is quasi–static while dynamic progressive buckling develops in high velocity impacts. In dynamic progressive buckling the entire length of a structure is involved in the deformation process and the deformation pattern varies from quasi–static progressive buckling shapes (Jones, 1989).

A number of collapse modes can be developed in a progressive buckling process, including axisymmetric, non–axisymmetric and mixed. Collapse can also happen through global bending. The amount of energy absorbed in the progressive buckling mode is significantly greater than in global bending mode since the former occurs in a more controlled manner (White et al., 1999) and on the other hand a greater amount of material is involved in plastic deformation.

The current project looks at the dynamic deformation of egg–box structures as energy absorbers. The collapse procedure in these structures can be categorised as an axisymmetric plastic deformation, initiating with the formation of travelling plastic hinges in the walls of the structure.

The properties of the materials used in the fabrication of egg–box structures, such as material rate dependency, can also affect their performance as energy absorbers, especially in dynamic loading. It is, therefore, necessary to take the effects of such characteristics into account when studying and predicting the behaviour of an energy absorbing structure.

A.3.2 Strain Rate Sensitivity

The stress–strain pattern can change with the rate of loading in structures that are fabricated from rate–dependent material (Reid and Harrigan 1998; Su et al. 1995). Materials such as certain aluminium alloys are sensitive to strain rate which can also be called visco–plastic material. Lu and Yu (2003), suggest that in visco–plastic material, the yield stress can also increase with strain rate.

In engineering equations, the effect of material strain rate should be taken into consideration for realistic calculations. A number of constitutive models exist for material strain rate sensitivity which can be utilised to reduce the number of

experimental tests. One well–known equation in material engineering, which accounts for material strain rate sensitivity, is the Cowper–Symonds relation which is commonly employed in structural impact problems (Reid et al., 1986). Automotive engineers use the Cowper–Symonds uniaxial equation to assess the strain rate effects on the structural response of energy absorbing structures under dynamic loading. The equation can also be implemented in material models for finite element analysis. The Cowper–Symonds constitutive equation can be shown in the following two forms;

$$\dot{\varepsilon} = \mathrm{C}\left(\frac{\sigma_\mathrm{d}}{\sigma_0} - 1\right)^{\mathrm{p}} \quad \sigma_\mathrm{d} \geq \sigma_0 \qquad \text{A.1}$$

$$\frac{\sigma_d}{\sigma_0} = 1 + \left(\frac{\dot{\varepsilon}}{C}\right)^{1/p} \quad \dot{\varepsilon} > 0 \qquad \text{A.2}$$

where ($\dot{\varepsilon}$) is the effective strain rate, σ_d is the dynamic yield stress, (σ_0) is the initial or static yield stress and (C) measured in s^{-1} and (p) are Cowper–Symonds material constants which represent, a characteristic at which $\sigma_d = 2\sigma_0$, and a measure of the rate sensitivity of the material, respectively. The latter two constants can be obtained from dynamic uniaxial or pure shear tests on the material (Jones, 1989) and are different even for different alloys of the same base material. Hence, it is vital to know the exact material specifications in order to find these components.

Finite element packages, such as those employed for the purpose of this study, use the above formulae, in conjunction with the specific material properties provided by the user, to assess the true behaviour of the materials forming the body being analysed.

A.3.3 Inertia Effect Characteristics

In severe impact loadings, structures can show signs of the presence of inertia effects. The collapse mode, initial peak load and load–deflection curve of a structure

can be extensively influenced by this effect. It is, therefore, necessary to investigate the behaviour of energy absorbing structures under both static and dynamic conditions.

According to Calladine et al. (1984), two general types of structures can be identified which deform plastically to absorb energy. The shape of the force–displacement curves of these structures is what distinguishes the two types. As illustrated in Figure A.3, the first type displays a relatively flat–topped curve, while in structures of the second type an initial peak load is followed by fall in the curve. The second group of structures are more sensitive to the impact velocity, i.e. more influenced by inertia.

In addition to Calladine's findings, the innovative type of cellular energy absorbing structures, such as egg–box and honeycomb, produce force–displacement curves which are a combination of the above two types, Figure A.4. Such curves display an initial peak followed by a steady plateau which transforms into a rapid steep rise at the densification point, as the entire structure collapses (Gibson et al., 1997). Due to the length and steadiness of the plateau, this group of energy absorbers are known to show ideal performances compared to their traditional counterparts.

The energy absorbing structure being studied in the current project is subjected to dynamic loading conditions in order to obtain realistic data on the collapse mode, initial peak load and load–deflection curves.

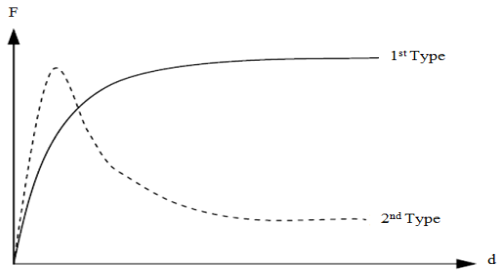

Figure A.3 – Two Types of Structural Collapse (Calladine, 1984)

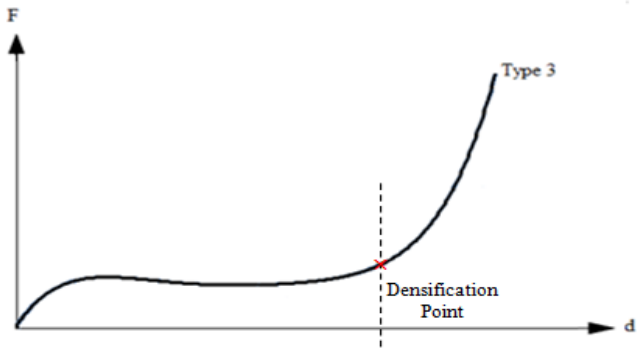

Figure A.4 – Structural Collapse Type Three

The effect of inertia on the energy absorption behaviour of a structure is strongly dependent on its physical and geometrical composition as well as the rate of the loading. For more substantial investigation on the effect of inertia on the characteristics of energy absorbers, the reader is referred to Karagiozova et al. (2000).

A.4. Energy Absorption by Structural Collapse

In order for energy absorbing structures to be used in practice, they should collapse in a predictable and manageable manner with a controlled force level. The energy absorption characteristics of a structure must be known in order to match the detailed design requirements. It would also be beneficial if such structures can be modified to accommodate specific ranges of applications.

Researchers studying this subject provide mathematical formulations expressing the relationship between the deformation behaviour of structures under applied forces and their energy absorption features. Studies such as Deshpande (2001 and 2003) and Shetty (2001) provide detailed information on the attributes of energy absorption per different units of measurement and the approaches towards formula derivation.

The force–deformation response of energy absorbing structures can measure their energy absorption performance. Collapse load can be defined as the amount of load required to cause a permanent deflection to a system. The deflection increases

as the crush progresses. An ideal energy absorber can be represented with a constant crushing load, from the initiation of the deformation process up to the maximum deflection. Energy absorption capacity can then simply be calculated as the rectangular area below the force–displacement curve up to the densification point.

The characteristics of EA structures and their energy absorption capacity are evaluated by a series of qualitative criteria. It is required to determine and meet these criteria at the design stage of an energy absorbing system. Details of such criteria are presented in this section.

A.4.1. Energy Absorbed Per Unit Volume

The energy absorption capability of a structure is primarily based on its plastic behaviour. For any given structure with a specific geometry, the area under the stress vs. strain curve associated with its deformation, up to a point of densification, gives its energy absorption capacity per unit volume.

Energy absorbed per unit volume becomes of significance when the structure being deformed is in some way restricted in the space, as well as situations where the ultimate energy absorption rate is achieved by mechanisms other than mere geometrical deformation of the structure.

A.4.2. Energy Absorbed Per Unit Mass

The specific energy absorption (SEA) also known as the energy absorbed per unit mass, (W_m,) is defined as the energy absorbed by a deformed structure when crushed with the energy of (E) per unit mass. This can be written as:

$$W_m = \frac{E_{Total}}{\rho x A} \qquad \text{A.3}$$

with (E_{Total}) representing the total energy absorbed in the crushing of the structure under a crush load of (F). The value $\varkappa$ is the displacement of the highest point of the structure after the impact, known as the crush distance. A represents the cross sectional area of the crushed portion of the structure which has a density of (ρ).

The crashworthiness of a structure is determined by its SEA value. The total energy absorbed by a structure, (E_{Total},) is equal to the area beneath its corresponding force vs. displacement curve. This value can be used as a comparison factor when studying the capabilities of different structures in terms of their level of energy absorption.

A.4.3. Energy Absorbed Per Unit Length

Here, length is defined as the distance of deformation and thus, the energy absorbed per unit length, (W_L) is defined as the energy absorbed per unit of deformation distance, ($\varkappa$). This can be shown as;

$$W_L = \frac{E_{Total}}{\varkappa} \qquad \text{A.4}$$

The energy absorbed per unit length provides a simple method for calculating the crashworthiness of structures where collapse is restricted to a well–defined crush zone. Such crashworthiness specifications allow for the structures to be verified by using appropriate test procedures or finite element simulation.

It is therefore evident that the selection of a suitable energy absorbing structure for a specific application will depend upon the geometry and material of the crushed structure, as well as the nature of the application under consideration.

From the definition of SEA it can be construed that the lighter the weight of a structure, the more crashworthy it would be. Hence, a practical energy absorber must have an acceptable and minimised weight.

A.5. Energy Absorbing Structures

Structures of certain geometries and materials have a considerable potential for absorbing the kinetic energy of an impact. Their energy absorption capability offers a unique combination of reduced structural weight and improved safety especially in the automotive and aircraft industry. Crash resistance of these structural parts provides a protective shell around the occupants of a vehicle.

In the past decade studies have demonstrated the ability of specific structures to absorb energy under dynamic crash conditions. Many energy absorbing structures have been studied experimentally.

Structures currently in use include thin–walled tubes such as: circular tubes, square/rectangular tubes, hat–section tubes, tapered rectangular tubes and conical tubes and cellular solids such as: metallic foams and polymeric (non–metallic) foams, honeycomb panels and egg–box components (Figure A.5). Analysing the characteristics of the latter type of energy absorbing structure is the concentration of the present study.

Figure A.5 – Commercially Used Energy Absorbing Structures

Energy absorbing structures are expected to perform in a predictable and controllable manner in order for load limitations to be specified per system. Investigations are made on the geometrical and material attributes of these structures to improve their performance and increase their crashworthiness per application.

A.5.1. Egg–box Structure

Amongst energy absorbing structures currently in employment, the repetitive cells of an egg–box structure, originated from the earlier work of Professor Shirvani and later patented under the name of PressLoad by Cellbond Composites Ltd. (Ashmead, 2000), offers high levels of energy absorption capacity and SEA. Egg–box structures are a group of energy absorbing cellular structures which, as suggested by the name, consist of panels shaped like egg–boxes (Figure A.6(a)).

In a regular egg–box arrangement, the unit cell is made up of alternated axisymmetric conical shells with flat tops geometrically classified by four parameters: cell height (h), apical angle of cell (ω), top diameter (d) and wall thickness (t), shown in Figure A.6(b).

The distance between two diagonal cells is defined by (p) where;

$$p = 2h\,tan\,\omega + d \qquad \text{A.5}$$

Another effective parameter in the deformation process is the radius of the fillet, (r), at the top of the peaks. This curvature is produced during the manufacturing process and is inevitable. It is practically impossible to create a specimen with $r = 0$. Although measuring and modelling this curvature is fairly complex, however, taking this factor into consideration results in a better valuation of the energy absorption characteristics of the specimen. A change of this parameter, when modelling the geometry, has been found to induce a significant effect on the initiation of the deformation where a sharp transition of $r = 0$ displays a stiff elastic response (Deshpande, 2003).

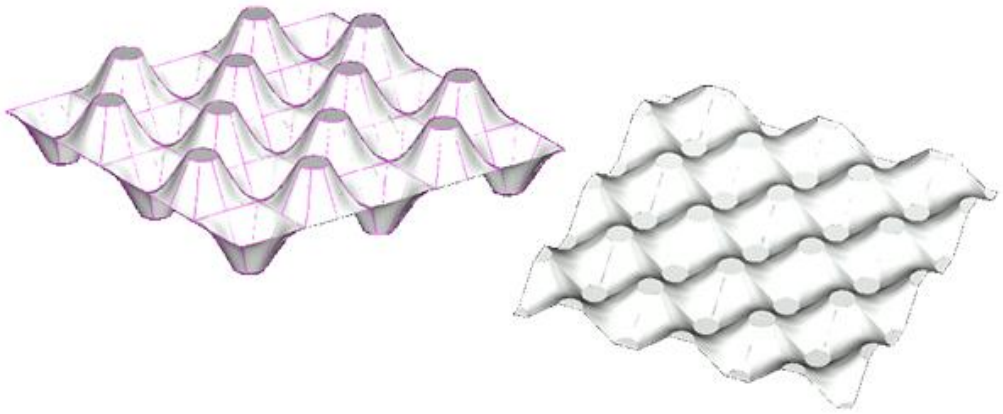

(a) Panel Concept Drawings

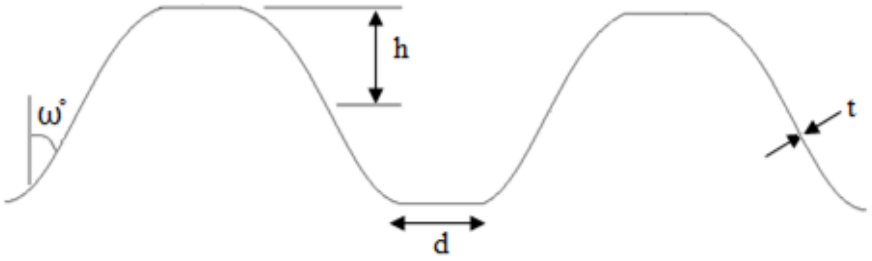

(b) Geometrical Characteristics

Figure A.6 – Egg–box Structure

In addition the peaks and trenches of the egg–box structure can be produced to different, usually small curvatures. The factor (*R*) is the radius of these arcs. For very large values of *R*, the peaks and trenches can practically be considered as being flat.

These geometrical factors in the egg–box structure can be adjusted to result in desired levels of energy absorption. Varying the peak to peak length, (*p*), angle, (*ω*), cell diameter, (*d*), or wall thickness, (*t*), in addition to the material type used and the level of constraints applied to the structure can result in diverse energy absorption characteristics for this structure. For example reducing the inter–peak distance, (*p*), gives a higher density of cones throughout the structure which in turn results in an increased stiffness and a higher stress level, i.e. greater amount of energy will be absorbed (Deshpande, 2003).

The geometrical appearance of the egg–box structure contributes towards its suitability as an energy absorber.

A.6. Analysis of Energy Absorbing Structures

In order to remain competitive in the highly dynamic market of safety material production, it is important for energy absorber developers to thoroughly understand the crashworthiness and impact mitigation of their products. Researchers use one or more of the following tools to carry out such comprehensive analysis; analytical, numerical and experimental techniques.

These three techniques can be used in conjunction for validation and verification of the outcomes of testing a certain structure. While structures currently in use can be improved and optimised, using these techniques, new design opportunities can also be discovered.

A.6.1. Experimental Methods

One commonly and traditionally used approach is controlling and manipulating the attributes of energy absorbing structures by the use of practical test machines, which can deliberately load specimens both statically and through dynamic impacts.

Experimental methods are valuable in terms of demonstrating the role of individual geometrical alterations in the behaviour of an energy absorber. They can however be extremely costly and time consuming, considering the need for repetition of single tests as well as tests performed on the great number of altered geometries. In addition, once a specimen undergoes loading and becomes deformed, there is no easy reverse approach; the material has to be recycled and formed into new structures, which means further expenses and in some cases impossible. Using these testing methods can be beneficial and even essential as validation tools when it comes to verifying results of numerical analysis.

Various methods of practical testing of energy absorber structures exist, which can be divided into two main categories of static loading and dynamic impact testing.

A.6.1.1. Static Loading of Egg–box Structures

Static loads, by definition, are, as explained earlier, constant mechanical forces that do not change with time. It is evident that in practice this would be impossible due to the presence of gravitational accelerations. Therefore, in mechanical physics, static loads are referred to the group of forces that are applied on a body, steadily and at very low rates. Testing structures under static loadings can be helpful in determining their maximum allowable load bearing capacities, as well as the mechanical properties of the materials forming them.

This particular mode of experimental testing becomes most valuable in the design of structures that are used towards human health and safety. In order to set safety margins on a structure, it is vital for a designer engineer to be aware of the maximum force a structure can support prior to collapsing. Energy absorbers are structures that directly deal with the safety of passengers in the transportation industry. It is therefore necessary for them to be statically loaded in order to study their attributes and limitations.

Figure A.7 – Plate Compression of Egg–box Energy Absorbing Structure (Experimental tests performed at Cellbond Composites Ltd)

In the static testing of egg–box energy absorbers, Figure A.7, the specimens are compressed using screw–driven plates at very minimal nominal strain rates, 10^{-6} – $10^{-3}s^{-1}$, or at low constant velocities such as 1mm/s. The compressive response of the specimen is then measured based on the level of constraint. The applied load is measured by placing a load cell on the test machine and is used to define the nominal compressive stress on the specimen; the nominal axial strain is measured via a clip gauge fixed between the loading platens, recording the distance travelled from the

initial location. The measured compressive stress vs. strain curves for every geometry can thus be produced and used to explore the deformation procedure of the egg–box.

A.6.1.2. Egg–box Structures under Dynamic Impact

Dynamic or impact loads are forces applied to physical bodies with a motion and can change with time. Dynamic loads can be categorised into three groups; low pace impact, high velocity impact and hyper velocity impact. This classification is based on the fact that, as the pace of impact increases, extreme changes become evident in the deformation mechanism of the target object and the energy transfer between this structure and the impactor.

A low pace impact is the situation where the impactor contacts the target for long periods of time. Such low velocity events can be considered as quasi-static loadings. The velocity limit which defines a quasi-static impact depends on the size ratio of the impactor to target. Cases where the impactor is significantly larger than the impacted structure could be counted as quasi-static (Nettels, 2000).

In contrast, in high pace impacts, the contact periods between the impactor and the target are much shorter in time. This type of impact occurs every day in road accidents as well as impacts in the ballistic range. The effects of high pace impacts are severe but, under certain circumstances, controllable. It is in the presence of this class of dynamic force when energy absorbing structures prove to be constructive.

Hyper pace impact refers to events where an exceedingly high velocity impactor crushes the target structure at such an elevated stress that the compound materials of the target act like fluids and exhibit minimal physical strength. It is unlikely for an impact with such magnitude to appear in the automotive and aviation disasters. Therefore, when examining the response of egg–box structures to dynamic impacts, this study concentrates on situations of high–pace impact.

The common testing method for energy absorbers subject to dynamic loads involves impacting the specimens in the vertical axial direction, under the effect of a drop–weight tower as shown in Figure A.8.

Figure A.8 – Dynamic Impact of Egg–box Structure

The loading mass and velocity of the impactor can be increased or decreased as appropriate. Zupan et al. (2003) suggest impacting egg–box panels of below $1m^2$ cross sectional area with an impactor mass of 5.5kg moving at a velocity of 6m/s. Similar to the static mode, the load is measured with a load cell placed on the impactor mass. The relative displacement of loading mass is measured by laser extensometer against time to prove the test acceleration. The measured compressive stress versus strain response of the specimen is resultantly produced to evaluate the behaviour and efficiency of a given egg–box absorber.

As mentioned previously, such techniques can be extremely costly in terms of both expenses and time. Moreover, in cases of irreversible material destruction, a good amount of metal or plastic can be wasted. This waste material is considered as contributing to global damage. Therefore it would be ideal to take advantage of non–experimental, repeatable methods which avert the need for structural production, destruction and recycling costs.

To generate a principle for measuring the energy absorption capacity of conical frusta, a mathematical approach is proposed. This formulation has been expanded to predict the characteristics of the egg–box structure, which is in fact made of a series of conical frusta (Deshpande, 2003). The next section provides a brief review of these calculations.

A.6.2. Mathematical Approach

An approach towards the determination of the energy absorption characteristics of EA structures is the development of mathematical models. To use these theory–based methods a series of assumptions and approximations need to be made. In other words, to allow for the application of mathematical formulations, the body being analysed needs to be simplified to a controllable model. The absence of physical and geometrical details in such modified assumptions leads to lack of accuracy in the calculations.

Despite the simplified outcome of mathematical modelling, this approach can be used as a valuable means of validation of the results of experimental or numerical analysis.

In most cases, mathematical calculations are based on two dimensional approximations of three dimensional systems. It would therefore be ideal to have a means of analysing the characteristics of the energy absorbers, using a method that would take into consideration the geometrical details of the structure in all three dimensions. Researchers are working on developing more accurate theoretical models for solving the behaviour of complex deformation patterns and structures.

In a recent study, a simple model is used to derive a general mathematical formulation for the travelling hinge deformation and the plastic buckling displayed in the crushing of a conical frustum (Deshpande et al., 2003).

The initial calculations are based on the approximate analyses done by Calladine (1986) on the inversion of a spherical shell when subjected to a central point load. It was assumed that the conical frustum being studied was being compressed between two solid platens, disregarding the friction. Two travelling plastic hinges were considered to form on each cross sectional side of the frustum, forming a knuckle. Equal and opposite longitudinal bending moments, resulting from the applied force, were identified on the inner and outer hinges, causing the knuckle to rotate instantaneously (Deshpande et al., 2003).

Through the combination of a series of equilibrium equations, a mathematical relation is derived representing the energy absorption rate by relating applied load of

(P) to the displacement of the top of the conical shell, u, for the travelling plastic hinge, expressed as:

$$\frac{P}{Yt^2} = \frac{2\pi\omega\tan\omega}{(2\omega-\sin 2\omega)^{1/2}}\left[\frac{a}{t}+\frac{u}{t}\cot\omega\right]^{1/2} \qquad \text{A.6}$$

where (Y) is the yield strength of the material, (t) is the wall thickness of the cone, a is the top radius and ω is the angle of the cone walls to the horizontal.

Once the above expression is verified against practical results, it is developed into equations, giving approximate numerical solutions for the energy absorption capacity and collapse strength of the egg–box absorber. To achieve this, it has been assumed that an egg–box comprises a two dimensional array of conical frusta of the same geometrical measurements and thus work out the stress vs. strain relationship of the egg–box to be equal to:

$$\frac{\sigma}{Y} = k\left(\frac{a}{t}+\frac{\varepsilon t}{2h}\cot\omega\right)^{1/2} \qquad \text{A.7}$$

$$k = \frac{\pi\omega\tan\omega}{2}\cdot\frac{1}{(2\omega-\sin 2\omega)^{1/2}}\cdot\frac{1}{\left(\frac{a}{t}+\cot\omega/2t\right)^2} \qquad \text{A.8}$$

where (σ) and (ε) are the nominal axial stress and strain, respectively, (h) is the depth of the egg–box cell and (k) is a geometrical constant defined in equation A.8.

In practice, force–displacement curves associated with the deformation of energy absorbers transit into a steep rise, starting at the densification point until the deformation process terminates and the structure collapses. According to Ashby et al. (2000), the densification process for cellular solids can begin at strain levels as low as 0.4 to as high as 0.94 depending on the material and the structural shape. This

process for egg-box structures starts at strain values of around 0.6-0.8 (Deshpande, 2003, Akisanya, 2006, Cheng, 2007). With (*H)* being the height of the egg-box panel and (*x)* the travelled distance of deformation, in mathematical terms, the value of the densification strain can be expressed as:

$$\varepsilon_D = \frac{x}{H} \approx 0.75 \qquad \text{A.9}$$

Through comparison against practical experiments, it can be concluded that equations A.7 and A.9 are rational mathematical approximation of the deformation behaviour of egg–box.

Despite their near agreement with the experimental data, these mathematical equations are all based on two dimensional approximations of the actual geometry. It can become too complicated, inaccurate and to some extent impossible, to use such formulations for energy absorbers with more complex geometrical features. For example, the small curvature present at the transition point of walls into peaks and trenches is ignored in the above calculations, while, as mentioned before, this small arc plays a significant role in the initial deformation of the egg–box structure. It would, therefore, be ideal to have a means of analysing the characteristics of the egg–box absorbers using a method that would take into consideration the geometrical details of the structure in all three dimensions.

Finite element analysis is a useful tool to solve just such a problem. Using numerical calculations and predictions, the FE method can in fact be used to determine the energy absorption characteristics of an EA structure prior to the geometrical design and manufacture. Further information on the background and application of the finite element method is provided in the next section.

A.6.3. Finite Element Numerical Analysis

For many engineering problems either due to the complexity of the nature of a system, or its boundary and initial conditions, it is not possible to obtain exact solutions. For such problems, approximate methods are used known as numerical solutions. These methods obtain exact solutions at approximated points called nodes whereas with exact methods, such as experimental tests, a single result applies to every point of the system or body through which, it would not be feasible to evaluate the role of each portion of the structure, hence the inability of modifying a single parameter towards optimisation of the structure.

This matrix–based method is mainly used for problems with complex geometry or boundary conditions. In finite element modelling the respective appearance of the information of a system in different matrices is important. Finite element analysis is a useful tool to solve three dimensional systems at more realistic approximations.

It is also important to note that the structure can only assume those shapes that can be represented by shape functions and, according to Hartmann et al. (2007), the accuracy of an FE solution depends fundamentally on how accurately a program can approximate the influence functions for stresses or displacements. Influence functions are the response of a structure to certain point loads. The more flexible a structure is modelled, the better it can react to such point loads, and hence the better the accuracy of the FE solution.

The FE numerical processing tools, allow for the study of the fundamental features of different energy absorbing structures. In addition, application–specific requirements can be met in terms of energy absorption capacity, appearance, material, etc. by designing individual optimised geometries prior to production.

Modern FE analysis packages are capable of simulating dynamic crash impacts by utilising explicit solvers. This technique allows for faster analysis of such problems, giving detailed information on material response and behaviour. In addition, these packages offer visual feedback on deformation modes and measured levels of stress, strain and energy absorption, by use of frame animation and graph processors (Figure A.9).

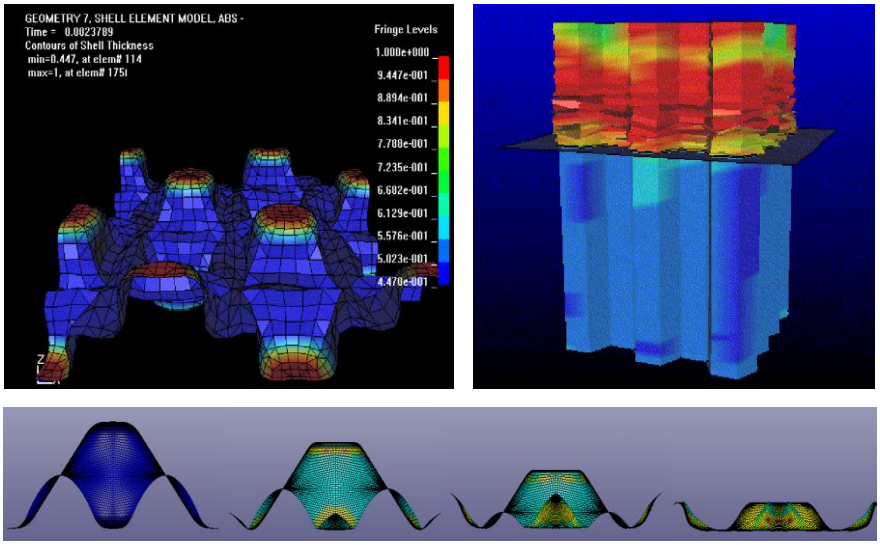

Figure A.9 – Typical Visual Feedback of Finite Element Packages

The finite element method is a numerical procedure based on the idea of building a complicated object, using simple blocks, plates or beams, or alternatively, dividing a complicated object into similar, easily manageable pieces, connected to each other at previously identified points known as nodes, to allow for detailed analysis of its attributes. The behaviour of each individual element can be described by a set of equations, which when combined with the other elements in a structure, form huge lists of simultaneous equations. Integral formulations are used to derive a solution for each element, which is then connected or assembled with the other individual solutions to form the complete solution for a system.

The accuracy of the final solution is based on the number, shape, location and accumulation of the elements and nodes defined as well as a realistic assumption of the boundary conditions. An important point to take into account is the behaviour of each individual element. A few good shaped elements can produce better results than many elements with poor geometries. There are many different shapes and types of elements including triangular and quadrilateral elements, which can be selected based on the geometrical outline and shape of the part being modelled.

To solve an engineering problem two sets of information are required; one is the details of the natural behaviour of a system, such as elastic modulus, thermal conductivity and viscosity and the other is information referring to the conditions of

a system under the effect of outer parameters, such as external forces, moments, temperature differences, pressure in fluids, etc. The first set of information can be generalised for systems of similar characteristics, while the mechanical properties applied to a system are particular to each system or body.

In dynamic analysis, to derive the result equations of a system, the work of the external forces absorbed by the work of the internal forces, inertial, and viscous forces for any small kinematical motion, which satisfies both compatibility and boundary conditions have to be taken into account. Displacement, velocity and acceleration change with time. It is also possible for the mass of the system to vary with time. Since the stiffness of the system is a function of both displacement and internal forces, the external disturbance will be a function of displacement as well as time, meaning the ultimate condition of the system will depend on the location of its points and the times in which these displacements have taken place.

It is evident that a demand for more accurate outcomes calls for a greater number of matrices and algebraic equations, increasing with higher complexities in structures. Solving all these equations and connecting them to form a final solution can be an extremely time consuming task when done in long hand. A much quicker technique of designing, visualising, refining and calculating the performance of a structure in different geometrical and mechanical conditions, is the use of, commercially available, solver packages.

Computers can be utilised to solve the astronomical number of equations and provide solutions to engineering problems. The availability of increasingly powerful, low cost processors has made finite element analysis accessible for many engineering disciplines. This ease of access has led to a substantial increase in manufacturing efficiency and competitiveness over the years.

A.7. Finite Element Software and Commercial Packages

For highly complex problems, highly professional finite element solver packages have been commercially designed, which substantially reduce the time and cost of experimental and mathematical analysis. Preliminary finite element software

with very basic abilities initially appeared in 1964. Today powerful commercial finite element packages exist, which offer highly interactive graphics and strong processors and are compatible with personal computers. Popular software currently in use for structural and mechanical analysis include ABAQUS®, ANSYS®, LS–DYNA®, NASTRAN®, RADIOSS®, PAMCRASH®, ADINA®, CRASH CAD® and LUSAS®, some of which are specifically designed to be used in crash analysis.

A.7.1. ANSYS® and LS–DYNA® Numerical Analysis Packages

The ANSYS® software is one of the highly established, widely distributed and popular commercial finite element analysis packages, which has continuously been in use and refined since 1970. Its historical background of development has resulted in a code with a vast range of capabilities.

As a powerful numerical finite element solver, ANSYS® package can be used to analyse a wide range of mechanical problems such as static and transient structural analysis. In fact, ANSYS® is most commonly used in this particular area of mechanical physics, since it can facilitate the analysis of structures as large as bridges or as small as vehicle parts.

ANSYS® allows for the simulation of problems in static and transient modes of mechanical loading. For both loading conditions ANSYS® can determine displacements and stresses of a simulated structure as well as nonlinear plasticity, stress stiffening, deflection, strain, hyper–elasticity, contact surfaces, etc., taking into consideration the time–varying loads in the transient mode.

A number of purpose–specific features are available in ANSYS® in addition to the above loading modes. Examples include fracture mechanics, composite material analysis, fatigue, and both p–Method and beam analyses (ANSYS® 13.0, 2010).

In ANSYS® the finite element analysis is performed in three stages, taking place in a GUI or graphical user interface. In the pre–processing phase a geometrical model is created and meshed. It is at this stage that all the physical requirements and limitation are simulated in the GUI. Next is the solution phase where all the quadratic equations are formed and then solved for each node of the model to give unanimous

final results on the performance of a modelled structure. These results can be viewed through the third phase, post–processing. Here graphs and time based animations can be produced to evaluate the outcomes of the simulated test.

In order to simulate dynamic loading conditions, the powerful pre–processors of ANSYS® have been combined with the equally powerful solver of another finite element package known as LS–DYNA®. This software is designed to be used for analysing static and dynamic problems with large deformation. LS–DYNA® uses explicit time integration as its base solution approach (LSTC, 2007).

LS–DYNA® was originally developed in the mid–seventies, starting under the name DYNA3D. This preliminary version had very basic capabilities and a number of issues were revealed with the different algorithms it used at that time. At this point the software was completely rewritten. After several attempts on introducing more complete and more comprehensive versions, by 1988 the package, now renamed to LS–DYNA®, was presented with a particular focus on the applications of the automotive industry. Throughout the past decade, progress has been made in the development of this software and with the emergence of newer versions, more options get added to the capabilities of LS–DYNA®, detailed in the LS–DYNA® User's Manual (LSTC, 2007).

A.7.2. ANSYS/LS–DYNA® Numerical Analysis Package

The combination of ANSYS® and LS–DYNA® gave existence to a powerful finite element package referred to as ANSYS/LS–DYNA®. This package is detailed further in this section.

ANSYS/LS–DYNA® was first introduced in 1996 to overcome challenges such as limited–duration events and large, permanent deformations which created great simulation challenges for the engineers. Researchers and designers used this product, to model a structure or system in ANSYS®, then obtaining the explicit dynamic solution using the powerful LS–DYNA® solver, and eventually reviewing the results in the ANSYS® post–processing GUI.

Through the years, this influential pairing has helped engineers understand the complicated combinations of nonlinearity they come across in crash tests and catastrophic failures.

The geometry and results information can also be transferred between ANSYS® and ANSYS/LS–DYNA® to help perform chronological implicit–explicit and explicit–implicit analyses, such as those required for drop–test, spring–back and other applications (ANSYS/LS–DYNA® User's Manual, 2011).

Since the solver in ANSYS/LS–DYNA® is an LS–DYNA® solver, the results can also be reviewed and modified in the LS–DYNA® post–processor environment. As a feature mentioned in the ANSYS/LS–DYNA® product details, this package supports both 2D and 3D explicit elements, and features an extensive set of single–surface, surface–to–surface and node–to–surface contacts as well as a unique contact analysis option that automatically creates contact surfaces for all simulated bodies in a system. In addition, ANSYS/LS–DYNA® provides options that allow for fast solution processing. Simulation results are delivered in a short period of time using solution techniques called symmetric multiprocessing (SMP) and massively parallel processing (MPP). This is achieved by optimising the power of multiple CPUs (ANSYS online, March 2011).

The availability of such computation powers increases model accuracies and details, since more exact and consistent simulations can be performed in shorter durations. However, in order for the finite element analysis tools to contribute efficiently in the design process of a structure, a practical compromise should be made between the preciseness requirements of a model and the time involved with its computation, a technique known as element sensitivity analysis.

A.8. Finite Element Modelling of Energy Absorbers

The finite element method (FEM) is an important tool in mechanical computation and structural engineering problems. Nonlinear FEM can be used to analyse large deformation plasticity problems to provide more accurate and detailed outcomes, as compared to the traditional methods.

Designing energy absorbing structures is a highly complicated process that may require several design iterations. Finite element analysis (FEA) is being used in the automotive industry to perform efficient, parametric studies of these structures. Using this method helps reduce or prevent the great number of costly and time–consuming practical testing.

Energy absorbing structures generally collapse in a complex manner under axial or multi–axial loading conditions. Due to this mode of deformation, the impact behaviour of an energy absorber could not be evaluated accurately using conventional analyses such as theoretical models.

The FE numerical processing tools, allow for the study of the fundamental features of different energy absorbing structures. These techniques have recently become one of the most important tools for simulating and analysing the behaviour of EA structures (Figure A.10).

An interactive model of a structure subjected to an impact load is simulated and analysed using the nonlinear FE–based package. This method makes it possible to obtain the entire history of the structural deformation process. The results of an FE model must be validated to ensure accurately reliable results have been achieved. The outcomes can be validated against results of experimental techniques or numerical and theoretical models.

Modern FE analysis packages are capable of simulating dynamic crash impacts by utilising explicit solvers. This technique allows for faster analysis of such problems, giving detailed information on material response and behaviour. In addition, these packages offer visual feedback on deformation modes and measured levels of stress, strain and energy absorption, by use of frame animation and graph processors.

The modelling of egg–box structures for dynamic loading conditions has been described extensively in the thesis.

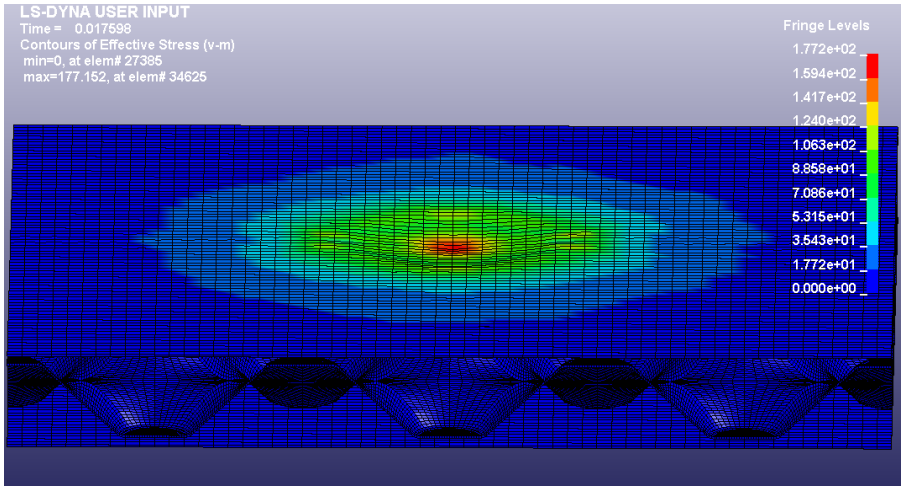

Figure A.10 – An Example of FE Analysis of Impacting an Energy Absorbing Structure (LS-DYNA®, personal interest research on egg-box sandwich structure, vertically impacted by an ellipsoid)

In addition, application–specific requirements can be met in terms of energy absorption capacity, appearance, material, etc. by designing individual optimised geometries prior to production.

A.8.1. Material Models

Modelling the base material of a structure is of importance in the FE simulation of the impact response of energy absorbers. The material model should represent the true properties of the physical material. Characteristics such as elasticity, plasticity, strain rate dependency, fracture and tearing response of materials at specific temperatures should be accurately modelled in order for the FE simulation to validly represent the physical structure.

As a powerful finite element code, one of the benefits of LS–DYNA® is its material modelling capabilities. More than 100 different material models are available to represent various types of highly nonlinear material behaviour including foam material and honeycomb structures.

A.9. Structural Optimisation

In the world of mathematical sciences and engineering, optimisation refers to the selection of the element or value, with the best available features, from a group of possible alternatives, given a defined domain of objectives. This means solving problems in which the aim is to minimise or maximise a characteristic of the design by analytically allocating values from a specified source, to a set of variables.

Optimisation problems of more than one objective increase complexity. For example, in the simplest double–objective problem there will be a design that amplifies objective No.1, while objective No.2 is in its lowest value and another design where objective No.2 is maximised and No.1 is ignored. There can also be countless designs that are a compromise of both criteria. An increase in the number of interest areas can add to the complexity of a problem, especially in cases where one criterion cannot change without affecting the other.

In structural engineering, for example, an optimised design can be defined as one that is adequately strong while it maintains a light weight. A simple judgment would reveal that these two objectives conflict. There can be a light weight design option, which is not necessarily strong, while another very strong design has an extraordinarily heavy weight. In addition, an infinite number of options could exist, that would be an assortment of weight and strength. This set of designs that cannot be optimised according to one criterion without influencing another is called a Pareto set (Lanzi, 2004).

The solution to such optimisation problems would be to keep changing the variables one at a time, while the rest are kept constant. This will give rise to a number of design combinations. This is where the concept of *application–specific* optimisation becomes important.

Despite the literal definition of the word optimum – the best – when it comes to practical optimisation, in a given criterion, a design can be *the best* fit for one purpose, but not necessarily for all. In the above example of structural engineering optimisation, for instance, selected out of the Pareto set, a design offering a reasonable level of strength at a low weight can be ideal for a structure which is designed to be transported, while for a similar structure, designed to be stable and

fixed, a slightly heavier but stronger option might be preferable. Therefore, a single design cannot be selected as the one and only optimal. Depending on the purpose and the location of a service, an application–specific optimisation can take place.

Application of the above techniques in the optimisation of energy absorbing structures is explained in the subsequent sections.

A.9.1. Optimising Energy Absorbing Structures

For any system to remain continuously successful in an industry, it needs to be constantly updated and improved. The same theory applies to the energy absorbing structures.

The regulations demanding safety limits on the vehicles are becoming increasingly precise and strict. Hence, the impact energy absorbing structures, which are employed as protective components in the vehicle bodies, need to meet up to the expectations of regulatory authorities. This necessitates continuous improvement of the performance of EA structures.

For industrial purposes, an energy absorbing structure is chosen for a particular function, based on its energy absorption capacity. It is desirable for this value to remain below a certain limit for a given stress level. Finding the structure that satisfies this requirement is known as purpose–specific optimisation. However, other influential factors come into the equation during the process of developing the best fit. Aspects such as structural size limits, durability, manufacturing costs and constraints, material recyclability, etc. play as equally important a role as the structural performance of an energy absorber.

The main purpose of structural optimisation is to improve a component using limited resources. The factors that are altered towards the improvement of a system are known as design variables. In energy absorbers, these factors can be associated with either the geometry or the material of the structure.

While geometrical aspects can be interconnected and changing one can affect the other, the effects of changing the materials of a structure can be compared

individually. The former case would result in a multi–variable optimisation where some variables have to be changed in accordance to another.

An efficient structural design is required to respond in an acceptable manner for various specifications. However, the optimisation of an energy absorbing structure is a comparative process. A structure can only be optimised for the loading and boundary conditions of the energy absorption system in which it is integrated. In other words, the structural optimisation of an energy absorber is merely valid for functioning under specifically identified circumstances and a design that fits perfectly into the requirements of one system may fail to be as adequate in a system with different boundary or loading conditions.

An extremely strong structure does not always succeed in becoming the optimum candidate if it is, for example, overweight or costly to manufacture. The presence and importance of all these factors increase the complexity of the optimisation process, especially with characteristics that contradict, such as durability of the materials and the costs of purchasing them. Therefore, based on its function, the optimisation of an energy absorbing system may be a multi–objective task where more than one characteristic identifies the crashworthiness of the system.

In general, it is required from an EA structure to absorb maximum amount of impact energy while it reduces the effect of the initial load of the impact. Simultaneously, the material from which the structure is made must be strong, have adequate elastic and plastic properties and be of a reasonably low density. Fulfilling all these requirements concurrently gives rise to an optimised energy absorbing structure.

Among many optimisation techniques (Vanderplaats, 2007), a practical method which can be used for the optimisation of energy absorbing structures is RSM or response surface methodology. The idea of this method was introduced by Box and Wilson (1951) where sequences of designed experiments are used to obtain an optimal response. Although this method is not exact, it provides a reasonable set of data which can be relied on as sources of evaluation for an optimisation problem. For the purpose of this study, hints have been taken from the RSM method.

A.9.2. Crashworthiness Optimisation of Application–specific Egg–box Models

Structural impact can be categorised into geometry and material optimisations, which can be accounted for individually. It means that for every material, there would be an improved geometry, which would perform desirably in a specific application.

For industrial purposes, based on their function, the egg–box absorbers are chosen so that their energy absorption capacity at a stress level would be below a prescribed limit. It is this limit that a model has to satisfy to be counted as an appropriate fit for a specified application. Among the designs that become eligible with regards to the energy absorption capacity, an optimised design would be one that takes a longer duration to transform the kinetic energy of the impact to the force, deforming the cell walls.

The total energy that the egg–box structure has the capacity to absorb during the deformation consists of both elastic and plastic strain energies. In an FE analysis, the total energy absorbed by an egg–box cell during crush can be defined as the area roofed by the curve displaying its reaction to the crush force over the deformation of its walls.

It is expected that an optimised egg–box cell will be able to absorb the maximum amount of energy in a unit structural weight. In addition to equation A.3, (W_m) (specific energy, in the unit of N.mm/ton) can also be defined as:

$$W_m = \frac{E_{total}}{m}, \qquad \text{A.10}$$

where (m) is the total mass of the egg–box cell under consideration. In terms of the corresponding force–displacement curve, a structure's improved behaviour will be displayed in a curve as a higher magnitude and a longer plateau.

From another point of view, the peak crushing force of the structure is also considered as a critical design objective. This is specifically of concern in cases

where the energy absorber is acting as a cushioning structure for vehicle occupants, in car doors and dashboards. In such conditions, preventing severe biomechanical injuries to the occupant's body is of major significance.

The challenge would be for the optimisation problem to account for both of these design objectives; bearing a major concern for the energy absorption capacity of the structure while, simultaneously, seeking designs of minimum peak crushing force.

A.9.3. Application of FEA in Structural Optimisation

As a result of the reliance of structural optimisation on nonlinear and conditional functions, analytical approaches fail to solve the practical design problems. On the contrary, numerical methods are ideal candidates for dealing with such problems.

With the development of nonlinear finite element analysis codes, the optimisation of energy absorbing structures becomes possible. The nature of optimisation is a comparative evaluation of variable combination. FE codes can take over the analysis of various combinations, providing prompt, inexpensive results which can consequently be assessed based on their contributing variables.

Finite element software prevent the need for costly experimental crash tests in the optimisation of energy absorbing structures. The highly powerful pre–processors of today's commercial FE packages facilitate the alteration of geometrical attributes and allow for repetitive tests. With a validated FE simulation, the performance of geometrically altered energy absorbers under various loading and boundary conditions can be promptly investigated and necessary modifications can be applied to a structure upon necessity.